RISK OF DIETARY HAZARDOUS SUBSTANCES AND IMPACT ON HUMAN MICROBIOTA: POSSIBLE ROLE IN SEVERAL DYSBIOSIS PHENOTYPES

EDITED BY: Margarita Aguilera, Mangesh Bhide, Els Van Pamel, Eric Houdeau, Bruno Lamas and Ana Rivas

PUBLISHED IN: Frontiers in Microbiology and Frontiers in Physiology

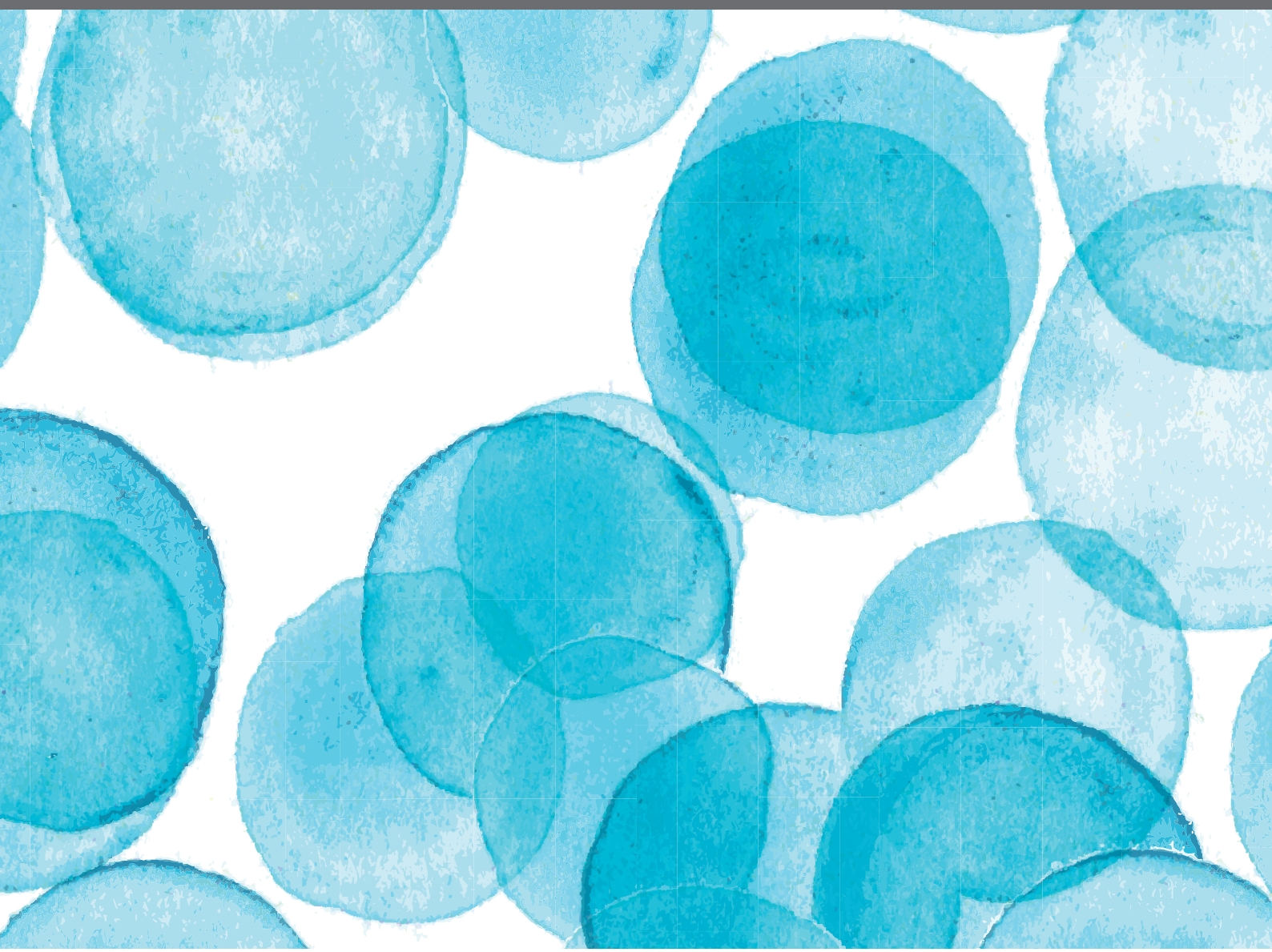

frontiers Research Topics

frontiers

Frontiers eBook Copyright Statement

The copyright in the text of individual articles in this eBook is the property of their respective authors or their respective institutions or funders. The copyright in graphics and images within each article may be subject to copyright of other parties. In both cases this is subject to a license granted to Frontiers.

The compilation of articles constituting this eBook is the property of Frontiers.

Each article within this eBook, and the eBook itself, are published under the most recent version of the Creative Commons CC-BY licence. The version current at the date of publication of this eBook is CC-BY 4.0. If the CC-BY licence is updated, the licence granted by Frontiers is automatically updated to the new version.

When exercising any right under the CC-BY licence, Frontiers must be attributed as the original publisher of the article or eBook, as applicable.

Authors have the responsibility of ensuring that any graphics or other materials which are the property of others may be included in the CC-BY licence, but this should be checked before relying on the CC-BY licence to reproduce those materials. Any copyright notices relating to those materials must be complied with.

Copyright and source acknowledgement notices may not be removed and must be displayed in any copy, derivative work or partial copy which includes the elements in question.

All copyright, and all rights therein, are protected by national and international copyright laws. The above represents a summary only. For further information please read Frontiers' Conditions for Website Use and Copyright Statement, and the applicable CC-BY licence.

ISSN 1664-8714
ISBN 978-2-88966-907-3
DOI 10.3389/978-2-88966-907-3

About Frontiers

Frontiers is more than just an open-access publisher of scholarly articles: it is a pioneering approach to the world of academia, radically improving the way scholarly research is managed. The grand vision of Frontiers is a world where all people have an equal opportunity to seek, share and generate knowledge. Frontiers provides immediate and permanent online open access to all its publications, but this alone is not enough to realize our grand goals.

Frontiers Journal Series

The Frontiers Journal Series is a multi-tier and interdisciplinary set of open-access, online journals, promising a paradigm shift from the current review, selection and dissemination processes in academic publishing. All Frontiers journals are driven by researchers for researchers; therefore, they constitute a service to the scholarly community. At the same time, the Frontiers Journal Series operates on a revolutionary invention, the tiered publishing system, initially addressing specific communities of scholars, and gradually climbing up to broader public understanding, thus serving the interests of the lay society, too.

Dedication to Quality

Each Frontiers article is a landmark of the highest quality, thanks to genuinely collaborative interactions between authors and review editors, who include some of the world's best academicians. Research must be certified by peers before entering a stream of knowledge that may eventually reach the public - and shape society; therefore, Frontiers only applies the most rigorous and unbiased reviews.
Frontiers revolutionizes research publishing by freely delivering the most outstanding research, evaluated with no bias from both the academic and social point of view. By applying the most advanced information technologies, Frontiers is catapulting scholarly publishing into a new generation.

What are Frontiers Research Topics?

Frontiers Research Topics are very popular trademarks of the Frontiers Journals Series: they are collections of at least ten articles, all centered on a particular subject. With their unique mix of varied contributions from Original Research to Review Articles, Frontiers Research Topics unify the most influential researchers, the latest key findings and historical advances in a hot research area! Find out more on how to host your own Frontiers Research Topic or contribute to one as an author by contacting the Frontiers Editorial Office: frontiersin.org/about/contact

RISK OF DIETARY HAZARDOUS SUBSTANCES AND IMPACT ON HUMAN MICROBIOTA: POSSIBLE ROLE IN SEVERAL DYSBIOSIS PHENOTYPES

Topic Editors:
Margarita Aguilera, University of Granada, Spain
Mangesh Bhide, University of Veterinary Medicine and Pharmacy in Košice, Slovakia
Els Van Pamel, Fisheries and Food Research (ILVO), Belgium
Eric Houdeau, INRA UMR1331 Toxicologie Alimentaire, France
Bruno Lamas, INRA UMR1331 Toxicologie Alimentaire, France
Ana Rivas, University of Granada, Spain

Citation: Aguilera, M., Bhide, M., Pamel, E. V., Houdeau, E., Lamas, B., Rivas, A., eds. (2021). Risk of Dietary Hazardous Substances and Impact on Human Microbiota: Possible Role in Several Dysbiosis Phenotypes. Lausanne: Frontiers Media SA. doi: 10.3389/978-2-88966-907-3

Table of Contents

frontiers in Microbiology

EDITORIAL
published: 23 April 2021
doi: 10.3389/fmicb.2021.669480

Editorial: Risk of Dietary Hazardous Substances and Impact on Human Microbiota: Possible Role in Several Dysbiosis Phenotypes

Margarita Aguilera[1,2]*, *Bruno Lamas*[3], *Els Van Pamel*[4], *Mangesh Bhide*[5], *Eric Houdeau*[3] and *Ana Rivas*[2]

[1] Department of Microbiology, Faculty of Pharmacy, University of Granada, Granada, Spain, [2] Department of Microbiology, Instituto de Investigación Biosanitaria ibs, Granada, Spain, [3] Research Center in Food Toxicology (Toxalim), INRAE, Toulouse University, ENVT, INP-Purpan, UPS, Toulouse, France, [4] Flanders Research Institute for Agriculture, Fisheries and Food (ILVO), Merelbeke, Belgium, [5] Department of Microbiology and Immunology, Institute of Immunology, University of Veterinary Medicine and Pharmacy, Kosice, Slovakia

OPEN ACCESS

Edited by:
Lorena Ruiz,
Institute of Dairy Products of Asturias (IPLA), Spain

Reviewed by:
Nico Jehmlich,
Helmholtz Centre for Environmental Research (UFZ), Germany
Ren-You Gan,
Institute of Urban Agriculture, Chinese Academy of Agricultural Sciences (CAAS), China

***Correspondence:**
Margarita Aguilera
maguiler@ugr.es

Specialty section:
This article was submitted to Food Microbiology, a section of the journal Frontiers in Microbiology

Received: 18 February 2021
Accepted: 09 March 2021
Published: 23 April 2021

Citation:
Aguilera M, Lamas B, Van Pamel E, Bhide M, Houdeau E and Rivas A (2021) Editorial: Risk of Dietary Hazardous Substances and Impact on Human Microbiota: Possible Role in Several Dysbiosis Phenotypes. Front. Microbiol. 12:669480. doi: 10.3389/fmicb.2021.669480

Keywords: xenobiotics, endocrine disruptors, microbiota, dysbiosis, probiotics

Editorial on the Research Topic

Risk of Dietary Hazardous Substances and Impact on Human Microbiota: Possible Role in Several Dysbiosis Phenotypes

The cumulative dietary exposure to hazardous substances such as endocrine disruptor chemicals (EDC) that are present in common and processed food is continuously increasing (Gálvez-Ontiveros et al., 2021). Prolonged exposure to EDC seems to affect human health by triggering obesity, insulin resistance, metabolic syndrome, and even infertility (Baker et al., 2017). Unfortunately, there is still a lack of knowledge on specific biomarkers necessary to better understand the mechanisms associated to specific EDC-related pathogenesis. The impact of EDC has been traditionally investigated through biomonitoring and epidemiological studies. However, analytical determinations of EDC in biological samples failed to provide consistent results. Thus, a paradigm shift in EDC-related disorders should take into consideration new scientific evidence supporting the fact that EDC may influence human health by modifying the human microbiota, as well as compiling evidence on the existence of microorganism species in the gut that are able to biodegrade such obesogens or contaminants (Gálvez-Ontiveros et al., 2020; López-Moreno et al., 2021). In this sense, relevant studies also support the development of predictive toxicological models that account for the gut-microbiota-immune axis (Lamas et al., 2020). For example, gut dysbiosis and immune system dysfunctions precede obese phenotype development in mice perinatally exposed to bisphenol A (BPA), a common EDC in human food (Malaisé et al., 2017, 2018). Therefore, discovering the association and role of microbiota as a metabolic mediator of food xenobiotics and endocrine pathophysiological outcomes has resulted in building multidisciplinary and integrative hypotheses. This research also provides opportunities to use microbial modulators like probiotics for restoring the dysbiotic taxa in EDC-related disorders (López-Moreno and Aguilera, 2020; López-Moreno et al., 2020). Importantly, EDC food risk assessment in relation to human microbiome variability and health outcomes is still at its very first phase of development, requiring integrative expertise and holistic analyses, i.e., a systemic approach.

The current Research Topic covers a collection of reviews, mini reviews, and original research articles focusing on dietary xenobiotics, human microbiota dysbiosis, and probiotics or prebiotics for modulating the associated pathophysiological phenotypes. In this sense, reviews agreed on the association of health disorders due to the impact of xenobiotics on the occurrence of microbiota dysbiosis.

In their mini review, Barnett and Gibson covered glyphosate's effects on the gut microbiome diversity and concluded that glyphosate residues on food could cause dysbiosis, given that opportunistic pathogens are more resistant to glyphosate compared to commensal bacteria. Moreover, glyphosate could inhibit exclusive pathways of bacteria, like the shikimate pathway. In addition, they postulated that the wheat sensitivity induced by the Western diet rich in high carbohydrates, seemed to be not only due to gluten but also to herbicides used to promote higher crop yields, and as a result of increased industrialized and processed food needs.

In their review, Aguilera et al. extensively analyzed the interactions of steroid hormones and EDC with gut microbiota. The authors innovatively suggest the term "endobolome" for stating gut microbiota genes and pathways involved in EDC metabolization. Microbiota disrupting chemicals (MDC) is the term to group the dietary xenobiotics that alter gut microbial components linked to chronic intestinal and systemic diseases. MDC allow distinguishing the role of contaminants from other microbiota natural modifiers. It is possible to develop specific research on the triad MDC-microbiota-host health axis.

Several original research papers published in this Research Topic focus on gut dysbiosis and pathogens, specifically on the characterisation of molecular pathways involved in the gut dysbiosis and possible modulation strategies. In this sense, the findings reported by Rubio-Gómez et al. suggest that dysbiosis or depletion of gut microbiota by antibiotics facilitated the colonization of the intestinal tract by multidrug-resistant pathogens (Pseudomonas aeruginosa PAO1). Fructooligosaccharides (FOS) and bifidogenic effects selectively reduced bacterial pathogenicity, decreasing growth, motility and biofilm by interfering with different canonical and signaling pathways. Wang et al. focused their study on *Vibrio parahaemolyticus*, which is a food-borne pathogen that can cause gut dysbiosis, disorders, diarrhea, and abdominal pain depending on the colonizer strain. Specific genes (*tdh* and *trh*) were only present in *V. parahaemolyticus* pathogenic strains, which showed strong activity to simulated gastric fluids. The study provided an innovative understanding to unlock the efficient control of pathogenic *V. parahaemolyticus*.

Three other research articles using mice models with induced gut dysbiosis focused on discovering mechanistic aspects after exposure to xenobiotics and obesogens. Li et al. showed that food additives such as polysorbate 80 (P80) exacerbate irradiation-induced gastrointestinal (GI) tract toxicity, microbiota dysbiosis, and tract injury. In summary, their findings demonstrated that P80 is a potential risk factor for cancer patients during radiotherapy and indicated that microbial butyrate might be a therapy to mitigate the co-morbidities.

Lin et al. tested, in high-fat diet (HFD)-induced obese mice, the effects of *Lactobacillus kefirnofaciens* M1 and *Lactobacillus mali* APS1, which are probiotics with, respectively, obesogenic and anti-obesogenic properties. The authors observed that M1/APS1 intervention influenced fat accumulation by regulating adipogenesis and inflammation-related marker expressions. Moreover, particular gut microbiota family taxa (*Christensenellaceae* and *Bacteroidales* S24-7) were negatively correlated with body weight gain through an increase in the esterified carnitine (acylcarnitine), which is essential for lipid intermediary metabolism and for energy expenditure and storage balance.

Liu et al. proved that the heavy metals arsenic (As), cadmium (Cd), and lead (Pb) modify the risk of disease by mediating on gut microbiota dysbiosis. Disease risk of As, Pb, and Cd exposure was more severe in HFD-fed mice compared to normal diet (ND)-fed mice, possibly due to a higher accumulation of heavy metals in the liver and kidneys. Specific increased microbes seemed to play a role in the heavy metal detoxification *via* absorption and faecal excretion. In ND-fed mice, relative abundance of *Bacteroides*, *Lactobacillus*, *Butyricimonas*, and *Dorea* increased after As exposure; *Faecoccus* and *Lactobacillus* increased after Cd exposure; and *Desulfovibrio*, and *Roseburia* increased after Pb exposure, while no difference in these same taxa was observed in HFD-fed mice microbiota. In summary, the enriched microbes that might respond to heavy metals in ND-fed mice did not respond or could not be enriched accordingly in HFD-fed mice.

Ren et al. described evidence that the natural dietary flavonoid, acacetin, attenuates dextran sulphate sodium (DSS)-induced colitis in mice by inhibiting inflammation (macrophages and inflammatory mediators). Acacetin was also able to restore the altered gut diversity microbiota profile caused by DSS reversing the reduction of Firmicutes, and the enrichment of Proteobacteria, Bacteroidetes, and Deferribacteres phyla. Overall, the results suggest that acacetin alleviated weight loss, diarrhea, colon shortening, inflammatory infiltration, and histological injuries.

Finally, xenobiotics in a diet and the environment could also affect other microbiotas encountered at body locations different from the gut. In this direction, Gonzalez et al. discovered temporal changes to the breast milk microbiome of healthy Guatemalan mothers from early to late lactation, according to several maternal factors and exposures. These included a general shift from *Staphylococcus* and *Streptococcus* species in early lactation to Sphingobium and Pseudomonas species in late lactation. Interestingly, species enriched in early lactation included putative commensal bacteria known to colonize the infant oral and intestinal tracts, whereas species enriched in late lactation, such as *Sphingomonas yanoikuyae*, *Pseudomonas putida*, *Stenotrophomonas maltophilia*, *Cloacibacterium normanense*, *Comamonas testosteroni*, *Ottowia beijingensis*, and *Flavobacterium cucumis*, showed common functional traits associated with hazardous substance biodegradation, like steroids and more general polycyclic aromatic hydrocarbon pathways.

In summary, together the articles in this Research Topic make a significant contribution to the evoked dysbiosis of the

microbiome following exposure to EDC, as a step toward a better comprehension of the endocrine-related pathophysiology.

AUTHOR CONTRIBUTIONS

MA: conceptualization and study design. AR: validation. MA, BL, EVP, EH: writing—original draft preparation. All authors: revision. All authors listed have made a substantial, direct and intellectual contribution to the work, and approved it for publication.

FUNDING

Research Topic was developed under the following Frameworks: (1) OBEMIRISK Project-GP/EFSA/ENCO/380 2018/03/G04: Knowledge platform for assessing the risk of Bisphenols on gut microbiota and its role in obesogenic phenotype: looking for biomarkers. (2) FEDER Infrastructure: IE_2019-198 Human Microbiota Reference Laboratory and (3) Europa Innovación: EIN-2019-103082.

REFERENCES

Baker, J., Al-Nakkash, L., and Herbst-Kralovetz, M. (2017). Estrogen–gut microbiome axis: physiological and clinical implications. *Maturitas* 103, 45–53. doi: 10.1016/j.maturitas.2017.06.025

Gálvez-Ontiveros, Y., Moscoso-Ruiz, I., Rodrigo, L., Aguilera, M., Rivas, A., and Zafra-Gómez, A. (2021). Presence of parabens and bisphenols in food commonly consumed in Spain. *Foods* 10:92. doi: 10.3390/foods10010092

Gálvez-Ontiveros, Y., Páez, S., Monteagudo, C., and Rivas, A. (2020). Endocrine disruptors in food: impact on gut microbiota and metabolic diseases. *Nutrients* 12:1158. doi: 10.3390/nu12041158

Lamas, B., Martins-Breyner, N., and Houdeau, E. (2020). Impacts of foodborne inorganic nanoparticles on the gut microbiota-immune axis: potential consequences for host health. *Part Fibre Toxicol.* 17:19. doi: 10.1186/s12989-020-00349-z

López-Moreno, A., and Aguilera, M. (2020). Probiotics dietary supplementation for modulating endocrine and fertility microbiota dysbiosis. *Nutrients* 12:757. doi: 10.3390/nu12030757

López-Moreno, A., Suárez, A., Avanzi, C., Monteoliva-Sánchez, M., and Aguilera, M. (2020). Probiotic strains and intervention total doses for modulating obesity-related microbiota dysbiosis: a systematic review and meta-analysis. *Nutrients* 12:1921. doi: 10.3390/nu12071921

López-Moreno, A., Torres-Sánchez, A., Acuña, I., Suárez, A., and Aguilera, M. (2021). Representative Bacillus sp. Am1 from gut microbiota harbor versatile molecular pathways for bisphenol a biodegradation. *Int J Mol Sci.* 22:2425 doi: 10.3390/ijms22052425

Malaisé, Y., Menard, S., Cartier, C., Gaultier, E., Lasserre, F., Lencina, C., et al. (2017). Gut dysbiosis and impairment of immune system homeostasis in perinatally-exposed mice to Bisphenol A precede obese phenotype development. *Sci. Rep.* 7:14472. doi: 10.1038/s41598-017-15196-w

Malaisé, Y., Ménard, S., Cartier, C., Lencina, C., Sommer, C., Gaultier, E., et al. (2018). Consequences of Bisphenol A perinatal exposure on immune responses and gut barrier function in mice. *Arch. Toxicol.* 92, 347–358. doi: 10.1007/s00204-017-2038-2

Conflict of Interest: The authors declare that the research was conducted in the absence of any commercial or financial relationships that could be construed as a potential conflict of interest.

Copyright © 2021 Aguilera, Lamas, Van Pamel, Bhide, Houdeau and Rivas. This is an open-access article distributed under the terms of the Creative Commons Attribution License (CC BY). The use, distribution or reproduction in other forums is permitted, provided the original author(s) and the copyright owner(s) are credited and that the original publication in this journal is cited, in accordance with accepted academic practice. No use, distribution or reproduction is permitted which does not comply with these terms.

frontiers in Microbiology

ORIGINAL RESEARCH
published: 20 February 2020
doi: 10.3389/fmicb.2020.00202

Full Transcriptomic Response of *Pseudomonas aeruginosa* to an Inulin-Derived Fructooligosaccharide

José Manuel Rubio-Gómez[1†], Carlos Molina Santiago[2†], Zulema Udaondo[3†], Mireia Tena Garitaonaindia[4], Tino Krell[5], Juan-Luis Ramos[5] and Abdelali Daddaoua[4]*

[1] Centro de Investigación Biomédica en Red de Enfermedades Hepáticas y Digestivas, Department of Pharmacology, School of Pharmacy, University of Granada, Granada, Spain, [2] Department of Microbiology, Instituto de Hortofruticultura Subtropical y Mediterránea "La Mayora", University of Málaga, Málaga, Spain, [3] Department of Biomedical Informatics, University of Arkansas for Medical Sciences, Little Rock, AR, United States, [4] Department of Biochemistry and Molecular Biology II, School of Pharmacy, University of Granada, Granada, Spain, [5] Department of Environmental Protection, Estación Experimental del Zaidín, Consejo Superior de Investigaciones Científicas, Granada, Spain

OPEN ACCESS

Edited by:
Eric Houdeau,
INRA UMR1331 Toxicologie Alimentaire, France

Reviewed by:
Jesús Muñoz-Rojas,
Meritorious Autonomous University of Puebla, Mexico
Mariam Sahrawy Barragan,
Spanish National Research Council (CSIC), Spain

***Correspondence:**
Abdelali Daddaoua
daddaoua@ugr.es

[†] These authors have contributed equally to this work

Specialty section:
This article was submitted to Microbial Symbioses, a section of the journal Frontiers in Microbiology

Received: 26 November 2019
Accepted: 28 January 2020
Published: 20 February 2020

Citation:
Rubio-Gómez JM, Santiago CM, Udaondo Z, Garitaonaindia MT, Krell T, Ramos J-L and Daddaoua A (2020) Full Transcriptomic Response of Pseudomonas aeruginosa to an Inulin-Derived Fructooligosaccharide. Front. Microbiol. 11:202. doi: 10.3389/fmicb.2020.00202

Pseudomonas aeruginosa is an ubiquitous gram-negative opportunistic human pathogen which is not considered part of the human commensal gut microbiota. However, depletion of the intestinal microbiota (Dysbiosis) following antibiotic treatment facilitates the colonization of the intestinal tract by Multidrug-Resistant *P. aeruginosa*. One possible strategy is based on the use of functional foods with prebiotic activity. The bifidogenic effect of the prebiotic inulin and its hydrolyzed form (fructooligosaccharide: FOS) is well established since they promote the growth of specific beneficial (probiotic) gut bacteria such as bifidobacteria. Previous studies of the opportunistic nosocomial pathogen *Pseudomonas aeruginosa* PAO1 have shown that inulin and to a greater extent FOS reduce growth and biofilm formation, which was found to be due to a decrease in motility and exotoxin secretion. However, the transcriptional basis for these phenotypic alterations remains unclear. To address this question we conducted RNA-sequence analysis. Changes in the transcript level induced by inulin and FOS were similar, but a set of transcript levels were increased in response to inulin and reduced in the presence of FOS. In the presence of inulin or FOS, 260 and 217 transcript levels, respectively, were altered compared to the control to which no polysaccharide was added. Importantly, changes in transcript levels of 57 and 83 genes were found to be specific for either inulin or FOS, respectively, indicating that both compounds trigger different changes. Gene pathway analyses of differentially expressed genes (DEG) revealed a specific FOS-mediated reduction in transcript levels of genes that participate in several canonical pathways involved in metabolism and growth, motility, biofilm formation, β-lactamase resistance, and in the modulation of type III and VI secretion systems; results that have been partially verified by real time quantitative PCR measurements. Moreover, we have identified a genomic island formed by a

cluster of 15 genes, encoding uncharacterized proteins, which were repressed in the presence of FOS. The analysis of isogenic mutants has shown that genes of this genomic island encode proteins involved in growth, biofilm formation and motility. These results indicate that FOS selectively modulates bacterial pathogenicity by interfering with different signaling pathways.

Keywords: RNA sequencing, rt-qPCR, adhesion, developmental process, molecular transducer, pathogenicity

INTRODUCTION

The human pathogen *Pseudomonas aeruginosa* causes a wide array of life-threatening acute and chronic infections, particularly in immunocompromised, cancer, burn wound, and cystic fibrosis patients (Juhas, 2015). This bacterium is moreover one of the leading causes of nosocomial infections affecting hospitalized patients (Buhl et al., 2015) and mortality associated with hospital-acquired *P. aeruginosa* infectious like ventilator-associated pneumonia or bacteremia is above 35% (Lynch et al., 2017).

Moreover, under continuous antibiotic treatment the intestinal microbiota integrity is compromised and bears depletion of the intestinal microbiota (Dysbiosis), hence, physiological colonization resistance subsequently facilitates the establishment of the *Pseudomonas aeruginosa* in the intestinal ecosystem which might be considered an important internal source for *P. aeruginosa* infection (Ohara and Itoh, 2003; Von Klitzing et al., 2017). It is important to note that pathological alterations of the intestinal microbiota (dysbiosis) is related with continuous antibiotic treatment, obesity, diabetes and fatty liver, and of course alterations of the intestinal barrier function (IBF) as in inflammatory bowel disease and metabolic syndrome (Cano et al., 2013; Miura and Ohnishi, 2014).

The severity and permanence of these infections are related to the ability of *P. aeruginosa* to resist the effect of antibiotics through the formation of biofilms (Mah et al., 2003; Hoiby et al., 2010; Taylor et al., 2014). Important research efforts have been made to study the molecular mechanisms related to the formation maturation and subsequent dispersion of the biofilm (Stoodley et al., 2002; Flemming et al., 2007). A number of surface proteins and appendages, including flagella and type IV pili, were found to be associated with biofilm formation (Klausen et al., 2003; Anyan et al., 2014). Furthermore, this species is characterized by its ability to synthesize the virulent factors exotoxin A and pyocyanin (Ortiz-Castro et al., 2014) that block protein synthesis consequently leading to cell death (Gaines et al., 2007).

Treatment of *P. aeruginosa* infections can be particularly challenging because this bacterium is intrinsically resistant to multiple antibiotics and can easily acquire new resistances (Breidenstein et al., 2011). In fact, over the past three decades, antibiotic resistance among *P. aeruginosa* has escalated globally, *via* the global dissemination of several multidrug-resistant epidemic clones (Miyoshi-Akiyama et al., 2017). *Pseudomonas aeruginosa* infections thus represent a severe threat to human health worldwide and the World Health Organization has declared this bacterium the second priority pathogen for research and development of new strategies to fight it (WHO, 2017).

Besides conventional treatments, one possible strategy is based on the use of functional foods with prebiotic activity which are non-digestible foods (mostly oligosaccharides) that selectively stimulate the growth of a limited number of host-friendly colonic bacteria (Froebel et al., 2019). Thus, from a chemical standpoint, resistance to human digestive enzymes and low absorption are key for these compounds to reach the distal parts of the gut, where they can be fermented by the microbiota, which in turn is selectively modified in the process. These additional actions of prebiotics tend to enhance the capacity of the mucosa to contain luminal microorganisms and their components, i.e., intestinal barrier function (IBF). Normally, passage of microorganisms and/or their components such as Lipopolysaccharides (LPS) to the mucosa and from there to the bloodstream (translocation) is minimal, and the immune system develops tolerance to the microbiota, without inflammation. Conversely, when IBF is compromised translocation ensues, depending on the nature of the dysfunction and the physiological/pathological context. Therefore, inflammation of the intestine is considered to stem from augmented translocation, which engages the adaptive immune system, ultimately resulting in uncontrolled inflammation. Thus, reinforcing IBF may be protective and is viewed as therapeutic in this context (Natividad and Verdu, 2012; Duseja and Chawla, 2014).

A significant number of natural compounds have been found to inhibit bacterial growth, although their mechanisms of action frequently remain unclear (Amer et al., 2010). Fructooligosaccharides (FOS) are short-chain oligosaccharides that are generated by hydrolysis of the polysaccharide inulin, which is composed of two to 60 fructose monomers. Inulin is found in different nutrients such as wheat, onion, garlic and banana (Lattimer and Haub, 2010) and is the most common used fiber in prebiotics that, when used in combination with other probiotics, is able to promote the growth of specific beneficial gut bacteria such as bifidobacteria (Gibson et al., 1995; Bosscher et al., 2006).

TABLE 1 | Statistics of RNA-seq data.

Sample	Raw reads	Mapped reads	Not mapped reads	Percent mapped
MM9-citrate	7472385	6322981	1149404	84.6%
Inulin	5368865	4575351	793514	85.2%
FOS	6598306	5580131	1018175	84.6%

Shown are means from two replicates.

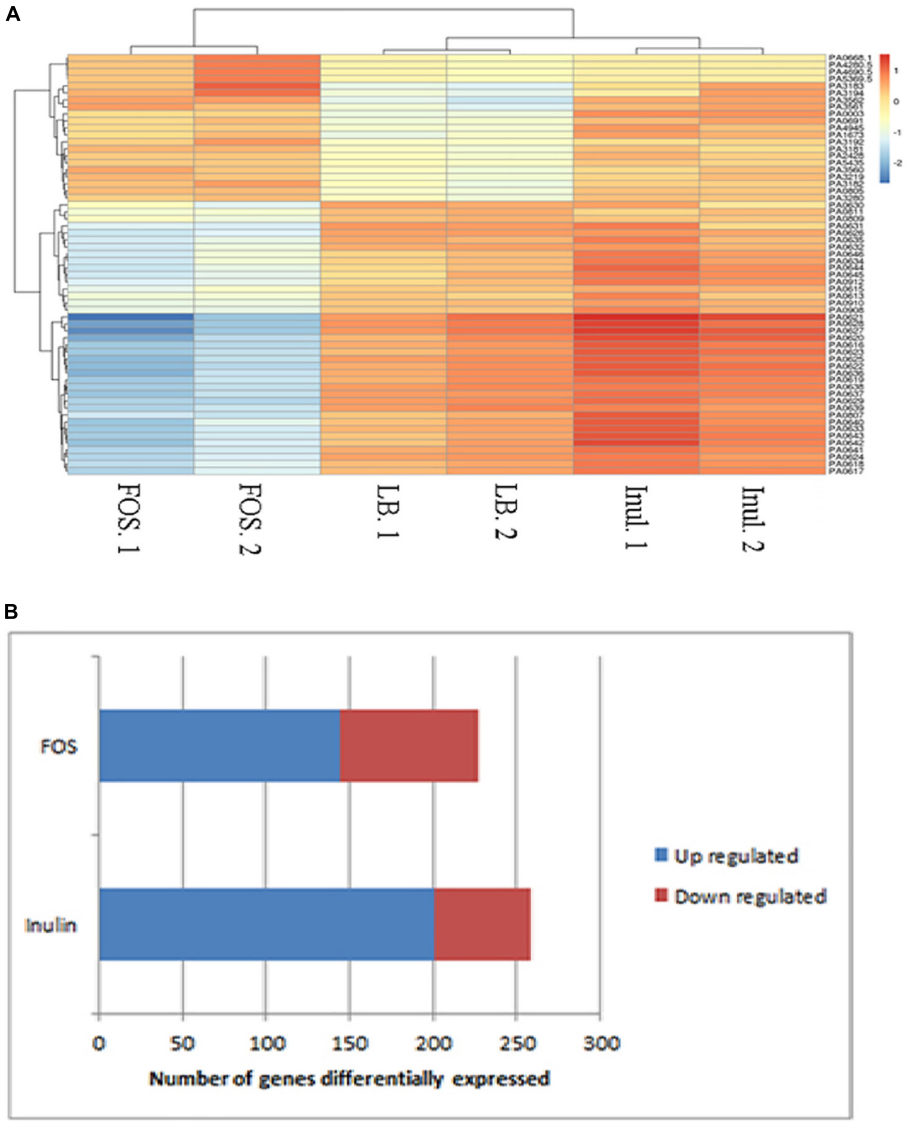

FIGURE 1 | Heat-map **(A)** analysis and hierarchical cluster **(B)** of the genes that are differentially induced and repressed in the presence of FOS or inulin as compared to the untreated control (M9 minimal medium). Blue: genes with increased expression; red: genes with reduced expression.

A number of studies illustrate that FOS and inulin exert a number of different effects on humans and animals. For example, most oraly delivered plant substrate supplements that prevent gastrointestinal infections such as prebiotin^{TM} and symbioram^{TM} contain inulin and FOS, indicating that these compounds are also able to reduce bacterial infection. Moreover, oligosaccharids and in particular inulin and FOS were found to have beneficial effects on intestinal immunity and intestinal barrier function (IBF) (Capitán-Cañadas et al., 2013, 2016). Another study has shown that oligosaccharides from goats milk as well as galactooligosaccharides, modulate cytokine production by intestinal epithelial cells and monocytes *via* a mechanism involving Toll-like receptor 4 (TLR4) (Capitán-Cañadas et al., 2013). TLRs are located on the cell membrane and in endosomes, where they recognize components of cell membranes (TLR2/6, TLR2/TLR4), nucleic acids (TLR3, 7, 8, and 9) and flagellin (TLR5). TLR4 is one of the non-pathogen recognition receptors (PRRs), which are key elements in the communication between the host and the microbiota (Sánchez de Medina et al., 2013). However, further clinical oral applications will require studies on the potential effects of these natural substrates on the human body, which corresponds to the research need addressed in this article.

In addition to the bacterial growth promoting role of inulin and FOS, we reported that FOS inhibited bacterial growth and biofilm formation of *P. aeruginosa* PAO1 (Ortega-González et al., 2014). Additionally, both compounds caused opposing effects on bacterial motility. While FOS inhibited motility, an increased motility was observed in the presence of inulin. Moreover, in co-cultures with eukaryotic cells (macrophages) FOS, and to a

lesser extent inulin, reduced the secretion of the inflammatory cytokines IL-6, IL-10, and TNF-α. We were also able to show that the reduction in cytokine secretion is due to a FOS-mediated modulation of the NF-κβ signal transduction pathway (Ortega-González et al., 2014). To gain insight into the detailed molecular processes triggered by FOS and inulin, we report here results from RNA-seq studies.

MATERIALS AND METHODS

Materials

Inulin and FOS were purchased from BENEO-Orafti (Tienen Belgium). Stock solutions at 200 g/L in modified M9 minimal medium were sterilized using 0.22 μm cut-off filters and aliquots were stored at −20°C.

Culture and Growth Conditions

Pseudomonas aeruginosa PAO1 was grown overnight at 37°C in minimum M9 medium. The resulting cultures were then used to inoculate 50 ml of minimum M9 medium supplemented by 5 mM of citrate (MM9) (in 250 ml Erlenmeyer flasks) to an initial OD_{600} of 0.01 and incubated with shaking at 200 rpm at 37°C. When cultures reached OD_{600} = 0.05, FOS or inulin were added to a final concentration of 20 mg/ml and cultures were harvested for analysis 1 h later.

RNA Extraction, Library Preparation and RNA Sequencing

Total RNA was extracted with the TRI reagent (Ambion) using the manufacturer's instructions. The RNase inhibitor RiboLock (Fermentas) was added to the samples and DNA was removed by treatment with DNase I (Fermentas). The integrity of the RNA samples was assessed with an Agilent 2100 Bioanalyzer (Agilent Technologies). Subsequently, the 23S, 16S, and 5S rRNAs were removed by subtractive hybridization using the MICROBExpress kit (Ambion) following the protocol reported by Gómez-Lozano et al. (2014). Removal of the rRNA was confirmed by an analysis with an Agilent 2100 Bioanalyzer (Agilent Technologies). Sequencing libraries were prepared using the TruSeq Stranded mRNA Sample Preparation kit (Illumina). After each step, the samples were validated using an Agilent 2100 Bioanalyzer (Agilent Technologies) and the final RNA concentration was measured using a Qubit 2.0 Fluorometer (Invitrogen). The libraries were sequenced using the Illumina HiSeq2000 platform with a paired-end protocol and read lengths of 100 nucleotides.

RNA-seq Analysis

The quality of sequenced reads was assessed using FastQC software, version 0.11.5 (Andrews and Fast, 2010). Single-end reads were aligned to the reference genome of *P. aeruginosa* PAO1 (GenBank accession number: AE004091.2) using SAMtools v 0.1.19 (Li et al., 2009). BAM files from SAM tools were used as input for the *feature counts* function (Liao et al., 2014) from the Rsubread package (Liao et al., 2013) of Bioconductor version 3.5 to generate a matrix of annotated genes with their corresponding raw counts. An average of 84.5% reads were successfully mapped to the reference genome. The count data were then analyzed to look for differential gene expression levels and statistical significance using DEseq2 (Love et al., 2014; Kimberly and Stephen, 2015).

The threshold to define differences in transcript levels was a statistical Log2 fold change. Genes were considered significantly differentially expressed when *p*-values were below 0.05.

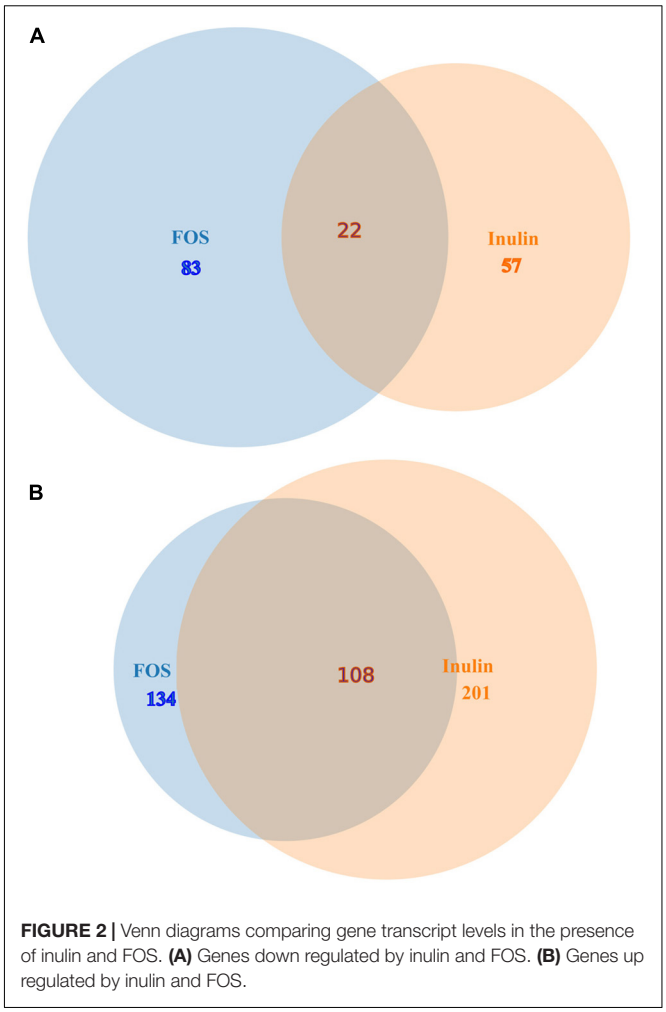

FIGURE 2 | Venn diagrams comparing gene transcript levels in the presence of inulin and FOS. **(A)** Genes down regulated by inulin and FOS. **(B)** Genes up regulated by inulin and FOS.

RNA-Sequencing Data Registration Number

The sequence reads have been deposited in the GEO database under accession N°: GSE124468. The following secure token has been created to allow for the review of record GSE124468: glshocwuzvkprop.

Analysis of Gene Expression by Quantitative Real Time PCR

Quantitative real time-PCR experiments were performed to validate RNA-seq results. Total RNA was obtained by the TRI reagent® /BCP method (Ambion). One μg of RNA

TABLE 2 | Transcript levels that were reduced in the presence of both, inulin and FOS.

Gene Id	Gene	Protein Function	Inulin		FOS	
			log2 fold change	*p*-value (10^{-6})	log2 fold change	*p*-value (10^{-6})
PA0090	*clpV1*	Type VI secretion ATPase	−0.9	0.000	−0.8	0.000
PA0296	*spuI*	Glutamylpolyamine synthetase	−0.6	0.008	−0.6	0.007
PA0795	*prpC*	Citrate synthase 2	−1.1	0.001	−0.9	0.002
PA1069	*nd*	Hypothetical protein	−0.7	0.000	−0.5	0.003
PA1171	*sltB2*	Soluble lytic transglycolase	−0.7	0.010	−0.6	0.008
PA1183	*dctA*	C4-dicarboxylate transport protein	−1.5	0.000	−1.2	0.000
PA1342	*aatj*	Probable binding protein component of ABC transporter	−1.0	0.000	−1.1	0.000
PA1585	*sucA*	2-oxoglutarate dehydrogenase	−0.5	0.008	−0.6	0.001
PA1588	*sucC*	Succinyl-CoA synthetase	−0.7	0.000	−0.6	0.002
PA1592	*nd*	Hypothetical protein	−0.9	0.000	−0.8	0.001
PA1787	*acnB*	Aconitate hydratase B	−0.5	0.003	−0.5	0.003
PA2007	*maiA*	Maleylacetatoacetate isomerase	−1.1	0.000	−0.7	0.003
PA2008	*fahA*	Fumarylacetoacetase	−1.1	0.000	−1.1	0.000
PA2040	*pauA4*	Glutamylpolyamine synthetase	−0.9	0.000	−0.7	0.002
PA2247	*bkdA1*	2-oxoisovalerate dehydrogenase	−0.9	0.001	−0.7	0.004
PA4055	*ribC*	Riboflavin synthase	−0.7	0.009	−0.7	0.005
PA4240	*rpsK*	30S ribosomal protein S11	−0.7	0.003	−1.0	0.000
PA4366	*sodB*	Superoxide dismutase	−0.7	0.000	−0.7	0.000
PA4370	*icmP*	Insulin-cleaving metalloproteinase outer membrane protein	−0.8	0.002	−0.9	0.000
PA4578	*nd*	Hypothetical protein	−0.9	0.000	−0.8	0.000
PA4824	*nd*	Hypothetical protein	−0.9	0.000	−0.8	0.000
PA4825	*mgtA*	Mg(2 +) transport ATPase P-type 2	−0.9	0.000	−0.8	0.000

The above table shows the list of the significant down regulated genes and control with a log2 fold change cut off ≥ 0.5 by taking significant p-value < 0.05.

was retrotranscribed following the protocol provided in the manufacturer protocol (iScript BioRad, Alcobendas, Spain) and DNA sequences were amplified with a MX3005P real time PCR instrument (Stratagene) using the primers listed in **Supplementary Table S3**. The genes of interest were amplified by PCR using the Go Taq@qPCR Master Mix (Promega, Madison, WI, United States) as well as 1 μl of the cDNA template and the primers listed in **Supplementary Table S3**. Forty PCR cycles were conducted using an annealing temperature of 61°C. The cycle threshold values were normalized to that of the reference transcript, 16S RNA, and data were normalized to the control.

Generation of Mutants in Genes of the Genomic Island PA0643, PA0644, and PA0646

To generate the PA0643:Gm, PA0644:Gm, and PA0646:Gm mutants 656, 241, and 636 pb DNA fragments, respectively, covering the central part of the genes were amplified by PCR from *P. aeruginosa* PA01 genomic DNA. The resulting products were cloned into plasmid pMBL to yield plasmids pMBL:PA0643, pMBL:PA0644, and pMBL:PA0646. Subsequently, the resulting plasmids were digested with *Bam*HI, which liberated the PA0643, PA0644, and PA0646 fragment. The plasmid pCHESI was also digested with *Bam*HI, to liberate the gentamicin resistance gene (Gm) in order to ligate it with the three DNA fragments. The resulting chimeric DNA was cloned into pMBL digested with *Bam*HI, to yield pMBL:PA0643ΩGm, pMBL:PA0644ΩGm and pMBL:PA0646ΩGm. The resulting plasmids were electroporated into *P. aeruginosa* PA01 for homologous double recombination. Mutant strains were selected on Gm plates and the correctness of the mutation was verified by Southern blotting (Sambrook et al., 1989; Molina-Fuentes et al., 2015).

Semi-Quantitative Determination of Biofilm Formation

Semi-quantitative determination of biofilm formation were performed as previously described (Christensen et al., 1985). *P. aeruginosa* PA0643, PA0644, and PA0646 mutants were tested in the biofilm-forming capacities in Minimum medium supplemented with 5 mM citrate. The determination of biofilm production was performed after 2, 4, and 6 h of growth by dissolving crystal violet from the biofilm with an ethanol-acetone mixture (70:30) and the absorbance measure at 590 nm.

Motility Assays

Assays were carried out to determine the effect of the PA0643, PA0644, and PA0646 deletion gene on swimming, twitching and swarming. For swimming assays, bacteria were placed with the help of a sterile tooth-pick at the center of plates containing a 5 mm layer of LB medium with 0.3% (w/v) Bacto agar, 0.2% casamino acids (w/v), and 30 mM glucose. Plates were incubated at 37°C for 24 h and the radial diffusion of bacteria, due to swimming, was inspected. To monitor twitching motility, bacteria were placed with a toothpick into a 2 mm thick layer containing 1.5% (w/v) Bacto agar, 0.2% (w/v) casamino acids,

TABLE 3 | Transcript levels that were increased in the presence of both, inulin and FOS.

Gene Id	Gene	Protein Function	Inulin		FOS	
			Log2 fold change	*p*-value (10^{-6})	Log2 fold change	*p*-value (10^{-6})
PA0003	*recF*	DNA replication and repair protein	1.8	0.000	1.2	0.000
PA0019	*def*	Peptide deformylase	1.0	0.000	0.8	0.000
PA0026	*plcB*	Phospholipase C	0.7	0.005	0.6	0.007
PA0408	*pilG*	Twitching motility protein	0.8	0.000	0.8	0.000
PA0576	*rpoD*	RNA polymerase sigma factor	0.6	0.000	0.7	0.000
PA0577	*dnaG*	DNA primase	0.6	0.002	0.5	0.003
PA0668	*tyrZ*	Tyrosyl-tRNA synthetase 2	0.9	0.000	0.7	0.000
PA0691	*phdA*	Prevent-host-death protein A	1.6	0.000	1.3	0.000
PA0692	*pdtB*	Phosphate depletion regulated TPS partner B	1.2	0.000	1.1	0.000
PA0693	*exbB2*	Transport protein	1.1	0.000	1.1	0.000
PA0730		3-hydroxyacyl-CoA-acyl carrier protein transferase.	0.8	0.000	0.6	0.004
PA0762	*algU*	RNA polymerase sigma factor	0.6	0.001	0.6	0.000
PA0768	*lepB*	Signal peptidase I	0.7	0.002	0.6	0.004
PA0782	*PutA*	Proline dehydrogenase	0.6	0.002	0.5	0.006
PA0805		Uncharacterized protein	1.2	0.000	1.2	0.000
PA0826		Uncharacterized protein	0.8	0.000	0.7	0.000
PA0842		Probable glycosyl transferase	0.6	0.007	0.6	0.005
PA0896	*aruF*	Arginine *N*-succinyltransferase	0.6	0.001	0.5	0.001
PA0979		Uncharacterized protein	1.2	0.000	1.0	0.000
PA1077	*flgB*	Flagellar basal body rod protein FlgB	0.6	0.007	0.6	0.004
PA1081	*flgF*	Flagellar basal-body rod protein FlgF	0.9	0.000	0.7	0.000
PA1084	*flgI*	Flagellar P-ring protein	0.6	0.000	0.5	0.002
PA1327		Serine protease	0.9	0.000	0.8	0.000
PA1382	*xqhB*	Probable type II secretion system protein	0.6	0.003	0.6	0.004
PA1414		Uncharacterized protein	1.9	0.001	1.7	0.004
PA1606		Uncharacterized protein	0.9	0.000	0.7	0.000
PA1608		Probable chemotaxis transducer	1.1	0.000	0.8	0.000
PA1610	*fabA*	Beta-hydroxydecanoyl-ACP dehydrase	0.8	0.000	0.8	0.000
PA1673		Uncharacterized protein	1.7	0.000	1.3	0.000
PA1796	*folD*	Cyclohydrolase	0.6	0.002	0.7	0.001
PA2022		UDP-glucose 6-dehydrogenase	1.0	0.000	0.9	0.000
PA2428		Uncharacterized protein	1.1	0.000	1.0	0.000
PA2548		Uncharacterized protein	0.8	0.000	0.9	0.000
PA2667	*mvaU*	Biosynthetic process	0.5	0.012	0.6	0.001
PA2738	*himA*	Integration host factor subunit alpha	0.7	0.000	0.8	0.000
PA2882		Probable two-component sensor	0.8	0.001	1.0	0.000
PA2971	*yceD*	Uncharacterized protein	1.0	0.000	0.6	0.003
PA3019	*uup*	Probable ATP-binding component of ABC transporter	0.8	0.000	0.6	0.002
PA3116		Probable aspartate-semialdehyde dehydrogenase	0.6	0.003	0.5	0.008
PA3147	*wbpJ*	Probable glycosyl transferase	0.7	0.001	0.7	0.000
PA3181	*edaA*	2-dehydro-3-deoxy-phosphogluconate aldolase	1.1	0.000	1.4	0.000
PA3183	*zwf*	Glucose-6-phosphate 1-dehydrogenase	1.7	0.000	2.0	0.000
PA3193	*glk*	Glucokinase	0.6	0.004	0.7	0.002
PA3194	*edd*	Phosphogluconate dehydratase	1.5	0.000	1.9	0.000
PA3195	*gapA*	Glyceraldehyde-3-phosphate dehydrogenase	1.0	0.001	1.1	0.000
PA3219		Uncharacterized protein	1.2	0.000	1.3	0.000
PA3280	*oprO*	Pyrophosphate-specific outer membrane porin	1.1	0.000	1.1	0.000
PA3296	*phoA*	Alkaline phosphatase	0.6	0.005	0.6	0.007
PA3305		Uncharacterized protein	2.3	0.001	1.9	0.004
PA3351	*flgM*	Two-component system	0.6	0.009	0.7	0.000
PA3382	*phnE*	Phosphonate transport protein	0.6	0.004	0.7	0.001
PA3383	*phnD*	Binding protein component of ABC phosphonate transporter	0.7	0.000	0.6	0.001

(Continued)

TABLE 3 | Continued

Gene Id	Gene	Protein Function	Inulin		FOS	
			Log2 fold change	*p*-value (10^{-6})	Log2 fold change	*p*-value (10^{-6})
PA3384	*phnC*	Phosphonates import ATP-binding protein	0.9	0.000	0.9	0.000
PA3496	*nd*	Uncharacterized protein	0.5	0.002	0.5	0.007
PA3560	*fruA*	Phosphotransferase system transporter	1.1	0.000	1.3	0.000
PA3561	*fruK*	1-phosphofructokinase	1.8	0.000	1.8	0.000
PA3562	*fruI*	Phosphotransferase system transporter enzyme I	2.0	0.000	2.0	0.000
PA3623	*nd*	Uncharacterized protein	0.7	0.001	0.7	0.004
PA3744	*rimM*	16S rRNA processing protein	0.8	0.000	0.6	0.004
PA3746	*ffh*	Signal recognition particle protein	0.6	0.002	0.5	0.004
PA3903	*prfC*	Peptide chain release factor 3	0.9	0.000	0.7	0.001
PA3990		Uncharacterized protein	1.3	0.000	0.9	0.000
PA4255	*rpmC*	50S ribosomal protein L29	0.9	0.000	0.8	0.000
PA4264	*rpsJ*	30S ribosomal protein S10	0.7	0.001	0.6	0.004
PA4270	*rpoB*	DNA-directed RNA polymerase beta chain	0.4	0.009	0.5	0.003
PA4280	*birA*	Regulation of transcription	0.7	0.000	0.7	0.000
PA4378	*lnaA*	Protein of response to stimulus	1.0	0.000	0.6	0.000
PA4418	*ftsI*	Peptidoglycan D.D-transpeptidase	1.1	0.000	0.9	0.000
PA4420	*yabC*	Uncharacterized protein	0.5	0.009	1.0	0.000
PA4421	*yabC*	Uncharacterized protein	1.2	0.000	1.1	0.000
PA4432	*rpsI*	30S ribosomal protein S9	0.7	0.012	0.8	0.000
PA4451	*yrbA*	Uncharacterized protein	0.7	0.000	0.9	0.000
PA4462	*rpoN*	RNA polymerase sigma-54 factor	0.9	0.000	0.6	0.000
PA4520		Probable chemotaxis transducer	0.4	0.009	0.5	0.003
PA4541	*lepA*	Large extracellular protease	0.7	0.000	0.6	0.000
PA4602	*glyA3*	Serine hydroxymethyltransferase	1.0	0.000	0.9	0.000
PA4690		Uncharacterized protein	0.5	0.009	0.6	0.005
PA4723	*dksA*	Suppressor protein	1.0	0.000	0.9	0.000
PA4741	*rpsO*	30S ribosomal protein S15	0.6	0.001	0.9	0.000
PA4747	*secG*	Secretion protein	0.6	0.003	0.7	0.001
PA4844	*ctpL*	Methyl-accepting chemotaxis protein	0.7	0.001	0.6	0.002
PA4853	*fis*	Putative Fis-like DNA-binding protein	0.7	0.006	1.0	0.000
PA4945	*miaA*	Delta 2-isopentenylpyrophosphate	0.8	0.000	0.6	0.004
PA4960	*serB*	Probable phosphoserine phosphatase	0.9	0.000	0.7	0.000
PA4961		Uncharacterized protein	0.7	0.000	0.7	0.000
PA4963		Uncharacterized protein	0.8	0.001	0.7	0.002
PA5013	*ilvE*	Branched-chain-amino-acid transferase	0.7	0.001	0.8	0.000
PA5015	*aceE*	Pyruvate dehydrogenase	0.7	0.001	0.6	0.005
PA5042	*pilO*	Type 4 fimbrial biogenesis protein	1.0	0.000	0.9	0.000
PA5045	*ponA*	Penicillin-binding protein 1A	1.3	0.000	1.0	0.000
PA5058	*phaC2*	Poly(3-hydroxyalkanoic acid) synthase 2	0.8	0.000	1.0	0.000
PA5066	*hisI*	Phosphoribosyl-AMP cyclohydrolase	0.6	0.000	0.5	0.005
PA5152		Probable ATP-binding component of ABC transporter	0.6	0.001	0.6	0.001
PA5170	*arcD*	Arginine/ornithine antiporter	0.7	0.000	0.6	0.000
PA5208		Uncharacterized protein	0.5	0.004	0.4	0.008
PA5235	*glpT*	Glycerol-3-phosphate transporter	1.0	0.000	0.9	0.000
PA5285	*sutA*	Uncharacterized protein	0.6	0.003	0.6	0.002
PA5286	*yjbQ*	Uncharacterized protein	0.7	0.002	0.7	0.003
PA5301	*pauR*	Polyamine catabolic process	0.7	0.002	0.6	0.002
PA5315	*rpmG*	50S ribosomal protein L33	0.6	0.002	0.6	0.001
PA5332	*crc*	Catabolite repression control protein	1.1	0.000	0.8	0.004
PA5348	*nd*	Probable DNA-binding protein	0.6	0.010	0.7	0.005
PA5367	*pstA*	Phosphate ABC transporter	0.9	0.005	1.2	0.000
PA5369	*pstS*	Phosphate ABC transporter	0.8	0.000	0.5	0.006
PA5435	*oadA*	Probable transcarboxylase activity	0.6	0.002	0.9	0.000

The above table shows the list of the significant up regulated genes and control with a log2 fold change cut off $\geq$ *0.5 by taking significant p-value* $<$ *0.05.*

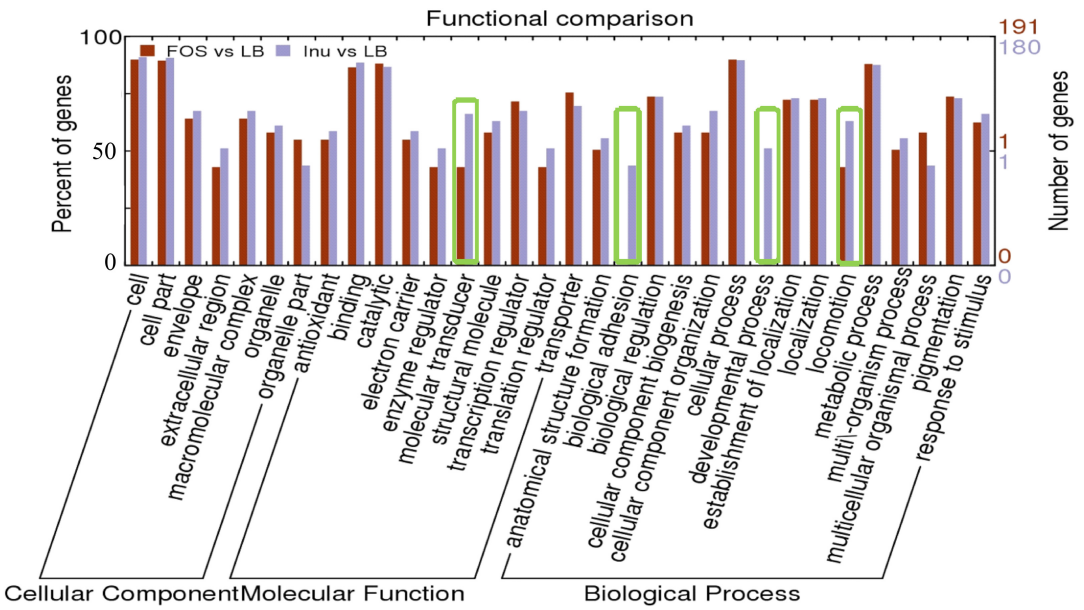

FIGURE 3 | Functional comparison of differentially expressed genes in the presence of FOS and inulin as compared to the control. Functions are organized into three groups: Cellular components, Molecular Function, and Biological Process. The functional groups with the main differences between FOS and inulin are "Molecular transducer," "Biological adhesion" "Developmental process" and "locomotion system."

and 30 mM glucose. After incubation at 37°C for 24 h, the expansion of bacteria on the plate was observed. For swarming assays, 5 μl of an overnight culture of bacteria were placed in the center of swarm plates, which are made of 0.5% (w/v) Bacto agar supplemented with 0.2% (w/v) casamino acids and 30 mM glucose. Plates were incubated at 37°C for 24 h, followed by an inspection of the surface movement of the bacteria. All motility assays were performed in triplicate.

Statistical Analysis

All results are expressed as means from three cultures with the corresponding standard deviations. Data were analyzed for statistical significance using the one-way ANOVA analysis and *a posteriori* least significance test. All analyses were carried out with the SigmaStat 2.03 program (Jandel Corporation, San Rafael, CA, United States). Fitting of dose-response curves was done using Origin 7.0 (OriginLab Corporation, Northampton, MA, United States). Differences were considered significant at $p < 0.05$.

RESULTS

FOS and Inulin Induce Differential Changes in *Pseudomonas aeruginosa* Transcript Levels

To understand the cellular response of *P. aeruginosa* PAO1 to FOS and inulin treatment, we conducted RNA-seq studies. Transcriptomic changes were determined in duplicate cultures grown in the absence and in the presence of either FOS or inulin at final concentrations of 20 mg/ml. Between 5,300,000 and up to 7,500,000 reads were obtained for inuline and FOS respectively, of which approximately 85% could be assigned to the 6,322 coding regions of the *P. aeruginosa* PAO1 reference genome (**Table 1**).

The heat map shown in **Figure 1A** illustrates genes with the most important alterations in transcript levels in the presence of FOS/inulin as compared to the control. For both compounds the number of genes with increased transcript levels were superior to those with decreased levels (see **Figure 1B**). FOS and inulin induced changes in the transcript level of 217 and 258 genes respectively, compared to the control to which no polysaccharide was added (**Figure 2**). Importantly, down changes in transcript levels of 57 and 83 genes were found to be specific for inulin or FOS, respectively (**Figure 2A**). Moreover, 201 and 134 genes showed an increase in transcript levels by inulin and FOS, respectively (**Figure 2B**) indicating that both compounds trigger different changes.

Supplementary Tables S1 and **S2** show the list of genes for which the expression level significantly increased or decreased in the presence of 20 mg/ml of inulin (**Supplementary Table S1**) and FOS (**Supplementary Table S2**). Analysis of the expression pattern showed that only 22 genes had decreased levels in the presence of both compounds (**Figure 2A** and **Table 2**). Among these genes the most prominent changes were observed for genes involved in: (1) Organic acid transport such as PA1342 (*aatj*), which encodes a C4-dicarboxylate transport protein and PA1183 (*dctA*), (2) Central metabolism, like a PA0795 (*prpC*), which regulates a citrate synthase, PA2008 (*fahA*) that controls a fumarylacetoacetase, and PA1585 (*sucA*) encoding a 2- oxoglutatate dehydrogenase, (3) Oxidative stress such as superoxide dismutase PA4366 and (4) Virulence system like

TABLE 4 | Genes with reduced transcript levels following exposure to FOS treatment.

Gene ID	Gene	Protein Function	log2 Fold Change	*p*-value (10^{-6})
PA0049		Uncharacterized protein	−1.2	0.001
PA0090	*clpV1*	Type VI secretion ATPase*	−0.8	0.000
PA0296	*spuI*	Glutamylpolyamine synthetase	−0.6	0.007
PA0612	*ptrB*	Positive regulation of cellular biosynthetic process	−0.9	0.002
PA0613		Uncharacterized protein	−1.3	0.000
PA0614		Uncharacterized protein	−1.1	0.000
PA0615		Uncharacterized protein	−1.3	0.000
PA0616		Uncharacterized protein	−2.5	0.000
PA0617		Uncharacterized protein	−2.1	0.000
PA0618		Uncharacterized protein	−1.9	0.000
PA0619		Uncharacterized protein	−2.4	0.000
PA0620		Uncharacterized protein	−2.5	0.000
PA0621		Uncharacterized protein	−3.2	0.000
PA0622		Uncharacterized protein	−2.5	0.000
PA0623		Uncharacterized protein	−2.3	0.000
PA0624		Uncharacterized protein	−2.3	0.000
PA0625		Uncharacterized protein	−2.5	0.000
PA0626		Uncharacterized protein	−2.1	0.000
PA0627		Uncharacterized protein	−3.7	0.000
PA0628		Uncharacterized protein	−2.9	0.000
PA0629		Uncharacterized protein	−2.6	0.000
PA0630		Uncharacterized protein	−1.8	0.000
PA0631		Uncharacterized protein	−2.9	0.000
PA0632		Uncharacterized protein	−2.1	0.000
PA0633		Uncharacterized protein	−2.2	0.000
PA0634		Uncharacterized protein	−1.5	0.000
PA0635		Uncharacterized protein	−1.9	0.000
PA0636		Uncharacterized protein	−2.5	0.000
PA0637		Uncharacterized protein	−2.8	0.000
PA0638		Uncharacterized protein	−2.6	0.000
PA0639		Uncharacterized protein	−2.5	0.000
PA0640		Uncharacterized protein	−2.1	0.000
PA0641		Uncharacterized protein	−2.1	0.000
PA0642		Uncharacterized protein	−2.2	0.000
PA0643		Uncharacterized protein	−2.2	0.000
PA0644		Uncharacterized protein	−2.0	0.000
PA0645		Uncharacterized protein	−1.9	0.000
PA0646		Uncharacterized protein	−1.5	0.000
PA0647		Uncharacterized protein	−1.3	0.000
PA0795		Uncharacterized protein	−0.9	0.002
PA0807	*ampD*	*N*-acetylmuramoyl-L-alanine amidase	−2.7	0.000
PA0809		Transporter activity	−1.7	0.000
PA0811		Transmembrane transport	−1.8	0.000
PA0812		Uncharacterized protein	−1.7	0.000
PA0908	*alpB*	Response to antibiotic	−2.0	0.000
PA0910	*alpD*	Response to DNA damage stimulus	−1.7	0.000
PA0911	*alpE*	Response to DNA damage stimulus	−1.4	0.000
PA0912		Uncharacterized protein	−2.4	0.000
PA1069		Uncharacterized protein	−0.5	0.003
PA1171	*sltB2*	Soluble lytic transglycolase	−0.6	0.008
PA1183	*dctA*	C4-dicarboxylate transport protein	−1.2	0.000
PA1337	*ansB*	Glutaminase-asparaginase	−0.9	0.002
PA1342	*aatj*	Probable binding protein component of ABC transport	−1.1	0.000
PA1585	*sucA*	2-oxoglutarate dehydrogenase	−0.6	0.001
PA1588	*sucC*	Succinyl-CoA synthetase	−0.6	0.002

(Continued)

TABLE 4 | Continued

Gene ID	Gene	Protein Function	log2 Fold Change	*p*-value (10^{-6})
PA1592	*nd*	Uncharacterized protein	−0.8	0.001
PA1787	*acnB*	Aconitrate hydratase B	−0.5	0.003
PA2001	*atoB*	Acetyl-CoA acetyltransferase	−1.0	0.002
PA2007	*maiA*	Maleylacetatoacetate isomerase	−0.7	0.003
PA2008	*fahA*	Fumarylacetoacetase	−1.1	0.000
PA2040	*pauA4*	Glutamylpolyamine synthetase	−0.7	0.002
PA2111		Uncharacterized protein	−1.1	0.000
PA2247	*bkdA1*	2-oxoisovalerate dehydrogenase	−0.7	0.004
PA2796	*tal*	Transaldolase	−0.8	0.004
PA3661		Uncharacterized protein	−1.0	0.001
PA3692	*lptF*	Lipotoxon F	−0.8	0.006
PA3866		Pyocin S4	−1.0	0.000
PA4055	*ribC*	Riboflavin synthase	−0.7	0.005
PA4237	*rplQ*	50S ribosomal protein L17	−0.6	0.005
PA4239	*rpsD*	30S ribosomal protein S4	−0.6	0.001
PA4240	*rpsK*	30S ribosomal protein S11	−1.0	0.000
PA4274	*rplk*	50S ribosomal protein L11	−0.7	0.002
PA4366	*sodB*	Superoxide dismutase	−0.7	0.000
PA4370	*icmP*	Insulin-cleaving metalloproteinase outer membrane protein	−0.9	0.000
PA4430		probable cytochrome b	−0.6	0.003
PA4578		Uncharacterized protein	−0.8	0.000
PA4774		Uncharacterized protein	−0.7	0.001
PA4823		Uncharacterized protein	−1.2	0.000
PA4824		Uncharacterized protein	−0.8	0.000
PA4825	*mgtA*	$Mg^{(2+)}$ transport ATPase P-type 2	−0.8	0.000
PA4826		Uncharacterized protein	−0.5	0.005
PA5149	*mviM*	Uncharacterized protein	−1.0	0.005
PA5169	*dctM*	C4-dicarboxylate transport	−1.0	0.001

The above table shows the list of the significant up regulated genes with a log2 fold change cut off ≥ 0.5 by taking significant p-value < 0.05.

the Type VI secretion ATPase (PA0090). These genes were outnumbered by the genes for which both compounds caused an increase in transcript levels (**Figure 2** and **Table 3**).

A significant number of these genes appear to be involved in sensing (transcriptional regulators, sensor kinases, and chemotaxis transducers), motility, glucose metabolism as well as control of transcription and protein synthesis (**Figure 2** and **Table 3**).

Functional Analysis of *Pseudomonas aeruginosa* Transcriptome Following Exposure to FOS and Inulin

GO terms (WEGO) enrichment analyses were conducted to characterize the DEG (Differentially expressed genes) profiles and K-means clustering was performed to further investigate their biological function. We found that the differentially expressed genes can be classified into 32 categories that belonged to three gene ontology (GO) categories, i.e., the biological process, the cellular component or the molecular function (**Figure 3**). There were more genes classified into biological processes than the other two categories and most genes were predicted to have a binding function, as these genes are primarily involved in protein metabolism (**Figure 3**).

The over-expressed DEGs were assigned to 15 GO categories based on biological processes (**Figure 3**) and the results showed that the response to the stimulus, metabolic process, biological regulation, the establishment of localization and pigmentation were among the most highly represented groups in the biological process category in the presence of inulin or FOS. However, "biological adhesion" and "developmental process" showed a drastic decrease in the number of genes between inulin or FOS samples. While in the "locomotion process" most of the inhibited genes (43%) are annotated in FOS samples (**Figure 3**).

Furthermore, DEGs were assigned to seven GO categories based on cellular component and the result showed that "Cell" and "Cell part" are similar and highly represented groups for FOS and inulin samples (**Figure 3**). However, the "extracellular region" and the "organelle part" are lower and distinctly represented in the presence of inulin or FOS (**Figure 3**).

Genes with altered transcript levels could be grouped into 10 GO terms with different molecular functions of which the categories "antioxidant," "binding," "electron carrier," "transcription regulator," "structural molecular", and "transcription regulator" were most populated (**Figure 3**). It is worth noting that, in the "molecular transducer" category a significantly higher number of genes were noted for inulin as compared to FOS. The individual genes that

TABLE 5 | Genes with increased transcript levels following exposure to FOS treatment.

Gene ID	Gene	Protein	Log2 fold Change	*p*-value (10^{-6})
PA0003	*recF*	DNA replication and repair protein	1.2	0.000
PA0019	*def*	Peptide deformylase	0.8	0.000
PA0026	*plcB*	Phospholipase C	0.6	0.007
PA0408	*pilG*	Twitching motility protein	0.8	0.000
PA0576	*rpoD*	RNA polymerase sigma factor	0.7	0.000
PA0577	*dnaG*	DNA primase	0.5	0.003
PA0668	*tyrZ*	Tyrosyl-tRNA synthetase 2	0.7	0.000
PA0691	*phdA*	Prevent-host-death protein A	1.3	0.000
PA0692	*pdtB*	Phosphate depletion regulated TPS partner B	1.1	0.000
PA0693	*exbB2*	Transport protein	1.1	0.000
PA0695		Uncharacterized protein	1.2	0.000
PA0715		Uncharacterized protein	0.6	0.007
PA0730		3-hydroxyacyl-CoA-acyl carrier protein transferase.	0.6	0.004
PA0762	*algU*	RNA polymerase sigma factor	0.6	0.000
PA0768	*lepB*	Signal peptidase I	0.6	0.004
PA0782	*putA*	Proline dehydrogenase	0.5	0.006
PA0805		Uncharacterized protein	1.2	0.000
PA0826		Uncharacterized protein	0.7	0.000
PA0842		Probable glycosyl transferase	0.6	0.005
PA0896	*aruF*	Arginine *N*-succinyltransferase	0.5	0.001
PA0952		Uncharacterized protein	1.1	0.001
PA0979		Uncharacterized protein	1.0	0.000
PA1077	*flgB*	Flagellar basal body rod protein FlgB	0.6	0.004
PA1081	*flgF*	Flagellar basal-body rod protein FlgF	0.7	0.000
PA1084	*flgI*	Flagellar P-ring protein	0.5	0.002
PA1327		Serine protease	0.8	0.000
PA1382	*xqhB*	Probable type II secretion system protein	0.6	0.004
PA1414		Uncharacterized protein	1.7	0.004
PA1606		Uncharacterized protein	0.7	0.000
PA1608		Probable chemotaxis transducer	0.8	0.000
PA1610	*fabA*	Beta-hydroxydecanoyl-ACP dehydrase	0.8	0.000
PA1673		Uncharacterized protein	1.3	0.000
PA1796	*folD*	Cyclohydrolase	0.7	0.001
PA1803	*lon*	Protein secretion by the type III secretion system	0.5	0.003
PA2022		UDP-glucose 6-dehydrogenase	0.9	0.000
PA2426	pvdS	Sigma factor	1.2	0.001
PA2428		Uncharacterized protein	1.0	0.000
PA2461		Uncharacterized protein	0.7	0.008
PA2548		Uncharacterized protein	0.9	0.000
PA2637	nuoA	NADH dehydrogenase I	0.6	0.004
PA2667	*mvaU*	Biosynthetic process	0.6	0.001
PA2685	*vgrG4*	protein secretion system type VI	0.5	0.005
PA2696		probable transcriptional regulator	1.0	0.004
PA2738	*himA*	Integration host factor subunit alpha	0.8	0.000
PA2756		Uncharacterized protein	0.7	0.000
PA2882		Probable two-component sensor	1.0	0.000
PA2971	*yceD*	Uncharacterized protein	0.6	0.003
PA3019	*uup*	Probable ATP-binding component of ABC transporter	0.6	0.002
PA3116		Probableaspartate-semialdehyde dehydrogenase	0.5	0.008
PA3147	*wbpJ*	Probable glycosyl transferase	0.7	0.000
PA3161	*him*	Integration host factor	0.6	0.005
PA3181	*eda*	2-dehydro-3-deoxy-phosphogluconate aldolase	1.4	0.000
PA3182	*pgl*	6-phosphogluconolactonase	2.0	0.000
PA3183	*zwf*	Glucose-6-phosphate 1-dehydrogenase	2.1	0.000

(Continued)

TABLE 5 | Continued

Gene ID	Gene	Protein	Log2 fold Change	*p*-value (10^{-6})
PA3190	*gltB*	Component of ABC sugar transporter	0.8	0.004
PA3192	*gltR*	Two-component response regulator	1.6	0.000
PA3193	*glk*	Glucokinase	0.7	0.002
PA3194	*edd*	Phosphogluconate dehydratase	1.9	0.000
PA3195	*gapA*	Glyceraldehyde-3-phosphate dehydrogenase	1.1	0.000
PA3219		Uncharacterized protein	1.3	0.000
PA3262		Peptidyl-prolyl cis-trans isomerase	0.8	0.001
PA3280	*oprO*	Pyrophosphate-specific outer membrane porin	1.1	0.000
PA3296	*phoA*	Alkaline phosphatase	0.6	0.007
PA3305		Uncharacterized protein	1.9	0.004
PA3345	*hptB*	Histidine phosphotransfer protein	0.5	0.008
PA3351	*flgM*	Two-component system	0.7	0.000
PA3382	*phnE*	Phosphonate transport protein	0.7	0.001
PA3383	*phnD*	Binding protein component of ABC phosphonate transporter	0.6	0.001
PA3384	*phnC*	Phosphonates import ATP-binding protein	0.9	0.000
PA3496		Uncharacterized protein	0.5	0.007
PA3560	*fruA*	Phosphotransferase system transporter	1.3	0.000
PA3561	*fruK*	1-phosphofructokinase	1.8	0.000
PA3562	*fruI*	Phosphotransferase system transporter enzyme I.	2.0	0.000
PA3563		Uncharacterized protein	0.7	0.004
PA3623		Uncharacterized protein	0.6	0.002
PA3744	*rimM*	16S rRNA processing protein	0.6	0.004
PA3746	*ffh*	Signal recognition particle protein	0.5	0.004
PA3903	*prfC*	Peptide chain release factor 3	0.7	0.001
PA3990		Uncharacterized protein	0.9	0.000
PA4255	*rpmC*	50S ribosomal protein L29	1.1	0.000
PA4264	*rpsJ*	30S ribosomal protein S10	0.8	0.000
PA4270	*rpoB*	DNA-directed RNA polymerase beta chain	0.9	0.000
PA4280	*birA*	Regulation of transcription	0.6	0.000
PA4335		Uncharacterized protein	1.1	0.001
PA4336		Uncharacterized protein	0.8	0.003
PA4378	*inaA*	Protein of response to stimulus	0.6	0.004
PA4418	*ftsI*	Peptidoglycan D.D-transpeptidase	0.5	0.003
PA4420	*yabC*	Uncharacterized protein	0.6	0.000
PA4421	*yabC*	Uncharacterized protein	0.9	0.000
PA4432	*rpsI*	30S ribosomal protein S9	0.6	0.005
PA4451	*yrbA*	Uncharacterized protein	0.9	0.000
PA4462	*rpoN*	RNA polymerase sigma-54 factor	0.9	0.000
PA4475		Uncharacterized protein	0.7	0.001
PA4520		Probable chemotaxis transducer	0.6	0.002
PA4525	pilA	Type 4 fimbrial precursor	0.9	0.000
PA4541	*lepA*	Large extracellular protease	1.0	0.000
PA4545	*comL*	Outer membrane lipoprotein	0.6	0.003
PA4602	*glyA3*	Serine hydroxymethyltransferase	0.6	0.004
PA4611		Uncharacterized protein	0.6	0.008
PA4690		Uncharacterized protein	1.1	0.000
PA4723	*dksA*	Suppressor protein	0.7	0.000
PA4741	*rpsO*	30S ribosomal protein S15	0.7	0.002
PA4747	*secG*	Secretion protein	0.8	0.000
PA4844	*ctpL*	Chemoreceptor for inorganic phosphate	0.6	0.005
PA4853	*fis*	Putative Fis-like DNA-binding protein	0.9	0.000
PA4941	*hflC*	Protease	0.5	0.004
PA4944	*hfq*	Motilities and Quorum sensing	0.6	0.001
PA4945	*miaA*	Delta 2-isopentenylpyrophosphate	1.0	0.000

(Continued)

TABLE 5 | Continued

Gene ID	Gene	Protein	Log2 fold Change	*p*-value (10^{-6})
PA4960	*serB*	Probable phosphoserine phosphatase	0.6	0.003
PA4961		Uncharacterized protein	0.5	0.005
PA4963		Uncharacterized protein	0.6	0.001
PA5013	*ilvE*	Branched-chain-amino-acid transferase	0.6	0.000
PA5015	*aceE*	Pyruvate dehydrogenase	0.4	0.008
PA5040	*pilQ*	Type IV pilus-dependent motility	0.5	0.004
PA5042	*pilO*	Type IV pilus-dependent motility	0.9	0.000
PA5043	*pilN*	Type IV pilus-dependent motility	0.7	0.005
PA5045	*ponA*	Penicillin-binding protein 1A	0.6	0.002
PA5058	*phaC2*	Poly(3-hydroxyalkanoic acid) synthase 2	0.7	0.003
PA5066	*hisI*	Phosphoribosyl-AMP cyclohydrolase	0.6	0.002
PA5152		Probable ATP-binding component of ABC transporter	0.6	0.001
PA5170	*arcD*	Arginine/ornithine antiporter	0.8	0.004
PA5208		Uncharacterized protein	0.7	0.005
PA5235	*glpT*	Glycerol-3-phosphate transporter	1.2	0.000
PA5255	algQ	Alginate regulatory protein	0.6	0.007
PA5285	*sutA*	Uncharacterized protein	0.5	0.006
PA5286	*yjbQ*	Uncharacterized protein	0.7	0.000
PA5288	*glnK*	Nitrogen regulatory protein	0.6	0.003
PA5301	*pauR*	Polyamine catabolic process	0.9	0.000
PA5315	*rpmG*	50S ribosomal protein L33	0.7	0.000
PA5332	*crc*	Catabolite repression control protein	0.7	0.000
PA5348		Probable DNA-binding protein	0.7	0.001
PA5367	*pstA*	Phosphate ABC transporter	0.7	0.001
PA5369	*pstS*	Phosphate ABC transporter	0.7	0.000
PA5435	*oadA*	Probable transcarboxylase activity	0.9	0.000

The above table shows the list of the significant up regulated genes with a log2 fold change cut off ≥ 0.5 by taking significant p-value < 0.05.

were classified into these different GO terms are provided in **Supplementary Tables S1, S2**.

Differential Gene Expression Pattern in the Presence of FOS

The differential expression analysis performed with DESeq2 in the presence of FOS showed that 83 gene transcript levels were reduced (**Table 4**), whereas 134 were increased (**Figure 2** and **Table 5**). A large number of genes with reduced transcript levels (43%) were annotated as hypothetical proteins of uncharacterized functions (**Table 4**). We observed a decrease in the expression of genes related to (1) Metabolic pathways like citrate synthase (*prpC*), glutaminase-asparaginase (*ansB*), glutamylpolyamine synthetase (*pauA4*), and riboflavin synthase (*ribC*), (2) Transport systems such as PA0811 and PA1342 (*aatj*) (3) Translation cellular processes like several ribosomal proteins (*rplQ*, *rpsD*, *rpsK,* and *rplK*) and (4) Virulence such as PA0090 (*clpV*); PA0612 (*ptrB*), PA3866 (*pyocin S4*), and PA4370 (*icmP*) (see **Table 4**).

Surprisingly, in addition to increasing the expression of genes involved in different metabolic pathways necessary for bacterial growth, we found that transcript levels of many genes that are related to *P. aeruginosa* motility were increased in the presence of FOS (**Table 5**), exemplified by genes involved in twitching motility (*pilG*), components of the flagellar motor or chemoreceptors including CtpL that mediates specific taxis to inorganic phosphate – a key regulator of *P. aeruginosa* virulence (Zaborin et al., 2009; Bains et al., 2012). In the same manner, transcript levels of many genes associated within the glucose metabolism were also increased including genes *eda*, *zwf*, *gapA, glk, edd,* or *gltR* (**Table 5**) suggesting that *P. aeruginosa* can catabolize these compounds.

Effect of FOS on Virulence Related Gene Transcript Levels

All the DEGs were mapped to KO terms in the KEGG database to identify FOS modulated genes that play a role in bacterial virulence, motility, or sensitivity to antibiotics and the corresponding genes are provided in **Table 6**.

Noteworthy are the increases observed for transcript levels of PA0668 which encodes a TyrZ: Tyrosyl-tRNA synthetase2 that inhibits growth and biofilm formation (Williams-Wagner et al., 2015), genes of the *pilMNOPQ* operon, which are important for the pilus assembly system (T4P) and promote surface-associated attachment (Ayers et al., 2009; Tammam et al., 2013; McCallum et al., 2016) showed increased transcript levels like *pilG* (PA0408) (Log2 fold = 0.8); *pilQ* (PA5040) (0.5 Log2 fold); *pilO* (PA5042) (0.9 Log2 fold); *pilN* (PA5043) (0.7 Log2 fold); or different genes of the *flg*

TABLE 6 | Genes with increased transcript levels in response to FOS that are related to bacterial pathogenicity.

Gene ID	Gene	Protein	Log2 Fold Change	Function	References
PA0408	*pilG*	Twitching motility protein	0.81	Twitching motility and Chemotaxis	Darzins, 1993; Darzins and Russell, 1997; Whitchurch et al., 2004
PA0668	*tyrZ*	Tyrosyl-tRNA synthetase 2	0.7	Inhibit growth and biofilm formation	Williams-Wagner et al., 2015
PA0692	*pdtB*	Phosphate depletion regulated TPS partner B	1.1	Type V secretion system	Faure et al., 2014
PA0762	*algU*	RNA polymerase sigma factor	0.6	Control expression of virulence genes	Stacey and Pritchett, 2016; Stacey et al., 2017
PA1077	*flgB*	Flagellar basal-body rod protein	0.63	Bacterial-type flagellum-dependent cell motility	Goodier and Ahmer, 2001
PA1081	*flgF*	Flagellar basal-body rod protein FlgF	0.75	Flagellar assembly	Goodier and Ahmer, 2001
PA1084	*flgI*	Flagellar P-ring protein	0.54	Flagellar assembly	Goodier and Ahmer, 2001
PA1382	*xqhB*	Probable type II secretion system protein	0.6	Type II secretion system	Stover et al., 2000
PA1608		Probable chemotaxis transducer	0.8	Chemotaxis system and biofilm formation	Southey-Pillig et al., 2005
PA2426	*pvdS*	Sigma factor	1.22	Sigma factor activity	Tiburzi et al., 2008
PA3183	*zwf*	Glucose-6-phosphate 1-dehydrogenase	2.13	Carbohydrate metabolic pathway	Udaondo et al., 2018
PA3192	*gltR*	Two component system	1.6	Carbohydrate metabolic and virulence	Daddaoua et al., 2014
PA3351	*flgM*	Negative regulator of flagellin synthesis FlgM	0.73	Flagellar assembly	Goodier and Ahmer, 2001
PA4520		Chemotaxis transducer	0.6	Chemotaxis system	Victoria et al., 2003
PA4747	*secG*	Secretion protein	0.7	Sec secretory pathway	Crowther et al., 2015
PA4844	*ctpL*	Chemoreceptor for inorganic phosphate	0.6	Chemotaxis to inorganic phosphate	Rico-Jiménez et al., 2016
PA5040	*pilQ*	Type 4 fimbrial biogenesis protein	0.5	Surface filaments involved in host colonization	Darzins, 1993; Darzins and Russell, 1997; Whitchurch et al., 2004
PA5042	*pilO*	Type 4 fimbrial biogenesis protein	0.9	Surface filaments involved in adhesion cell, twitching motility	Martin et al., 1995; Leighton et al., 2018; Ayers et al., 2009
PA5043	*pilN*	Type 4 fimbrial biogenesis protein	0.7	Surface filaments involved in host colonization	Ayers et al., 2009
PA5045	*ponA*	Penicillin-binding protein 1A	1.0	*ampR*-β-lactamase modulation	Handfield et al., 1997
PA5332	*crc*	Catabolite repression control protein	0.8	Virulence, Quorum Sensing	Milojevic et al., 2013; Chakravarthy et al., 2017
PA5435	*oadA*	Probable transcarboxylase activity	0.9	Virulence	Bains et al., 2012
PA5369	*pstS*	Phosphate ABC transporter transporter control protein	0.8	Virulence	Zaborin et al., 2009

operon that encode proteins of the flagellar motor such as *flgB* (PA1077) (0.6 Log2 fold); *flgF* (PA1081) (0.7 Log2 fold); *flgI* (PA1084) (0.5 Log2 fold); and *flgM* (PA3351) (0.7 Log2 fold). Moreover, the transcript levels of three chemoreceptors were increased in the presence of FOS, of which two (PA1608, PA4520) are of unknown function, whereas PA4844 (*ctpl*) encodes a specific chemoreceptor for inorganic phosphate (Rico-Jiménez et al., 2016). In addition, the *zwf1* gene encoding a glucose-6-phosphate dehydrogenase that is involved in *P. aeruginosa* virulence (Udaondo et al., 2018) showed much higher transcript levels (2.13 Log2 fold) in the presence of FOS. In the same manner, transcript levels of *gltR* encoding the response regulator of the GtrS/GltR two component system (TCS) were significantly increased (1.6 Log2 fold) (**Table 6**). This TCS was found to regulate the expression of *toxA* encoding the primary virulence factor exotoxin A (Udaondo et al., 2018).

However, the results (**Table 7**) show several virulence related genes with reduced transcript levels, such as PA0090 encoding the ClpV1 protein, involved in the type VI secretion system (Bönemann et al., 2009), or the PtrB component of the type III secretion system (TTSS) that coordinates TTSS repression and pyocin synthesis under DNA damage (Weihui and Shouguang, 2005). The latter observation agrees with the reduced

TABLE 7 | Genes with decreased transcript levels in response to FOS that are related to bacterial pathogenicity.

Gene ID	Gene	Protein	Fold change	Function	References
PA0090	*clpV*	Type VI secretion ATPase	−0.84	Biofilm formation and secretion system type VI	Bönemann et al., 2009
PA0296	*spuI*	Glutamylpolyamine synthetase	−0.55	Polyamine toxicity	Dong-Kwon and Chung-Dar, 2006
PA0612	*ptrB*	Protease	−0.85	Suppresses the Type III Secretion System	Weihui and Shouguang, 2005
PA0807	*ampD*	*N*-acetylmuramoyl-L-alanine amidase	−2.68	β-lactam resistance	Amber and Nancy Hanson, 2008
PA0908	*alpB*	Outer membrane protein AlpB	−1.98	Cellular response to antibiotic	Alvarez-Ortega et al., 2010
PA1183	*dctA*	C4-dicarboxylate transport protein	−1.23	Growth process	Valentini et al., 2011
PA3692	*lptF*	Lipotoxon F	−0.78	Integral component of membrane and survival factor	Heath-Damron et al., 2009
PA3866		*Pyocin S4,* soluble (S-type) pyocins	−0.95	Virulence factor	Ameer et al., 2012
PA4370	*icmP*	Insulin-cleaving metalloproteinase outer membrane protein precursor	−0.93	Pathogenicity	Christian et al., 2015

TABLE 8 | Quantitative real time PCR experiments to quantify the effect of FOS on the transcript levels of genes that belong to the genomic island and that are related to bacterial pathogenicity in *P. aeruginosa*.

Gene ID	Gene	Protein	Relative expression levels	*P*-value
PA0807	*ampD*	*N*-acetylmuramoyl-L-alanine amidase	−6.1	0.04
PA0908	*alpB*	Outer membrane protein AlpB	−5.8	0.04
PA1183	*dctA*	C4-dicarboxylate transport protein	−7.2	0.02
PA0296	*spuI*	Glutamylpolyamine synthetase	−7.1	0.04
PA3866	*Pyocin S4*	Soluble (S-type) pyocins	−10.7	0.01
PA4370	*icmP*	Insulin-cleaving metalloproteinase outer membrane	−10.4	0.02
PA4844	*ctpL*	Chemoreceptor for inorganic phosphate	+ 0.65	0.09

Experiments were conducted using P. aeruginosa cultures grown in the presence and absence of 20 mg/ml of FOS. The cycle threshold values were normalized to that of the reference transcript, 16S RNA, and data of relative expression levels were normalized to the control lacking FOS.

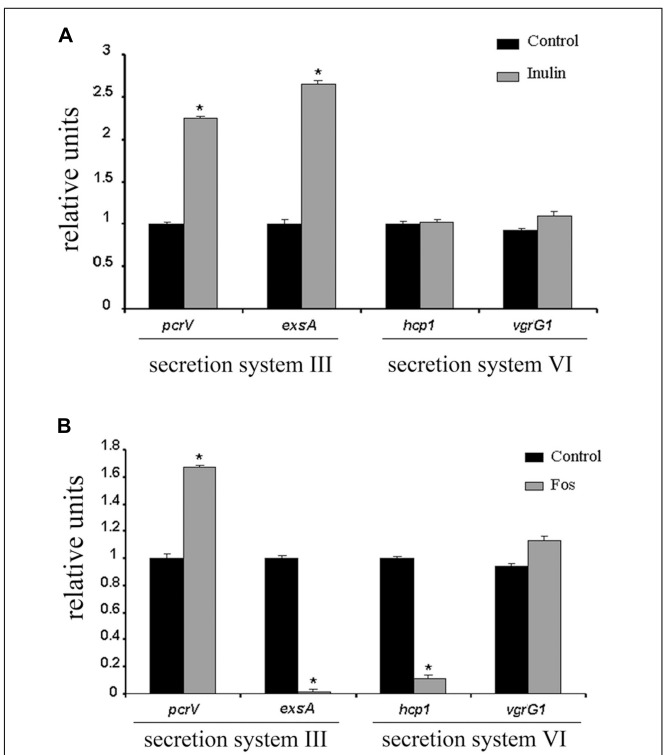

FIGURE 4 | Quantitative RT-PCR validations of the effect of FOS and inulin on the expression of secretion system genes. rt-qPCR studies of *P. aeruginosa* of cultures grown in the presence and absence of 20 mg/ml inulin **(A)** or FOS **(B)**. The expression of genes encoding proteins of secretion systems III and VI are shown. *$P < 0.05$ vs. Control.

transcript level of the gene (PA3866) encoding the pyocin S4 (Ameer et al., 2012).

In addition, the results shown in **Table 7** reveal reduced transcript levels for PA3692 (*lptF*), encoding an outer membrane protein (alipotoxon), which plays a key role in *P. aeruginosa* survival under harsh environmental conditions, including lung colonization in patients with cystic fibrosis (Heath-Damron et al., 2009). Furthermore, the reduction in transcript levels for PA0807 (*ampD*) and PA0908 (*alpB*), encoding proteins involved in responses to antibiotics, or in PA0296, involved in polyamine toxicity, may indicate that FOS modulates sensitivity to antibiotics (Amber and Nancy Hanson, 2008; Shah and Swiatlo, 2008; Alvarez-Ortega et al., 2010) and polyamines (Dong-Kwon and Chung-Dar, 2006). These data have been confirmed by real time quantitative PCR (rt-qPCR) experiments (**Table 8**).

Moreover, FOS treatment resulted in lower transcript levels of the *dctA* gene (PA1183) which is associated with the normal growth of *P. aeruginosa* (Valentini et al., 2011) and of the *icmP* gene (PA4370) encoding an metalloproteinase outer membrane protein, which has been shown to degrade the plasminogen activator (Christian et al., 2015) and plays a key role in the *Pseudomonas aeruginosa* pathogenicity. These FOS mediated alterations in transcript levels have been confirmed by rt-qPCR studies (see **Table 8**). Altogether, data suggest that FOS acts

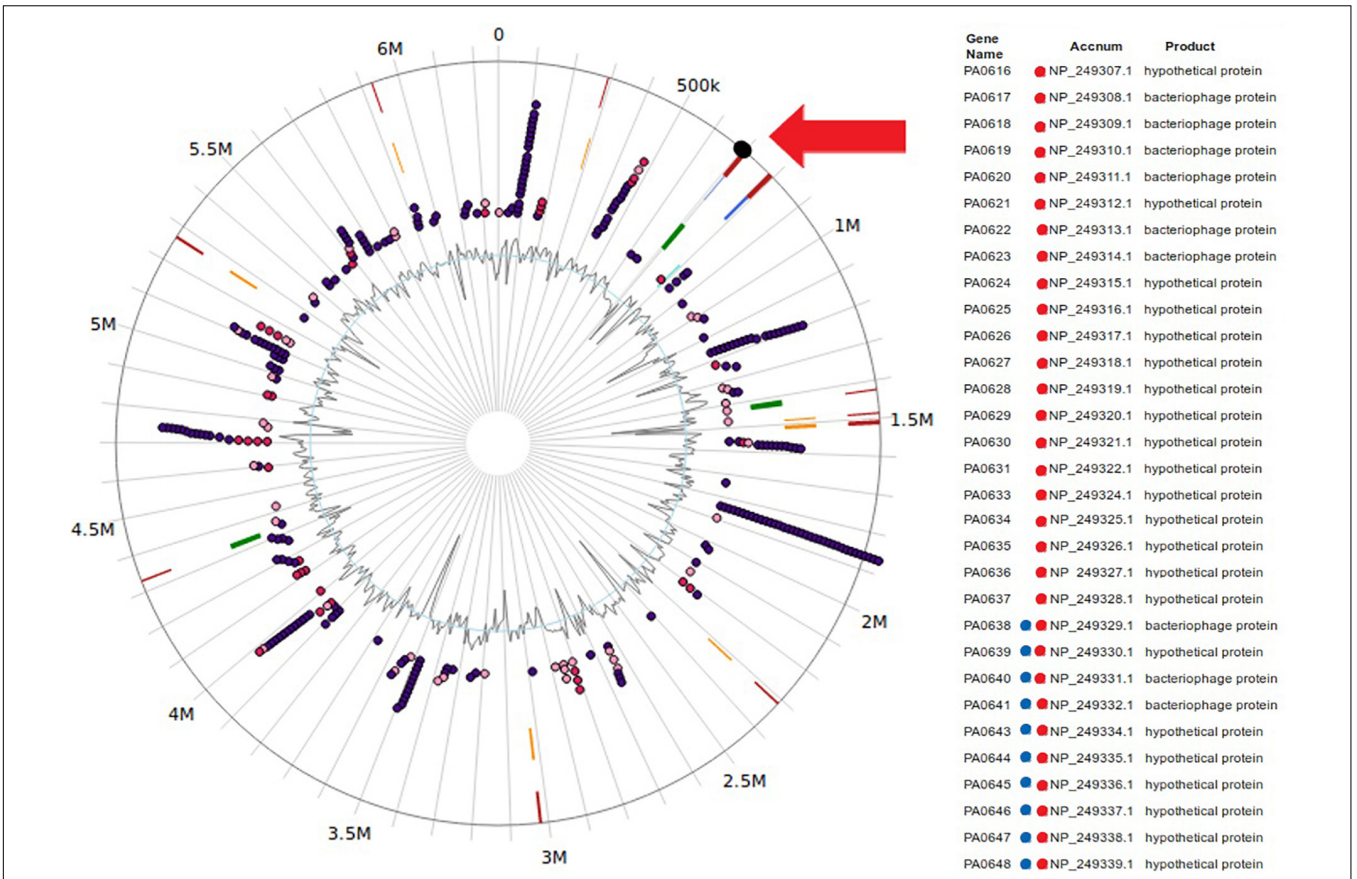

FIGURE 5 | Location of the genomics island with genes widely repressed by FOS-treatment in *Pseudomonas aeruginosa* PAO1 genome. Figure were made using IslandViewer4 (Bertelli et al., 2017). Genes ids with a red dot represent genes repressed in presence of FOS treatment. Genes with blue dot represent genes identified in a genomic island in *P. aeruginosa* PAO1 genome.

as a signal molecule that modulates bacterial virulence through distinct signaling pathways.

Confirmation That FOS Reduces Expression of Structural Proteins of Secretion System III and VI

To confirm that FOS mediates changes in secretion system genes, we have conducted rt-qPCR experiments to determine the influence of FOS and inulin on the expression of 4 genes that encode proteins that are part of type III and VI secretion systems. The products of the *pcrV* and *exsA* genes control the activation of the type III secretion system (Lee et al., 2010), whereas the proteins encoded by *hcp1* and *vgrG1* are necessary for the type VI secretion system (Hachani et al., 2011).

We found that inulin caused a significant increase in *pcrV* and *exsA* transcript levels, whereas those of *hcp1* and *vgrG1* did not vary (**Figure 4A**). In contrast, the expression of *exsA* and *hcp1* were dramatically down regulated by factors of approximately 20 and 7, respectively, in the presence of FOS (**Figure 4B**). FOS but not inulin down regulated the expression of two components of the type III and VI secretion system.

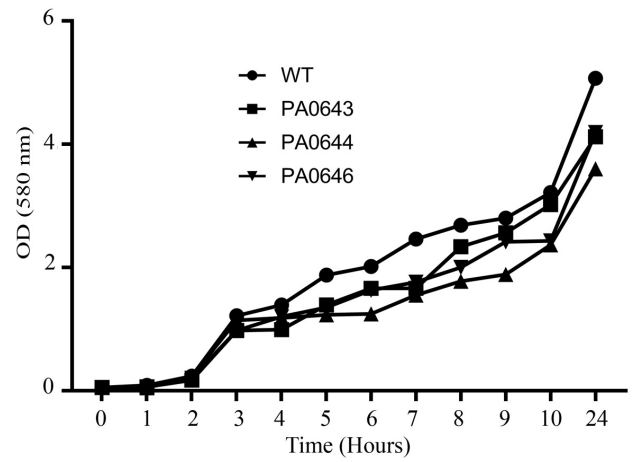

FIGURE 6 | The effect of PA0643, PA0644, and PA0646 deletion on the growth of *P. aeruginosa* PAO1. Shown are results from growth experiments that were conducted in M9 minimum medium at 37°C for 24 h. Representative data from one of three independent experiments with similar results are shown.

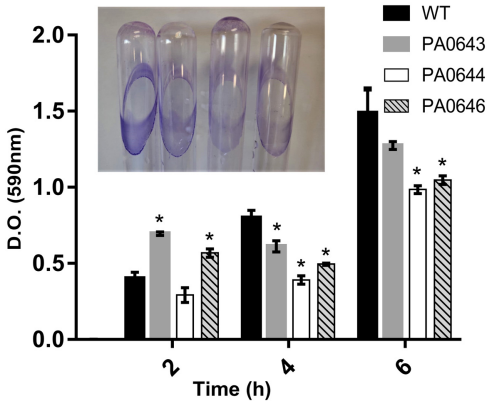

FIGURE 7 | The effect of PA0643, PA0644, and PA0646 deletion on biofilm formation of *P. aeruginosa* PAO1. Biofilm formation was monitored in minimum medium supplemented with 5 mM of citrate and quantified after 2, 4, and 6 h. The OD at 590 nm of crystal violet (CV) stained and resuspended bacteria from biofilms was recorded. Shown are means and standard deviations with $n = 3–6$; $^*P < 0.05$ vs. WT.

Identification of Genomics Islands Widely Repressed by FOS-Treatment in *Pseudomonas aeruginosa* PAO1

Due to their relevance to human health, extensive efforts have been made to study genomic islands, which are large genetic elements acquired through horizontal transmission (Juhas et al., 2009; Stephen and Julian, 2015; Mao and Lu, 2016).

Our data, using RNAseq sequence analysis, indicates the presence of a genomic island in PAO1 of ∼17 kb comprising 15 genes that had been inserted into the 3′-end of the PA0639 gene (**Figure 5**) through a phage encoded R2/F2 pyocin (Chang et al., 2005). Most of its genes were clearly repressed in the presence of FOS. Unfortunately, most of these genes code for proteins with unknown functions. Furthermore, in order to determine the biological role of this genomic island, various isogenic mutants were constructed and submitted to a phenotypic analysis that investigates changes in growth, biofilm formation, and motility. Interestingly, PA0643, PA0644, and PA0646 mutants showed reduced growth inhibition compared to the wild-type strain (**Figure 6**). In addition, while the PA0643 mutant strain did not cause any significant changes, the PA0644 and PA0646 isogenic mutant demonstrated a reduction in biofilm formation at 4 and 6 h (**Figure 7**). Moreover, PA0643, PA0644, and PA0646 mutants were tested for their ability to swim, swarm, and twitch and the results showed that the mutants exhibited differences in all three types of motility (**Figure 8**). While PA0643, PA0644, and PA0646 mutants caused the same reduced change in swarming motility, it was found that PA0644 and PA0646 mutants significantly inhibited (at least 50–60% of WT) the swimming motility. Interestingly, the twitching motility has been drastically reduced in the case of the PA0646 mutant (**Figure 8**). Markedly, this is the first study which shows that the deletion of PA0643, PA0644, and PA0646 genes are able to block *P. aeruginosa* swarming, swimming, and twitching motility. However, further studies are required to elucidate the function of these proteins.

DISCUSSION

Various factors appear to be implicated in the ability of *P. aeruginosa* to cause health problems. While surface structures, including pili and the polysaccharide, seem to favor biofilm formation and adhesion of *P. aeruginosa* to host cells (Pollack, 1984/1992; Prince, 1992) promoting colonization, its exotoxins in combination with various secretion systems deteriorate the host's defenses. The identification of signal molecules and the study of their corresponding molecular mechanism, which is associated with these processes, are of utmost interest.

Prebiotics have been shown to exert beneficial effects on human health by altering the intestinal microbiota and also by inhibiting the progression of some pathogenic strains (Knol et al., 2005), due to an indirect effect caused by the selective growth of host friendly bacteria. To our knowledge, antimicrobial properties have been described for a number of oligosaccharides (Daddaoua et al., 2006) and in a previous study, it was shown that FOS as a prebiotic had specific effects on *P. aeruginosa*, since it reduced growth,

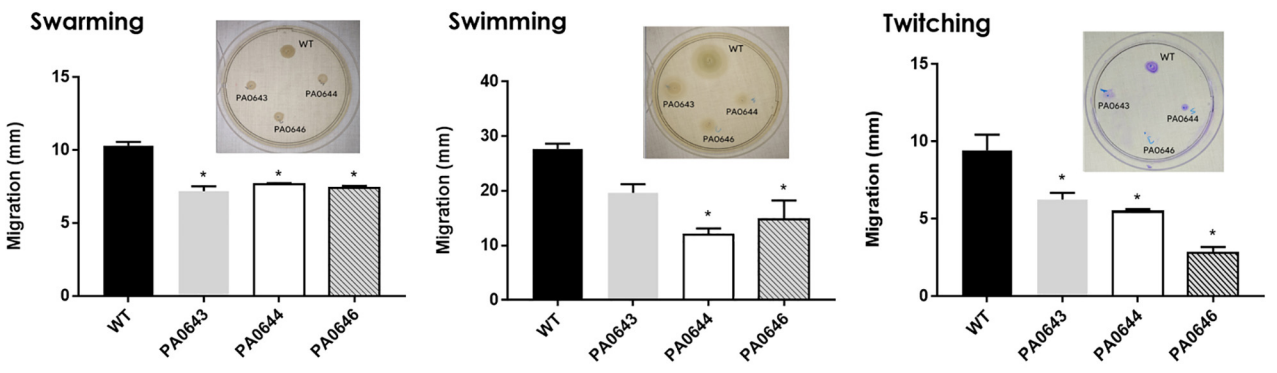

FIGURE 8 | Effect of PA0643, PA0644, and PA0646 deletion on the motility of *P. aeruginosa* PAO1. Motility assays were carried out as described in section "Materials and Methods." Shown are means and standard deviations with $n = 3–6$; $^*P < 0.05$ vs. WT.

limited the formation of biofilm, impaired motility, and reduced the inflammatory response (Ortega-González et al., 2014). Although, inulin and FOS are structurally related oligosaccharides, they differ in chain length and both compounds can be used as a carbon and energy source for *P. aeruginosa* growth.

The present study demonstrates that FOS induces a number of important changes in *P. aeruginosa* transcript levels some of which are related to bacterial survival (**Figure 1**) and provides an initial insight into the corresponding molecular mechanisms. As shown in **Figure 2**, in the 162 genes with reduced transcript levels by FOS and inulin, only 13% of them were affected by both compounds. Similarly, of the 443 genes with increased levels only 24% of gene transcript levels were altered by both compounds. Therefore, these compounds can be considered as signal molecules; however, their molecular mechanisms remain unknown.

RNA-Seq and rt-qPCR based comparative RNA profiling of *P. aeruginosa* PAO1 in the presence of FOS or inulin, not only highlighted known functions required for survival metabolism, but revealed a decrease in transcript levels of genes associated with carbohydrate metabolism and growth such as PA1183 (*dctA)* which has been shown to be associated previously with bacterial growth (Valentini et al., 2011). Thus, the growth reduction may be due to a reduction in transcript levels of genes associated with carboxylic acid transport, carboxylic acid metabolism, and reduction in ribosomal proteins.

Furthermore, these studies revealed a decrease of *spuI* gene transcript levels (PA0296), confirmed by rt-qPCR (**Table 8**), which control the expression of polyamine toxicity and of pyocins (PA3866), which are virulence factors that are induced by DNA-damaging agents, such as UV light and mitomycin C (Dean-Scholl and Martin, 2008).

The current analysis clearly shows that the pathogenesis of *P. aeruginosa* in the presence of FOS is compromised due to a decrease in several virulence-associated genes; i.e., *alpB* (PA0908), a holin-like protein that is required for lysis and the *icmP* gene (PA4370), which has been shown to degrade plasminogen activator (Christian et al., 2015) and may play a role in *P. aeruginosa* pathogenicity (**Tables 5**, **8**).

Secretion of exotoxins through type III secretion systems (T3SSs) (Filloux, 2011) are related to acute infections in *P. aeruginosa*, while type VI secretion systems are often associated with chronic infections and biofilm formation (Silverman et al., 2012).

Here we show by rt-qPCR that FOS lowers the transcript levels of *exsA* encoding a transcriptional activator of the secretion system type (T3SS) as well as those of a key protein necessary for the secretion system type VI (T6SS) function, encoded by the *hcp* gene (**Figure 4**).

Interestingly, the RNA seq analysis data coincide with a report that demonstrated that the repression of the *ptrB* gene (PA0612) is implicated in the regulation of the T3SS under DNA damage stress conditions (Weihui and Shouguang, 2005). In addition, this report demonstrates that a repression of *clpV* (PA0090) regulates the biofilm formation and T6SS (**Table 5**). Altogether, our study is consistent with the notion that the FOS mediated reduction in pathogenicity is mediated by the secretion systems III and VI.

Further, we obtained initial data suggesting that FOS modulates bacterial resistance to antibiotics, since FOS reduced the expression of *ampD* (PA0807) transcription levels which leads to the constitutive hyperproduction of the beta-lactamase AmpC and consequently to an increase of the β-lactam resistance (Lindberg et al., 1987). Furthermore, the data shows that FOS lowers transcript levels of *alpB* (PA0908) a gene product which is related to cell responses to antibiotics (Alvarez-Ortega et al., 2010).

The RNA seq analysis demonstrated the presence of an island with different genes of unknown function, whose expression was completely inhibited in the presence of FOS (**Figure 5** and **Table 4**). The deletion of the PA0643, PA0644, and PA0646 genes caused alterations in bacterial growth (**Figure 6**), biofilm formation (**Figure 7**) and motility (**Figure 8**). The alteration of the transcript levels of this island is thus another possible mechanism by which FOS reduces bacterial pathogenesis.

CONCLUSION

FOS containing supplements are currently being used to prevent gastrointestinal infections (Yasuda et al., 2012), suggesting that it is a valid strategy to combat *Pseudomonas* infection by potentially including FOS in antimicrobial cocktails. The present study is a contribution to close the gap of knowledge that exists in the corresponding molecular mechanisms.

DATA AVAILABILITY STATEMENT

All datasets generated for this study are included in the article/**Supplementary Material**.

AUTHOR CONTRIBUTIONS

JR-G, CS, and MG provided advice on experimental design. ZU and CS collected and assembled the data. AD designed the study, supervised and analyzed the data, and wrote the manuscript. TK and J-LR revised the manuscript. All authors reviewed and commented on the manuscript.

FUNDING

This work was supported by grants from the Spanish Ministry for Economy and Competitiveness (AGL2017-85270-R). CS is funded by the program Juan de la Cierva-Formación (FJCI-2015-23810).

SUPPLEMENTARY MATERIAL

The Supplementary Material for this article can be found online at: https://www.frontiersin.org/articles/10.3389/fmicb.2020.00202/full#supplementary-material

REFERENCES

Alvarez-Ortega, C., Wiegand, I., Olivares, J., Hancock, R. E., and Martínez, J. L. (2010). Genetic determinants involved in the susceptibility of *Pseudomonas aeruginosa* to beta lactam antibiotics. *Antimicrob. Agents Chemother.* 54, 4159–4167 doi: 10.1128/aac.00257-10

Amber, S. J., and Nancy Hanson, D. (2008). Role of ampD homologs in overproduction of AmpC in clinical isolates of *Pseudomonas aeruginosa*. *Antimicrob. Agents Chemother.* 52, 3922–3927. doi: 10.1128/AAC.00341-08

Ameer, E., Qing, W., and Pierre, C. (2012). The soluble pyocins S2 and S4 from *Pseudomonas aeruginosa* bind to the same FpvAI receptor. *Microbiologyopen* 1, 268–275. doi: 10.1002/mbo3.27

Amer, L. S., Bishop, B. M., and Van Hoek, M. L. (2010). Antimicrobial and antibiofilm activity of cathelicidins and short, synthetic peptides against *Francisella*. *Biochem. Biophys. Res. Commun.* 396, 246–251. doi: 10.1016/j.bbrc.2010.04.073

Andrews, S., and Fast, Q. C. (2010). *A Quality Control Tool for High Throughput Sequence Data*. Available at: http://www.bioinformatics.babraham.ac.uk/projects/fastqc/

Anyan, M. E., Amiri, A., Harvey, C. W., Tierra, G., Morales-Soto, N., Driscoll, C. M., et al. (2014). Type IV pili interactions promote intercellular association and moderate swarming of *Pseudomonas aeruginosa*. *Proc. Natl. Acad. Sci. U.S.A.* 50, 18013–18018. doi: 10.1073/pnas.1414661111

Ayers, M., Sampaleanu, L. M., Tammam, S., Koo, J., Harvey, H., Howell, P. L., et al. (2009). PilM/N/O/P proteins form an inner membrane complex that affects the stability of the *Pseudomonas aeruginosa* type IV pilus secretin. *J. Mol. Biol.* 394, 128–142. doi: 10.1016/j.jmb.2009.09.034

Bains, M., Fernandez, L., and Hancock, R. E. (2012). Phosphate starvation promotes swarming motility and cytotoxicity of *Pseudomonas aeruginosa*. *Appl. Environ. Microbiol.* 78, 6762–6768. doi: 10.1128/AEM.01015-12

Bertelli, C., Laird, M. R., Williams, K. P., Simon Fraser University Research Computing Group, Lau, B. Y., Hoad, G., et al. (2017). IslandViewer 4: expanded prediction of genomic islands for larger-scale datasets. *Nucleic Acids Res.* 45, W30–W35.

Bönemann, G., Pietrosiuk, A., Diemand, A., Zentgraf, H., and Mogk, A. (2009). Remodelling of VipA/VipB tubules by ClpV-mediated threading is crucial for type VI protein secretion. *EMBO J.* 28, 315–325. doi: 10.1038/emboj.2008.269

Bosscher, D., Van Loo, J., and Franck, A. (2006). Inulin and oligofructose as prebiotics in the prevention of intestinal infections and diseases. *Nutr. Res. Rev.* 19, 216–226. doi: 10.1017/S0954422407249686

Breidenstein, E. B., de la Fuente-Nunez, C., and Hancock, R. E. (2011). *Pseudomonas aeruginosa*: all roads lead to resistance. *Trends Microbiol.* 19, 419–426. doi: 10.1016/j.tim.2011.04.005

Buhl, M., Peter, S., and Willmann, M. (2015). Prevalence and risk factors associated with colonization and infection of extensively drug-resistant *Pseudomonas aeruginosa*: a systematic review. *Expert Rev. Anti Infect. Ther.* 13, 1159–1170. doi: 10.1586/14787210.2015.1064310

Cano, P. G., Santacruz, A., Trejo, F. M., and Sanz, Y. (2013). Bifidobacterium CECT 7765 improves metabolic and immunological alterations associated with obesity in high-fat diet-fed mice. *Obesity (Silver Spring)* 21, 2310–2321. doi: 10.1002/oby.20330

Capitán-Cañadas, F., Ocón, B., Aranda, C. J., Anzola, A., Suárez, M. D., Zarzuelo, A., et al. (2016). Fructooligosaccharides exert intestinal anti-inflammatory activity in the CD4+ CD62L+ T cell transfer model of colitis in C57BL/6J mice. *Eur. J. Nutr.* 55, 1445–1454. doi: 10.1007/s00394-015-0962-6

Capitán-Cañadas, F., Ortega-González, M., Guadix, E., Zarzuelo, A., Suárez, M. D., de Medina, F. S., et al. (2013). Prebiotic oligosaccharides directly modulate proinflammatory cytokine production in monocytes via activation of TLR4. *Mol. Nutr. Food Res.* 58, 1098–1110. doi: 10.1002/mnfr.201300497

Chakravarthy, S., Butcher, B. G., Liu, Y., D'Amico, K., Coster, M., and Filiatrault, M. J. (2017). Virulence of *Pseudomonas syringae* pv. tomato DC3000 is influenced by the catabolite repression control protein Crc. *Mol. Plant Microbe Interact.* 30, 283–294. doi: 10.1094/MPMI-09-16-0196-R

Chang, W., Small, D. A., Toghrol, F., and Bentley, W. E. (2005). Microarray analysis of *Pseudomonas aeruginosa* reveals induction of pyocin genes in response to hydrogen peroxide. *BMC Genomics* 6:115. doi: 10.1186/1471-2164-6-115

Christensen, G. D., Simpson, W. A., Younger, J. J., Baddour, L. M., Barrett, F. F., Melton, D. M., et al. (1985). Adherence of coagulase-negative staphylococci to plastic tissue culture plates: a quantitative model for the adherence of staphylococci to medical devices. *J. Clin. Microbiol.* 22, 996–1006. doi: 10.1128/jcm.22.6.996-1006.1985

Christian, L., Melanie, B., Chaves-Moreno, D., Andreas, O., Christian, H., Stephan, F., et al., (2015). Metaproteomics approach to elucidate host and pathogen protein expression during catheter-associated urinary tract infections (CAUTIs). *Mol. Cell. Proteomics* 14, 989–1008. doi: 10.1074/mcp.M114.043463

Crowther, G. J., Weller, S. M., Jones, J. C., Weaver, T., Fan, E., Van Voorhis, W. C., et al. (2015). The bacterial sec pathway of protein export: screening and follow-up. *J. Biomol. Screen.* 20, 921–926. doi: 10.1177/1087057115587458

Daddaoua, A., Molina-Santiago, C., de la Torre, J., Krell, T., and Ramos, J. L. (2014). GtrS and GltR form a two-component system: the central role of 2-ketogluconate in the expression of exotoxin A and glucose catabolic enzymes in *Pseudomonas aeruginosa*. *Nucleic Acids Res.* 42, 7654–7663. doi: 10.1093/nar/gku496

Daddaoua, A., Puerta, V., Requena, P., Martinez-Ferez, A., Guadix, E., de Medina, F. S., et al. (2006). Goat milk oligosaccharides are anti-inflammatory in rats with hapten-induced colitis. *J. Nutr.* 136, 672–676. doi: 10.1093/jn/136.3.672

Darzins, A. (1993). The *pilG* gene product, required for *Pseudomonas aeruginosa* pilus production and twitching motility, is homologous to the enteric, single-domain response regulator CheY. *J. Bacteriol.* 175, 5934–5944. doi: 10.1128/jb.175.18.5934-5944.1993

Darzins, A., and Russell, M. A. (1997). Molecular genetic analysis of type-4 pilus biogenesis and twitching motility using *Pseudomonas aeruginosa* as a model system–a review. *Gene* 192, 109–115. doi: 10.1016/s0378-1119(97)00037-1

Dean-Scholl, D., and Martin, D. W. Jr. (2008). Antibacterial efficacy of R-Type pyocins towards *Pseudomonas aeruginosa* in a murine peritonitis model. *Antimicrob. Agents Chemother.* 52, 1647–1652. doi: 10.1128/AAC.01479-07

Dong-Kwon, H., and Chung-Dar, L. (2006). Polyamines increase antibiotic susceptibility in *Pseudomonas aeruginosa*. *Antimicrob. Agents Chemother.* 50, 1623–1627 doi: 10.1128/aac.50.5.1623-1627.2006

Duseja, A., and Chawla, Y. K. (2014). Obesity and NAFLD: the role of bacteria and microbiota. *Clin. Liver Dis.* 18, 59–71

Faure, L. M., Garvis, S., De Bentzmann, S., and Bigot, S. (2014). Characterization of a novel two-partner secretion system implicated in the virulence of *Pseudomonas aeruginosa*. *Microbiology* 160, 1940–1952. doi: 10.1099/mic.0.079616-0

Filloux, A. (2011). Protein secretion systems in *Pseudomonas aeruginosa*: an essay on diversity, evolution. and function. *Front. Microbiol.* 2:155. doi: 10.3389/fmicb.2011.00155

Flemming, H. C., Neu, T. R., and Wozniak, D. J. (2007). The EPS matrix: the "house of biofilm cells". *J. Bacteriol.* 189, 7945–7947. doi: 10.1128/jb.00858-07

Froebel, L. K., Jalukar, S., Lavergne, T. A., Lee, J. T., and Duong, T. (2019). Administration of dietary prebiotics improves growth performance and reduces pathogen colonization in broiler chickens. *Poult. Sci.* 98, 6668–6676. doi: 10.3382/ps/pez537

Gaines, J. M., Carty, N. L., Tiburzi, F., Davinic, M., Visca, P., Colmer-Hamood, J. A., et al. (2007). Regulation of the *Pseudomonas aeruginosa toxA*, *regA* and *ptxR* genes by the iron-starvation sigma factor PvdS under reduced levels of oxygen. *Microbiology* 153, 4219–4233. doi: 10.1099/mic.0.2007/011338-0

Gibson, G. R., Beatty, E. R., and Wang, X. (1995). Cummings JH Selective stimulation of bifidobacteria in the human colon by oligofructose and inulin. *Gastroenterology* 108, 975–982. doi: 10.1016/0016-5085(95)90192-2

Gómez-Lozano, M., Marvig, R. L., Tulstrup, M. V. L., and Molin, S. (2014). Expression of antisense small RNAs in response to stress in *Pseudomonas aeruginosa*. *BMC Genomics* 15:783. doi: 10.1186/1471-2164-15-783

Goodier, R. I., and Ahmer, B. M. (2001). SirA orthologs affect both motility and virulence. *J. Bacteriol.* 183, 2249–2258. doi: 10.1128/jb.183.7.2249-2258.2001

Hachani, A., Lossi, N. S., Hamilton, A., Jones, C., and Bleves, S. (2011). Type VI secretion system in *Pseudomonas aeruginosa*: secretion and multimerization of VgrG proteins. *J. Biol. Chem.* 286, 12317–12327. doi: 10.1074/jbc.M110.193045

Handfield, J. 1, Gagnon, L., Dargis, M., and Huletsky, A. (1997). Sequence of the *ponA* gene and characterization of the penicillin-binding protein 1A of *Pseudomonas aeruginosa* PAO1. *Gene* 199, 49–56. doi: 10.1016/s0378-1119(97)00345-4

Heath-Damron, F., Napper, J., Allison-Teter, M., and Hongwei, D. Yu. (2009). Lipotoxin F of *Pseudomonas aeruginosa* is an AlgU-dependent and

alginate-independent outer membrane protein involved in resistance to oxidative stress and adhesion to A549 human lung epithelia. *Microbiology* 155, 1028–1038. doi: 10.1099/mic.0.025833-0

Hoiby, N., Ciofu, O., and Bjarnsholt, T. (2010). *Pseudomonas aeruginosa* biofilms in cystic fibrosis. *Future Microbiol.* 5, 1663–1674. doi: 10.2217/fmb.10.125

Juhas, M. (2015). *Pseudomonas aeruginosa* essentials: an update on investigation of essential genes. *Microbiology* 161, 2053–2060. doi: 10.1099/mic.0.000161

Juhas, M., Van der Meer, J. R., Gaillard, M., Harding, R. M., Hood, D. W., and Crook, D. W. (2009). FEMS genomic islands: tools of bacterial horizontal gene transfer and evolution. *Microbiol. Rev.* 33, 376–393. doi: 10.1111/j.1574-6976.2008.00136.x

Kimberly, R. K., and Stephen, M. B. (2015). RNA sequencing and analysis. *Cold Spring Harb. Protoc.* 11, 951–969.

Klausen, M., Heydorn, A., Ragas, P., Lambertsen, L., and Aaes-Jorgensen, A. (2003). Biofilm formation by *Pseudomonas aeruginosa* wild type, flagella and type IV pili mutants. *Mol. Microbiol.* 48, 1511–1524. doi: 10.1046/j.1365-2958.2003.03525.x

Knol, J., Boehm, G., Lidestri, M., Negretti, F., and Jelinek, J. (2005). Increase of faecal bifidobacteria due to dietary oligosaccharides induces a reduction of clinically relevant pathogen germs in the faeces of formula-fed preterm infants. *Acta Paediatr. Suppl.* 94, 31–33. doi: 10.1111/j.1651-2227.2005.tb02152.x

Lattimer, J. M., and Haub, M. D. (2010). Effects of dietary fiber and its components on metabolic health. *Nutrients* 2, 1266–1289. doi: 10.3390/nu2121266

Lee, P. C., Stopford, C. M., Svenson, A. G., and Rietsch, A. (2010). Control of effector export by the *Pseudomonas aeruginosa* type III secretion proteins PcrG and PcrV. *Mol. Microbiol.* 75, 924–941. doi: 10.1111/j.1365-2958.2009.07027.x

Leighton, T. L., Mok, M. C., Junop, M. S., Howell, P. L., and Burrows, L. L. (2018). Conserved, unstructured regions in *Pseudomonas aeruginosa* PilO are important for type IVa pilus function. *Sci. Rep.* 8:2600. doi: 10.1038/s41598-018-20925-w

Li, H., Handsaker, B., Wysoker, A., Fennell, T., Ruan, J., Homer, N., et al. (2009). The sequence alignment/map format and samtools. *Bioinformatics* 25, 2078–2079. doi: 10.1093/bioinformatics/btp352

Liao, Y., Smyth, G. K., and Shi, W. (2013). The Subread aligner: fast accurate and scalable read mapping by seed-and-vote. *Nucleic Acids Res.* 41:e108. doi: 10.1093/nar/gkt214

Liao, Y. G. K., Smyth, G. K., and Shi, W. (2014). Feature counts: an efficient general purpose program for assigning sequence reads to genomic features. *Bioinformatics* 30, 923–930. doi: 10.1093/bioinformatics/btt656

Lindberg, F., Lindquist, S., and Normark, S. (1987). Inactivation of the *ampD* gene causes semiconstitutive overproduction of the inducible *Citrobacter freundii* beta-lactamase. *J. Bacteriol.* 169, 1923–1928. doi: 10.1128/jb.169.5.1923-1928.1987

Love, M. I., Huber, W., and Anders, S. (2014). Moderated estimation of fold change and dispersion for RNA-seq data with DESeq2. *Genome Biol.* 15:550.

Lynch, J. P. III, Zhanel, G. G., and Clark, N. M. (2017). Emergence of antimicrobial resistance among *Pseudomonas aeruginosa*: implications for therapy. *Semin. Respir. Crit. Care Med.* 38, 326–345. doi: 10.1055/s-0037-1602583

Mah, T. F., Pitts, B., Pellock, B., and Walker, G C,. (2003). A genetic basis for *Pseudomonas aeruginosa* biofilm antibiotic resistance. *Nature* 426, 306–310. doi: 10.1038/nature02122

Mao, J., and Lu, T. (2016). Population-dynamic modeling of bacterial horizontal gene transfer by natural transformation. *Biophys. J.* 110, 258–268. doi: 10.1016/j.bpj.2015.11.033

Martin, P. R., Watson, A. A., McCaul, T. F., and Mattick, J. S. (1995). Characterization of a five-gene cluster required for the biogenesis of type 4 fimbriae in *Pseudomonas aeruginosa*. *Mol. Microbiol.* 16, 497–508. doi: 10.1111/j.1365-2958.1995.tb02414.x

McCallum, M., Tammam, S., Little, D. J., Robinson, H., Koo, J., Shah, M., et al. (2016). PilN binding modulates the structure and binding partners of the *Pseudomonas aeruginosa* type IVa pilus protein pilm. *J. Biol. Chem.* 291, 11003–11015. doi: 10.1074/jbc.M116.718353

Milojevic, T., Grishkovskaya, I., Sonnleitner, E., Djinovic-Carugo, K., and Bläsi, U. (2013). The *Pseudomonas aeruginosa* catabolite repression control protein Crc is devoid of RNA binding activity. *PLoS One* 8:e64609. doi: 10.1371/journal.pone.0064609

Miura, K., and Ohnishi, H. (2014). Role of gut microbiota and toll-like receptors in nonalcoholic fatty liver disease. *World J. Gastroenterol.* 20, 7381–7391. doi: 10.3748/wjg.v20.i23.7381

Miyoshi-Akiyama, T., Tada, T., Ohmagari, N., Viet Hung, N., Tharavichitkul, P., Pokhrel, B. M., et al. (2017). Emergence and spread of epidemic multidrug-resistant *Pseudomonas aeruginosa*. *Genome Biol. Evol.* 9, 3238–3245. doi: 10.1093/gbe/evx243

Molina-Fuentes, Á., Pacheco, D., Marín, P., Philipp, B., Schink, B., and Marqués, S. (2015). Identification of the gene cluster for the anaerobic degradation of 3,5-Dihydroxybenzoate (α-Resorcylate) in *Thauera aromatica* strain AR-1. *Appl. Environ. Microbiol.* 81, 7201–7214. doi: 10.1128/AEM.01698-15

Natividad, J. M., and Verdu, E. F. (2012). Modulation of intestinal barrier by intestinal microbiota: pathological and therapeutic implications. *Pharmacol. Res.* 69, 42–51. doi: 10.1016/j.phrs.2012.10.007

Ohara, T., and Itoh, K. (2003). Significance of *Pseudomonas aeruginosa* colonization of the gastrointestinal tract. *Intern. Med.* 42, 1072–1076. doi: 10.2169/internalmedicine.42.1072

Ortega-González, M., Sánchez de Medina, F., Molina-Santiago, C., López-Posadas, R., Pacheco, D., Krell, T., et al. (2014). Fructooligosacharides reduce *Pseudomonas aeruginosa* PAO1 pathogenicity through distinct mechanisms. *PLoS One* 22:e85772. doi: 10.1371/journal.pone.0085772

Ortiz-Castro, R., Pelagio-Flores, R., Méndez-Bravo, A., Ruiz-Herrera, L. F., Campos-García, J., and López-Bucio, J. (2014). Pyocyanin, a virulence factor produced by *Pseudomonas aeruginosa*, alters root development through reactive oxygen species and ethylene signaling in *Arabidopsis*. *Mol. Plant Microbe Interact.* 27, 364–378. doi: 10.1094/MPMI-08-13-0219-R

Pollack, M. (1984/1992). The virulence of *Pseudomonas aeruginosa*. *Rev. Infect. Dis.* 6(Suppl. 3), S617-S626.

Prince, A. (1992). Adhesins and receptors of *Pseudomonas aeruginosa* associated with infection of the respiratory tract. *Microb. Pathog.* 13, 251–260. doi: 10.1016/0882-4010(92)90035-m

Rico-Jiménez, M., Reyes-Darias, J.-A., Ortega, Á., Peña, A. I. D., Morel, B., and Tino, K. (2016). Two different mechanisms mediate chemotaxis to inorganic phosphate in *Pseudomonas aeruginosa*. *Sci. Rep.* 6:28967. doi: 10.1038/srep28967

Sambrook, J., Fritsch, E. F., and Maniatis, T. (1989). *Molecular Cloning: A Laboratory Manual*, 2nd Edn. Cold Spring Harbor, NY: Cold Spring Harbor Laboratory.

Sánchez de Medina, F., Ortega-González, M., González-Pérez, R., Capitán-Cañadas, F., and Martínez-Augustin, O. (2013). Host-microbe interactions: the difficult yet peaceful coexistence of the microbiota and the intestinal mucosa. *Br. J. Nutr.* 109, S12-S20

Shah, P., and Swiatlo, E. (2008). A multifaceted role for polyamines in bacterial pathogens. *Mol. Microbiol.* 68, 4–16. doi: 10.1111/j.1365-2958.2008.06126.x

Silverman, J. M., Brunet, Y. R., Cascales, E., and Mougous, J. D. (2012). Structure and regulation of the type VI secretion system. *Annu. Rev. Microbiol.* 66, 453–472. doi: 10.1146/annurev-micro-121809-151619

Southey-Pillig, C. J., Davies, D. G., and Sauer, K. (2005). Characterization of temporal protein production in *Pseudomonas aeruginosa* biofilms. *J. Bacteriol.* 187, 8114–8126. doi: 10.1128/jb.187.23.8114-8126.2005

Stacey, S. D., and Pritchett, C. L. (2016). *Pseudomonas aeruginosa* AlgU contributes to posttranscriptional activity by increasing rsmA expression in a mucA22 Strain. *J. Bacteriol.* 198, 1812–1826. doi: 10.1128/JB.00133-16

Stacey, S. D., Williams, D. A., and Pritchett, C. L. (2017). The *Pseudomonas aeruginosa* two-component regulator AlgR directly activates rsmA expression in a phosphorylation independent manner. *J Bacteriol.* 199:e00048-17. doi: 10.1128/JB.00048-17

Stephen, D. B., and Julian, P. (2015). Genomic perspectives on the evolution and spread of bacterial pathogens. *Proc. Biol. Sci.* 282:20150488. doi: 10.1098/rspb.2015.0488

Stoodley, P., Sauer, K., Davies, D. G., and Costerton, J. W. (2002). Biofilms as complex differentiated communities. *Annu. Rev. Microbiol.* 56, 187–209. doi: 10.1146/annurev.micro.56.012302.160705

Stover, C. K., Pham, X. Q., Erwin, A. L., Mizoguchi, S. D., Warrener, P., Hickey, M. J., et al. (2000). Complete genome sequence of *Pseudomonas aeruginosa* PAO1, an opportunistic pathogen. *Nature* 406, 959–964.

Tammam, S., Sampaleanu, L. M., Koo, J., Manoharan, K., Daubaras, M., Burrows, L. L., et al. (2013). PilMNOPQ from the *Pseudomonas aeruginosa* type IV pilus system form a transenvelope protein interaction network that interacts with PilA. *J. Bacteriol.* 195, 2126–2135. doi: 10.1128/JB.00032-13

Taylor, P. K., Yeung, A. T. Y., and Hancock, R. E. W. (2014). Antibiotic resistance in *Pseudomonas aeruginosa* biofilms: towards the development of novel anti-biofilm therapies. *J. Biotechnol.* 191, 121–130. doi: 10.1016/j.jbiotec.2014.09.003

Tiburzi, F., Imperi, F., and Visca, P. (2008). Intracellular levels and activity of PvdS, the major iron starvation sigma factor of *Pseudomonas aeruginosa*. *Mol. Microbiol.* 67, 213–227. doi: 10.1111/j.1365-2958.2007.06051.x

Udaondo, Z., Ramos, J., Segura, A., Krell, T., and Daddaoua, A. (2018). Regulation of carbohydrate degradation pathways in *Pseudomonas* involves a versatile set of transcriptional regulators. *Microb. Biotechnol.* 11, 442–454. doi: 10.1111/1751-7915.13263

Valentini, M., Storelli, N., and Lapouge, K. (2011). Identification of C_4-Dicarboxylate transport systems in *Pseudomonas aeruginosa* PAO1. *J. Bacteriol.* 193, 4307–4316. doi: 10.1128/jb.05074-11

Victoria, E. W., Daniel, B., Luciano, P., Brooks, A. I., and Iglewski, B. H. (2003). Microarray analysis of *Pseudomonas aeruginosa* quorum-sensing regulons: effects of growth phase and environment. *J. Bacteriol.* 185, 2080–2095. doi: 10.1128/jb.185.7.2080-2095.2003

Von Klitzing, E., Bereswill, S., and Heimesaat, M. M. (2017). Multidrug-resistant *Pseudomonas aeruginosa* induce systemic pro-inflammatory immune responses in colonized mice. *Eur. J. Microbiol. Immunol.* 7, 200–209. doi: 10.1556/1886.2017.00022

Weihui, W., and Shouguang, J. (2005). PtrB of *Pseudomonas aeruginosa* suppresses the type III secretion system under the stress of DNA damage. *J. Bacteriol.* 187, 6058–6068. doi: 10.1128/jb.187.17.6058-6068.2005

Whitchurch, C. B., Leech, A. J., Young, M. D., Kennedy, D., Sargent, J. L., Bertrand, J. J., et al. (2004). Characterization of a complex chemosensory signal transduction system which controls twitching motility in *Pseudomonas aeruginosa*. *Mol. Microbiol.* 52, 873–893. doi: 10.1111/j.1365-2958.2004.04026.x

WHO (2017). Global Priority List of Antibiotic-Resistant Bacteria to Guide Research, Discovery and Development of New Antibiotics. Available at: http://www.who.int/medicines/publications/global-priority-list-antibiotic-resistant-bacteria/en/

Williams-Wagner, R. N., Grundy, F. J., Raina, M., Ibba, M., and Henkin, T. M. (2015). The *Bacillus subtilis* tyrZ gene encodes a highly selective tyrosyl-tRNA synthetase and is regulated by a MarR regulator and T box riboswitch. *J. Bacteriol.* 197, 1624–1631. doi: 10.1128/JB.00008-15

Yasuda, A., Inoue, K., Sanbongi, C., Yanagisawa, R., and Ichinose, T. (2012). Dietary supplementation with fructooligosaccharides attenuates allergic peritonitis in mice. *Biochem. Biophys. Res. Commun.* 422, 546–550. doi: 10.1016/j.bbrc.2012.05.007

Zaborin, A., Romanowski, K., Gerdes, S., Holbrook, C., Lepine, F., Long, J., et al. (2009). Red death in *Caenorhabditis elegans* caused by *Pseudomonas aeruginosa* PAO1. *Proc. Natl. Acad. Sci. U.S.A.* 106, 6327–6332. doi: 10.1073/pnas.0813199106

Conflict of Interest: The authors declare that the research was conducted in the absence of any commercial or financial relationships that could be construed as a potential conflict of interest.

Copyright © 2020 Rubio-Gómez, Santiago, Udaondo, Garitaonaindia, Krell, Ramos and Daddaoua. This is an open-access article distributed under the terms of the Creative Commons Attribution License (CC BY). The use, distribution or reproduction in other forums is permitted, provided the original author(s) and the copyright owner(s) are credited and that the original publication in this journal is cited, in accordance with accepted academic practice. No use, distribution or reproduction is permitted which does not comply with these terms.

frontiers in Microbiology

ORIGINAL RESEARCH
published: 03 March 2020
doi: 10.3389/fmicb.2020.00212

Comparison on the Growth Variability of *Vibrio parahaemolyticus* Coupled With Strain Sources and Genotypes Analyses in Simulated Gastric Digestion Fluids

Yangmei Wang[1], Yong Zhao[1,2,3], Yingjie Pan[1,2,3] and Haiquan Liu[1,2,3,4]**

[1] College of Food Science and Technology, Shanghai Ocean University, Shanghai, China, [2] Shanghai Engineering Research Center of Aquatic Product Processing & Preservation, Shanghai, China, [3] Laboratory of Quality & Safety Risk Assessment for Aquatic Product on Storage and Preservation (Shanghai), Ministry of Agriculture Shanghai, Shanghai, China, [4] Engineering Research Center of Food Thermal-Processing Technology, Shanghai Ocean University, Shanghai, China

Vibrio parahaemolyticus is a food-borne pathogen that causes pathogenic symptoms such as diarrhea and abdominal pain. Currently no studies have shown that either pathogenic and non-pathogenic *V. parahaemolyticus* possess growth heterogeneity in a human environment, such as in gastric and intestinal fluids. The *tlh* gene is present in both pathogenic and non-pathogenic *V. parahaemolyticus* strains, while the *tdh* and *trh* genes are only present in pathogenic strains. This study firstly applied simulated human gastric fluids to explore growth variability of 50 strains of *V. parahaemolyticus* at 37°C. The bacterial growth curves were fitted by primary modified Gompertz model, and the maximum growth rate (μ_{max}), lag time (LT), and their CV values were calculated to compare the stress response of pathogenic and non-pathogenic *V. parahaemolyticus* to simulated human gastric fluids. Results showed that the simulated human gastric fluids treatment significantly increased the μ_{max} of pathogenic strains and shortened the lag time, while decreased the μ_{max} of non-pathogenic strains and prolonged the lag time. Meanwhile, the CV values of genotypes ($tlh^+/tdh^+/trh^-$) evidently increased, showing that the pathogenic genotype ($tlh^+/tdh^+/trh^-$) strains had strong activity to simulated gastric fluids. All of the results indicated that the *V. parahaemolyticus* strains exhibited a great stress-resistant variability and growth heterogeneity to the simulated gastric fluids, which provides a novel insight to unlock the efficient control of pathogenic *V. parahaemolyticus*.

Keywords: *Vibrio parahaemolyticus*, growth heterogeneity, simulate gastric fluids, maximum growth rate, gene heterogeneity

OPEN ACCESS

Edited by:
Giovanna Suzzi,
University of Teramo, Italy

Reviewed by:
Learn-Han Lee,
Monash University Malaysia, Malaysia
Pendru Raghunath,
Texila American University, Guyana

***Correspondence:**
Yong Zhao
yzhao@shou.edu.cn
Haiquan Liu
hqliu@shou.edu.cn

Specialty section:
This article was submitted to Food Microbiology, a section of the journal Frontiers in Microbiology

Received: *18 October 2019*
Accepted: *30 January 2020*
Published: *03 March 2020*

Citation:
Wang Y, Zhao Y, Pan Y and Liu H (2020) Comparison on the Growth Variability of Vibrio parahaemolyticus Coupled With Strain Sources and Genotypes Analyses in Simulated Gastric Digestion Fluids. Front. Microbiol. 11:212. doi: 10.3389/fmicb.2020.00212

INTRODUCTION

Vibrio parahaemolyticus is a gram-negative non-spore halophilic bacteria, which inhabits primarily coastal marine and estuarine environments and is widely found in various marine products (Alonsohernando et al., 2013). Cross-contamination due to the transportation and sale of seafood can also be found in large quantities in freshwater products (Jing et al., 2014). *V. parahaemolyticus*

is a common food-borne pathogen, which can cause pathogenic symptoms such as diarrhea, vomiting, acute gastroenteritis, dehydration, shock, and even death after the ingestion of the bacteria (Baker-Austin et al., 2010). *V. parahaemolyticus* has become the major pathogen causing food-borne infection in many countries and coastal areas, such as Japan, Southeast Asia, the United States, and Taiwan (Yamasaki et al., 2009). According to reports of patients in China, due to *V. parahaemolyticus*, there have been 6.65 million cases of acute diarrhea, about 7.281 million cases of acute gastroenteritis, and the proportion of food-borne *V. parahaemolyticus* infection was about 68.0%. Thus, it is essential to control and prevent *V. parahaemolyticus*. Additionally, approximately 95% of *V. parahaemoliticus* cases are non-pathogenic and 5% are pathogenic in the environment (Nordstrom et al., 2007). The use of multiplex-PCR can comprehensively detect *V. parahaemolyticus*. All *V. parahaemolyticus* can amplify the *tlh* gene, which is unique to *V. parahaemolyticus*. The detection of *tdh* and *trh* genes as pathogenic isolates is also the main cause of human food-borne diseases (Letchumanan et al., 2015).

Although most environmental strains are not pathogenic, there are a small number of pathogenic strains with virulence factors that serve as the most critical in causing food-borne diseases. The reason that pathogenic *V. parahaemolyticuscan* causes human diarrhea, which is contained in seafood. And it is related to pathogenic factors, including the initial adhesion of pathogenic bacteria to host cells; and the release of pathogenic bacteria to the host cells with various biological activities such as toxins, proteins, and polysaccharides plays a toxic role. Usually, most pathogenic isolates and a few environmental sources of *V. parahaemolyticus* are pathogenic, which is associated with its cell-associated factors (such as colistin) (Obaidat et al., 2017), extracellular factors (such as hemolytic toxins) (Takahashi et al., 2000), and proteases (such as mucinase) (Jun et al., 2003).

Previous studies' identified methods for the pathogenic isolates of *V. parahaemolyticus* mainly include: MLSA reveals that pathogenic isolates have a higher genetic diversity than non-pathogenic isolates (de Jesus Hernandez-Diaz et al., 2015). The pathogenic isolates include two hemolysin genes (*tdh* and *trh*) and a horizontally acquired type-three secretion system (T3SS2) (Xu et al., 2015). The comparative genomics method is used to analyze the differences in the genomes of pathogenic and non-pathogenic isolates, and there are more conserved genes in pathogenic isolates (Hazen et al., 2015). Using Whole Gene Sequencing (WGS) characterization, the pathogenic isolates containing *tdh* and *trh* genes account for the highest proportion of increasing cases of *V. parahaemolyticus* each year (Haendiges et al., 2015).

Current researches on *V. parahaemolyticus* have been mostly applied to single strain in pure cultures or in food. Studies have demonstrated that there are differences in the growth kinetics between temperature and salinity leading to pathogenicity and growth rate of the strains. There was an inseparable relationship between environmental factors and strain activity (Fujikawa et al., 2009). *V. parahaemolyticus* had different growth activities under four different temperature conditions (10, 20, 30, and 37°C) (Liu et al., 2016), and found that of the strains at 37°C, 3% had a good growth rate: As the temperature and salinity conditions become increasingly tense, their growth vigor was also more inhibited accordingly. Moreover, only a small amount of research has shown the pathogenicity of *V. parahaemolyticus*, which was present in the small intestine (Ritchie et al., 2012b), but few studies have been done on the growth kinetic parameters of *V. parahaemolyticus* under gastric digestion fluids. And there is also limited knowledge of the pathogenesis of diarrhea caused by *V. parahaemolyticus*. Therefore, it is of great significance to study the heterogeneity of growth of *V. parahaemolyticus* in gastric digestion fluids.

The main virulence factor of *V. parahaemolyticus* is hemolytic toxin—the others are heat-resistant hemolytic toxin (TDH), hemolytic toxin associated with heat-resistant hemolytic toxin (TRH), and heat-labile hemolytic toxin (TLH) (Takahashi et al., 2000; Dou et al., 2013). TDH is an enzyme that can digest the cell walls of blood cells and can produce a β-type hemolytic ring on blood agar medium, called Kanagawa (KP +) (Zhang and Chen, 2018). Almost all pathogens isolated *V. parahaemolyticus* produce a biologically active protein: TDH or TRH. The most direct characterization of the TDH-producing strain is the presence of beta-type hemolysis on the blood-stained plate, which is positive for Kanagawa (KP+) and is used as the most important marker for the pathogenicity of the strain. Pathogenic strains that produce only TRH (trh^+), although negative for KP, also have enterotoxin activity, so these strains are generally considered to be pathogenic strains. Most environmental strains have neither *tdh* nor *trh,* and are called non-pathogenic strains. And epidemiological investigations have shown that the pathogenicity of *V. parahaemolyticus* is highly correlated with TDH (Guo et al., 2014). Otherwise, as a food-borne pathogen that is orally ingested, *V. parahaemolyticus* must survive human digestion to cause disease in humans. It is well known that in the gastric digestion fluids with pH 0.9–1.5, *V. parahaemolyticus* can neither survive nor cause people to become sick. However, the pH value of the stomach will rise rapidly within half an hour after ingestion. Therefore, for the food-borne pathogen *V. parahaemolyticus*, the bacterial concentration reaches 10^4 CFU/ml, while the stomach provides favorable conditions for growth and colonization. It can cause other symptoms, such as diarrhea (Ritchie et al., 2012a).

Maximum growth rate (μ_{max}) and lag time (LT) are the most important parameters for fitting microbiology models. Predicting microbes is a precise method for risk assessment (Lou et al., 2015). Currently, risk assessment studies based on *V. parahaemolyticus* focus on models established by single strains under different environmental conditions (Yang and Jiao, 2008). Few papers have analyzed the differences in the growth kinetic parameters of highly pathogenic *V. parahaemolyticus* from diverse sources. As *V. parahaemolyticus* is the most common pathogenic microorganism in aquatic products, establishing a perfect predictive model has market significance for ensuring the quality of aquatic products and predicting the shelf life of aquatic products.

MATERIALS AND METHODS

Bacterial Strains and Preparation of Inoculum

This study was carried out in accordance with the recommendations of the World Medical Association's Declaration of Helsinki and the Shanghai First Maternity and Infant Hospital Ethics Committee. The protocol was approved by the Shanghai First Maternity and Infant Hospital (ethics approval acceptance number: KS1940). The medical ethics committee approved the project to amend the project according to ethical requirements, conformed to ethical requirements, and agreed to implement it. All subjects gave written informed consent, or written informed consent was provided by parents/guardians for participants that were under the age of 16.

All *V. parahaemolyticus* virulence genes information were identified in our previous studies (Li et al., 2017; Niu et al., 2018a). A total of 50 strains of *V. parahaemolyticus* were used in this study, of which clinical isolates (VPC, n = 23) were recovered from the patients who presented with acute diarrhea in gastroenteritis outpatient clinics in the Shanghai hospital. And each fecal specimen was collected after informed consent was obtained from the patient or, if the patient was a child, from the child's parent/guardian. Environment isolates (VPE, n = 27) were recovered from shrimp in freshwater or seawater in our previous study. The sources and genotypes of all of the strains are listed in **Table 1**. All *V. parahaemolyticus* strains were stored −80°C in 25% glycerol test tubes. Strains were streaked onto a thiosulfate-bile salt-sucrose agar medium (TCBS; Beijing Guotuqiao Technology Co., Ltd., Beijing, China) and cultured at 37°C for 8–12 h. A single colony from TCBS plate was transferred into 9 ml TSB (Beijing Luqiao Technology Co., Ltd., Beijing, China) at pH 8.0 and 3.0% (w/w) NaCl concentration, and then incubated overnight at 37°C and 220 rpm to prepare the test inoculum. The overnight culture was then diluted with 0.1% peptone water (PW; Beijing Luqiao Technology Co., Ltd., Beijing, China) to an optical density (OD) value for 1.2 ± 0.02 (about 10^9 CFU/ml) at 600 nm (OD 600). The automated turbidimetric system Bioscreen C (Oy Growth Curves Ab Ltd., Raisio, Finland) was used to test the corresponding OD values at regular intervals (Niu et al., 2018b).

Preparation of Simulated Digestion Fluids

Simulated human gastric fluids were prepared according to the formula of Minekus simulated digestive fluids (Minekus et al., 2014), and sterilized by 0.22 um filter. 1 M HCl and 1 M NaOH were used to adjust the pH (SGF was 4.0). The gastric fluids should be pre-warmed to 37°C before use, and to avoid precipitation, the $CaCl_2(H_2O)_2$ solutions were finally added to the mixture. The above inoculum was appropriately serially diluted ten-fold with a 0.1% PW solution, mixed with SGF digestion solution, and treated at 37°C, 110 rpm constant temperature shaker for 120 min.

Growth Curve Experiments

Microbial culture growth is often divided into four periods: lag time, logarithmic growth phase, stationary phase, and decay phase. The growth curve has the culture time as the abscissa and the logarithm of the number of bacteria or the growth rate as the ordinate. It represents the dynamic change of the whole process of growth, reproduction, and even death of bacteria in a new suitable environment. The automated turbidity system Bioscreen C (Oy Growth Curves Ab Ltd., Raisio, Finland) is used to detect the OD value of the wideband filter (600 nm) at regular time intervals. Changes in OD value can be observed throughout the total time period. The initial inoculum of each strain prepared was diluted ten-fold with five gradients in TSB. With strain concentration of approximately 10^4 CFU/ml, the inoculated TSB was transferred to a 100-well microtiter plate and then placed in automated turbidimetric system Bioscreen C. Three OD measurement replicates were tested throughout this process. In addition, three independent experiments were performed at each growth condition, and there were three samples per strain completely utilized for testing. In this way, the total OD growth curve described will reach 900 patterns (3 replicates × 3 independent experiments × 2 growth conditions × 50 types of *V. parahaemolyticus*).

Maximum Specific Growth Rate and Lag Time

Following the study by Lianou (Lindqvist, 2006; Alexandra and Koutsoumanis, 2011), the Bioscreen gradient dilution method is used to calculate the maximum specific growth rate of the strain as: $\log(\mathrm{Ni}) = K - \mu_{\max} \times t_{det}$.

In the formula: t_{det} is the time (h) when the OD 600 nm of *V. parahaemolyticus* reaches the Bioscreen C detectable level (10^6–10^7 CFU/mL); $\mu_{\max}$ is the maximum specific growth rate of *V. parahaemolyticus* growth rate [log CFU/(mL h)]; Ni is the initial concentration of *V. parahaemolyticus* (CFU/mL) in the selected sample well; and K is a constant.

Growth Kinetics Fitting: Using the modified Gompertz model, the growth data of *V. parahaemolyticus* under different growth conditions were fitted by Origin Pro 8.0 software (Origin Lab Corp., Northampton, MA, United States).

$$y = A + C \exp\left\{-\exp\left[\frac{\mu_{\mathrm{m}}}{A}(\lambda - t) + 1\right]\right\}$$

were A means the initial total number of bacteria (log CFU/mL), C represents the difference between the maximum bacterial species and the initial bacterial species, log CFU/mL, μ_m represents maximum specific growth rate, λ is the time to reach the relative maximum growth rate (h), and y represents total number of bacteria at time (log CFU/mL).

Statistical Analysis Methods

The prediction model is evaluated through the coefficient of determination R^2, the root mean square error (RMSE), the Fisher's F test P-value, the accuracy factor A_f, the bias factor B_f, and other parameters (Zhang et al., 2015). When R^2 is close to 1, it means that the reference value of its prediction model is

TABLE 1 | The sources and genotypes of 50 strains of *V. parahaemolyticus*.

No	Genotype			Source	No	Genotype			Source
	tlh	*tdh*	*trh*			*tlh*	*tdh*	*trh*	
VPE01	+	−	+	Freshwater	VPE48	+	−	−	Freshwater
VPE02	+	−	−	Seawater	VPE49	+	−	−	Seawater
VPE03	+	−	+	Freshwater	VPC16	+	+	−	Pathogenic
VPE04	+	−	−	Freshwater	VPC18	+	+	−	Pathogenic
VPE05	+	−	−	Seawater	VPC25	+	+	−	Pathogenic
VPE07	+	+	−	Seawater	VPC26	+	+	−	Pathogenic
VPE08	+	−	+	Freshwater	VPC29	+	+	−	Pathogenic
VPE09	+	+	−	Seawater	VPC32	+	+	−	Pathogenic
VPE10	+	+	−	Seawater	VPC36	+	+	−	Pathogenic
VPE11	+	−	−	Seawater	VPC40	+	+	−	Pathogenic
VPE17	+	+	−	Seawater	VPC41	+	+	−	Pathogenic
VPE27	+	−	−	Freshwater	VPC44	+	+	−	Pathogenic
VPE28	+	+	−	Freshwater	VPC45	+	+	−	Pathogenic
VPE29	+	−	+	Freshwater	VPC46	+	+	−	Pathogenic
VPE32	+	−	−	Seawater	VPC47	+	+	−	Pathogenic
VPE36	+	−	+	Freshwater	VPC49	+	+	−	Pathogenic
VPE37	+	+	−	Seawater	VPC50	+	+	−	Pathogenic
VPE38	+	−	−	Freshwater	VPC51	+	+	−	Pathogenic
VPE40	+	−	+	Freshwater	VPC54	+	+	+	Pathogenic
VPE42	+	+	+	Human	VPC55	+	+	−	Pathogenic
VPE43	+	+	−	Human	VPC89	+	+	−	Pathogenic
VPE44	+	−	−	Freshwater	VPC90	+	+	−	Pathogenic
VPE45	+	−	−	Seawater	VPC94	+	−	+	Pathogenic
VPE46	+	−	−	Freshwater	VPC97	+	+	−	Pathogenic
VPE47	+	−	−	Freshwater	VPC100	+	+	−	Pathogenic

higher; otherwise, when it is close to 0, its reference value is lower. When A_f is equal to 1, it means that the predicted value and the observed value are equal. If the A_f value is larger, it indicates that the average accuracy of the model is lower. The B_f value in the range of (0.9–1.05) indicates that the prediction model has a small deviation. The parameter formula of each prediction model is as follows:

$$R^2 = \left[1 - \frac{\sum (\text{pred} - \text{obs})^2}{\sum (\text{obs} - \text{mean})^2}\right]$$

$$\text{RMSE} = \sqrt{\frac{\sum (\text{obs} - \text{pred})^2}{n}}$$

$$A_\text{f} = 10\left(\frac{\sum |\text{L}_\text{g}(\text{pred}/\text{obs})|}{n}\right)$$

$$B_\text{f} = 10\left(\frac{\sum \text{L}_\text{g}(\text{pred}/\text{obs})}{n}\right)$$

Under the condition of gastric digestive fluids treatment, the coefficient of variation (CV) of the μ_{max} is calculated as follows:

$$\text{CV} = \frac{\text{Standard deviation of } \mu_{max}}{\text{Mean value of } \mu_{max}} \times 100\%$$

In addition, a significant difference test using *P*-values was also used to verify differences in growth rates of strains from different conditions. The level of statistical significance ($P < 0.05$) was tested by the least significant difference (LSD) method. Statistical analysis were analyzed using the SPSS statistical package 17.0 (SPSS Inc., Chicago, IL, United States).

RESULTS

Changes in Maximum Growth Rate After Gastric Digestion Fluids Treatment

The growth curves of 50 strains of *V. parahaemolyticus* were measured in an automated turbidity system Bioscreen C. The Modified Gompertz model was used to evaluate μ_{max}(Nauta and Dufrenne, 1999; Boonyawantang et al., 2012). Almost all test values were fitted to the equations given above statistical formula. All RMSE values tended to 0, and A_f and B_f were close to 1. The results showed goodness-of-fit with the Modified Gompertz model.

The maximum specific growth rates of *V. parahaemolyticus* from different sources after treatment with gastric digestive fluids (SGF) are shown in **Figure 1**. As shown in **Figure 1A**, which compares with control groups (before treatment with gastric digestive fluids), the μ_{max} of 89% of environmental *V. parahaemolyticus* strains were significantly reduced. Among them, the μ_{max} (OD × h^{-1}) of VPE01, VPE05, VPE37, and

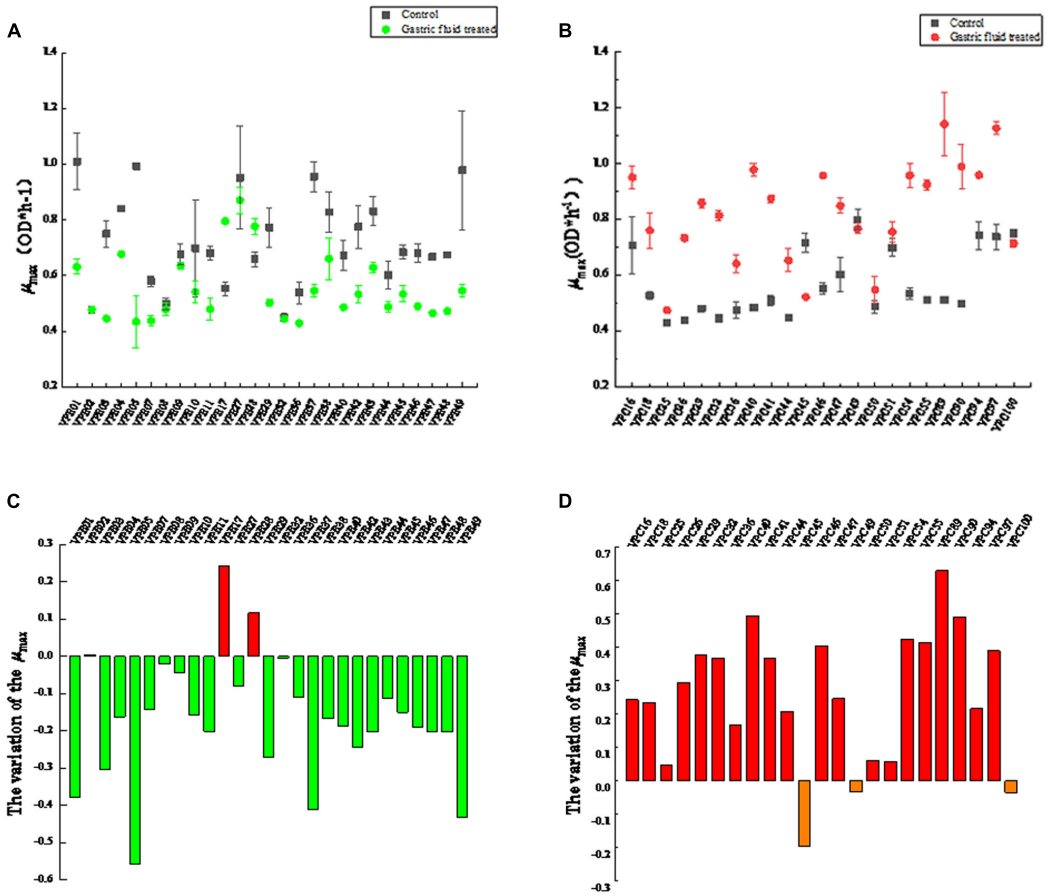

FIGURE 1 | Maximum specific growth rates (μ_{max}) of *V. parahaemolyticus* strains from different sources after SGF. **(A)** Maximum specific growth rate of environmental strains. **(B)** Maximum specific growth rate of pathogenic strains. **(C)** The change of maximum specific growth rate of environmental strains in SGF treatment. **(D)** The change of maximum specific growth rate of pathogenic strains in SGF treatment.

VPE49 decreased sharply. The μ_{max} of VPE01 decreased from 1.001 to 0.63, the μ_{max} of VPE05 went down from 0.889 to 0.434, the μ_{max} of VPE37 dropped from 0.982 to 0.541, and the μ_{max} of VPE49 decreased from 0.979 to 0.565. Results indicated that the μ_{max} of environmental strains treated with gastric fluids were decreased, which had poor tolerance to gastric fluids and poor adaptability to external stress environments.

Interestingly, the μ_{max} changes of the pathogenic *V. parahaemolyticus* were completely opposite to that of environmental strains. The value of μ_{max} ($OD \times h^{-1}$) of most strains were significantly different ($P < 0.01$) between control and treatment groups. As shown in **Figure 1B**, the μ_{max} of most strains fluctuated between 0.4 and 0.6 in control groups. After gastric fluids treatment, the μ_{max} of the strains fluctuated between 0.64 and 1.1, increasing by 1.8 times. Among them, VPC40, VPC89, and VPC90 increased significantly. The μ_{max} of VPC40 increased from 0.483 to 0.979, the μ_{max} of VPC89 increased sharply from 0.511 to the highest point of 1.142, and the μ_{max} of VPC90 increased from 0.498 to 0.989. Also as shown in **Figure 1D**, the μ_{max} changes of VPC40, VPC89, and VPC90 were 0.496, 0.631, and 0.491, respectively. Other pathogenic isolates had increased to varying degrees. Meanwhile, the μ_{max} of VPC45, VPC49, and VPC100 decreased on the contrary: The reductions were 0.196, 0.013, and 0.036, respectively. The reason for these reductions will be the focus of future experiments.

Tendency of Lag Time (LT) (λ)

The biologically accepted definition is the time when a microbial population undergoes a mutation in the environment and begins to reproduce after self-adjustment. In the geometric sense, the microbial lag period refers to the time interval when the logarithmic growth phase of the microorganism reaches the maximum specific growth rate (Aguirre and Koutsoumanis, 2016). The lag time (LT) exhibited changes, as shown in **Figure 2**. The LT of most strains were significantly different ($P < 0.05$) between control and treatment groups. In control groups, the LT values of environment-derived isolates were different, with about 60% of the isolates strains having LT of less than 3 h (**Figure 2A**). The LT of 92.5% of the strains increased in the treatment groups after SGF, on the other hand. Among them, the LT of VPE10 reached a maximum of 6.2965, the LT of VPE27 fell to a low of 2.1563, and the LT of VPE36 and VPE02 fluctuated insignificantly. However, as shown in **Figure 2B**, for pathogenic-derived strains, the LT of the strains was about 3 h,

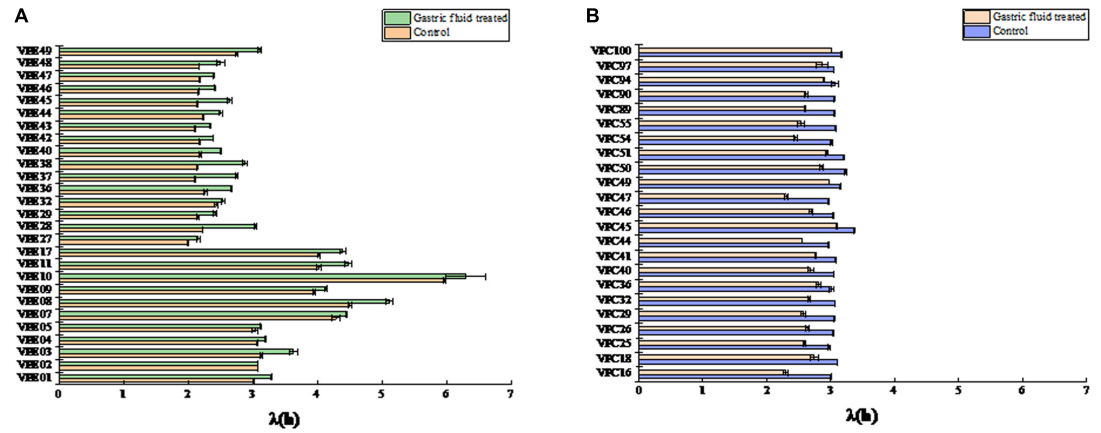

FIGURE 2 | The lag time (λ) of *V. parahaemolyticus* strains from different sources after SGF. **(A)** Lag time (λ) of environmental strains. **(B)** Lag time (λ) of pathogenic strains.

which was not significantly different in control groups. While, after SGF treatment, the LT of almost all pathogenic-derived isolates strains were shortened significantly, and about 91% of the strains had a LT of less than 3 h. The shortening of the pathogenic strains LT corresponded to the stress of gastric fluids treatment.

Evaluation of Growth Variability After SGF

In order to study the effect of SGF treatment on the growth rate of *V. parahaemolyticus*, the growth variability of the strain was studied by coefficient of variation (CV). The maximum specific growth rate and CV values of environmental isolate strains after SGF treatment were shown in **Figure 3A**. After SGF treatment, the maximum specific growth rate of the environmental isolate strains decreased, and the CV value of the strain μ_{max} also fluctuated. When the μ_{max} of VPE1, VPE5, VPE37, and VPE49 decreased the most, the CV values of μ_{max} were 4.3%, 9.5%, 3.9%, and 0.9%, respectively. The results showed that the CV value of μ_{max} of VPE5 was the largest, which revealed the largest growth heterogeneity in the gastric fluids environment, and there was growth heterogeneity between the various strains of *V. parahaemolyticus* after SGF treatment.

Results depicted the difference in the μ_{max} coefficient of variation CV of pathogenic isolate strains after SGF treatment (**Figure 3B**). The CV value of most strains fluctuated between 0.26 and 4.00%. After SGF treatment, the CV value of μ_{max} of VPC18, VPC50, VPC89, and VPC90 increased sharply, which were 8.44, 8.97, 10.07, and 8.17%, respectively. The CV values of μ_{max} of VPC25 and VPC46 fell respectively by 0.55 and 0.26%. The CV values of μ_{max} of pathogenic isolates, which were easier to grow in gastric fluids, were significantly higher than those of environmental isolates. When pathogenic *V. parahaemolyticus* grows to a pathogenic amount in human stomach, it has the potential of causing diarrhea and gastroenteritis.

The CV value of LT was significantly different ($P < 0.01$) between environmental isolates and pathogenic isolates after SGF treatment (**Figure 3C**). As shown in **Figure 3C**, the CV values of LT of environmental isolates fluctuated between 0.16% and 1.50%, while the CV values of LT of VPE03 and VPE48 exceeded 1.5%, which were 1.56 and 2.61%, respectively. As shown in **Figure 3D**, the CV values of LT of pathogenic isolates fluctuated between 0.14 and 1.3%, while all of the CV values of LT of VPC16, VPC18, VPC40, VPC55, and VPC97 strains were larger than the fluctuation range, which were 1.64, 2.29, 1.78, 2.04, and 3.35, respectively. By comparing the growth kinetic parameter, the CV value of μ_{max} and LT more comprehensively represents the growth heterogeneity for *V. parahaemolyticus* strains.

Comparison of Growth Variability From Different Sources

Table 1 shows the sources of different types of *V. parahaemolyticus*, divided into environmental and pathogenic strains. Among them, environmental strains can be roughly divided into two categories: freshwater and seawater. The box diagrams of the four types are: environment group, pathogenic group, different sources strains before SGF treatment, and different sources strains after SGF treatment (**Figure 4**). The average of the maximum specific growth rate μ_{max} was counted, and significant differences were calculated by the *P*-value. In addition, the *P*-values of the differences were 0.001 [environment group, SGF treatment (**Figure 4A**)], 0.000 [pathogen group, SGF treatment (**Figure 4B**)], 0.001 [environment group and pathogenic group before SGF (**Figure 4C**)], and 0.000 [Environment group and pathogenic group after SGF (**Figure 4D**)]. All four groups performed significant difference analysis.

Effects of Genotypes on Growth Variation After Treatment With Different Sources

Genetic heterogeneity has a certain influence on the growth variation of *V. parahaemolyticus*. To further describe the growth characteristics of *V. parahaemolyticus*, 50 strains from different sources (shown in **Table 1**) were classified by genotype.

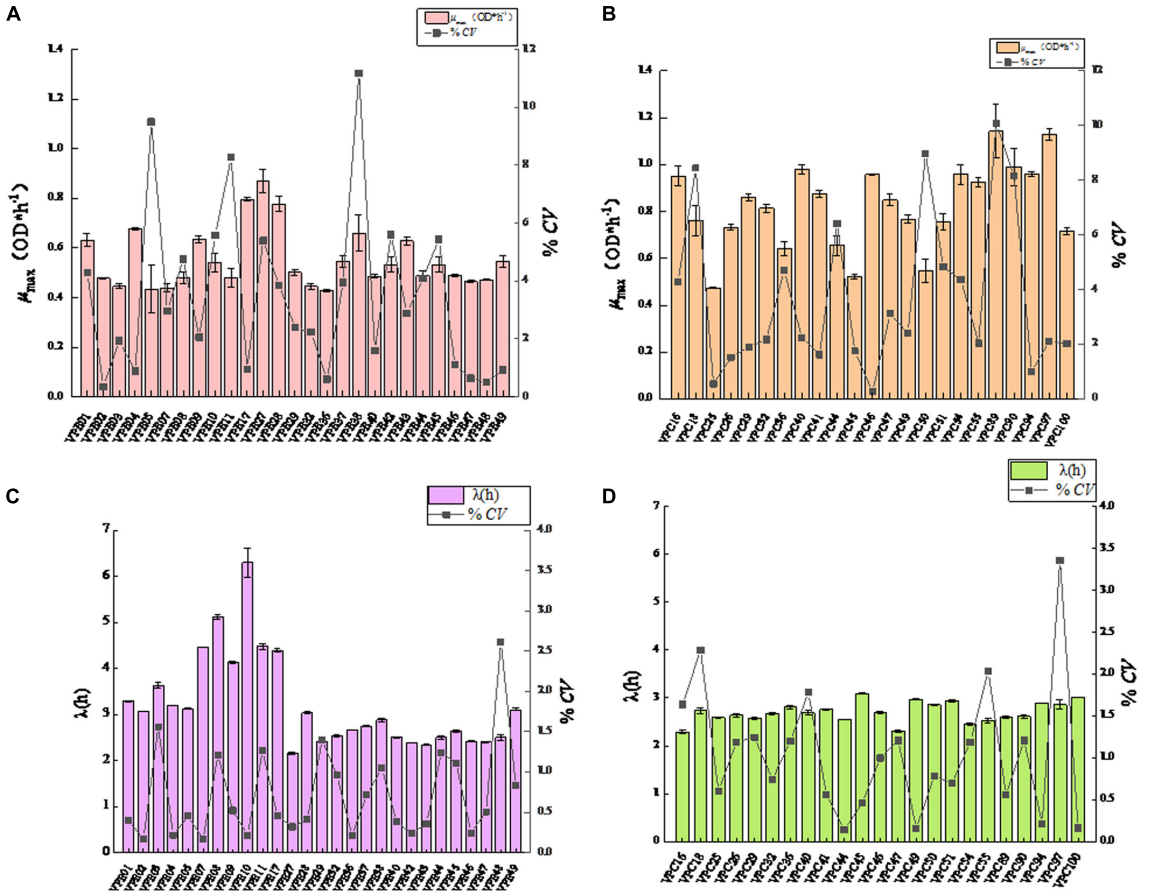

FIGURE 3 | Mean value curve of maximum specific growth rates (μ_{max}) and coefficient of variation curve of μ_{max} among strains (CV-Strain) after SGF treatment. **(A)** Mean value curve of maximum specific growth rates (μ_{max}) and coefficient of variation curve of μ_{max} among strains (CV-Strain) of environmental strain. **(B)** Mean value curve of maximum specific growth rates (μ_{max}) and coefficient of variation curve of μ_{max} among strains (CV-Strain) of pathogenic strain. **(C)** Mean value curve of lag time (λ) and coefficient of variation curve of lag time (λ) among strains (CV-Strain) of environmental strains. **(D)** Mean value curve of lag time (λ) and coefficient of variation curve of lag time (λ) among strains (CV-Strain) of pathogenic strains.

Based on different virulence factors, *V. parahaemolyticus* could be divided into four categories: (1) $tlh^+/tdh^-/trh^-$, (2) $tlh^+/tdh^+/trh^-$, (3) $tlh^+/tdh^-/trh^+$, and (4) $tlh^+/tdh^+/trh^+$ (Letchumanan et al., 2014), which were used to explore the internal causes of the growth variability of *V. parahaemolyticus*. In these virulence genes, all clinical and environmental strains of *V. parahaemolyticus* had been expressed as *tlh* in previous studies (Okada et al., 2009). Today, the most important virulence factors of the recognized *V. parahaemolyticus* are heat-resistant direct hemolysin (TDH) and heat-resistant hemolysin (TRH), which are encoded by the *tdh* and *trh* genes, respectively, as an important basis to distinguish pathogenic and non-pathogenic *V. parahaemolyticus.*

The changes of *V. parahaemolyticus* of different genotypes after SGF treatment are shown in **Figure 5**. In control conditions, $tlh^+/tdh^-/trh^-$ (green) exhibited the maximum growth variability compared to the other three genotypes, which had CV values at higher levels (**Figure 5A**). As shown in **Figure 5B**, $tlh^+/tdh^+/trh^+$ (black) and $tlh^+/tdh^-/trh^+$ (red) performed moderate variability in growth. After SGF treatment, the CV value of $tlh^+/tdh^+/trh^-$ (blue) was the highest of those of other genotypes ($tlh^+/tdh^-/trh^-$, $tlh^+/tdh^-/trh^+$, and $tlh^+/tdh^+/trh^+$).

DISCUSSION

Effects of SGF on Growth Variability

Predictive microbiology model is an important research topic in the field of food safety (Yoon et al., 2008; Stan-Lotter et al., 2010). One should use a modified Gompertz model for growth kinetic analysis of pathogenic and non-pathogenic *V. parahaemolyticus* in broth and oysters, and use two-dimensional models (such as Davey and square root models) to fit lag time and the maximum growth rate (Yoon et al., 2014). Pathogenic *V. parahaemolyticus* strains in *Vannamei* have different growth kinetic parameters (Lou et al., 2015). The prediction model of *V. parahaemolyticus* was used to study the growth variation of pathogenic and non-pathogenic strains. The maximum specific growth rate (μ_{max}) and lag time (LT) are the two most important parameters of

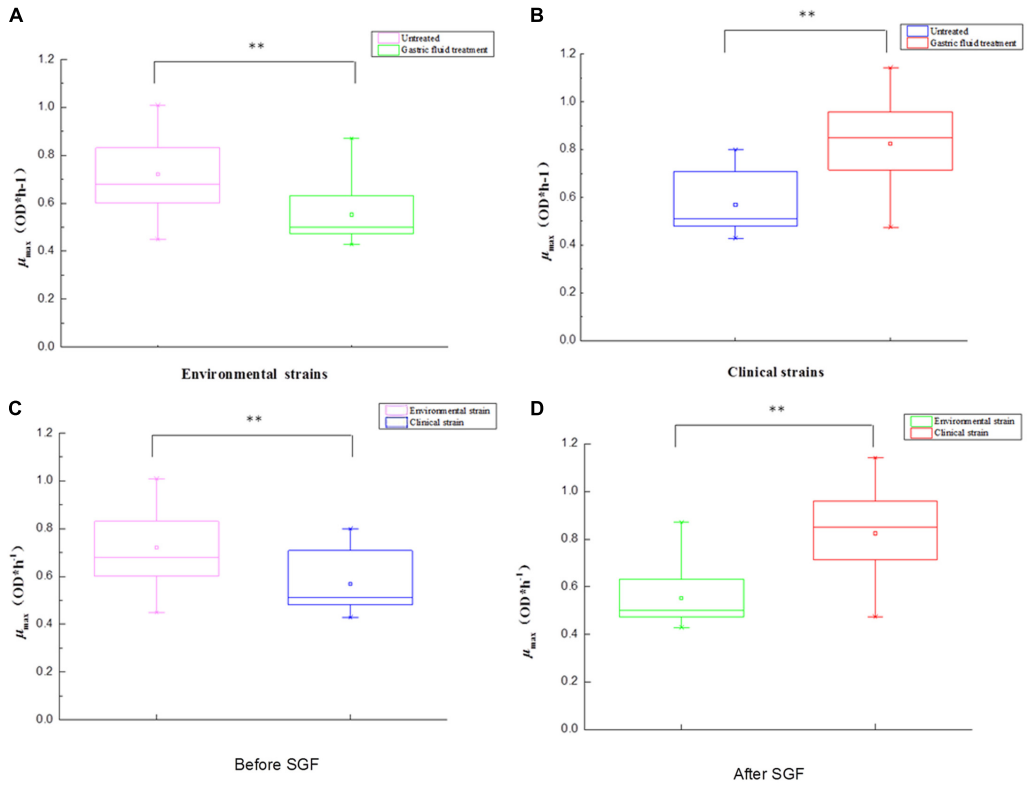

FIGURE 4 | The box plot between environment and pathogens for *V. parahaemolyticus* strains under gastric fluids treatment in the following growth conditions. **(A)** The environmental strains with $P = 0.001$ (control group and SGF treatment). **(B)** The pathogenic strains with $P = 0.000$ (control group and SGF treatment). **(C)** The environmental strains and pathogenic strains with $P = 0.001$ before SGF treatment. **(D)** The environmental strains and pathogenic strains with $P = 0.000$ after SGF treatment. **Statistical significance ($p < 0.05$).

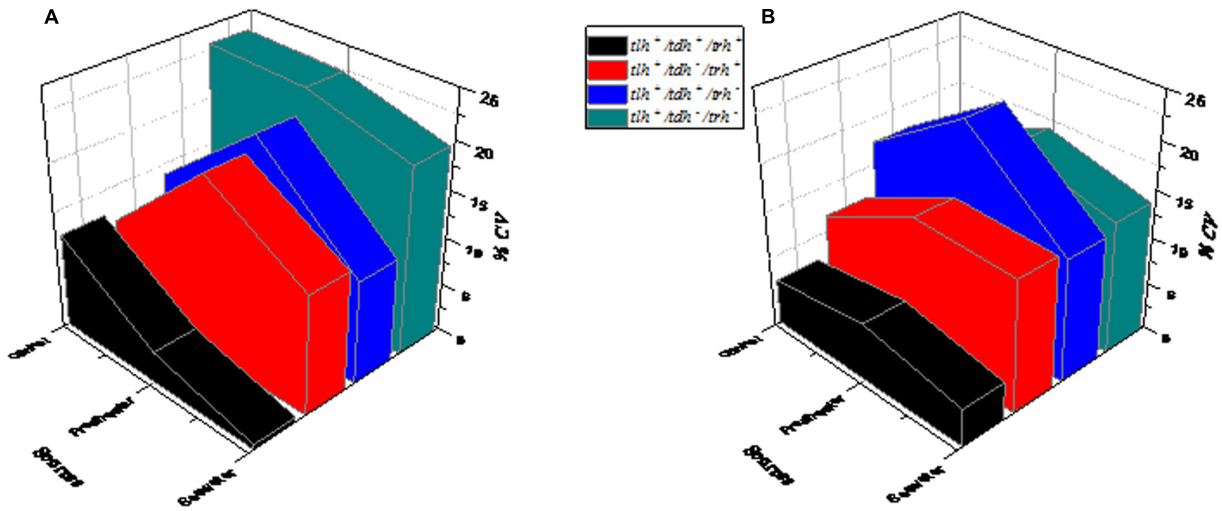

FIGURE 5 | The influence of the genotype on the growth variability of *V. parahaemolyticus* strains from different sources. **(A)** Control group (not treated with SGF). **(B)** After SGF treatment.

microbial dynamics. It was obvious that 37°C was considered to be the optimal growth condition in the control group (**Figure 1**), which had already been verified by the similar completion in laboratory experiments (Baker-Austin et al., 2010; Fernandez-Piquer et al., 2011). However, the most effective obstacle of the survival and onset of *V. parahaemolyticus* is the human stomach.

After SGF treatment, *V. parahaemolyticus* showed different variability. The maximum specific growth rate of environmental strains decreased (**Figure 1A**), while the lag time was increased simultaneously (**Figure 2A**). In fact, most environmental strains were adapted to the natural environment, while SGF was not adjusted to the growth of those strains. Interestingly, the growth of the pathogenic *V. parahaemolyticus* was opposite to SGF stress. The maximum specific growth rate of the pathogenic strains increased (**Figure 1B**), whereas the lag period was shortened (**Figure 2B**). The value of μ_{max} of pathogenic VPC89 was 1.1418, and the lag time was only 2.59 h. This data indicates that VPC89 had a short lag time, rapidly entered into the log phase, which grew rapidly to reach the maximum bacterial concentration in a short time. Studies have shown that the length of the lag time can reflect the strain's ability to respond to the new environment. The CV value of μ_{max} and LT more clearly reflected the heterogeneity of *V. parahaemolyticus* after SGF (**Figure 3**). And the pathogenic bacteria was significantly different ($P < 0.01$) than that of environmental strains (**Figure 4**), which meant the pathogenic bacteria had a stronger ability to adapt to the SGF environment. This situation brought certain risks to food control and to human health (Arroyo-Lopez et al., 2014).

Impact of SGF on Pathogenicity

In this study, the differences in maximum growth rates and lag time between pathogenic and non-pathogenic isolates were observed after SGF treatment. The *V. parahaemolyticus* with high maximum growth rates in SGF generally presented a positive correlation with virulence factors and pathogenicity. Extracellular enzymes, endotoxin lipopolysaccharides, and heat-labile capsular polysaccharides have enhanced the pathogenicity of pathogenic strains. The pathogenic *V. parahaemolyticus* contains the *tdh* gene (Petronella and Ronholm, 2018), which is located in the coding region adjacent to the chromosome. The *tdh* gene with genetic characteristics was more easily expressed than the *trh* gene during SGF (Yoshitsugu et al., 2013; Shimohata and Takahashi, 2010).

According to the strain information data collected in **Table 1**, since there was only one strain containing $tlh^+/tdh^+/trh^+$, the characteristics of this genotype would not be typical, and the black curve provided some references for different trends. Besides, the genotype $tlh^+/tdh^+/trh^-$ is found in almost all pathogenic isolated strains. In addition, the secretory systems of *V. parahaemolyticus* play an indispensable role in the pathogenesis. Almost all pathogenic *V. parahaemolyticus* have a type III secretion system (T3SS), which is the main contributor to the pathogenicity of *V. parahaemolyticus* (Rohinee et al., 2012). The type III secretion system is a bacterial protein secretion device, which mediates bacterial cytotoxicity in a manner that induces programmed cell death or autophagy of host cells (Kwon-Sam et al., 2004; Okada et al., 2010). Li et al. (2016) reported that the *vtr*A/*vtr*C complex of *V. parahaemolyticus* can induce *vtr*B to activate T3SS2, and *vtr*A and *vtr*B deletion mutants cannot produce TDH and T3SS2 related proteins (Gotoh et al., 2010). *vop*V, *vop*Z, and *vop*L are the three major secretory effector proteins of T3SS2, and they play an important role in the pathogenicity and intestinal colonization of hemolytic *V. parahaemolyticus*.

These facts indicated that the maximum growth rate of pathogenic strains was increased, the lag time was decreased after SGF treatment, and the CV values of genotypes ($tlh^+/tdh^+/trh^-$) increased evidently more than those of other genotypes ($tlh^+/tdh^-/trh^-$, $tlh^+/tdh^-/trh^+$ and $tlh^+/tdh^+/trh^+$), as shown in **Figure 5**. Therefore, the results suggested a relationship between the expression of virulence genes and the ($tlh^+/tdh^+/trh^-$) genotype of *V. parahaemolyticus*, and it was more adaptable to the changes of gastric fluids environment.

CONCLUSION

The growth kinetics characteristics of 50 pathogenic and non-pathogenic *V. parahaemolyticus* strains with different genotypes and from different sources were determined in simulated gastric fluids. Compared to the control group, the μ_{max} of 87% of pathogenic strains significantly increased, while the μ_{max} of 89% of non-pathogenic strains decreased. However, the LT of all pathogenic strains was shortened, and the LT of all non-pathogenic strains was prolonged in simulated gastric fluids. Meanwhile, the CV values of genotypes ($tlh^+/tdh^+/trh^-$) increased evidently more than those of other genotypes ($tlh^+/tdh^-/trh^-$, $tlh^+/tdh^-/trh^+$, and $tlh^+/tdh^+/trh^+$). Therefore, more attention should be paid to the clinical genotypes ($tlh^+/tdh^+/trh^-$) associated with severe virulence, which is of great significance for the prevention and maintenance of human health. The generated knowledge will facilitate the incorporation of strain variability in predictive microbiology and microbial risk assessment and will hence provide an efficient way and scientific guidance to control the pathogens in the food industry.

DATA AVAILABILITY STATEMENT

All datasets generated for this study are included in the article/supplementary material.

AUTHOR CONTRIBUTIONS

YZ, YP, and HL conceived and supervised the study. YW designed and performed the experiments, analyzed the data, and wrote the manuscript. YZ and HL revised the manuscript.

FUNDING

This research was supported by the National Natural Science Foundation of China (31671779 and 31972188), the National Key R&D Program of China (2018YFC1602205 and 2018YFC1602200), the Shanghai Agriculture Applied Technology Development Program (T20170404), and the Innovation Program of Shanghai Municipal Education Commission (2017-01-07-00-10-E00056).

REFERENCES

Aguirre, J. S., and Koutsoumanis, K. P. (2016). Towards lag phase of microbial populations at growth-limiting conditions: the role of the variability in the growth limits of individual cells. *Int. J. Food Microbiol.* 2016, 1–6. doi: 10.1016/j.ijfoodmicro.2016.01.021

Alexandra, L., and Koutsoumanis, K. P. (2011). Effect of the growth environment on the strain variability of *Salmonella enterica* kinetic behavior. *Food Microbiol.* 28, 828–837. doi: 10.1016/j.fm.2010.04.006

Alonsohernando, A., Alonsocalleja, C., and Capita, R. (2013). Growth kinetic parameters of Gram-positive and Gram-negative bacteria on poultry treated with various chemical decontaminants. *Food Control* 33, 429–432. doi: 10.1016/j.foodcont.2013.03.009

Arroyo-Lopez, F. N., Blanquet-Diot, S., Denis, S., Thevenot, J., Chalancon, S., Alric, M., et al. (2014). Survival of pathogenic and lactobacilli species of fermented olives during simulated human digestion. *Front. Microbiol.* 5:540. doi: 10.3389/fmicb.2014.00540

Baker-Austin, C., Stockley, L., Rangdale, R., and Martinez-Urtaza, J. (2010). Environmental occurrence and clinical impact of *Vibrio vulnificus* and *Vibrio parahaemolyticus*: a european perspective. *Environ. Microbiol. Rep.* 2, 7–18. doi: 10.1111/j.1758-2229.2009.00096.x

Boonyawantang, A., Mahakarnchanakul, W., Rachtanapun, C., and Boonsupthip, W. (2012). Behavior of pathogenic *Vibrio parahaemolyticus* in prawn in response to temperature in laboratory and factory. *Food Control* 26, 479–485. doi: 10.1016/j.foodcont.2012.02.009

de Jesus Hernandez-Diaz, L., Leon-Sicairos, N., Velazquez-Roman, J., Flores-Villasenor, H., Guadron-Llanos, A. M., Javier Martinez-Garcia, J., et al. (2015). A pandemic *Vibrio parahaemolyticus* O3:K6 clone causing most associated diarrhea cases in the Pacific Northwest coast of Mexico. *Front. Microbiol.* 6:221. doi: 10.3389/fmicb.2015.00221

Dou, Y., Pei-Hong, H. U., and Peng-Cheng, G. U. (2013). Research progress in *Vibrio parahaemolyticus* TDH toxin and detection methods. *Mod. Food Sci. Technol.* 29, 215–218.

Fernandez-Piquer, J., Bowman, J. P., Ross, T., and Tamplin, M. L. (2011). Predictive models for the effect of storage temperature on *Vibrio parahaemolyticus* viability and counts of total viable bacteria in pacific oysters (*Crassostrea gigas*). *Appl. Environ. Microbiol.* 77, 8687–8695. doi: 10.1128/aem.05568-5511

Fujikawa, H., Kimura, B., and Fujii, T. (2009). Development of a predictive program for *Vibrio parahaemolyticus* growth under various environmental conditions. *Biocontrol Sci.* 14:127. doi: 10.4265/bio.14.127

Gotoh, K., Kodama, T., Hiyoshi, H., Izutsu, K., Park, K.-S., Dryselius, R., et al. (2010). Bile acid-induced virulence gene expression of *Vibrio parahaemolyticus* Reveals a novel therapeutic potential for bile acid sequestrants. *PLoS One* 5:e13365. doi: 10.1371/journal.pone.0013365

Guo, Z., Cui, X., Wang, J., Sun, X., Pan, Y., and Zhao, Y. (2014). Metabolome response to tdh expression of pathogenic *Vibrio parahaemolyticus* induced by different temperatures. *Acta Microbiol. Sin.* 54, 882–888.

Haendiges, J., Timme, R., Allard, M. W., Myers, R. A., Brown, E. W., and Gonzalez-Escalona, N. (2015). Characterization of *Vibrio parahaemolyticus* clinical strains from Maryland (2012-2013) and comparisons to a locally and globally diverse *V. parahaemolyticus* strains by whole-genome sequence analysis. *Front. Microbiol.* 6:125. doi: 10.3389/fmicb.2015.00125

Hazen, T. H., Lafon, P. C., Garrett, N. M., Lowe, T. M., Silberger, D. J., Rowe, L. A., et al. (2015). Insights into the environmental reservoir of pathogenic *Vibrio parahaemolyticus* using comparative genomics. *Front. Microbiol.* 6:204. doi: 10.3389/fmicb.2015.00204

Jing, J. W., Wen, S. S., Meng, T. J., Hai, Q. L., Zhang, W., Xiao, H. S., et al. (2014). Fate of *Vibrio parahaemolyticus* on shrimp after acidic electrolyzed water treatment. *Int. J. Food Microbiol.* 179, 50–56. doi: 10.1016/j.ijfoodmicro.2014.03.016

Jun, I. J., Kim, Y. H., Kim, M. J., Hwang, H. S., Lee, T. H., and Cha, J. (2003). Isolation and characterization of mucinase complex secreted from *Vibrio parahaemolyticus*. *J. Microbiol. Biotechnol.* 13, 731–737.

Kwon-Sam, P., Takahiro, O., Mitsuhiro, R., Myoung-Ho, J., Kazuhisa, O., Tetsuya, I., et al. (2004). Functional characterization of two type III secretion systems of *Vibrio parahaemolyticus*. *Infect. Immun.* 72:6659. doi: 10.1128/IAI.72.11.6659-6665.2004

Letchumanan, V., Chan, K. G., and Lee, L. H. (2014). *Vibrio parahaemolyticus*: a review on the pathogenesis, prevalence, and advance molecular identification techniques. *Front. Microbiol.* 5:705. doi: 10.3389/fmicb.2014.00705

Letchumanan, V., Yin, W.-F., Lee, L.-H., and Chan, K.-G. (2015). Prevalence and antimicrobial susceptibility of *Vibrio parahaemolyticus* isolated from retail shrimps in Malaysia. *Front. Microbiol.* 6:33. doi: 10.3389/fmicb.2015.00033

Li, H., Tang, R., Lou, Y., Cui, Z., Chen, W., Hong, Q., et al. (2017). A comprehensive epidemiological research for clinical *Vibrio parahaemolyticus* in shanghai. *Front. Microbiol.* 8:1043. doi: 10.3389/fmicb.2017.01043

Li, P., Rivera-Cancel, G., Kinch, L. N., Salomon, D., Tomchick, D. R., Grishin, N. V., et al. (2016). Bile salt receptor complex activates a pathogenic type III secretion system. *eLife* 5:e15718. doi: 10.7554/elife.15718

Lindqvist, R. (2006). Estimation of Staphylococcus aureus growth parameters from turbidity data: characterization of strain variation and comparison of methods. *Appl. Environ. Microbiol.* 72, 4862–4870. doi: 10.1128/AEM.00251-256

Liu, B., Liu, H., Pan, Y., Xie, J., and Zhao, Y. (2016). Comparison of the effects of environmental parameters on the growth variability of *Vibrio parahaemolyticus* coupled with strain sources and genotypes analyses. *Front. Microbiol.* 7:994. doi: 10.3389/fmicb.2016.00994

Lou, Y., Zhang, Z. H., Xiao, L. L., Guo, D. F., Liu, H. Q., Pan, Y. J., et al. (2015). Growth kinetic parameters of multi-drug and single-drug resistant *Vibrio parahaemolyticus* strains in pure culture and in *Penaeus vannamei*. *Mod. Food Sci. Technol.* 31, 181–186.

Minekus, M., Alminger, M., Alvito, P., Ballance, S., Bohn, T., Bourlieu, C., et al. (2014). A standardised static in vitro digestion method suitable for food – an international consensus. *Food Funct.* 5, 1113–1124. doi: 10.1039/c3fo60702j

Nauta, M. J., and Dufrenne, J. B. (1999). Variability in growth characteristics of different E. *coli O*157:H7 isolates, and its implications for predictive microbiology. *Quant. Microbiol.* 1, 137–155. doi: 10.1023/a:1010087808314

Niu, B., Hong, B., Zhang, Z., Mu, L., Malakar, P. K., Liu, H., et al. (2018a). A novel qPCR method for simultaneous detection and quantification of viable pathogenic and non-pathogenic *Vibrio parahaemolyticus* (tlh plus, tdh plus, and ureR(+)). *Front. Microbiol.* 9:1747. doi: 10.3389/fmicb.2018.01747

Niu, B., Mu, L., Xiao, L., Zhang, Z., Malakar, P. K., Liu, H., et al. (2018b). Reduction of infection risk meditated by co-culturing *Vibrio parahaemolyticus* and *Listeria monocytogenes* in refrigerated cooked shrimp. *J. Sci. Food Agric.* 98, 4454–4461. doi: 10.1002/jsfa.8969

Nordstrom, J., Vickery, M., Blackstone, G., and Murray, S. A. (2007). Development of a multiplex real-time PCR assay with an internal amplification control for the detection of total and pathogenic *Vibrio parahaemolyticus* bacteria in oysters. *Appl. Environ. Microbiol.* 73, 5840–5847. doi: 10.1128/AEM.00460-467

Obaidat, M. M., Salman, A., and Roess, A. A. (2017). Virulence and antibiotic resistance of *Vibrio parahaemolyticus* isolates from seafood from three developing countries and of worldwide environmental, seafood, and clinical isolates from 2000 to 2017. *J. Food Prot.* 80:2060. doi: 10.4315/0362-028X.JFP-17-156

Okada, N., Iida, T., Park, K.-S., Goto, N., Yasunaga, T., Hiyoshi, H., et al. (2009). Identification and characterization of a novel type III secretion system in trh-positive *Vibrio parahaemolyticus* strain TH3996 reveal genetic lineage and diversity of pathogenic machinery beyond the species level. *Infect. Immun.* 77, 904–913. doi: 10.1128/iai.01184-1188

Okada, N., Matsuda, S., Matsuyama, J., Park, K. S., de los Reyes, C., Kogure, K., et al. (2010). Presence of genes for type III secretion system 2 in *Vibrio mimicus* strains. *BMC Microbiol.* 10:302. doi: 10.1186/1471-2180-10-302

Petronella, N., and Ronholm, J. (2018). The mechanisms that regulate *Vibrio parahaemolyticus* virulence gene expression differ between pathotypes. *Microb. Genom.* 4:9. doi: 10.1099/mgen.0.000182

Ritchie, J. M., Haopeng, R., Xiaohui, Z., Tetsuya, I., Toshio, K., Susuma, I., et al. (2012a). Inflammation and disintegration of intestinal villi in an experimental model for *Vibrio parahaemolyticus*-induced diarrhea. *PLoS Pathog.* 8:e1002593. doi: 10.1371/journal.ppat.1002593

Ritchie, J. M., Rui, H., Zhou, X., Iida, T., Kodoma, T., Ito, S., et al. (2012b). Inflammation and disintegration of intestinal villi in an experimental model for *Vibrio parahaemolyticus*-induced diarrhea. *PLoS Pathog.* 8:e1002593.

Rohinee, P., Hamel, O. S., Asta, S., and Martin, L. (2012). Genetic diversity of clinical and environmental *Vibrio parahaemolyticus* strains from the Pacific

Northwest. *Appl. Environ. Microbiol.* 78, 8631–8638. doi: 10.1128/AEM.01531-12

Shimohata, T., and Takahashi, A. (2010). Diarrhea induced by infection of *Vibrio parahaemolyticus*. *J. Med. Invest.* 57, 179–182. doi: 10.2152/jmi.57.179

Stan-Lotter, H., Fendrihan, S., Dornmayr-Pfaffenhuemer, M., Gerbl, F., Legat, A., Gruber, C., et al. (2010). Presence of T3SS2 and other virulence-related genes in tdh -negative *Vibrio parahaemolyticus* environmental strains isolated from marine samples in the area of the Venetian Lagoon, Italy. *FEMS Microbiol. Ecol.* 70, 506–514. doi: 10.1111/j.1574-6941.2009.00764.x

Takahashi, A., Kenjyo, N., Imura, K., Myonsun, Y., and Honda, T. (2000). Cl-Secretion in colonic epithelial cells induced by the *Vibrio parahaemolyticus* hemolytic toxin related to thermostable direct hemolysin. *Infect. Immun.* 68, 5435–5438. doi: 10.1128/iai.68.9.5435-5438.2000

Xu, F., Ilyas, S., Hall, J. A., Jones, S. H., Cooper, V. S., and Whistler, C. A. (2015). Genetic characterization of clinical and environmental *Vibrio parahaemolyticus* from the Northeast USA reveals emerging resident and non-indigenous pathogen lineages. *Front. Microbiol.* 6:272. doi: 10.3389/fmicb.2015.00272

Yamasaki, S., Migita, Y., Nakamura, M., Ura, N., Harakudo, Y., Misawa, N., et al. (2009). Effect of environmental factors on the occurrence of *Vibrio vulnificus* in costal waters of nagasaki prefecture, Japan. *J. Jpn. Vet. Med. Assoc.* 62, 649–655. doi: 10.12935/jvma.62.649

Yang, Z. Q., and Jiao, X. A. (2008). Molecular characterization and microbial growth kinetics model of *Vibrio parahaemolyticus* isolates from different sources. *Chin. J. Zoon.* 24, 210–215.

Yoon, J. H., Bae, Y. M., Jung, S. Y., Cha, M. H., Ryu, K., Park, K. H., et al. (2014). Predictive modeling for the growth of *Listeria monocytogenes* and *Salmonella Typhimurium* on fresh-cut cabbage at various temperatures. *J. Korean Soc. Appl. Biol. Chem.* 57, 631–638. doi: 10.1007/s13765-014-4096-y

Yoon, K. S., Min, K. J., Jung, Y. J., Kwon, K. Y., Lee, J. K., and Oh, S. W. (2008). A model of the effect of temperature on the growth of pathogenic and nonpathogenic *Vibrio parahaemolyticus* isolated from oysters in Korea. *Food Microbiol.* 25, 635–641. doi: 10.1016/j.fm.2008.04.007

Yoshitsugu, N., Jun, O., Tetsuya, I., and Mitsuaki, N. (2013). The urease gene cluster of *Vibrio parahaemolyticus* does not influence the expression of the thermostable direct hemolysin (TDH) gene or the TDH-related hemolysin gene. *Microbiol. Immunol.* 47, 233–239. doi: 10.1111/j.1348-0421.2003.tb03392.x

Zhang, H., and Chen, M. (2018). Comparison of different methods to identify tdh-positive pathogenic *Vibrio parahaemolyticus* isolates. *Curr. Microbiol.* 75, 1–5. doi: 10.1007/s00284-017-1332-1339

Zhang, Z., Liu, H., Lou, Y., Xiao, L., Liao, C., Malakar, P. K., et al. (2015). Quantifying viable *Vibrio parahaemolyticus* and *Listeria monocytogenes* simultaneously in raw shrimp. *Appl. Microbiol. Biotechnol.* 99, 6451–6462.

Conflict of Interest: The authors declare that the research was conducted in the absence of any commercial or financial relationships that could be construed as a potential conflict of interest.

Copyright © 2020 Wang, Zhao, Pan and Liu. This is an open-access article distributed under the terms of the Creative Commons Attribution License (CC BY). The use, distribution or reproduction in other forums is permitted, provided the original author(s) and the copyright owner(s) are credited and that the original publication in this journal is cited, in accordance with accepted academic practice. No use, distribution or reproduction is permitted which does not comply with these terms.

frontiers in Microbiology

ORIGINAL RESEARCH
published: 26 June 2020
doi: 10.3389/fmicb.2020.01450

Gut Microbiota Metabolite Fights Against Dietary Polysorbate 80-Aggravated Radiation Enteritis

Yuan Li[1†], Huiwen Xiao[1†], Jiali Dong[1], Dan Luo[1], Haichao Wang[1,2,3], Shuqin Zhang[1], Tong Zhu[1], Changchun Zhu[1], Ming Cui[1] and Saijun Fan[1]**

[1] Tianjin Key Laboratory of Radiation Medicine and Molecular Nuclear Medicine, Institute of Radiation Medicine, Chinese Academy of Medical Sciences and Peking Union Medical College, Tianjin, China, [2] Department of Emergency Medicine, North Shore University Hospital, Manhasset, NY, United States, [3] Laboratory of Emergency Medicine, The Feinstein Institute for Medical Research, Manhasset, NY, United States

OPEN ACCESS

Edited by:
Margarita Aguilera, University of Granada, Spain

Reviewed by:
Emilie Viennois, INSERM U1149 Centre de Recherche sur l'Inflammation, France
Alexander Rodriguez-Palacios, Case Western Reserve University, United States

***Correspondence:**
Ming Cui
cuiming0403@bjmu.edu.cn
Saijun Fan
fansanjun@irm-cams.ac.cn

[†] *These authors have contributed equally to this work*

Specialty section:
This article was submitted to Microbial Symbioses, a section of the journal Frontiers in Microbiology

Received: *19 December 2019*
Accepted: *04 June 2020*
Published: *26 June 2020*

Citation:
Li Y, Xiao H, Dong J, Luo D, Wang H, Zhang S, Zhu T, Zhu C, Cui M and Fan S (2020) Gut Microbiota Metabolite Fights Against Dietary Polysorbate 80-Aggravated Radiation Enteritis. Front. Microbiol. 11:1450. doi: 10.3389/fmicb.2020.01450

Radiation therapy is a cornerstone of modern management methods for malignancies but is accompanied by diverse side effects. In the present study, we showed that food additives such as polysorbate 80 (P80) exacerbate irradiation-induced gastrointestinal (GI) tract toxicity. A 16S ribosomal RNA high-throughput sequencing analysis indicated that P80 consumption altered the abundance and composition of the gut microbiota, leading to severe radiation-induced GI tract injury. Mice harboring fecal microbes from P80-treated mice were highly susceptible to irradiation, and antibiotics-challenged mice also represented more sensitive to radiation following P80 treatment. Importantly, butyrate, a major metabolite of enteric microbial fermentation of dietary fibers, exhibited beneficial effects against P80 consumption-aggravated intestinal toxicity via the activation of G-protein-coupled receptors (GPCRs) and maintenance of the intestinal bacterial composition in irradiated animals. Moreover, butyrate had broad therapeutic effects on common radiation-induced injury. Collectively, our findings demonstrate that P80 are potential risk factors for cancer patients during radiotherapy and indicate that butyrate might be employed as a therapeutic option to mitigate the complications associated with radiotherapy.

Keywords: emulsifier, radiation enteropathy, intestinal microbiota, gut microbiota metabolite, GPR43

INTRODUCTION

Pelvic and abdominal cancers are common malignancies affecting gastrointestinal (GI), genitourinary and gynecologic functions (Pal et al., 2019). Due to their large sizes and ease of spread to other abdominal organs and the lymphatic system, pelvic and abdominal cancers are increasingly being routinely treated via radiotherapy (Liauw et al., 2013; Citrin, 2017). After radiotherapy, many patients with pelvic and abdominal cancers suffer from GI syndromes (GIS) (Peterson et al., 2010; Hauer-Jensen et al., 2014), such as malabsorption, bacterial enteritis and diarrhea, which adversely affect treatment and can even lead to death. These acute and chronic complications have become major challenges for radiation oncologists and medical physicists. Therefore, the identification of potential risk factors that may negatively influence the prognosis of cancer patients after radiotherapy and development of novel therapeutic approaches are urgently needed.

Emulsifiers are a class of detergent-like molecules that are commonly added to processed foods, pharmaceutical preparations and cosmetics. Commonly used dietary emulsifiers include Tween, Span, sodium stearyl lactate (SSL) and propylene glycol esters of fatty acids. For example, Tween 80 (or polysorbate-80, P80) is a widely used food additive that lends a smooth and stable consistency to cake, chocolate, ice cream and other packaged snacks. In addition, P80 is also used as a dispersal agent, solubilizer and stabilizer for insoluble medicinal preparations (e.g., etoposide and docetaxel injections) for cancer therapy (Iusuf et al., 2015; Al-Ali et al., 2018). Because of its potential toxicity and carcinogenicity, P80 has been used in limited doses (up to 1.0%) (Food Safety Commission [of Japan], 2007; Roberts et al., 2013). However, the growing consumption of P80 over the past half-century is associated with the increasing incidence of various chronic inflammatory and metabolic diseases (Chassaing et al., 2015), particularly in conjunction with alterations in the compositions and translocation of the intestinal microbiota (Roberts et al., 2010). Ironically, cancer patients would be given foods and medicines containing P80 during radiotherapy. Therefore, whether consumption of P80 adversely impairs the efficacy of radiotherapy remains poorly understood.

The GI tract is inhabited by a community of trillions of microbes that are collectively termed the gut microbiota (Gopalakrishnan et al., 2018). The gut microbiota provides crucial benefits to hosts, including the facilitation of food digestion and development of the metabolic and immune systems (Holmes et al., 2012; Wrzosek et al., 2013). Meanwhile, perturbance or translocation of enteric microbes may also result in a series of pathological processes (Clemente et al., 2012; Lichtman et al., 2016), such as chronic colitis (Gevers et al., 2014), *Clostridium difficile*-associated disease (Ghose, 2013; Peng et al., 2018) and Crohn's disease (Mottawea et al., 2016). Disorders of the gut microbiota are also comorbid with a series of psychiatric illnesses and systemic metabolic diseases, such as anxiety (Heijtz et al., 2011), human immunodeficiency virus (HIV) infection (Sun et al., 2016) and non-alcoholic fatty liver disease (Chu et al., 2019). Indeed, substantial evidence suggests a positive association between radiotherapy and the development of colitis (Kirsch et al., 2010; Andreyev et al., 2013), as well as significant alterations of the composition of the gut microbiota after radiotherapy (Cui et al., 2016, 2017a).

In this study, we aimed to determine whether P80 consumption leads to detrimental alteration of the gut microbiota and exacerbates radiation-induced intestinal injury (RIII). Our observations demonstrated that P80 consumption altered the composition of the gut microbiota and worsened radiation-induced GI toxicity. Importantly, administration of butyrate by the oral route mitigated the harmful effects of P80 in irradiated animals. Taken together, our findings identified that P80 is a risk factor for cancer patients during radiotherapy and indicated that butyrate might be employed as a therapeutic option for protection against radiation-associated GI toxicity in preclinical settings.

MATERIALS AND METHODS

Animals

This experiment tested groups (12 mice per group) of 6–8 weeks old male C57BL/6J mice, housed using Individual Ventilated Cage as six mice per cage to provide a study power of 80%. Experimental mice were treated with 200 ul P80 (1.0% in sterile water) administered via oral route for 7 days, sterile water was used as control. No specialist equipment was used. Cyclical bias were controlled as follows. Mice were randomly allocated to treatment groups, no more than six mice per cage to ensure the active area of each mouse was not less than 0.01 m^2. Mice were maintained on clean sawdust substrates and fed an autoclaved (60 min wet cycle) pellet food (Cat#1022, HFK Bioscience, Beijing, China, ≤5%CHO, ≥18%PRO, ≥4%FAT/kg) and autoclaved filtered water (pH around 5) *ad libitum*. To prevent dirty bedding, the bedding material were changed every 2 days and mice in the same cohort were blended and re-separated every 2 days throughout the whole experiments to avoid the effects of coprophagy on gut microbiome. Food/water were replaced every 4 days. A co-housing protocol was used before the start of all experiments. Fresh murine feces were collected routinely in the morning the day after cage replacement and stored for about 30 days at −80°C until analysis.

Polysorbate-80 (P80) Administration

P80 was purchased from Sigma (Spain, Cat#59924). In this study, P80 consumption was performed by oral gavage of 200 μl for 7 days (the concentration of P80, 1.0% in sterile water) to mice before exposed to abdominal irradiation and last until the end of the experiment. The same water was used as vehicle for the water-treated group (control).

Radiation-Induced Intestinal Injury Model

A Gammacell® 40 Exactor (Atomic Energy of Canada Lim, Canada) was used for all experiments. Male (approximately 20 g in body weight) mice were treated with a single dose of 12 Gy or 15 Gy γ-ray at a rate of 1.0 Gy/min (test by dose rate meter carried by the Exactor) total abdominal irradiation (TAI) using a specific steel chamber, and radiation dose was monitored by a dose rate meter. After irradiation, the mice were returned to the animal facility for daily observation and treatment as described above. Mice in all groups were monitored for survival status throughout the 30-day course of the experiment, and then sacrificed to collect tissue samples for gross structural and functional examinations.

Hematoxylin and Eosin (HE) Staining

Following euthanasia, the small intestines and colons of mice were fixed in 4% buffered formalin overnight at room temperature and then embedded in paraffin. Tissues were sectioned at 5 μm thickness and dipped in hematoxylin and eosin (Solarbio, China) using standard protocols.

Periodic Acid-Schiff (PAS) Staining

Small intestine tissues were fixed in Carnoy (60% dry ethanol, 30% chloroform, 10% glacial acetic acid) (Jiangtian Chemical Technology, China) solution overnight, and 5 μm paraffin sections were deparaffinized and oxidized in 1% periodic acid (Solarbio, China) for 10 min, after rinsing, tissues were incubated in Schiff's reagent (Solarbio, China) for 10 min, washed in warm water, and counterstained with hematoxylin (Solarbio, China) for 30 s, washed and dehydrated before mounting.

Fecal Microbiota Analysis

For this study, stool samples were freshly collected from five mice in different cages as described before (Cui et al., 2017b), and then stored at −80°C until use. DNA was extracted from the stool samples using the Power fecal® DNA Isolation Kit (MoBio, Carlsbad, CA, United States). The DNA was recovered with 30 μl of buffer in the kit. The 16S ribosomal RNA (rRNA) V4 gene amplification and sequencing were done using the Illumina MiSeq technology. The library was sequenced on an Illumina HiSeq 2500 and 250 bp paired-end reads were generated. Sequence analyses were performed by Uparse software (Uparse v7.0.1001[1]). Sequences with ≥97% similarity were assigned to the same OTUs. Representative sequence for each OTU was screened for further annotation. For each representative sequence, the Silva123 Database was used based on RDP classifier (Version 2.2[2]) algorithm to annotate taxonomic information. Statistical difference of 16S rRNA high-throughput sequencing was assessed by Tukey's HSD. The primers are listed in **Supplementary Table S1**.

Butyrate Administration

For butyrate treated group mice, sodium butyrate (Tokyo Chemical Industry, Japan) was gavaged every day for 10 consecutive days after 12 Gy TAI. Fresh feces were collected before and after 7 days of P80 treatment, as well as 7 days after butyrate remedy, respectively, for downstream analysis.

Antibiotic Cocktail (ABX) Administration

ABX consisted of ciprofloxacin (0.125 g/l), metronidazole (0.1 g/l), vancomycin (0.05 g/l), streptomycin (100 U/l) and penicillin (100 U/l). Mice were exposed to ABX in drinking water after TAI. The same water was used for the water-treated (TAI+P80) group.

Short Chain Fatty Acids (SCFAs) Measurements

Quantification of short chain fatty acids was performed by high performance liquid chromatography (HPLC) (Thermo Fisher, United States) in supernatants of fecal samples reconstituted in PBS. In brief, 1 ml of fecal solution was acidified with 1/10 volume of H_2SO_4 (0.01 M), and passed through a condenser to isolate volatile compounds within a sample. Following filtration through 0.45 μm membrane, equal volume of samples was loaded onto the HPLC Chromatographic column: C18 AQ (4.6*250 mm), sulfuric acid (0.01 M) was used as the mobile phase, and the level of SCFAs were determined by external standard calibration method.

Fecal Microbiota Transplantation (FMT)

For FMT experiments, fresh transplant materials were prepared on the same day of transplantation within 4 h before gastric perfusion to prevent changes in bacterial composition (Cui et al., 2017b). Particularly, 200 mg of stools from the P80-treated mice was re-suspended in 2 ml sterile saline, vortexed for 30 s and allowed to stand for 30 min anaerobically. Eight-week-old male C57BL/6J recipient mice were orally administered daily with the supernatant for 10 days before 12 Gy TAI and maintained on sterile water throughout the experiment.

Quantitative Real-Time Polymerase Chain Reaction (qRT-PCR)

Total RNA was separated from the tissues or cells using Trizol (Invitrogen, United States) according to the manufacturer's protocol. cDNA was synthesized from total RNA using poly(A)- tailed total RNA and reverse transcription primer with ImPro-II Reverse Transcriptase (Promega, United States), according to the manufacturer's protocol. The RT-PCR was performed using DreamTaq^{TM} Hot Start Green PCR Master Mix (Thermo Fisher Scientific, CA, United States) according to the manufacturer's protocol. The qRT-PCR was performed according to the instructions of Fast Start Universal SYBR Green Master (Rox) (Roche Diagnostics GmbH, Germany). GAPDH was used as the housekeeping gene. The expression of gene was indicated with $2^{-\Delta\Delta Ct}$ and normalized to GAPDH. Specifically, the calculated $2^{-\Delta\Delta Ct}$ in control group was set to 1, the expression of gene in experimental group was valued as $2^{-\Delta\Delta Ct(\text{experimental group})}/2^{-\Delta\Delta Ct(\text{control group})}$. The primers used in this study were listed in **Supplementary Table S2**.

Residual P80 Measurements

Quantification of residual P80 was performed by HPLC in supernatants of fecal samples. The chromatographic analysis was carried out on a Dionex Ultimate 3000 (Dionex, United States), and the mobile phase consisted of 20 mM ammonium acetate and acetonitrile (9:1). Following filtration through 0.45 μm membrane, equal volume of samples was loaded onto the HPLC. Flow rate was 0.6 ml/min, and the column temperature was 30°C.

Immunohistochemistry Staining (IHC)

Following euthanasia, the colons of mice were fixed in carnoy fixation overnight at room temperature and then embedded in paraffin. Tissues were sectioned at 5 μm thickness, and blocked with 5% BSA (Solarbio, China) for 1 h at room temperature and then incubated with primary antibodies overnight at 4°C and incubated with fluorescein isothiocyanate (FITC)-conjugated goat anti-rabbit IgG antibody (ZSGB Bio, China) for 1 h at room temperature, then stained by DAB Staining Kit (ZSGB Bio, China), followed by hematoxylin nuclear counterstaining. The primary antibody of rabbit anti-MUC2 (Abcam, United States) was used.

[1]http://drive5.com/uparse/

[2]http://sourceforge.net/projects/rdp-classifier/

Quantification of Fecal LCN2 and IL-10

Frozen fecal samples were re-suspended in PBS containing 0.1% Tween 20 (Jiangtian Chemical Technology, China) to a final concentration of 0.1 g/ml, then vortexed to produce a homogenous fecal suspension, followed by centrifuging for 10 min at 14,000 × *g* and 4°C. LCN2 and IL-10 levels were measured from the clear supernatant using Mouse Lipocalin (LCN2) ELISA kit (Solarbio, China) or Mouse IL-10 ELISA kit (Solarbio, China) according to the manufacturer's protocol. Read the OD 450 nm value with a microtiter plate reader (Rayto, China). Specifically, with the OD value of absorbance as the ordinate (Y) and the concentration of the standard LCN2 (or IL-10) to be measured as the abscissa (X), the corresponding curve is made. The content of the LCN2 (or IL-10) to be measured in the sample can be converted from the standard curve to the corresponding concentration according to its OD value.

Cell Culture

The human enterocyte HIEC-6 cell line was cultured in RPMI-1640 medium (Gibco, CA, United States) supplemented with 10% fetal bromide serum (FBS) (Gibco, CA, United States) at 37°C in a 100% humidified atmosphere of 5% CO_2.

Cell Transfection

For cell transfection, the cells were cultured in a 6-well plate for 24 h and then were transfected with siRNA. All transfections were performed using polyetherimide (PEI) (Sigma, Spain) according to the manufacturer's protocol. si-GPR43 was synthesized by RiboBio (Guangzhou, China). The sequences of siRNA were listed in **Supplementary Table S3**.

Statistical Analysis

Each experiment was repeated at least three times. Significance was assessed by comparing the mean values (6 standard deviation; SD) using Student's *t*-test between each two cohort as follows: $^{*}p < 0.05$, $^{**}p < 0.01$, $^{***}p < 0.001$. Statistically difference of 16S rRNA high throughput sequencing was assessed by TukeyHSD and the data were analyzed controlling for cage-clustering. Kaplan–Meier analysis was performed for survival analysis, and significance between survival curves was determined by a log rank test. Results with $p < 0.05$ were considered statistically significant. The statistical tests were clarified in related legends. Kernel-density-violin plots were used to determine the sample sizes and data distribution (Basson et al., 2020a).

RESULTS

P80 Consumption Shifts the Gut Microbial Profile

In light of a recent finding that chronic P80 consumption (for 12 weeks) caused detrimental alteration of the gut microbial profile and promoted colitis (Chassaing et al., 2015), we examined whether inflammation and alteration of the gut microbiota were induced by a relatively short-term P80 challenge (for 7 days) in mice. Chronic P80-induced gains in overall weight and decrease in colon length were not observed in short-term P80-treated mice (**Figure 1A** and **Supplementary Figure S1A**; body weights not shown), while short-term consumption of P80 led to loose stools (**Figure 1A**). Given the important role of *Glut1* (*Slc2a1*), *Pgk*, and multidrug resistance protein (*MDR*) in the maintenance of epithelial integrity (Zaki et al., 2010; Kelly et al., 2013; Winkler et al., 2015; Cui et al., 2017b; Xiao et al., 2018), we observed a significant reduction in the expression of *Glut1* (but not *MDR* and *Pgk*) in the P80-challenged animals (**Figure 1B** and **Supplementary Figures S1B,C**). In addition, the *tumor necrosis factor-α (TNF-α)* and pro-inflammatory cytokine *interleukin 6* (*IL-6*) exhibited increased expressions in the small intestines of mice subjected to short-term P80 treatment (**Figures 1C,D**). Although short-term P80 consumption induced mild colitis in mice, it did not cause histopathologic epithelial damage in the intestines (**Supplementary Figure S1D**). Next, we performed 16S rRNA sequencing analysis to detect alterations in the intestinal microbiota after short-term P80 treatment. The results revealed a marked decrease in the numbers of intestinal bacterial species after short-term P80 consumption (**Figure 1E** and **Supplementary Figures S1E,F**). Principal component analysis (PCA) further confirmed that short-term P80 administration significantly altered the composition of the intestinal bacteria (**Figure 1F** and **Supplementary Figure S1G**), leading to increased abundances of *Lactobacillus* but decreased abundances of the *Allobaculum* genus (**Figure 1G**).

P80 Consumption Aggravates RIII

To determine the effects of P80 consumption on RIII, we repetitively administered (oral gavage) P80 daily for 7 consecutive days before subjecting the mice to TAI. Notably, P80 treatment reduced the survival rate (**Figure 2A**, $p = 0.0028$) and impaired weight recovery (**Figure 2B**) in irradiated mice. At 30 days post-TAI, mice were sacrificed to assess intestinal injury. The irradiated mice with P80 challenge presented relatively short colons, indicating severe intestinal inflammation (**Figure 2C** and **Supplementary Figure S2A**). Histological analysis revealed that P80 consumption decreased the number of intact intestinal villi and goblet cells in the irradiated mice (**Figures 2D,E**), suggesting that oral gavage of P80 aggravated the radiation-impaired small intestinal epithelial integrity. Further determination of the levels of *Glut1*, *MDR*, and *Pgk* in the small intestines revealed significant reduction in expressions of these genes in the P80-challenged animals (**Figures 2F,G** and **Supplementary Figure S2B**). Given *IL-18* plays a role in the maintenance of epithelial integrity (Zaki et al., 2010), we observed a significant reduction in *IL-18* expression in the P80-challenged animals (**Figure 2H**).

P80 Consumption Exacerbates Radiation-Induced GI Toxicity Through the Gut Microbiota

To elucidate the mechanism underlying the P80-mediated aggravation of irradiation injury, we performed 16S rRNA sequencing using fecal pellets from the mice to characterize the composition of the gut microbiota. The mice were fed the

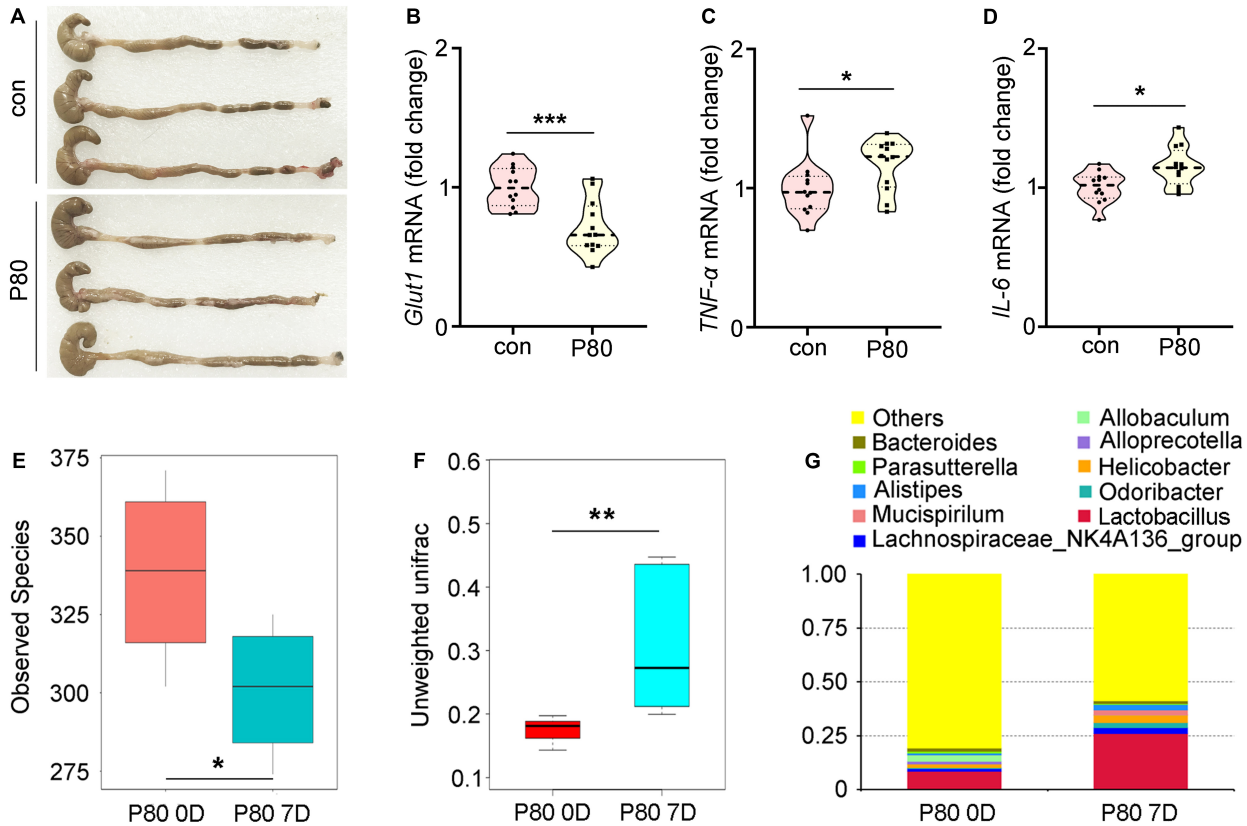

FIGURE 1 | P80 consumption promotes intestinal inflammation and alters the gut microbiota. **(A)** The length of colon tissues from mice with or without consumption of P80 by oral gavage was shown. **(B–D)** The expression levels of *Glut1* **(B)**, *TNF-α* **(C)** and *IL-6* **(D)** in small intestines were examined by qRT-PCR. Significant differences are indicated: $^{*}p < 0.05$, $^{***}p < 0.001$; Student's *t*-test, $n = 12$ per group. **(E)** The observed species number of intestinal bacteria in mice before and after 7 days of consumption of P80 was examined by 16S rRNA high throughput sequencing. The top and bottom boundaries of each box indicate the 75th and 25th quartile values, respectively, and lines within each box represent the 50th quartile (median) values. Ends of whiskers mark the lowest and highest diversity values in each instance. Statistically significant differences are indicated: $^{*}p < 0.05$; TukeyHSD, $n = 5$. **(F)** The β diversity of intestinal bacteria in mice before and after 7 days of consumption of P80 was examined by 16S rRNA high throughput sequencing. Statistically significant differences are indicated: $^{**}p < 0.01$; TukeyHSD, $n = 5$. **(G)** The relative abundances of enteric bacteria at the phylum level in mice before and after 7 days of consumption of P80 were assessed using 16S rRNA high throughput sequencing.

same rodent chow and sterile water in a specific-pathogen-free (SPF) animal facility for at least 3 days to make the microbiota of the mice accordant (**Figure 3A**). Interestingly, TAI exposure alone did not change the α-diversity of the enteric bacteria (**Figure 3B** and **Supplementary Figure S3A**), while TAI following P80 consumption altered the α-diversity of the gut microbiota (**Figure 3C** and **Supplementary Figure S4A**). We also assessed the species number of enteric bacteria in irradiated mice with or without P80 treatment and observed no significant alterations (**Figure 3D**). Furthermore, PCA analysis and unweighted_unifrac algorithm further confirmed that, when the initial community configurations were similar (**Figures 3E,I**), TAI alone did not change the composition of the gut microbiota (**Figures 3F,J**), but P80 consumption significantly shifted that in irradiated animals (**Figures 3G,K**). Notably, although the species number of intestinal bacteria showed no changes in irradiated mice with or without P80 consumption, the PCA showed a separation of microbiota composition between the two cohorts (**Figure 3H**), unweighted_unifrac algorithm further confirmed that P80-challenged mice exhibited significant changes in the gut microbial composition following TAI (**Figure 3L**). To elaborate, TAI elevated the relative frequency of *Bacteroides* but reduced that of the *Lachnospiraceae_NK4A136* group at the genus level (**Supplementary Figure S3B**), whereas P80 administration increased the relative frequency of *Bacteroidetes* but decreased that of *Lactobacillus* in TAI-exposed mice (**Supplementary Figure S4B**). Further analysis of the gut bacterial composition at the genus level revealed increased abundances of *Candidatus_Stoquefichus*, *Parabacteroides*, *Bacteroides*, *Turicibacter*, *Erysipelatoclostridium* and *Ruminococcus_1* in the irradiated mice (**Supplementary Figure S3C**). In contrast, mice exposed to irradiation after P80 consumption harbored high relative abundances of bacterial genera belonging to the phyla *Firmicutes* and *Bacteroidetes*, such as *Lactobacillus*, *Anaerotruncus*, *Roseburia* and *Rikenella*, but low relative abundances of bacterial genera belonging to the phyla *Proteobacteria* and *Actinobacteria*, including *Parasutterella* and *Akkermansia* (**Supplementary Figure S4C**).

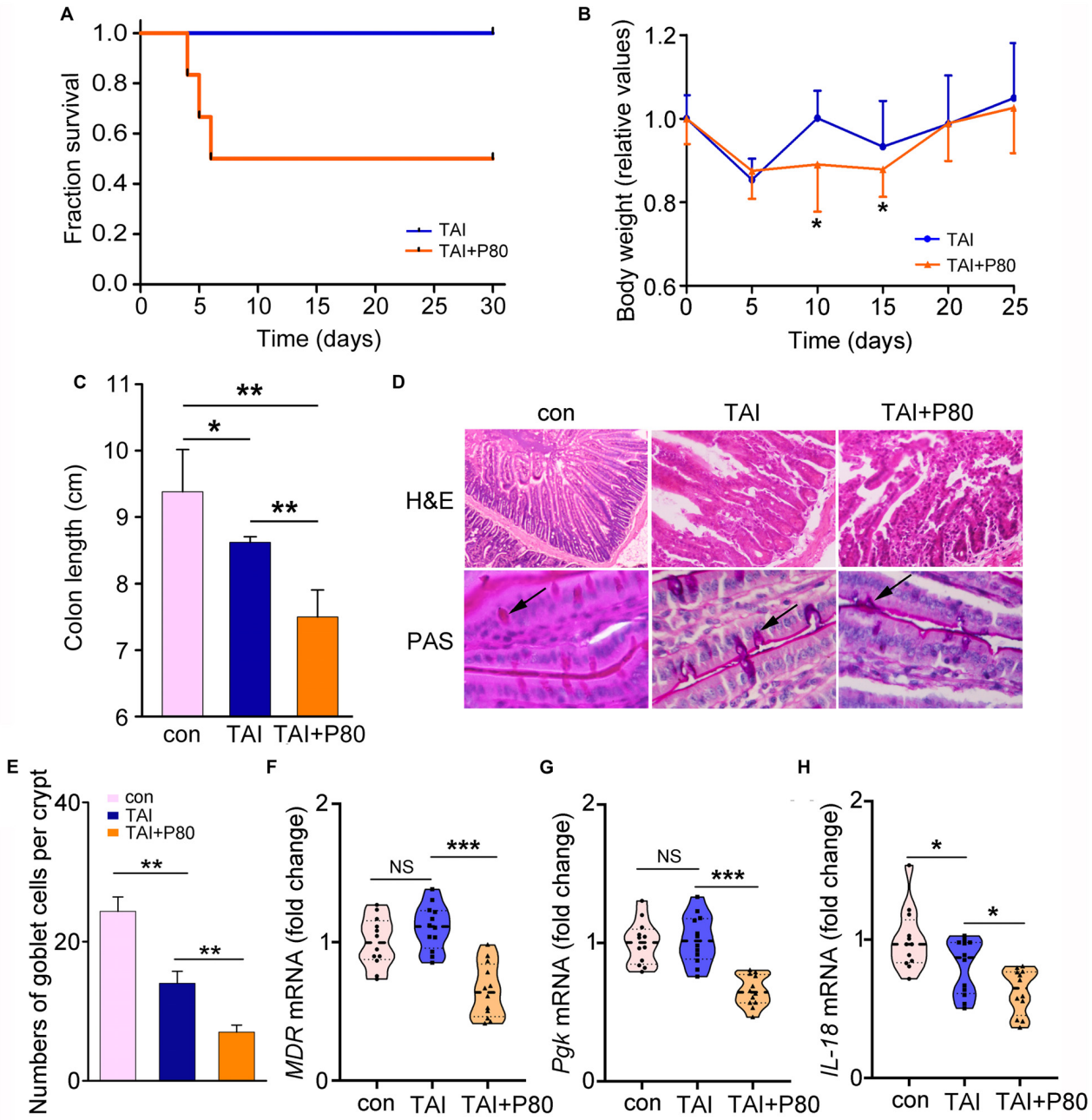

FIGURE 2 | P80 consumption aggravates RIII. **(A)** Mice received 7 days of oral gavage with water or P80 before TAI. Kaplan–Meier survival analysis was performed. $p = 0.0028$ by log-rank test, $n = 12$ per group. **(B)** The body weight was measured using two-way group ANOVA ($^*p < 0.05$), $n = 12$ per group. **(C)** The length of colon tissues from irradiated mice was measured at 30 days after TAI. Statistically significant differences are indicated: $^*p < 0.05$, $^{**}p < 0.01$; Student's *t*-test, $n = 12$ per group. **(D)** The morphologies of the small intestines of mice were shown by HE and PAS staining. **(E)** The number of goblet cells per crypt was counted. Statistically significant differences are shown relative to the "TAI" group: $^{**}p < 0.01$; Student's *t*-test between each two cohorts, $n = 5$ per group. **(F–H)** The expression levels of *MDR* **(F)**, *Pgk* **(G)** in small intestines and *IL-18* **(H)** in colon tissues were examined by qRT-PCR. Significant differences are indicated: none significance (NS), $^*p < 0.05$, $^{***}p < 0.001$; Student's *t*-test, $n = 12$ per group.

To eliminate the effects of residual P80 in stools on recipients, we performed HPLC to measure the residual P80 in feces of mice that received water (control group) or P80 for 7 consecutive days. The results showed no significant difference between the two groups, indicating that P80 remains undetectable in feces after oral gavage (**Supplementary Figure S5A**). Thus, we performed FMT (**Figure 4A**) and antibiotic treatment to validate the role of gut microbes in P80-exacerbated radiation toxicity. Although FMT did not affect the body weights of the animals (**Figure 4B**), mice

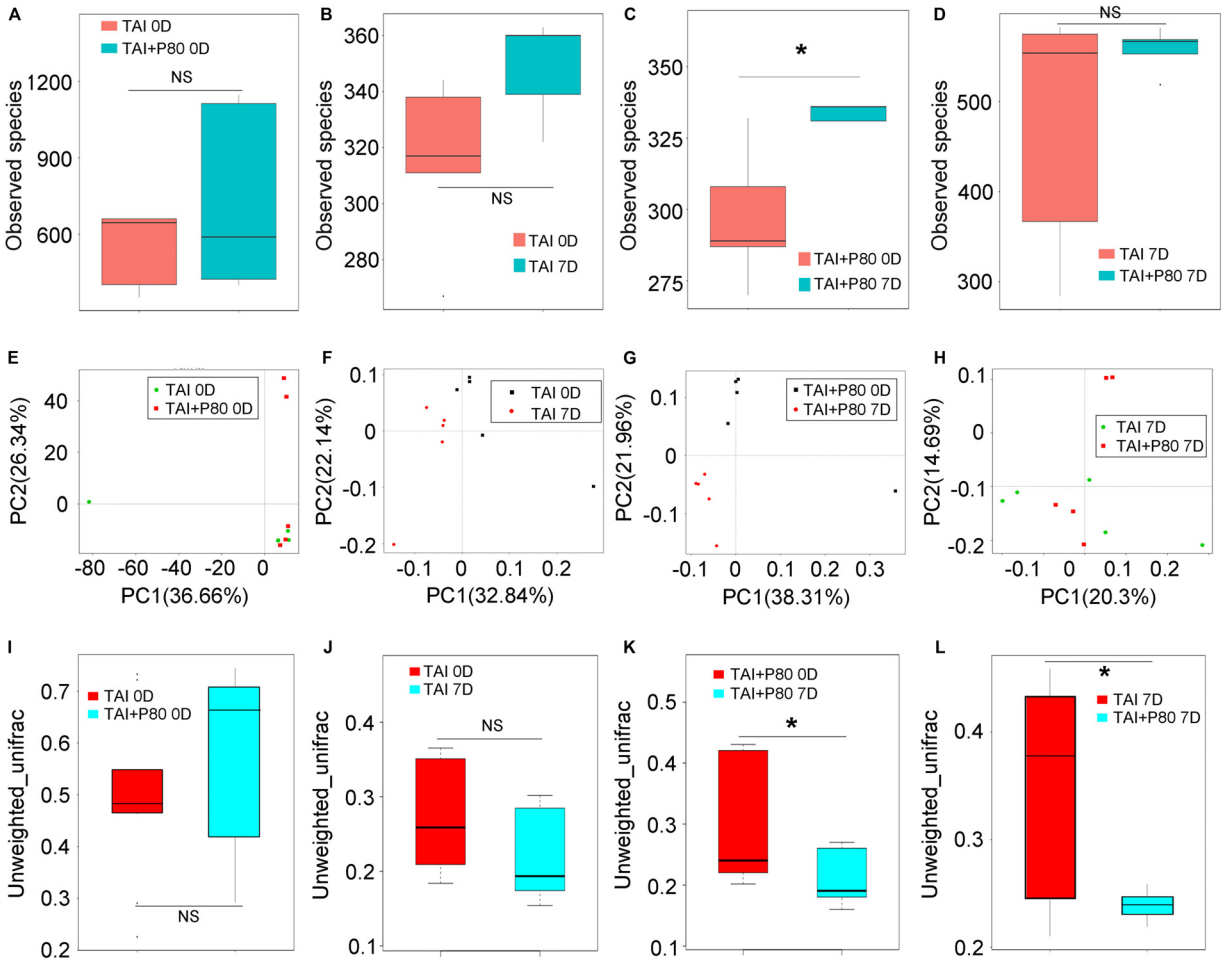

FIGURE 3 | P80 alters the gut microbiota composition of irradiated mice. **(A–D)** The observed species number of intestinal bacteria was examined by 16S rRNA sequencing before (or at 7 days after) 12 Gy TAI. Mice were treated with water (TAI group) or P80 (TAI+P80 group), respectively. Statistically significant differences are indicated: none significance (NS), *$p < 0.05$; TukeyHSD, $n = 5$ per group. **(E–L)** The PCA **(E–H)** and β diversity **(I–L)** of intestinal bacteria in mice before (or at 7 days after) TAI were examined by 16S rRNA sequencing. The top and bottom boundaries of each box indicate the 75th and 25th quartile values, respectively, and lines within each box represent the 50th quartile (median) values. Ends of whiskers mark the lowest and highest diversity values in each instance. Statistically significant differences are indicated: none significance (NS), *$p < 0.05$; TukeyHSD, $n = 5$ per group.

that received gut microbes from P80-challenged mice exhibited susceptibility to irradiation, leading to slightly decreased survival rates (**Figure 4C**, $p = 0.2589$), relatively short colons (**Figure 4D** and **Supplementary Figure S5B**) and reduced levels of intestinal integrity markers (**Figure 4E** and **Supplementary Figures S5C,D**). Consistent with the results of FMT, when we used an antibiotic cocktail (ABX, named "TAI+P80+ABX") to eliminate the intestinal microbiota of P80-treated mice following TAI, the mice that were administered ABX exhibited increased weight loss (**Figure 4F**), decreased colon lengths (**Figure 4G** and **Supplementary Figure S5E**) and reduced intestinal integrity (**Figure 4H** and **Supplementary Figures S5F,G**), suggesting that alteration of the gut microbiota might be a response to P80 consumption-exacerbated GI toxicity after radiation exposure. Notably, ABX administration induced relatively low grade inflammation (*TNF*-α, $p = 0.014$; *IL-6*, $p = 0.117$) (**Figure 4I** and **Supplementary Figure S5H**); however, it might be inadequate to alleviate P80-aggravated RIII.

Butyrate Replenishment Attenuates P80-Aggravated GI Toxicity Following Irradiation

Given the protective effects of SCFAs against intestinal epithelial injury (Fukuda et al., 2011; Smith et al., 2013; Kelly et al., 2015), we measured the concentrations of SCFAs in fecal pellets of mice in different cohorts using HPLC. The acetate levels remained unchanged in irradiated and P80-treated animals (**Supplementary Figure S6A**). However, the butyrate levels decreased in the feces of irradiated animals and further decreased in the animals subjected to P80 exposure combined with irradiation (**Figure 5A**). In contrast, the propionate levels increased in the feces of irradiated mice and further

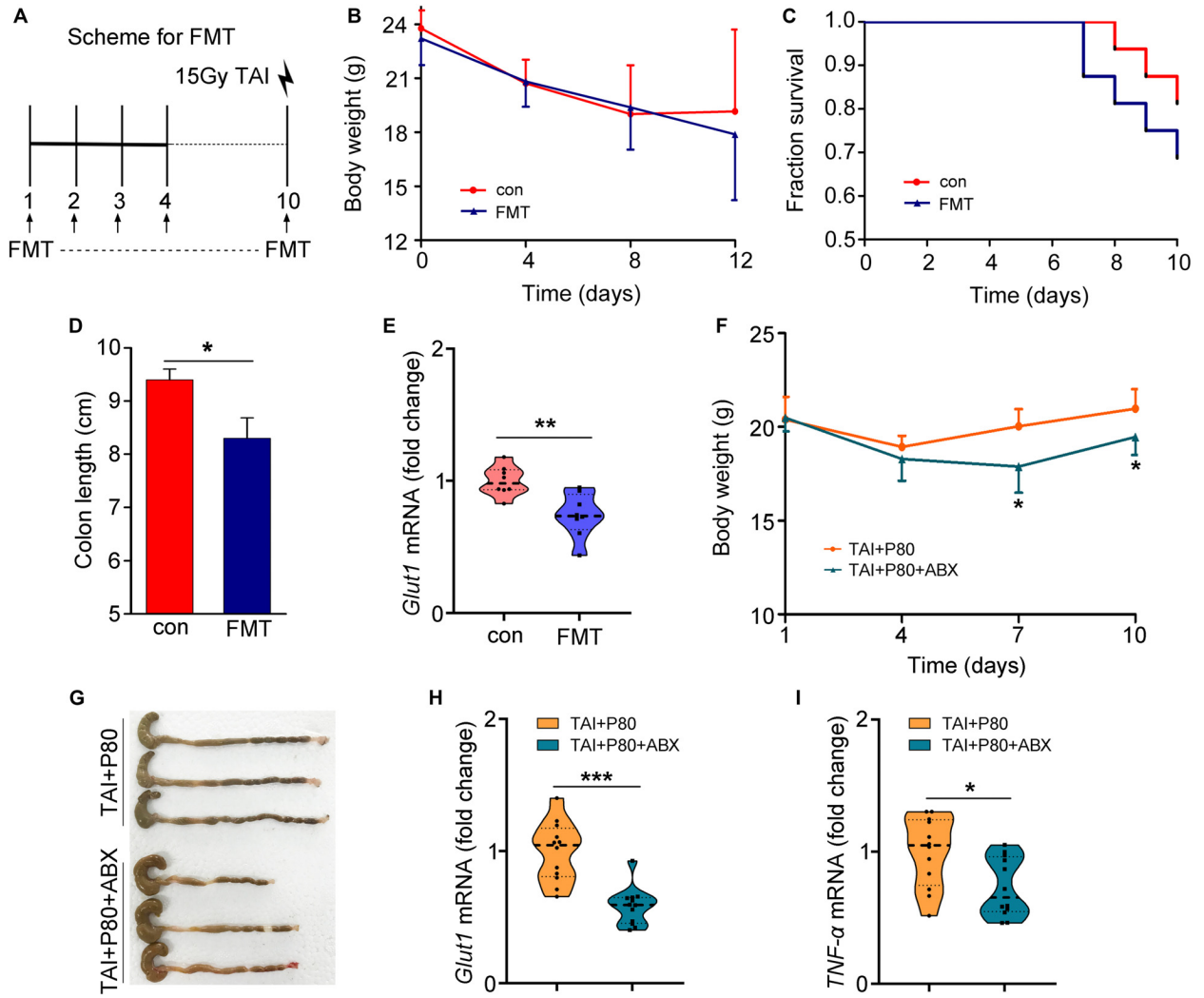

FIGURE 4 | Alteration in the gut microbiota aggravates RIII. **(A–E)** Mice were separated into two groups randomly. Before 15 Gy γ ray exposure, one cohort was treated with saline as control (named saline-treated FMT), the other was treated with intestinal microbes of P80-challenged mice in saline (named P80-treated FMT). **(A)** Scheme for FMT. **(B)** Mice received 10 days of oral gavage with saline or FMT, the body weight was measured after TAI using two-way group ANOVA (*$p < 0.05$). $n = 8$ per group. **(C)** Kaplan–Meier survival analysis of mice was performed after TAI. $p = 0.2589$ by log-rank test between con and FMT group, $n = 8$ per group. **(D)** The length of colon tissues was measured at 15 days after TAI. Statistically significant differences are indicated: *$p < 0.05$; Student's *t*-test, $n = 8$ per group. **(E)** The expression level of *Glut1* was examined in small intestine tissues by qRT-PCR. Significant differences are indicated: **$p < 0.01$; Student's *t*-test, $n = 8$ per group. **(F–I)** Mice were separated into two groups randomly. Before 12 Gy γ ray exposure, mice were treated with P80 by oral gavage for 7 days, then one cohort was treated with sterile water (named TAI+P80), the other was treated with antibiotic cocktail (named TAI+P80+ABX). **(F)** Mice received water or ABX treatment, the body weight was measured using two-way group ANOVA (*$p < 0.05$), $n = 12$ per group. **(G)** The length of colon tissues was shown at 15 days after TAI. **(H,I)** The expression levels of *Glut1* **(H)** and *TNF*-α **(I)** in small intestine tissues were examined by qRT-PCR. Significant differences are indicated: *$p < 0.05$, ***$p < 0.001$; Student's *t*-test, $n = 12$ per group.

elevated by irradiation following P80 exposure (**Supplementary Figure S6B**). Thus, we evaluated the therapeutic potency of butyrate toward P80-exacerbated GI injury following TAI. Using a mouse model of TAI, we observed that butyrate improved survival rate reduction (slightly, from 78.6% to 85.7%) and body weight loss of P80-challenged mice following radiation in a dose-dependent manner (**Figures 5B,C**), suggesting that butyrate treatment might alleviate P80-aggravated irradiation injury. We chose the effective concentration of butyrate (high, 7.5 mg/ml) to further study its role in protecting radiation enteritis. As shown in **Figure 5** and **Supplementary Figure S6**, oral gavage of butyrate restored the length and structure of the colon (**Figures 5D,E** and **Supplementary Figure S6C**), as well as increased the number of intact intestinal villi and goblet cells in the small intestines (**Figure 5F**). The genes involved in maintenance of epithelial integrity were upregulated in the butyrate-treated cohort (**Figure 5G** and **Supplementary Figures S6D–F**). Moreover, butyrate treatment eliminated the alterations in LCN2 and IL-10 levels in feces driven by P80 consumption (**Figures 5H,I**),

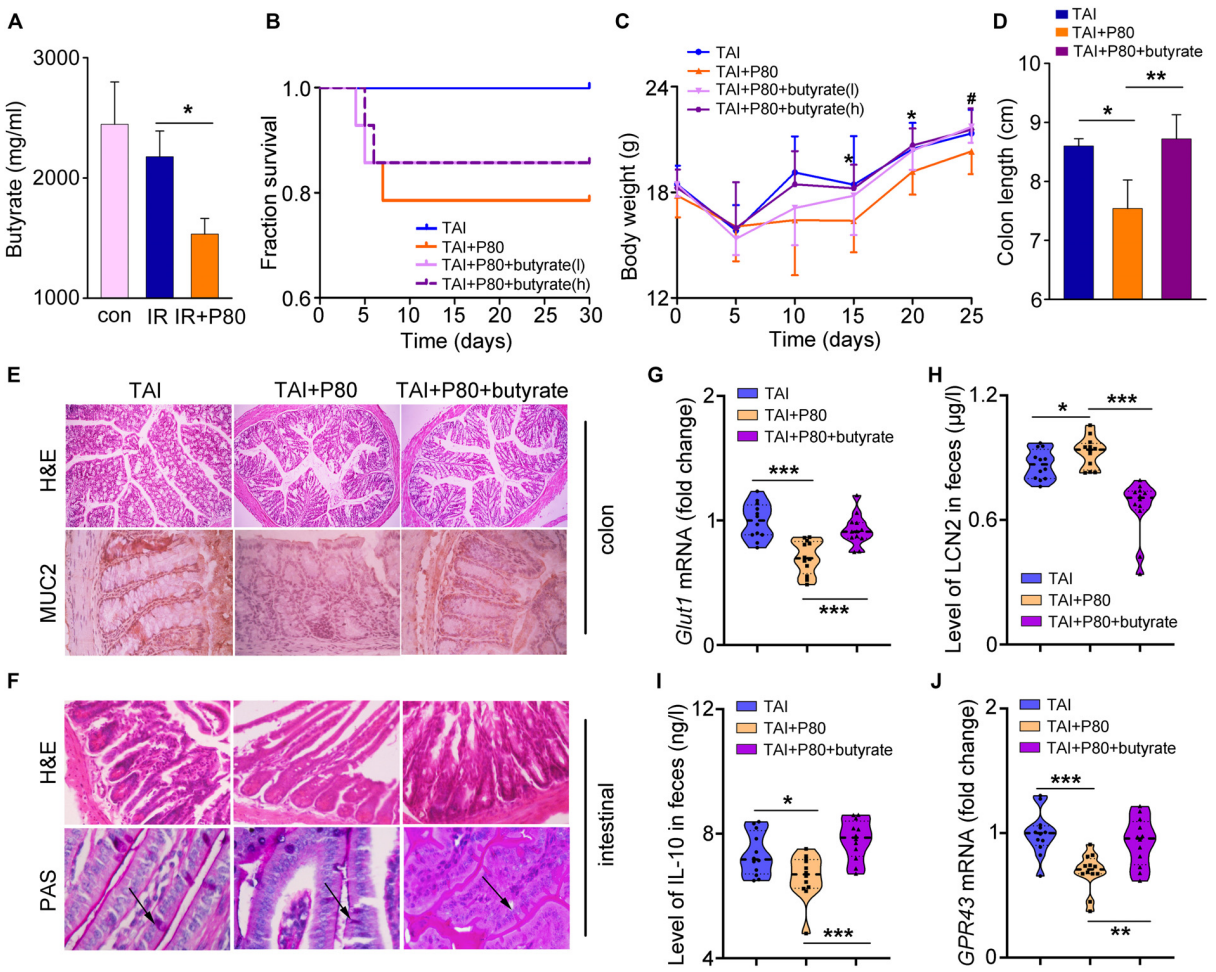

FIGURE 5 | Butyrate prevents the P80-aggravated irradiation injury. **(A)** The concentration of butyrate in different fecal samples was analyzed by HPLC. Significant differences are indicated: $^{*}p < 0.05$; Student's *t*-test, $n = 12$ per group. **(B)** Kaplan–Meier survival analysis of mice after irradiation was performed. $p = 0.0102$ between TAI and TAI+P80 group by log-rank test; $n = 14$ per group. TAI group was treated with water before and after TAI as control, TAI+P80 group was treated with P80 for 7 days before irradiation and water after irradiation, TAI+P80+butyrate group was treated with P80 before irradiation and different concentrations of butyrate after irradiation (low, 3.75 mg/ml; high, 7.5 mg/ml). **(C)** The body weight of mice was measured after 12 Gy TAI using two-way group ANOVA ($^{\#}p < 0.05$ compared between TAI+P80 and TAI+P80+butyrate (l), $^{*}p < 0.05$ compared between TAI+P80 and TAI+P80+butyrate (h); $n = 14$ per group. **(D)** The length of colon tissues was measured at 30 days after TAI. Significant differences are indicated: $^{*}p < 0.05$, $^{**}p < 0.01$; Student's *t*-test. **(E)** The morphology of the colon (upper panel) was shown by HE staining. Immunohistochemical showed expression of MUC2 in the colons of mice (lower panel). **(F)** The morphology of the small intestines was shown by HE and PAS staining. The arrows pointed to the goblet cells. **(G)** The expression level of *Glut1* in small intestine tissues was examined by qRT-PCR. Significant differences are indicated: $^{***}p < 0.001$; Student's *t*-test, $n = 12$ per group. **(H)** Fecal level of the inflammatory marker LCN2 was examined by ELISA. Statistically significant differences are indicated: $^{*}p < 0.05$, $^{***}p < 0.001$; Student's *t*-test, $n = 12$ per group. **(I)** The concentration of IL-10 in feces was examined by ELISA. Significant differences are indicated: $^{*}p < 0.05$, $^{***}p < 0.001$; Student's *t*-test, $n = 12$ per group. **(J)** The expression level of *GPR43* in the colons was examined by qRT-PCR. Significant differences are indicated: $^{**}p < 0.01$, $^{***}p < 0.001$; Student's *t*-test, $n = 12$ per group.

indicating that butyrate might be able to combat low-level intestinal inflammation.

Given that butyrate is an important energy substrate (Buzzetti et al., 2016), we observed that butyrate treatment upregulated the expression of *Mgam*, *Glut2* and *Sglt1* expression (**Supplementary Figures S6G–I**), which are essential genes for digestion and energy absorption (Sainz et al., 2015; Barron et al., 2016; Buzzetti et al., 2016). Previous studies have shown that the mechanism underlying the SCFAs effect partially involves G-protein-coupled receptors (GPCRs) (Macia et al., 2015). Therefore, we measured the expression of *GPR41* and *GPR43*, both of which are major GPCRs activated by SCFAs. The results showed that the levels of these two GPCRs were increased in the butyrate-treated cohort (**Figure 5J** and **Supplementary Figure S6J**).

To determine whether butyrate could alleviate common radiation-induced injury, we performed water (as a control) or butyrate administration by the oral route. As expected, butyrate treatment resulted in significant gains in body weight and amelioration of tissue damage (**Figures 6A,B**). Butyrate also reduced multiple parameters of inflammation in mice, including colon length (**Figures 6C,D**) and expression levels of integrity markers in intestines (**Figures 6E–H**). To determine

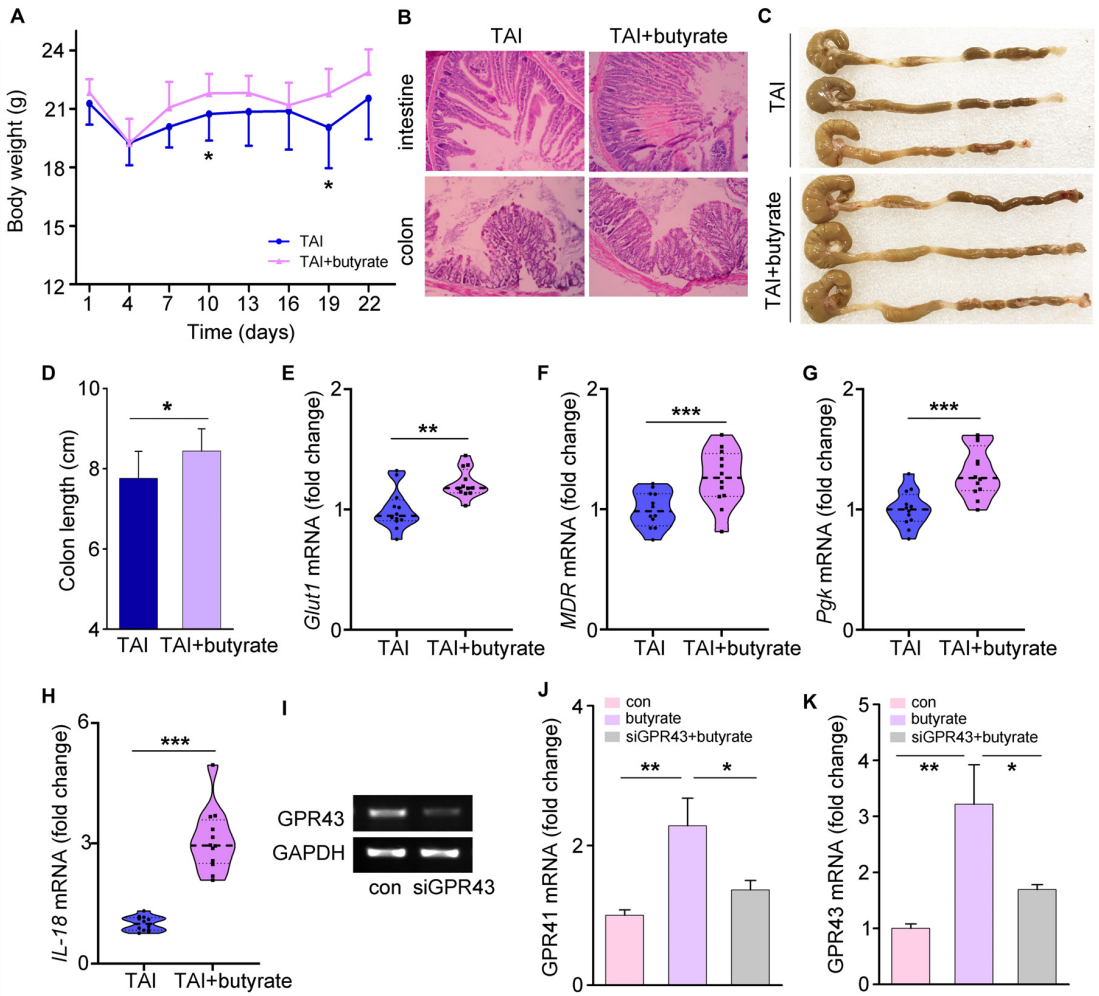

FIGURE 6 | Butyrate educates P80-aggravated GI injury involving GPCRs. **(A)** The body weight of mice was measured after 12 Gy TAI using two-way group ANOVA (*$p < 0.05$), $n = 12$ per group. **(B)** The morphologies of the intestine (upper panel) and colon (lower panel) of mice were shown by HE staining. **(C,D)** The length of colon tissues of mice was measured at 30 days after 12 Gy TAI. Significant differences are indicated: *$p < 0.05$; Student's *t*-test, $n = 12$ per group. **(E–H)** The expression levels of *Glut1* **(E)**, *MDR* **(F)** and *Pgk* **(G)** in small intestines and *IL-18* **(H)** in colon tissues of mice were examined by qRT-PCR. Significant differences are indicated: **$p < 0.01$, ***$p < 0.001$; Student's *t*-test, $n = 12$ per group. **(I)** The expression level of GPR43 in the HIEC-6 cells with butyrate and with or without knockdown of the GPR43 expression was examined by quantitative PCR. **(J,K)** The expression levels of GPR41 **(J)** and GPR43 **(K)** in HIEC-6 cells with or without siGPR43 transfection were examined by qRT-PCR. Significant differences are indicated: *$p < 0.05$, **$p < 0.01$; Student's *t*-test.

the mechanism underlying the modulation of radiation injury by butyrate, we supplied HIEC-6 cells with butyrate and with or without knockdown of the GPR43 expression by siRNA (**Figure 6I**). Similar to the results obtained in mouse models, butyrate treatment significantly upregulated the expression of GPR41 and GPR43, while GPR43 siRNA transfection downregulated GPR41 and GPR43 (**Figures 6J,K**).

Oral Gavage of Butyrate Prevents P80-Mediated Alteration of the Gut Microbiota

To elucidate the mechanism underlying butyrate-mediated protection, we performed 16S rRNA sequencing to assess the intestinal bacterial composition of mice with or without butyrate replenishment (**Figure 7A**). For comparison, the gut bacterial taxonomic proportions of mice from the control group (non-irradiated and non-P80-treated) exhibited no statistically significant difference before and after 14 days of feeding (**Supplementary Figures S7A–D**). However, supplementation with butyrate significantly attenuated the P80-induced shift in the gut microbial profile (**Figures 7B,C**). PCA further confirmed that supplementation with butyrate attenuated the P80-induced intestinal bacterial composition (**Figures 7D,E**). Specifically, the P80-treated mice harbored increased abundances of *Proteobacteria* and decreased abundances of *Firmicutes* after TAI. However, oral gavage of butyrate stabilized the abundance of *Proteobacteria* and increased the abundance of *Firmicutes* (**Figure 7F**). Moreover, butyrate administration elevated the relative abundances of *Parabacteroides*, *[Eubacterium],*

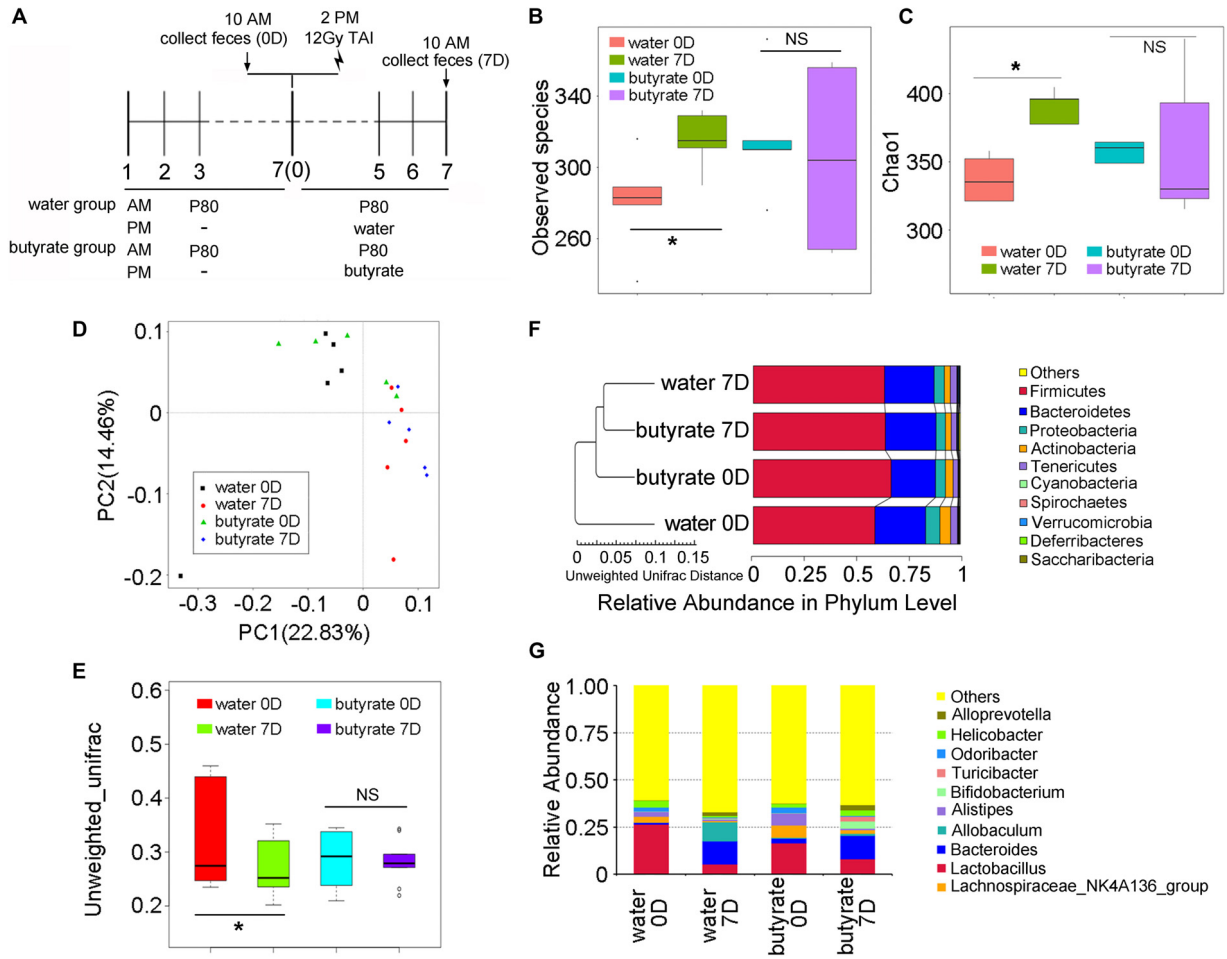

FIGURE 7 | Butyrate alters the fecal microbiota. **(A)** Experimental design. "Water" group is short for "TAI+P80+water" group, "butyrate" group is short for "TAI+P80+butyrate" group. **(B,C)** The observed species number **(B)** and Chao 1 index **(C)** of intestinal bacteria of mice were examined by 16S rRNA sequencing. Statistically significant differences are indicated: non significance (NS), $*p < 0.05$; TukeyHSD, $n = 5$ per group. **(D,E)** The PCA **(D)** and β diversity **(E)** of intestinal bacteria in irradiated mice were examined by 16S rRNA sequencing. Statistically significant differences are indicated: non significance (NS), $*p < 0.05$; TukeyHSD, $n = 5$ per group. **(F)** The relative abundance of intestinal bacteria at the phylum level of irradiated mice was assessed using 16S rRNA sequencing. **(G)** The relative abundance of enteric bacteria at the genus level of irradiated mice was assessed using 16S rRNA sequencing.

Rikenellaceae, Turicibacter and *Bifidobacterium* at the genus level and concurrently reduced the abundances of *Odoribacter, Anaerotruncus* and the *Lachnospiraceae_NK4A136 group* (**Figure 7G** and **Supplementary Figure S7E**).

DISCUSSION

During the past half-century, we have witnessed a steep rise in the consumption of food and medicine additives. These agents include spices, sweeteners, preservatives and emulsifiers, which are added to preserve the flavor or enhance the taste, appearance, or other qualities of foods and medicines. The primary basis for approving the usage of the additives is the notion that they fail to favor toxicity at concentrations reasonably greater than the approved concentrations. Of late, mounting evidence corroborates that many of these additives may have harmful effects on human health. For instance, artificial sweeteners have recently been reported to cause glucose intolerance in humans (Suez et al., 2014). Similarly, there is an on-going debate regarding a possible association between the addition of thiomersal in vaccines and the development of autism (Siva, 2012). Dietary emulsifiers, such as carboxymethylcellulose (CMC) and P80, have been reported to impair the mucus layer and alter the composition of the intestinal microbiota, resulting in colitis and metabolic syndrome (Chassaing et al., 2015). The intestinal tract is home to a complex and diverse microbial flora, which interacts with the gut epithelium to maintain an effective mucosal barrier that is important for the maintenance of homeostasis (Brown et al., 2015; Zanvit et al., 2015). Recent investigations have demonstrated that non-nutritive sweeteners and dietary emulsifiers consumption shape the gut microbiome, resulting in intestinal disturbance and inflammation, spurring the development of the metabolic syndrome and detrimentally

influence anxiety-related and social behaviors (Suez et al., 2014; Chassaing et al., 2015; Holder et al., 2019). For more than 10 years, microbial configuration has been associated with radiosensibility in both humans and mouse models (Sokol and Adolph, 2018). Notably, the data presented in our previous studies have shown that regular work-rest cycle and FMT fought against radiation toxicity via modulating gut microbiome (Cui et al., 2016, 2017b). Specifically, it has been reported in our previously studies that TAI had no effect on the abundance of the intestinal bacterial of mice after 3 days (Cui et al., 2017a), 5 days (Xiao et al., 2018) and 6 or 12 days (Li et al., 2020) of TAI. In addition, recently study reported that after 1 month of TAI, there was no significant change in the abundance of gut microbiota (Lu et al., 2019). All the studies prove that TAI unchanges the α-diversity of gut microbiota in hosts. However, in light of PCA analysis in this study and principal coordinates analysis (PCoA) analysis in our another study (Li et al., 2020), TAI exposure spurred the separation of gut microbiota, suggesting that TAI might alter the composition of intestinal microbe configurations. Moreover, germ-free mice, which lack colonizing microbes, are resistant to radiation-induced lesions, indicating that the gut microbiota indeed relates to radiation-induced intestinal damage (Crawford and Gordon, 2005). Accordingly, we conjectured that P80 might be a potential risk factor for cancer patients receiving radiotherapy. To test this hypothesis, we performed TAI exposure mouse models with P80 consumption. As expected, the experimental mice exhibited more deteriorate symptom. It suggests that P80 might be an adverse agent for cancer patients receiving radiotherapy. Therefore, the medication and diet of cancer patients with radiation therapy need monitoring. In particular, the intake of P80 should be strictly limited so as not to impair the prognosis. Cage-clustering effect is a key interference factor for studies on gut microbes using mouse models (Rodriguez-Palacios et al., 2018; Basson et al., 2020b). Here, it should be noted that although we controlled the cyclical bias by maintaining relative clean bedding material and providing sterile diet and water, the cage-clustering effect always exists in this system as the limitation of studies using mouse data, unless mice are housed individually, or statistical methods are used to control for cage effects.

The human GI tract harbors trillions of microbes, constituting a bioreactor fueled by dietary macronutrients to produce bioactive molecules. Many microbial products might emerge as messengers between gut microbes and hosts, and play pivotal roles in governing the physiological processes of hosts, ranging from metabolism to brain function. For example, a great majority of 5-hydroxytryptamine is synthesized in the GI tract, modulating various biological processes, including the function of the GI, cardiac and respiratory systems as well as platelet aggregation (Kishi et al., 2013). Likewise, other microbial products, such as betaine, trimethylamine *N*-oxide (TMAO) and choline, are also involved in the development of cardiovascular diseases (Wang et al., 2011). Bile acids, which are major intestinal metabolites, may have beneficial effects on obesity and hepatic insulin sensitivity (Tagawa et al., 2015; Kusumoto et al., 2017). SCFAs are a group of major fermentation products from dietary fibers by microorganisms in the gut, serve as histone deacetylases inhibitors and GPCRs ligands governing host metabolism and immunity (Chung et al., 2016; Koh et al., 2016). In comparison with radiation-free mice here, TAI exposure downregulated butyrate levels, a member of SCFAs, which was further decreased in fecal pellets of mice subjected to P80 challenge. Since *Allobaculum* is thought to be a beneficial bacterium, which plays anti-inflammatory role, protects gut barrier function and regulates host metabolism and immunity by producing SCFAs in the intestine (Cox et al., 2014; Ma et al., 2020). Thus, P80-treated mice may harbor lower relative abundance of *Allobaculum* in the intestinal microbiota. Butyrate supplementation hinders the development of hepatitis and colitis (Zhang et al., 2016; Sheng et al., 2017), implying that butyrate might be harnessed to protect against radiation toxicity. To test this hypothesis, we performed a butyrate "rescue" experiment in which butyrate was artificially supplied via the oral route. We treated P80-challenged mice with butyrate at concentration of 3.75 mg/ml and 7.5 mg/ml and results showed that butyrate performed therapeutic effects in a dose-dependent manner. Then, we used the optimal dose of butyrate (7.5 mg/ml) throughout the study. As expected, butyrate replenishment significantly restored the P80-shifted gut microbial composition, and mitigated P80-aggravated GI toxicity in irradiated animals. Generally, radiation-induced GI tract injury represents as shortening of colon, losing of intestinal villi and decreasing of goblet cells. In addition, emulsifiers intake propelled epithelial damage of small intestine and shortened colons. All the evidence indicates that small intestine might be vulnerable to external stimulus and shows structural damage, and contraction in length of colon might be a marker for GI tract toxicity following radiation. Concerning the possible mechanism by which SCFAs modulate host responses, previous study suggests that human genome possesses approximately 800 GPCRs, and lately a cluster of four GPCR genes is identified in close proximity to the *CD22* gene on chromosome 19q13.1. Luminal SCFAs are sensed by GPCRs, releasing bioactive factors to impact satiety, inflammation and intestinal transit (Koh et al., 2016). In line with the previous implications, the underlying mechanism by which butyrate performs radiation protective effects partly dependents on binding and activating GPCR. In addition, 16S rRNA sequencing indicated butyrate replenishment reconstructed the enteric bacteria composition of irradiated mice, suggesting that the gut microbe pattern is the essential element to sustain butyrate-mediated radiation toxicity. Taken together, our findings suggest that butyrate, a metabolite of the gut microbiota, can be employed as a therapeutic agent to attenuate P80-aggravated GI injury following radiotherapy.

DATA AVAILABILITY STATEMENT

The data can be found in NCBI, under accession PRJNA636288 (https://www.ncbi.nlm.nih.gov/Traces/study/?acc=PRJNA636288).

ETHICS STATEMENT

The animal study was reviewed and approved by Chinese Academy of Medical Sciences, Institute of Radiation Medicine.

AUTHOR CONTRIBUTIONS

YL, JD, DL, SZ, TZ, CZ, and MC contributed to the data curation. HX contributed to the formula analysis. MC and SF contributed to the funding acquisition. DL contributed to the methodology. YL, MC, and SF contributed to the project administration. MC supervised the study. YL wrote the original draft of the manuscript. YL, HX, JD, HW, and MC reviewed and edited the manuscript. All authors contributed to the article and approved the submitted version.

FUNDING

This work was supported by grants from the National Natural Science Foundation of China under grant number (81872555, 81730086, and 81572969), CAMS Innovation Fund for Medical Sciences under grant number (2016-I2M-1-017 and 2016-I2M-B&R-13), the Drug Innovation Major Project of China under grant number (2018ZX09711001-007-008), the PUMC Graduate Innovation Fund (2016-1001-07). HW was supported by the U.S. National Center of Complementary and Alternative Medicine (NCCAM, R01AT005076) and the National Institute of General Medical Sciences (NIGMS, R01GM063075, and R41GM123858).

ACKNOWLEDGMENTS

We thank Haichao Wang for helping us interpret the data and significantly revise the manuscript.

SUPPLEMENTARY MATERIAL

The Supplementary Material for this article can be found online at: https://www.frontiersin.org/articles/10.3389/fmicb.2020.01450/full#supplementary-material

REFERENCES

Al-Ali, A., Quach, J., Bundgaard, C., Steffansen, B., Holm, R., and Nielsen, C. U. (2018). Polysorbate 20 alters the oral bioavailability of etoposide in wild type and mdr1a deficient Sprague-Dawley rats. *Int. J. Pharm.* 543, 352–360. doi: 10.1016/j.ijpharm.2018.04.006

Andreyev, H. J., Benton, B. E., Lalji, A., Norton, C., Mohammed, K., Gage, H., et al. (2013). Algorithm-based management of patients with gastrointestinal symptoms in patients after pelvic radiation treatment (ORBIT): a randomised controlled trial. *Lancet* 382, 2084–2092. doi: 10.1016/S0140-6736(13)61648-7

Barron, C. C., Bilan, P. J., Tsakiridis, T., and Tsiani, E. (2016). Facilitative glucose transporters: implications for cancer detection, prognosis and treatment. *Metabolism* 65, 124–139. doi: 10.1016/j.metabol.2015.10.007

Basson, A. R., Cominelli, F., and Rodriguez-Palacios, A. (2020a). Patterns of 'analytical irreproducibility' in multimodal diseases. *bioRxiv* [Preprint] doi: 10.1101/2020.03.22.002469

Basson, A. R., LaSalla, A., Lam, G., Kulpins, D., Moen, E. L., Sundrud, M. S., et al. (2020b). Artificial microbiome heterogeneity spurs six practical action themes and examples to increase study power-driven reproducibility. *Sci. Rep.* 10, 1–19. doi: 10.1038/s41598-020-60900-y

Brown, E. M., Wlodarska, M., Willing, B. P., Vonaesch, P., and Han, J. (2015). Diet and specific microbial exposure trigger features of environmental enteropathy in a novel murine model. *Nat. Commun.* 6:7806. doi: 10.1038/ncomms8806

Buzzetti, E., Pinzani, M., and Tsochatzis, E. A. (2016). The multiple-hit pathogenesis of non-alcoholic fatty liver disease (NAFLD). *Metabolism* 65, 1038–1048. doi: 10.1016/j.metabol.2015.12.012

Chassaing, B., Koren, O., Goodrich, J. K., Poole, A. C., Srinivasan, S., Ley, R. E., et al. (2015). Dietary emulsifiers impact the mouse gut microbiota promoting colitis and metabolic syndrome. *Nature* 519, 92–96. doi: 10.1038/nature14232

Chu, H., Duan, Y., Yang, L., and Schnabl, B. (2019). Small metabolites, possible big changes: a microbiota-centered view of non-alcoholic fatty liver disease. *Gut* 68, 359–370. doi: 10.1136/gutjnl-2018-316307

Chung, W. S., Walker, A. W., Louis, P., Parkhill, J., Vermeiren, J., Bosscher, D., et al. (2016). Modulation of the human gut microbiota by dietary fibres occurs at the species level. *BMC Biol.* 14:3. doi: 10.1186/s12915-015-0224-3

Citrin, D. E. (2017). Recent developments in radiotherapy. *N. Engl. J. Med.* 377, 2200–2201. doi: 10.1056/NEJMc1713349

Clemente, J. C., Ursell, L. K., Parfrey, L. W., and Knight, R. (2012). The impact of the gut microbiota on human health: an integrative view. *Cell* 148, 1258–1270. doi: 10.1016/j.cell.2012.01.035

Cox, L. M., Yamanishi, S., Sohn, J., Alekseyenko, A. V., Leung, J. M., Cho, I., et al. (2014). Altering the intestinal microbiota during a critical developmental window has lasting metabolic consequences. *Cell* 158, 705–721. doi: 10.1016/j.cell.2014.05.052

Crawford, P. A., and Gordon, J. I. (2005). Microbial regulation of intestinal radiosensitivity. *Proc. Natl. Acad. Sci. U.S.A.* 102, 13254–13259. doi: 10.1073/pnas.0504830102

Cui, M., Xiao, H., Li, Y., Dong, J., Luo, D., Li, H., et al. (2017a). Total abdominal irradiation exposure impairs cognitive function involving miR-34a-5p/BDNF axis. *Biochim. Biophys. Acta Mol. Basis Dis.* 1863, 2333–2341. doi: 10.1016/j.bbadis.2017.06.021

Cui, M., Xiao, H., Li, Y., Zhou, L., Zhao, S., Luo, D., et al. (2017b). Faecal microbiota transplantation protects against radiation-induced toxicity. *EMBO Mol. Med.* 9, 448–461. doi: 10.15252/emmm.201606932

Cui, M., Xiao, H., Luo, D., Zhang, X., Zhao, S., Zheng, Q., et al. (2016). Circadian rhythm shapes the gut microbiota affecting host radiosensitivity. *Int. J. Mol. Sci.* 17, 1–12. doi: 10.3390/ijms17111786

Food Safety Commission [of Japan]. (2007). *Evaluation Report of Food Additives (Polysorbates 20, 60, 65 and 80)*. Available online at: https://www.fsc.go.jp/english/evaluationreports/foodadditive/polysorbate_report.pdf

Fukuda, S., Toh, H., Hase, K., Oshima, K., Nakanishi, Y., Yoshimura, K., et al. (2011). Bifidobacteria can protect from enteropathogenic infection through production of acetate. *Nature* 469, 543–547. doi: 10.1038/nature09646

Gevers, D., Kugathasan, S., Denson, L. A., Vázquez-Baeza, Y., Van Treuren, W., Ren, B., et al. (2014). The treatment-naive microbiome in new-onset Crohn's disease. *Cell Host Microbe* 15, 382–392. doi: 10.1016/j.chom.2014.02.005

Ghose, C. (2013). Clostridium difficile infection in the twenty-first century. *Emerg. Microbes Infect.* 2:e62. doi: 10.1038/emi.2013.62

Gopalakrishnan, V., Helmink, B. A., Spencer, C. N., Reuben, A., and Wargo, J. A. (2018). The influence of the gut microbiome on cancer, immunity, and cancer immunotherapy. *Cancer Cell* 33, 570–580. doi: 10.1016/j.ccell.2018.03.015

Hauer-Jensen, M., Denham, J. W., and Andreyev, H. J. (2014). Radiation enteropathy–pathogenesis, treatment and prevention. *Nat. Rev. Gastroenterol. Hepatol.* 11, 470–479. doi: 10.1038/nrgastro.2014.46

Heijtz, R. D., Wang, S., Anuar, F., Qian, Y., Bjorkholm, B., Samuelsson, A., et al. (2011). Normal gut microbiota modulates brain development and behavior. *PNAS* 108, 3047–3052. doi: 10.1073/pnas.1010529108

Holder, M. K., Peters, N. V., Whylings, J., Fields, C. T., Gewirtz, A. T., Chassaing, B., et al. (2019). Dietary emulsifiers consumption alters anxiety-like and social-related behaviors in mice in a sex-dependent manner. *Sci. Rep.* 9:172. doi: 10.1038/s41598-018-36890-3

Holmes, E., Kinross, J., Gibson, G. R., Burcelin, R., Jia, W., Pettersson, S., et al. (2012). Therapeutic modulation of microbiota-host metabolic interactions. *Sci. Transl. Med.* 4, 136r–137r. doi: 10.1126/scitranslmed.3004244

Iusuf, D., Hendrikx, J. J., van Esch, A., van de Steeg, E., Wagenaar, E., Rosing, H., et al. (2015). Human OATP1B1, OATP1B3 and OATP1A2 can mediate the in vivo uptake and clearance of docetaxel. *Int. J. Cancer* 136, 225–233. doi: 10.1002/ijc.28970

Kelly, C. J., Glover, L. E., Campbell, E. L., Kominsky, D. J., Ehrentraut, S. F., Bowers, B. E., et al. (2013). Fundamental role for HIF-1alpha in constitutive expression of human beta defensin-1. *Mucosal Immunol.* 6, 1110–1118. doi: 10.1038/mi.2013.6

Kelly, C. J., Zheng, L., Campbell, E. L., Saeedi, B., Scholz, C. C., Bayless, A. J., et al. (2015). Crosstalk between microbiota-derived short-chain fatty acids and intestinal epithelial HIF augments tissue barrier function. *Cell Host Microbe* 17, 662–671. doi: 10.1016/j.chom.2015.03.005

Kirsch, D. G., Santiago, P. M., di Tomaso, E., Sullivan, J. M., Hou, W. S., Dayton, T., et al. (2010). p53 controls radiation-induced gastrointestinal syndrome in mice independent of apoptosis. *Science* 327, 593–596. doi: 10.1126/science.1166202

Kishi, T., Yoshimura, R., Fukuo, Y., Okochi, T., Matsunaga, S., Umene-Nakano, W., et al. (2013). The serotonin 1A receptor gene confer susceptibility to mood disorders: results from an extended meta-analysis of patients with major depression and bipolar disorder. *Eur. Arch. Psychiatry Clin. Neurosci.* 263, 105–118. doi: 10.1007/s00406-012-0337-4

Koh, A., De Vadder, F., Kovatcheva-Datchary, P., and Backhed, F. (2016). from dietary fiber to host physiology: short-chain fatty acids as key bacterial metabolites. *Cell* 165, 1332–1345. doi: 10.1016/j.cell.2016.05.041

Kusumoto, Y., Irie, J., Iwabu, K., Tagawa, H., Itoh, A., Kato, M., et al. (2017). Bile acid binding resin prevents fat accumulation through intestinal microbiota in high-fat diet-induced obesity in mice. *Metabolism* 71, 1–6. doi: 10.1016/j.metabol.2017.02.011

Li, Y., Dong, J., Xiao, H., Zhang, S., Wang, B., Cui, M., et al. (2020). Gut commensal derived-valeric acid protects against radiation injuries. *Gut Microbes* doi: 10.1080/19490976.2019.1709387 [Epub ahead of print],

Liauw, S. L., Connell, P. P., and Weichselbaum, R. R. (2013). New paradigms and future challenges in radiation oncology: an update of biological targets and technology. *Sci. Transl. Med.* 5, 172s–173s. doi: 10.1126/scitranslmed.3005148

Lichtman, J. S., Ferreyra, J. A., Ng, K. M., Smits, S. A., Sonnenburg, J. L., and Elias, J. E. (2016). Host-microbiota interactions in the pathogenesis of antibiotic-associated diseases. *Cell Rep.* 14, 1049–1061. doi: 10.1016/j.celrep.2016.01.009

Lu, L., Li, W., Sun, C., Kang, S., Li, J., Luo, X., et al. (2019). Phycocyanin ameliorates radiation-induced acute intestinal toxicity by regulating the effect of the gut microbiota on the TLR4/Myd88/NF-kappaB pathway. *JPEN J. Parenter. Enteral. Nutr.* doi: 10.1002/jpen.1744 [Epub ahead of print],

Ma, Q., Li, Y., Wang, J., Li, P., Duan, Y., Dai, H., et al. (2020). Investigation of gut microbiome changes in type 1 diabetic mellitus rats based on high-throughput sequencing. *Biomed. Pharmacother.* 124:109873. doi: 10.1016/j.biopha.2020.109873

Macia, L., Tan, J., Vieira, A. T., Leach, K., Stanley, D., Luong, S., et al. (2015). Metabolite-sensing receptors GPR43 and GPR109A facilitate dietary fibre-induced gut homeostasis through regulation of the inflammasome. *Nat. Commun.* 6:6734. doi: 10.1038/ncomms7734

Mottawea, W., Chiang, C., Mühlbauer, M., Starr, A. E., Butcher, J., Abujamel, T., et al. (2016). Altered intestinal microbiota-host mitochondria crosstalk in new onset Crohn's disease. *Nat. Commun.* 7:13419. doi: 10.1038/ncomms13419

Pal, S. K., Miller, M. J., Agarwal, N., Chang, S. M., Chavez-MacGregor, M., Cohen, E., et al. (2019). Clinical cancer advances 2019: annual report on progress against cancer from the American society of clinical oncology. *J. Clin. Oncol.* 37, 834–849. doi: 10.1200/JCO.18.02037

Peng, Z., Ling, L., Stratton, C. W., Li, C., Polage, C. R., Wu, B., et al. (2018). Advances in the diagnosis and treatment of Clostridium difficile infections. *Emerg. Microbes Infect.* 7:15. doi: 10.1038/s41426-017-0019-4

Peterson, D. E., Bensadoun, R. J., and Roila, F. (2010). Management of oral and gastrointestinal mucositis: ESMO clinical practice guidelines. *Ann. Oncol.* 21, v261–v265. doi: 10.1093/annonc/mdq197

Roberts, C. L., Keita, A. V., Duncan, S. H., O'Kennedy, N., Soderholm, J. D., Rhodes, J. M., et al. (2010). Translocation of Crohn's disease *Escherichia coli* across M-cells: contrasting effects of soluble plant fibres and emulsifiers. *Gut* 59, 1331–1339. doi: 10.1136/gut.2009.195370

Roberts, C. L., Rushworth, S. L., Richman, E., and Rhodes, J. M. (2013). Hypothesis: increased consumption of emulsifiers as an explanation for the rising incidence of Crohn's disease. *J. Crohns Colitis.* 7, 338–341. doi: 10.1016/j.crohns.2013.01.004

Rodriguez-Palacios, A., Aladyshkina, N., Ezeji, J. C., Erkkila, H. L., Conger, M., Ward, J., et al. (2018). 'Cyclical bias' in microbiome research revealed by a portable germ-free housing system using nested isolation. *Sci. Rep.* 8:3801. doi: 10.1038/s41598-018-20742-1

Sainz, N., Barrenetxe, J., Moreno-Aliaga, M. J., and Martinez, J. A. (2015). Leptin resistance and diet-induced obesity: central and peripheral actions of leptin. *Metabolism* 64, 35–46. doi: 10.1016/j.metabol.2014.10.015

Sheng, L., Jena, P. K., Hu, Y., Liu, H. X., Nagar, N., Kalanetra, K. M., et al. (2017). Hepatic inflammation caused by dysregulated bile acid synthesis is reversible by butyrate supplementation. *J. Pathol.* 243, 431–441. doi: 10.1002/path.4983

Siva, N. (2012). Thiomersal vaccines debate continues ahead of UN meeting. *Lancet* 379:2328. doi: 10.1016/s0140-6736(12)61002-2

Smith, P. M., Howitt, M. R., Panikov, N., Michaud, M., Gallini, C. A., Bohlooly-Y, M., et al. (2013). The microbial metabolites, short-chain fatty acids, regulate colonic Treg cell homeostasis. *Science* 341, 569–573. doi: 10.1126/science.1241165

Sokol, H., and Adolph, T. E. (2018). The microbiota: an underestimated actor in radiation-induced lesions? *Gut* 67, 1–2. doi: 10.1136/gutjnl-2017-314279

Suez, J., Korem, T., Zeevi, D., Zilberman-Schapira, G., Thaiss, C. A., Maza, O., et al. (2014). Artificial sweeteners induce glucose intolerance by altering the gut microbiota. *Nature* 514, 181–186. doi: 10.1038/nature13793

Sun, Y., Ma, Y., Lin, P., Tang, Y. W., Yang, L., Shen, Y., et al. (2016). Fecal bacterial microbiome diversity in chronic HIV-infected patients in China. *Emerg. Microbes Infect.* 5:e31. doi: 10.1038/emi.2016.25

Tagawa, H., Irie, J., Itoh, A., Kusumoto, Y., Kato, M., Kobayashi, N., et al. (2015). Bile acid binding resin improves hepatic insulin sensitivity by reducing cholesterol but not triglyceride levels in the liver. *Diabetes Res. Clin. Pract.* 109, 85–94. doi: 10.1016/j.diabres.2015.04.025

Wang, Z., Klipfell, E., Bennett, B. J., Koeth, R., Levison, B. S., Dugar, B., et al. (2011). Gut flora metabolism of phosphatidylcholine promotes cardiovascular disease. *Nature* 472, 57–63. doi: 10.1038/nature09922

Winkler, E. A., Nishida, Y., Sagare, A. P., Rege, S. V., Bell, R. D., Perlmutter, D., et al. (2015). GLUT1 reductions exacerbate Alzheimer's disease vasculo-neuronal dysfunction and degeneration. *Nat. Neurosci.* 18, 521–530. doi: 10.1038/nn.3966

Wrzosek, L., Miquel, S., Noordine, M. L., Bouet, S., Joncquel, C. M., Robert, V., et al. (2013). *Bacteroides* thetaiotaomicron and Faecalibacterium prausnitzii influence the production of mucus glycans and the development of goblet cells in the colonic epithelium of a gnotobiotic model rodent. *BMC Biol.* 11:61. doi: 10.1186/1741-7007-11-61

Xiao, H. W., Li, Y., Luo, D., Dong, J. L., Zhou, L. X., Zhao, S. Y., et al. (2018). Hydrogen-water ameliorates radiation-induced gastrointestinal toxicity via MyD88's effects on the gut microbiota. *Exp. Mol. Med.* 50:e433. doi: 10.1038/emm.2017.246

Zaki, M. H., Boyd, K. L., Vogel, P., Kastan, M. B., Lamkanfi, M., and Kanneganti, T. (2010). The NLRP3 inflammasome protects against loss of epithelial integrity and mortality during experimental colitis. *Immunity* 32, 379–391. doi: 10.1016/j.immuni.2010.03.003

Zanvit, P., Konkel, J. E., Jiao, X., Kasagi, S., and Zhang, D. (2015). Antibiotics in neonatal life increase murine susceptibility to experimental psoriasis. *Nat. Commun.* 6:8424. doi: 10.1038/ncomms9424

Zhang, M., Zhou, Q., Dorfman, R. G., Huang, X., Fan, T., Zhang, H., et al. (2016). Butyrate inhibits interleukin-17 and generates Tregs to ameliorate colorectal colitis in rats. *BMC Gastroenterol.* 16:84. doi: 10.1186/s12876-016-0500-x

Conflict of Interest: The authors declare that the research was conducted in the absence of any commercial or financial relationships that could be construed as a potential conflict of interest.

Copyright © 2020 Li, Xiao, Dong, Luo, Wang, Zhang, Zhu, Zhu, Cui and Fan. This is an open-access article distributed under the terms of the Creative Commons Attribution License (CC BY). The use, distribution or reproduction in other forums is permitted, provided the original author(s) and the copyright owner(s) are credited and that the original publication in this journal is cited, in accordance with accepted academic practice. No use, distribution or reproduction is permitted which does not comply with these terms.

frontiers in Microbiology

ORIGINAL RESEARCH
published: 08 July 2020
doi: 10.3389/fmicb.2020.01454

Investigating the Mechanistic Differences of Obesity-Inducing *Lactobacillus kefiranofaciens* M1 and Anti-obesity *Lactobacillus mali* APS1 by Microbolomics and Metabolomics

*Yu-Chun Lin[1,2], Yung-Tsung Chen[3], Kuan-Yi Li[2] and Ming-Ju Chen[2]**

[1]*Livestock Research Institute, Council of Agriculture, Executive Yuan, Tainan, Taiwan,* [2]*Department of Animal Science and Technology, National Taiwan University, Taipei, Taiwan,* [3]*Institute of Biotechnology, National Taiwan University, Taipei, Taiwan*

Many studies have investigated the anti-obesity effects of probiotics in animal models and humans. However, few studies have focused on the mechanisms of obesity-inducing probiotics. In a previous study, we demonstrated that specific bacterial strains isolated from kefir, *Lactobacillus kefirnofaciens* M1 and *Lactobacillus mali* APS1, possess obesity and anti-obesity effects, respectively, in high-fat diet (HFD)-induced obese mice. Thus, in the present study, we systematically investigated whether APS1 and M1 affect energy homeostasis and lipid metabolism in HFD-induced obese mice and how this might be achieved. We observed that the M1/APS1 intervention influenced fat accumulation by regulating adipogenesis and inflammation-related marker expression both *in vitro* and in a HFD induced C57BL/6J mice model. We also observed putative links between key taxa and possible metabolic processes of the gut microbiota. Notably, families *Christensenellaceae* and *S24_7* were negatively correlated with body weight gain through increase in the essential esterized carnitine for energy expenditure. These results suggest the importance of specific probiotic interventions affecting leanness and obesity of subjects under a HFD, which are operated by modulating the tripartite relationship among the host, microbiota, and metabolites.

Keywords: ***Lactobacillus kefiranofaciens*** **M1,** ***Lactobacillus mali*** **APS1, obesity, microbolomics, metabolomics**

OPEN ACCESS

Edited by:
Margarita Aguilera, University of Granada, Spain

Reviewed by:
Carolina Gómez Llorente, University of Granada, Spain
Diwas Pradhan, National Dairy Research Institute (ICAR), India

****Correspondence:***
Ming-Ju Chen
cmj@ntu.edu.tw

Specialty section:
This article was submitted to Food Microbiology, a section of the journal Frontiers in Microbiology

Received: *05 January 2020*
Accepted: *04 June 2020*
Published: *08 July 2020*

Citation:
Lin Y-C, Chen Y-T, Li K-Y and Chen M-J (2020) Investigating the Mechanistic Differences of Obesity-Inducing Lactobacillus kefiranofaciens M1 and Anti-obesity Lactobacillus mali APS1 by Microbolomics and Metabolomics. Front. Microbiol. 11:1454. doi: 10.3389/fmicb.2020.01454

INTRODUCTION

Diet-caused dysbiosis is an important contributor affecting the development of obesity by suppressing the metabolic capacity of gut microbiota and creating a chronic state of inflammation (Malaisé et al., 2017; Wilkins et al., 2019; Amabebe et al., 2020). Impaired gut permeability caused by dysbiosis leads to a continuous translocation of bacteria, which further jeopardizes the metabolism of nutrients and affects energy extraction, expansion and storage (Pindjakova et al., 2017; Nagpal et al., 2018; Amabebe et al., 2020; Tilg et al., 2020). Additionally, a low-grade activation of the innate immune system and a chronic state inflammatory response often accompany the excessive accumulation of lipid in overweight and obesity subjects due

to physiological adaptive response to the stress of adipocyte (Shoelson et al., 2007; Reilly and Saltiel, 2017).

Clear evidence shows that the gut microbiome plays a crucial role in the functioning of the digestive tract and harvesting energy from the diet as well as modulating the immune system (Bäckhed et al., 2004; Maruvada et al., 2017; John et al., 2018; Zhang et al., 2019; Crovesy et al., 2020). Studies of gut microbiome in both animal models and humans revealed that bacterial species from the Bacteroidetes and Firmicutes phyla are dominated, which comprise more than 90% of the gut microbiota (Huttenhower et al., 2012; Hall et al., 2017). Besides, phyla of Actinobacteria, Proteobacteria and Verrucomicrobia are three important phyla based on the species level and their relative abundances (Mack et al., 2016; Hall et al., 2017).

Microbiome-targeted therapies such as probiotics, prebiotic-resistant starches, and fecal microbiota transplant (FMT) provide novel opportunities to prevent and treat the development of obesity and metabolic syndrome by manipulation of the gut microbiome (Kamada et al., 2013; Hill et al., 2014; Parekh et al., 2015; Maruvada et al., 2017). Accumulating evidence indicates that supplementation with specific probiotics in dietary interventions could affect the host metabolism and modulate the glucose homeostasis in an animal model and human studies (Holmes et al., 2012; Cano et al., 2013; Yadav et al., 2013; Cheng et al., 2015; Aoki et al., 2017). Some species within the *Lactobacillus* demonstrated anti-obesity (Karimi et al., 2015; Li et al., 2016) or anti-diabetic (Honda et al., 2012; Li et al., 2016) effects in animal models or humans.

Two strains, *Lactobacillus kefirnofaciens* M1 (M1) and *Lactobacillus mali* APS1 (APS1), were isolated from Taiwanese kefir grain and sugary kefir grain, respectively, in our lab (Chen et al., 2008). *L. kefirnofaciens* M1 has been demonstrated to have an immune-modulating activity *in vitro* (Hong et al., 2009) and anti-allergic (Hong et al., 2010), anti-asthma (Hong et al., 2011), and anti-colitis (Chen et al., 2012) effects in a murine model. The immunoregulatory effects of *L. kefirnofaciens* M1 involve upregulating the regulatory T (Treg) cell and inhibiting secretion of proinflammatory and inflammatory cytokines. *L. mali* APS1 demonstrated a beneficial effect on accelerating weight loss (Chen et al., 2018b) and on ameliorating hepatic steatosis (Chen et al., 2018a) in a murine model of diet-induced obesity. *L. mali* APS1 also possesses an anti-colitis effect. For intestinal barrier protection, both *L. kefirnofaciens* M1 and *L. mali* APS1 could improve epithelial barrier function *in vitro* by increasing the transepithelial electrical resistance (TEER) and significantly upregulating the level of the chemokine CCL-20 (Chen et al., 2012). The features of both strains suggest a potential to modulate chronic inflammatory activities and strengthen the gut epithelial layer of obese individuals. Surprisingly, M1 and APS1 exhibited opposite results on body weight and glucose homeostasis in high-fat diet (HFD)-induced obese mice. M1 possesses obesity effects, and APS1 has anti-obesity and anti-T2D effects (Lin et al., 2016b).

Many studies have investigated the anti-obesity or anti-diabetic effects of probiotics in animal models or humans. However, few studies have focused on the mechanisms of obesity-inducing probiotics. Thus, in the present study, we further systematically investigated whether APS1 and M1 affected energy and glucose homeostasis in HFD-induced obese mice by regulating adipogenesis and inflammation-related proteins through modulating metabolites *via* manipulating the gut microbiota composition.

MATERIALS AND METHODS

M1 and APS1 Preparation

L. kefiranofaciens M1 and *L. mali* APS1 were grown in MRS broth (Difco Laboratories, Detroit, MI) and incubated at 37 and 30°C for 36 and 12 h, respectively. To prepare the probiotic treatments, the bacterial cells were harvested by centrifugation (3,000 × *g* for 15 min) during the log phase. Cultures were washed and suspended in saline three times. After washing, the bacteria were resuspended in saline and adjusted to 5×10^8 CFU/ml for following *in vitro* and *in vivo* studies. The preparation of bacterial cell-free excretory supernatants (CFSs) and intracellular cell-free extracts (CFEs) was adopted from Zeng et al. (2016). Briefly, M1 and APS1 strains were harvested by centrifugation at 3,000 × *g* for 10 min, washed three times and resuspended in phosphate-buffered saline (PBS; adjusted to 10^9 CFU/ml). The cell pellets of M1 and APS1 were resuspended before ultrasonic disruption (Mucroson XL 2000, Minsonix Inc., Farmingdale, NY, USA) in 3-s pulses for 30 s in an ice bath. The cell fractions were separated by ultracentrifugation at 3,000 × *g* for 10 min.

In vitro Cell Culture

Cell Preparation

Both RAW264 macrophage cell line and 3T3-L1 preadipocytes, purchased from Bioresource Collection and Research Center, Food Industry Research and Development Institute (Hsinchu, Taiwan), were cultured in Dulbecco's Modified Eagle's Medium (DMEM; Corning, Lowell, MA, USA) containing 10% fetal bovine serum (FBS) and 1% antibiotic-antimycotic in a humidified atmosphere of carbon dioxide (CO_2) 5/95% air atmosphere at 37°C.

3T3-L1 Adipocyte Differentiation

3T3-L1 was first cultured in preadipocyte medium containing DMEM media with 10% bovine calf serum 25 mmol/L glucose, 10% bovine serum, 100 units/ml penicillin, and 100 μg/ml streptomycin in a humidified incubator set to 37°C and 5% CO_2. Differentiation of 3T3-L1 preadipocytes into mature adipocytes was performed using a 3T3-L1 differentiation kit (Biovision, Milpitas, CA, USA) according to the manufacturer's instructions. For initiate differentiation, cell cultures were replaced medium with differentiation medium containing differentiation cocktail and incubated for 3 days in a humidified incubator at 37°C with 5% CO_2. After differentiation induction, cell cultures were maintained in a maintenance medium containing 1 μl of insulin to 1 ml of DMEM/F12 (1:1) with 10% FBS and the medium replaced in every 2–3 days. After 7–10 days, lipid droplet accumulation was observed by light microscopy BX-50 (OLYMPUS, Tokyo, Japan).

Co-culture of M1/APS1, Adipocytes, and Macrophages

After differentiation, 3T3-L1 cells were cocultured with RAW264 using the Transwell inserting with a 3 μm porous membrane (Corning, Lowell, MA, USA) to separate adipocytes (lower well) from macrophages (upper well). After 24-h incubation, 10^7 CFU/ml of L. kefiranofaciens M1/L. *mali* APS1 were co-cultured with upper layer RAW264, at 37°C for 24 h. The cells in the lower well were lysed in Trizol for further study. For CFS/CFE, to examine the effect of M1 and APS1 on the differentiation of preadipocytes into mature adipocytes, 3T3-L1 preadipocytes were treated with 10% of CFE or CFS of M1 and APS1 in culture medium during the differentiation period.

Oil Red O Staining of Lipid Droplets in 3T3-L1

3T3-L1 cells were washed with DPBS and fixed with 4.0% formaldehyde (Sigma-Aldrich, St. Louis, MO, USA). After being fixed, the cells were stained with Oil red O solution (Sigma-Aldrich) containing 0.5% Oil red O in isopropanol for 30 min at room temperature (RT) and then washed three times with distilled water. The appearance of lipid accumulation was visualized by bright-field microscopy BX-50 (OLYMPUS, Tokyo, Japan). The area ratio (%) of Oil red O staining was determined by ImageJ 1.3 image analysis software (National Institutes of Health).

In vivo Animal Model

A total of 40 male (7-week-old) C57BL/6J mice were purchased from BioLasco Corp., Ltd. (Ilan, Taiwan). The tested mice were housed in cages (one mouse per cage) under a controlled RT and 12 h light-dark cycle and provided food and filtered water *ad libitum*. All animal husbandry and experimental activities were conducted in accordance with national legal requirements. The studies were conducted in compliance with relevant guidelines, approved by the Institutional Animal Care and Use Committee of Livestock Research Institute, Council of Agriculture, Taiwan (Approval No: LRI IACUC 106-32). After 1 week of acclimatization, the mice were divided into four groups (n = 10 per group): a normal diet (ND) group that received the control diet (D12450B; Research Diets, Inc., New Brunswick, NJ, USA), a HFD group that received a HFD (D12492; Research Diets, Inc.) with oral administrated PBS, an M1 intervention group that was simultaneously fed a HFD and daily intragastric administration of 10^8 CFU/mouse *L. kefiranofaciens* M1, and an APS1 intervention group that was simultaneously fed a HFD and *L. mali* APS1 10^8 CFU/mouse intragastrically. All groups started from 8 weeks of age and continued until 16 weeks of age. The energy content of the HFD consisted of 60% fat, 20% carbohydrates, and 20% protein (5.24 kcal/g). The body weight and food intake of all mice were measured once a week. At the end of the experiment, all of the tested mice were fasted for 8 h, then anesthetized with isoflurane and sacrificed for serum and tissue collection. For RNA extraction, the adipose tissue was freshly harvested and then frozen stored in RNA*later* (Applied Biosystems, Foster City, CA, USA).

Quantitative Real-Time Polymerase Chain Reaction Analysis

To analyze adipogenesis-related gene expression *in vitro* and *in vivo* models, the total RNA was isolated from the samples using the SPLIT RNA Extraction Kit (Lexogen, Vienna, Austria) based on the product manual. Extracted total RNA was further purified with Ambion™ RNase Inhibitor (Applied Biosystems) and TURBO DNA-free™ Kit (Applied Biosystems), and then saved for further cDNAs synthesis. cDNAs were synthesized from 1 mg total RNA using a High-Capacity cDNA Reverse Transcription Kit with RNase Inhibitor (Applied Biosystems). cDNAs were then analyzed by qPCR using a Power SYBR Green PCR Master mix (Applied Biosystems), which is performed using a StepOnePlus Real-Time PCR System (Applied Biosystems) for qPCR analyses. Specific primer sequences were adopted from Breasson et al. (2017). Relative quantification of gene expressions was performed using the comparative Ct method and normalized by an internal control, glyceraldehyde-3-phosphate dehydrogenase (GAPDH). Results were expressed as fold difference relative to a relevant control sample.

Immunohistochemistry

After anesthetizing, epididymal white adipose tissue (eWAT) of the test animal was collected and fixed in 4% formaldehyde. Tissues were then paraffin-embedded and sectioned at 5 μm thickness. For Immunohistochemistry (IHC), sections were heated to 62°C to remove wax and then rehydrated prior to treatment with blocking serum (PBS or 0.5% Triton X-100 with 5% serum) for 1 h at RT. The appropriate volume of diluted primary anti-F4/80 (#70076, Cell Signaling Technology, Inc., Danvers, MA, USA) or anti-CD11c (#45581, Cell Signaling Technology) antibody was added and incubated overnight at 4°C. After washing, the sections were incubated at RT with HRP-conjugated anti-Rabbit-IgG secondary antibody (#31460, Thermo Fisher Scientific) for 1 h. Positive cells were visualized with diaminobenzidine (DAB; TA-060, Thermo Fisher Scientific) and counterstained with Mayer's hematoxylin under a light microscope SG-EX30 microscope (SAGE vision, Taiwan). Each group had four sections and each section had three visual fields.

Analysis of SCFA

The fecal samples were collected at the end of animal study and immediately stored at −80°C. Fecal short chain fatty acids (SCFAs) were analyzed using gas chromatography-flame ionization detector (GC-FID) with a modified method described by Mehrpouya-Bahrami et al. (2017). Briefly, 30 mg of each fecal sample was weighed and suspended in 300 μl saturated NaCl solution, and then homogenized for approximately 2 min. Second, subsequently, the samples were acidified with 20 μl of 10% sulfuric acid (Sigma-Aldrich, St. Louis, MO, USA). After acidification, 400 μl of diethyl ether was added to the samples for SCFAs extraction, and then centrifuged for 15 min at 14,000 × g under 4°C. The supernatant was quantified using a GC-FID to measure acetate, propionate, and butyrate.

Western Blot Analysis

The fresh epididymal adipose of the tested mice was frozen immediately in liquid nitrogen after collection and used for preparation of the whole cell lysate. Two microgram total protein from adipose tissue, was separated by SDS-PAGE using 4–20% Tris-glycine gels (Invitrogen). After electrophoresis, proteins were transferred onto polyvinylidene difluoride (PVDF; Millipore IPVH 00010) membranes by iBlot 2 Dry Blotting System (Invitrogen) and blocked with 5% BSA (UniRegion Bio-Tech, Taipei. Taiwan) in Tris-buffered saline with 0.1% Tween 20 (TBST) at RT for 1 h. The member was then washed three times for 5 min each with 5 ml PBS with Tween-20 (PBST). After that, the membranes were subsequently incubated overnight at 4°C with primary antibodies (1:1,000 dilute with 1X PBST and 5% BSA) used for immunoblotting as follows: acetyl-CoA carboxylase (ACC; C83B10; anti-ACC, #3676, Cell Signaling Technology, Inc.), anti-fatty acid synthase (anti-FAS, #3180, Cell Signaling Technology, Inc.) and anti-β-actin antibody (BA3R, Thermo Fisher Scientific). Further, the membrane was washed three times for 5 min with 5 ml TBST, and then incubated with Goat Anti-Rabbit IgG Antibody, Peroxidase Conjugated (Millipore AP132P at 1:1,000) and Goat anti-mouse IgG, F(ab')2-HRP (Santa Cruz, sc-3697 at 1:1,000) in 5 ml of blocking buffer with gentle agitation for 1 h at RT. After being washed a further three times with TBST, the anti-specific protein was visualized by the enhanced chemiluminescence detection system (Millipore). Quantification of the protein level in the luminescent bands was performed by ImageJ software (NIH).

Analysis of Satiety Hormones

Total gastric inhibitory peptide (GIP), total ghrelin, Peptide YY (PYY), pancreatic polypeptide (PP), leptin, and resistin levels in mouse serum were measured using the Milliplex® MAP Kit and mouse metabolic hormone 96-well plate assay (Millipore Corporation) according to the manufacturer's instructions.

DNA Extraction and Sequencing of Gut Microbiota

The bacteria genomic DNA in the fecal samples from the ND, HFD, HFDM1, and HFDAPS1 groups was extracted by a QIAamp DNA Stool kit (QIAGEN, Hilden, Germany) according to the manufacturer's instruction. The bacterial 16S ribosomal RNA variable region V3–V4 was amplified by PCR using a primer with a sample-specific barcode (V3F: 5′-CCTACGGGNGGCWGCAG-3′; V4R: 5′-GACTACHVGGGTATCTAATCC-3′) for microbiome analysis as described previously (Chang et al., 2015). PCR products were employed for microbiome analysis on an Illumina MiSeq sequencing platform according to the manufacturer's instructions. The raw reads were denoised and filtered using QIIME (v1.7.0) to remove sequences that containing a short variable region (<90 bp) or undetermined bases (>2 bases) to get effective tags in V3–V4 variable region. All 16S rRNA gene sequencing data were submitted to the NCBI's sequence read archive (SRA) database under the accession number PRJNA634807. Operational taxonomic unit (OTU) clustering and species annotation of barcoded PCR amplicons from the various fecal samples were performed from representative sequences using UPARSE software (Version 7.0.1001[1]) and the Greengenes database based on ribosomal database project classifier (Version 2.2), respectively. Chao 1 and Shannon index of alpha diversity and partial least squares-discriminant analysis (PLS-DA) plots were measured with QIIME (Version v1.7.0) using R software (Version 2.15.3). The abundance of specific bacteria at the genus- and species-level at $p < 0.05$ was determined using the non-parametric Kruskal-Wallis test. Taxonomic cladograms were derived from a Linear discriminant analysis Effect Size (LEfSe) analysis with linear discriminant analysis (LDA) scores greater than 3 and significance at $\alpha < 0.05$, as determined by Kruskal-Wallis test. To clarify a co-occurrence network of the predominant microbiota, we performed a bivariate correlation analysis for the 15 most abundant families and obesity-related indicators using Spearman's correlation coefficient and R and SAS software version 9.4 (SAS Institute Inc., Cary, North Carolina, USA) with a value of p as 0.05. The correlation heatmaps between gut microbiota and inflammation markers and serum metabolites were generated by R and SAS software version 9.4 (SAS), and then created using GraphPad Prism software (Prism 7, GraphPad Software Inc., CA, USA).

Non-Targeted Serum Metabolomics Profile Investigation

Blood plasma samples were collected from the tested mice and stored at −80°C until analysis. The metabolomic profile analysis was conducted by the commission service of the Metabolomics Core Laboratory at the Center of Genomic Medicine, National Taiwan University (Taipei, Taiwan) using ultraperformance liquid chromatography (LC; Infinity 1290, Agilent Technologies, CA, USA) coupled with a quadrupole-time of flight (Q-TOF) mass spectrometer (6540, Agilent Technologies, Santa Clara, CA, US) with electrospray ionization. The Acquity HSS T3 column (2.1 × 100 mm, 1.8 μm pore size; Waters, Milford, MA, USA) was used and maintained at 40°C. Metabolites were identified by analysis of the spectra of mass spectrometry (MS) using XCMS2 (Benton et al., 2008), TIPick (Ho et al., 2013), and Batch Normalizer (Wang et al., 2013) methods.

Statistical Analyses

The values are expressed as the mean ± standard deviation. In addition to the gut microbiota, all statistical analyses were performed by GraphPad PRISM 7 (GraphPad Software, Inc.). Significant differences among the experimental results expect for relative bacterial abundance were estimated by a one-way ANOVA with *post hoc* Tukey's test. A probability level $p < 0.05$ was considered statistically significant. Differences in the abundance of specific bacteria were determined using the non-parametric Kruskal-Wallis test.

[1]http://drive5.com/uparse/

RESULTS

APS1 and M1 Interventions Affect TG Lipid Accumulation Through Modulating Adipogenesis, Lipogenesis, and Inflammation in 3T3-L1 Cells

After confirmation of no cytotoxicity effect on the cells (data no shown), we first *in vitro* evaluated the effect of M1 and APS1 on adipocyte differentiation and key lipogenesis markers involving in adipocytes. Results indicated that the M1 group in viable cells could induce significantly more production of lipid droplets than the CT and APS1 groups. Whereas, CFS and CFE from APS1 could significantly inhibit lipid accumulation relative to the control ($p < 0.05$; **Figure 1A**). Consistently, APS1 intervention showed a tendency to downregulate the mRNA expression of adipogenesis and lipogenesis markers

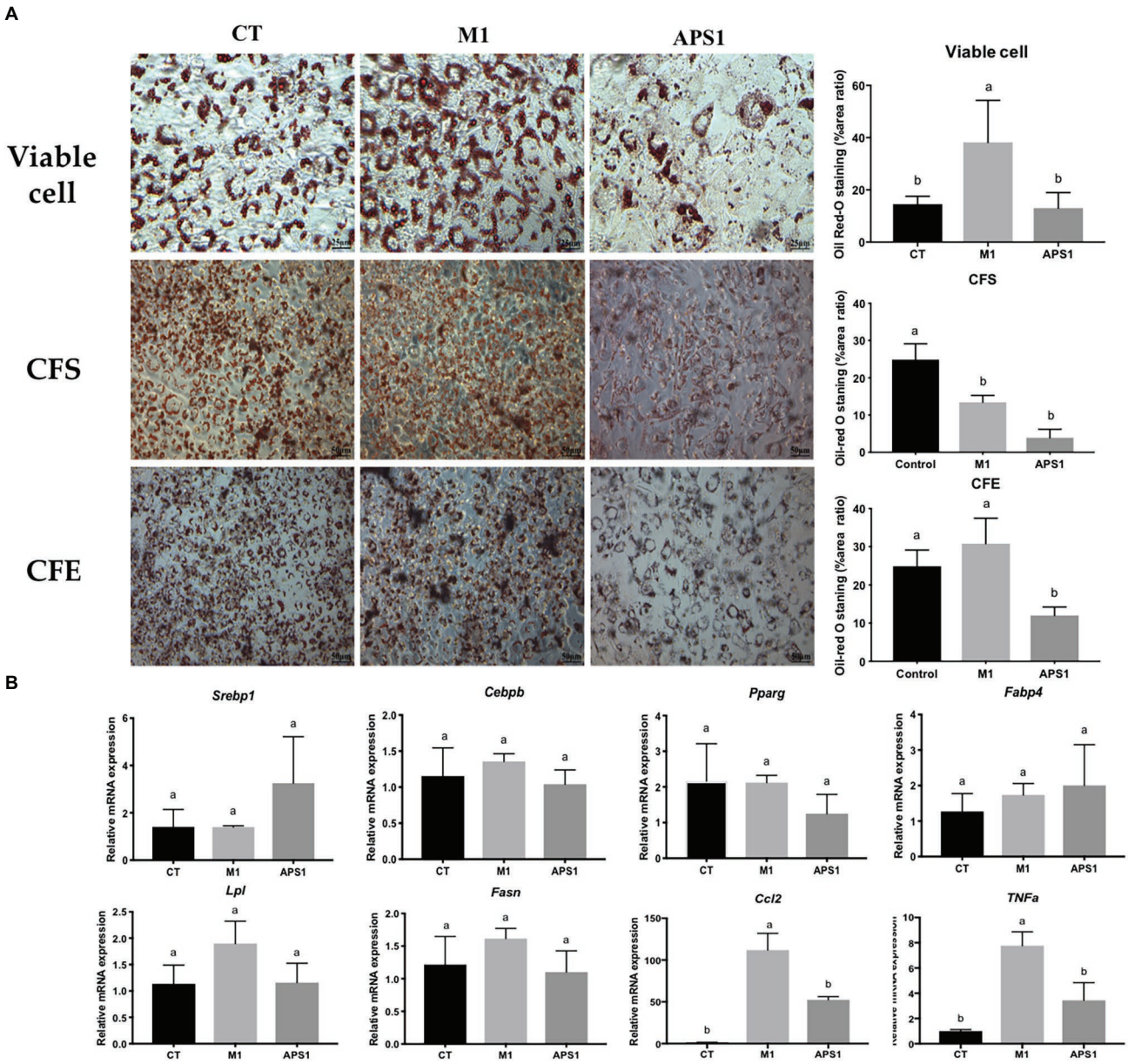

FIGURE 1 | Effects of M1 and APS1 on modulation of adipogenesis in 3T3-L1 cells. **(A)** Lipid accumulation and the area ratio by ImageJ (%) in 3T3-L1 cells treated by viable cell, intracellular cell-free extract (CFE), bacterial cell-free excretory supernatant (CFS) of M1 and APS1 with Oil red O staining; and **(B)** modulation of adipogenesis and macrophage-derived *Tnf* and *Ccl2* relative mRNA levels in 3T3-L1 adipocytes after treated with viable M1 and APS1. Relative quantification of gene expressions was performed using the comparative Ct method with normalization to glyceraldehyde-3-phosphate dehydrogenase (GAPDH). Results were expressed as fold difference relative to a relevant control sample. Data are expressed as the mean ± SD ($n = 3$). Labeled means without a common superscript letter differ, $p < 0.05$.

(*Pparg*, *Lpl*, and *Fasn*) in 3T3-L1 cells when compared with the M1 group without significant difference ($p > 0.05$; **Figure 1B**). Conversely, treating cells with M1 promoted inflammation by upregulating biomarkers of inflammatory cytokines (*Ccl2* and *Tnf-α*; $p < 0.05$) (**Figure 1B**). *In vitro* results demonstrated that APS1 and M1 might affect lipid accumulation by modulating adipogenesis, lipogenesis, and inflammation.

APS1 and M1 Interventions Affect the Obesity-Induced Mass/Size and Inflammation of Adipose Tissue by Regulating Adipogenesis, Macrophage Recruitment, and M1/M2 Status *in vivo*

In vivo results indicate that APS1 intervention (5×10^8 CFU/mouse/day) not only significantly decreased the body weight and mean diameters of adipocytes, but also reduced the weights of eWAT (by 36.68%), rpWAT (by 28.53%), and iWAT (by 27.57%) relative to the HFD group ($p < 0.05$; **Figures 2A–C**). Whereas, the body weight of mice treated with M1 (10^8 CFU/mouse) for 8 weeks was significantly higher than that of HFD mice ($p < 0.05$; **Figure 2A**). However, no significant difference was observed in mean diameters of adipocytes and the weights of retroperitoneal, intrascapular, epididymal, and visceral white adipose tissues between the HFDM1 and HFD groups ($p > 0.05$; **Figures 2B,C**).

We then investigated the possible underlying molecular mechanisms. Results showed that APS1 intervention could downregulate adipogenesis-related gene, *Fasn* (**Figure 2D**). Conversely, upregulation of adipogenic gene expression, *Pparg*, was observed in the HFDM1 group (**Figure 2D**). After studying mRNA expression, western blot analysis revealed that APS1 intervention showed a tendency to reduce the levels of FAS and ACC as compared with the HFDM1 group ($p > 0.05$; **Figure 2E**).

Besides adipogenesis, the effects of *L. kefiranofaciens* M1 and *L. mali* APS1 on types of macrophages accumulating on the adipose tissue of HFD-induced obese mice were also investigated. We found that APS1 intervention could significantly downregulate mRNA expressions of macrophage markers (F4/80, CD11c), inflammatory markers (*Tnf-α*, *MCP-1*), and M1 activated macrophage (*IL-1ra*), as well as upregulate M2 activated macrophage *CCR2* relative to the M1 and HFD groups ($p < 0.05$). Whereas, M1 intervention showed significantly higher mRNA expressions of macrophage markers (*CD68*, CD11c), inflammatory markers (*MCP-1*), and M1 activated macrophage (*IL-1ra*; $p < 0.05$) when compared with other groups (**Figures 3A–C**). The further IHC analysis for macrophage markers indicated that the fat subjects (HFD and HFDM1 groups) had larger adipocytes with higher F4/80 and CD11c in the eWAT than the lean subjects (NC and HFDAPS1 groups; **Figure 3D**).

APS1 and M1 Interventions Regulate Metabolites and Fecal SCFAs Affecting Lipid Metabolism in HFD-Induced Obese Mice

Next, we studied the roles of metabolites and SCFAs specifically changed by the APS1 and M1 interventions on body weight gain and lipid metabolism. The PCA plot of non-targeted metabolomic profiling showed a significant separation among all tested groups using 24 significant detectable metabolites, explaining 31.3% of the variation (**Figure 4**). Among the metabolites, eight compounds, including 3-hydroxy 3-methylglutaric acid (HMG), corticosterone, glycerophosphocholine (GPC), glycine, L-isoleucine, octanoyl-L-carnitine (OLC), propionyl-L-carnitine (PLC), and traumatic acid, demonstrated significant differences among the four groups ($p < 0.05$; **Table 1**). After analysis by the Kyoto Encyclopedia of Genes and Genomes (KEGG) database, the metabolites were related to lipid metabolism, energy expenditure, lipid peroxidation, anti-inflammation, fat oxidation, and anti-oxidative stress (**Table 1**).

Besides, the mice fed with APS1 also had significantly increased excretion levels of cecal acetate, propionic acid and butyric acid ($p < 0.05$; **Figure 5A**). Upregulation of SCFAs was not observed in the HFDM1 group. Accompany the SCFAs, the HFD group showed significantly higher leptin, PP, and resistin than the ND group ($p < 0.05$; **Figure 5B**). The mice that received the APS1 significantly reduced the production of resistin compared to the HFD group ($p < 0.05$). Administration of M1 could downregulate the production of leptin and resistin (**Figure 5B**).

APS1 and M1 Interventions Modulated Enriched Taxa in HFD-Induced Obese Mice

We then investigated whether the modulating effects of M1 and APS1 on features of obesity and adipose low-grade inflammation were associated with changes in metabolites *via* the gut microbiota using NGS. First, the alpha-diversity analysis of Chao 1 showed no significant difference ($p > 0.05$) in the richness of gut microbiota among the groups (**Figure 6A**). However, a significant Shannon diversity index ($p < 0.05$) was observed between the ND and HFDAPS1 groups (**Figure 6A**). Next, we performed a supervised PLS-DA based on OUT levels to evaluate the variant of gut microbial composition among the treated groups. Our PLS-DA plot shows that PLS1 and PLS2 explain 15 and 6.45% of the variation of gut microbiota composition, respectively, effectively separating each group (**Figure 6A**).

To further identify the specific bacterial taxa that were predominant as the biomarkers among the groups, the LEfSe was calculated. A total of 25 influential taxonomic clades (LDA score >3) were recognized (**Figure 6B**). The most impacted taxa in the ND group were the family *S24_7* (within the phylum Bacteroidetes), the order Bacteroidales (within the phylum Bacteroidetes), the family *Christenseneliaceae* (within the phylum Firmicutes), and species *Lactococcus garvieae* (within the phylum Firmicutes). After 8-week HFD feeding, the order Actinomycetales and family *Caulobacteraceae* (within the order Caulobacterales) were more predominant in the HFD group than in the other groups. Administrating APS1 specifically influenced 11 taxonomic clades in the mice, including the genera *Adlercreutzia* (within phylum Actinobacteria), *Actinomycetospora*

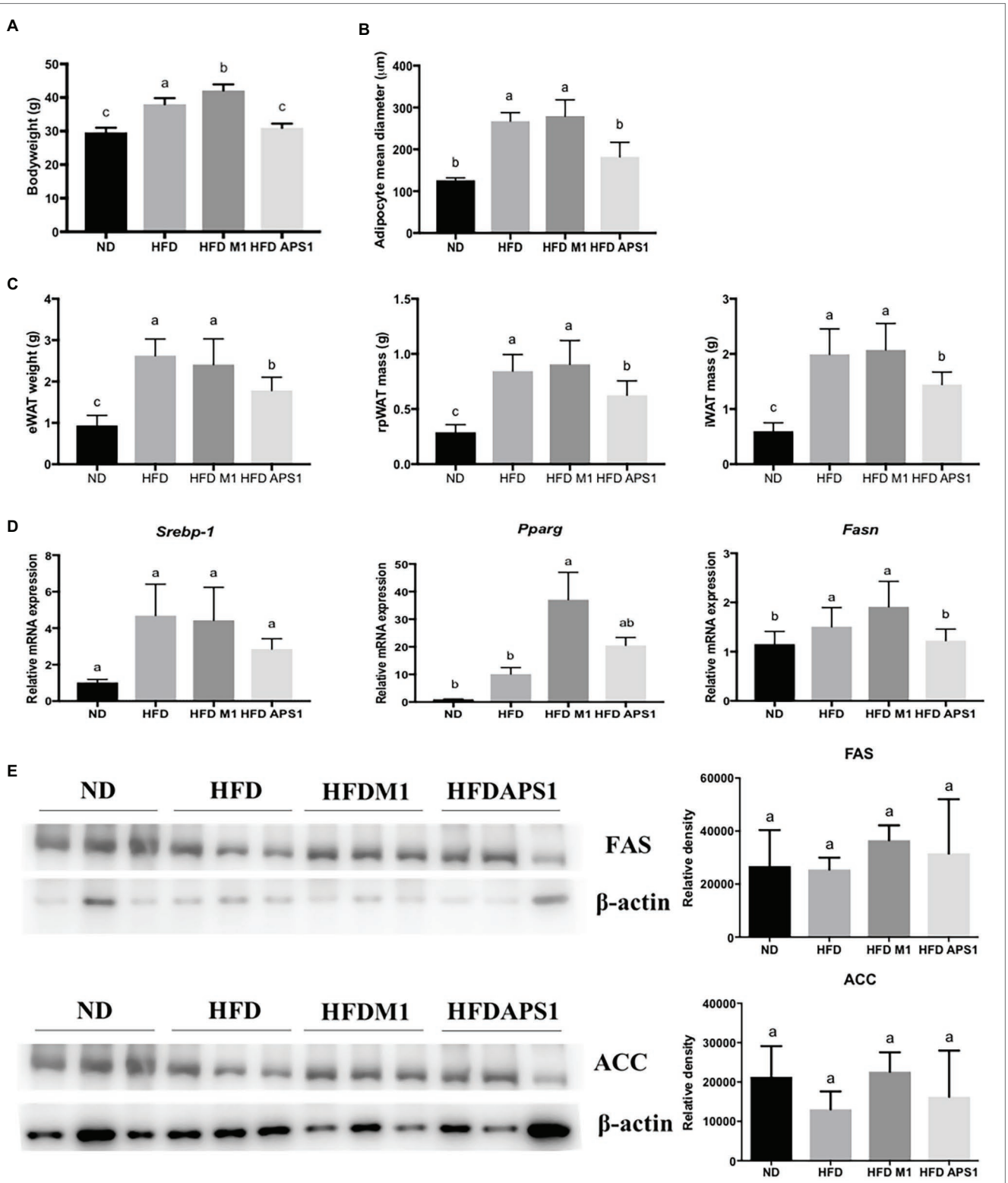

FIGURE 2 | M1 and APS1 regulate fat hypertrophy and mRNA expressions of adipogenesis in mouse adipose tissue. M1 and APS1 interventions modulated **(A)** body weight; **(B)** the mean diameters of epididymal white adipose tissue (eWAT) adipocytes; **(C)** the weight of eWAT, rpWAT and iWAT; **(D)** adipogenesis-related mRNA expressions in mouse eWAT; **(E)** Western blot analyses of fatty acid synthase (FAS) and acetyl-CoA carboxylase (ACC) in adipose tissue. Relative quantification of gene expressions was performed using the comparative Ct method with normalization to GAPDH. Results were expressed as fold difference relative to a relevant control sample. Data are expressed as the mean ± SEM of 8–10 mice per group. Labeled means without a common superscript letter differ, $p < 0.05$.

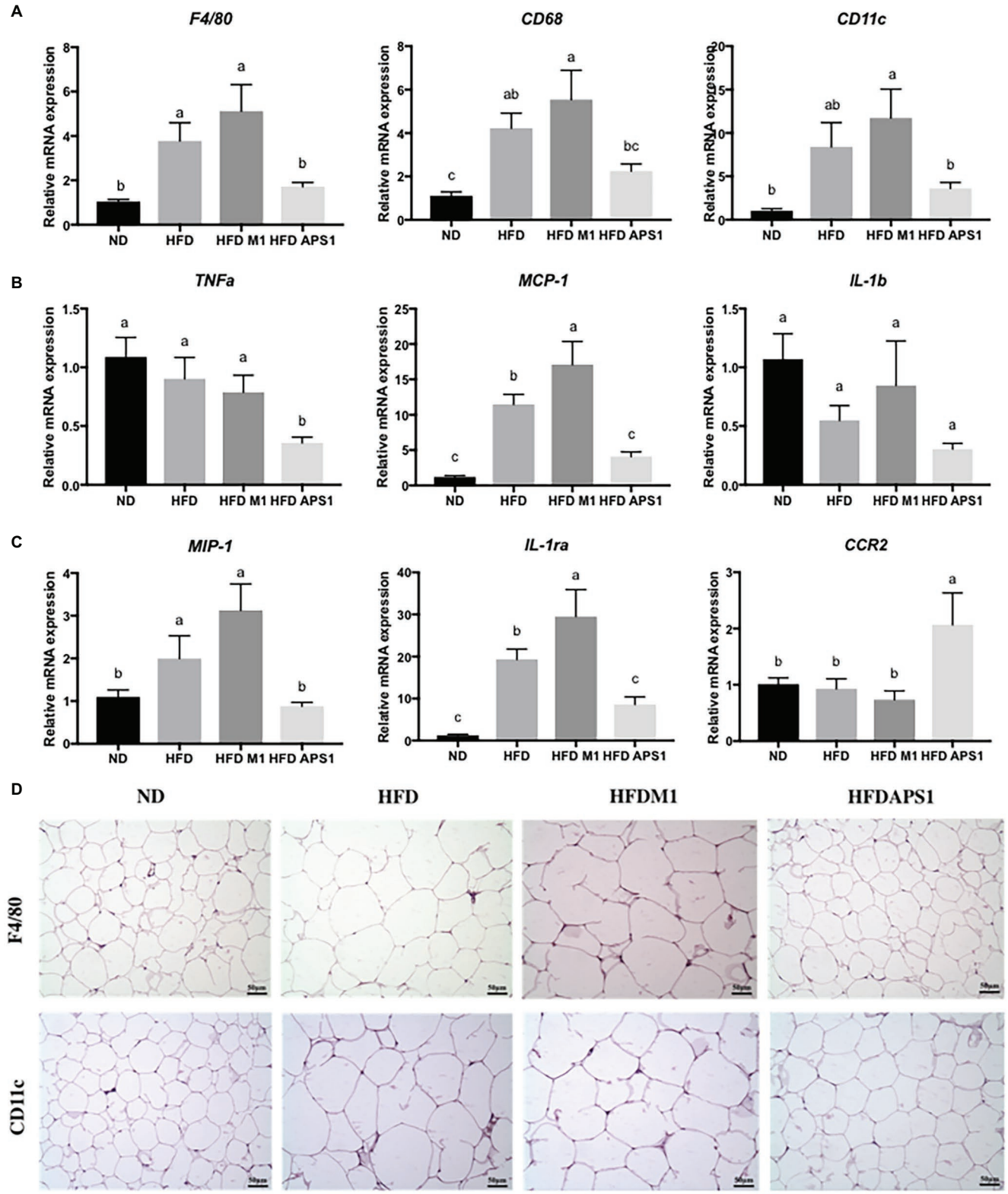

FIGURE 3 | Effects of M1 and APS1 on expression of **(A)** macrophage markers; **(B)** inflammatory markers; **(C)** M1- and M2-activated macrophages and **(D)** immunohistochemistry (IHC) analysis of F4/80 and CD11c in adipose tissues of high-fat diet (HFD)-induced obese mice. Relative quantification of gene expressions was performed using the comparative Ct method with normalization to GAPDH. Results were expressed as fold difference relative to a relevant control sample. Data are expressed as the mean ± SEM of 8–10 mice per group. Labeled means without a common superscript letter differ, $p < 0.05$.

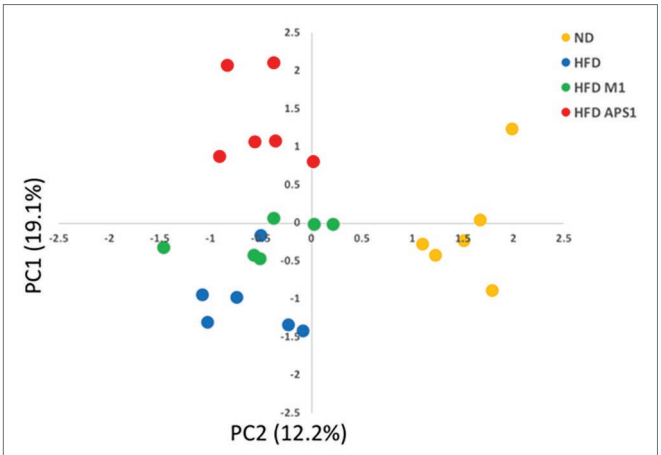

FIGURE 4 | PCA plot of metabolomics profile based on PC1 and PC2 from mean intensity values of total detected metabolites.

(within phylum Actinobacteria), and the species *Candidatus nitrososphaera* (within phylum Actinobacteria). When orally administered M1, the most influential taxa were the class Clostridia (within the phylum Firmicutes), the family *Streptococcaceae* (within the phylum Firmicutes), and *Lactococcus* genus (within the phylum Firmicutes).

M1 and APS1 Interventions Affect Body Weight Gain by Manipulating the Network of Co-occurring Predominant Bacteria at the Family Level

After identifying the specific bacterial taxa that were predominant as the biomarkers among four groups, the roles of these biomarkers in body weight gain and adipose inflammation were investigated. First, we constructed a module of the microbiome network among eight LEfSe selected families from all groups (**Figure 6C**). We observed that *S24_7* was positively correlated with *Christensenellaceae*. *Streptococcaceae* was negatively correlated with *S24_7* and *Christensenellaceae*. We further correlated eight LEfSe selected families with body weight gain and lipid weight. The families *S24_7* and *Christensenellaceae* showed a negative correlation with body weight gain and lipid weight while *Streptococcaceae* had a positive correlation with lipid weight. We validated these results by determining the relative abundance of specific bacteria at the family level of taxonomic cladograms, where we also found that the families *S24_7* and *Streptococcaceae* were enriched in lean and fat subjects, respectively (**Figure 6D**).

M1 and APS1 Mediate Obesity-Related Adipose Inflammation by Regulating the Metabolites *via* Specific Bacterial Taxa

Finally, using Spearman's correlations, we verified that M1 and APS1 modulate inflammation and lipid metabolism by regulating the metabolites *via* microbiota (**Figure 7**). Serum OLC, PLC, and traumatic acid showed positive correlations with families *S24_7* and *Christensenellaceae*, and species *garvieae*, and had negative correlations with phylum Firmicute, family *Streptococcaceae*, and genus *Lactococcus* (**Figure 7**). Circulating isoleucine was positively correlated with the *Streptococcaceae* family and *Lactococcus* genus and negatively correlated with families *S24_7* and *Christensenellaceae* in the whole study population (**Figure 7**). Four taxa, including *S24_7* and phylum Bacteroides, had significant negative correlations with serum GPC. Serum HMG showed negative correlations with family *Paenibacillaceae* and genus *Actinomycetospora*, but positive correlations with *S24_7*, *Christensenellaceae*, and *garvieae*.

DISCUSSION

In a previous study, we demonstrated that specific bacterial strains isolated from kefir, *L. kefirnofaciens* M1 and *L. mali* APS1, possess obesity and anti-obesity effects, respectively, in HFD-induced obese mice. In the present study, we investigated the mechanism contributing to the opposite effects in body weight, further underscoring the importance of the tripartite relationship among the host, microbiota, and metabolites. Our findings highlight three interdependent effects of the gut microbiome on adipogenesis, lipogenesis, and inflammation through APS1 and M1 interventions.

First, we observed that APS1 and M1 interventions elucidated different regulations on gene expression of lipid metabolism and cellular crosstalk in both cell line and adipose tissue. The HFDM1 group might be more effective at extracting energy from food and stimulating lipogenesis through upregulating an essential nuclear hormone receptor (*Pparg*). Conversely, the HFDAPS1 group suppressed lipid accumulation by downregulating the mRNA expression of adipose *Pparg* and *Fasn*, as well as observed tendency for reduced SREBP 1 and ACC at protein level. Adipocyte differentiation is regulated by complex modulation of various transcription factors and specific proteins. The PPARγ is considered key early regulators of adipogenesis, while FAS and ACC are the two major enzymes of *de novo* lipogenesis, which are abundantly expressed in adipose tissues under the control of SREBP1 (Nishimura et al., 2014; Moseti et al., 2016; Gross et al., 2017). SREBP1, the primary substrate for AKT-mediated lipid metabolism, promotes lipid biosynthesis and inhibits lipolysis (Niso-Santano et al., 2015; Yan and Zheng, 2017; Choi et al., 2018).

Besides, because of obesity, the HFDM1 group demonstrated low-grade inflammation in visceral adipose tissue through enhancing production of inflammation-related cytokines, *Ccl2* and *Tnf-α*. Additionally, low-grade inflammation also affects adipocyte function with macrophage infiltration of adipose tissue. The adipose tissue macrophages (ATMs) are characterized as proinflammatory macrophages (M1) and noninflammatory macrophages (M2) according to their polarization state (Lumeng et al., 2007; Chang et al., 2015).

TABLE 1 | The detected [by liquid chromatography–mass spectrometry (LC-MS)] differential metabolites of plasma sample among the normal diet (ND), high-fat diet (HFD), HFDM1, and HFDAPS1 groups.

Metabolites	Ion (m/z)	Mean intensity[1,2]				*p* value	Physiological function
		HFD/ND	ND/HFD	HFDM1/HFD	HFDAPS1/HFD		
3-Hydroxy 3-methylglutaric acid	161.046	0.097	10.271	3.286	3.912	0.00193	Lipid metabolism
Corticosterone	369.204	0.351	2.848	1.979	4.919	0.00634	Energy expenditure
Glycerophosphocholine	258.108	3.999	0.250	0.709	0.404	0.03595	Lipid peroxidation
Glycine	76.039	0.508	1.970	1.189	1.768	0.01156	Anti-inflammation
l-isoleucine	132.101	2.331	0.429	1.101	0.994	0.03404	Protein metabolism
Octanoyl-l-carnitine	288.217	0.078	12.755	1.186	1.977	0.00097	Fat oxidation
Propionyl-l-carnitine	218.139	0.502	1.992	1.189	1.243	0.00853	Fat oxidation
Traumatic acid	227.129	0.054	18.589	0.609	5.223	0.00108	Anti-oxidative stress

[1]*n = 6 per group.*

[2]*Fold change was calculated by dividing the mean of the peak intensity of each metabolite from the ND, HFD, HFDM1, and HFDAPS1 groups.*

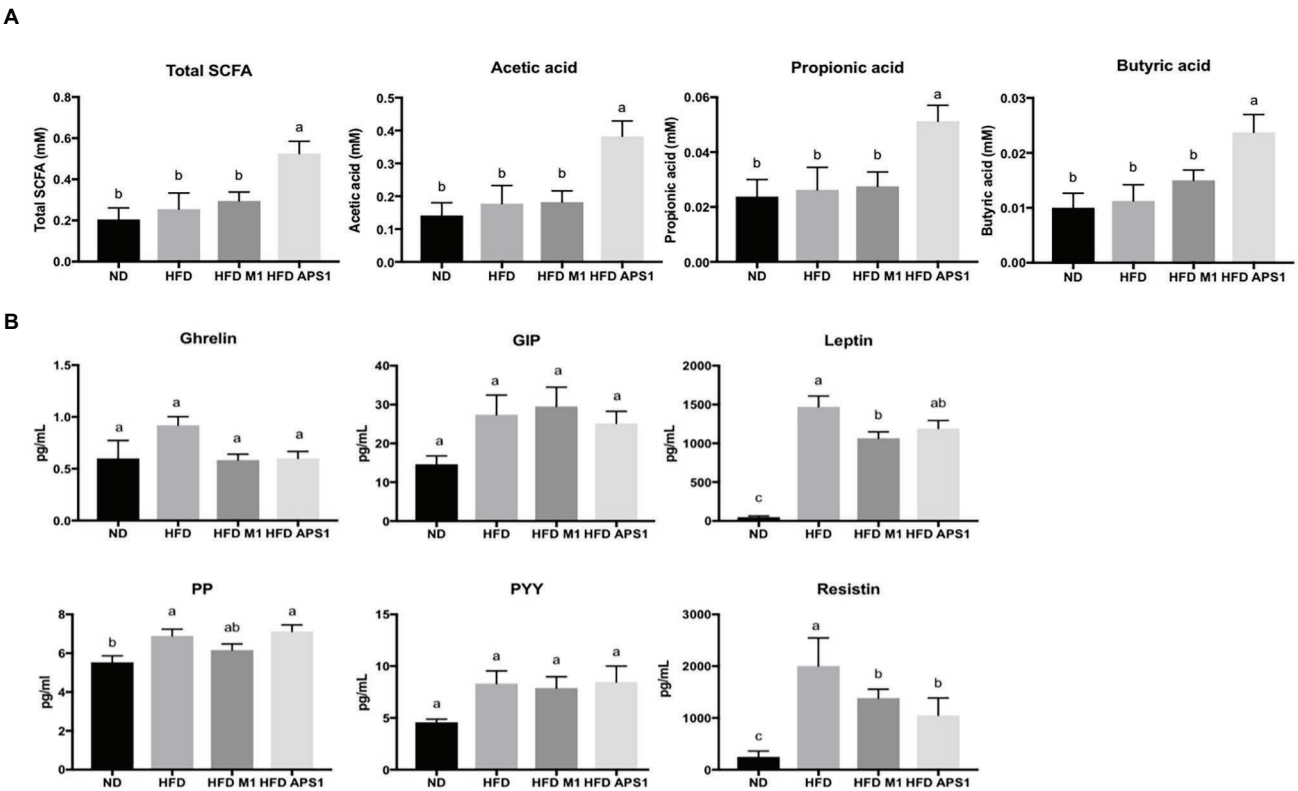

FIGURE 5 | Effects of M1 and APS1 interventions on **(A)** fecal short chain fatty acids (SCFAs) excretion and **(B)** expression of satiety hormones in HFD-induced obese mice. (n = 8 per group). The data are expressed as the mean ± SEM. Labeled means without a common superscript letter differ, $p < 0.05$.

Obesity induces the accumulation of M1 ATMs, whereas, M2 ATMs predominate in lean mice (Kitade et al., 2012). In the present study, administration of *L. kefiranofaciens* M1 with HFD upregulated M1 activating marker (*IL-1ra*), leading to a proinflammatory environment (*MCP-1*) relative to the HFD group. Conversely, APS1 invention upregulated M2 activating macrophages in HFD-induced obese mice *via* significantly downregulating relative mRNA expressions of M1 macrophage and M1 activating markers (*MIP-1*, *IL-1ra*). Thus, our findings provide a possible link between probiotic intervention, obesity, and inflammation.

Secondary, we observed that the abundance of obesity- or inflammation-associated bacteria in intestinal microbiota was regulated by the APS1 and M1 interventions. Microbial diversity has previously been identified as a significant factor influenced by diet (Clarke et al., 2014), which is decreased among the overweight (Le Chatelier et al., 2013) and increased in lean individuals (Wang et al., 2010; Lu et al., 2016).

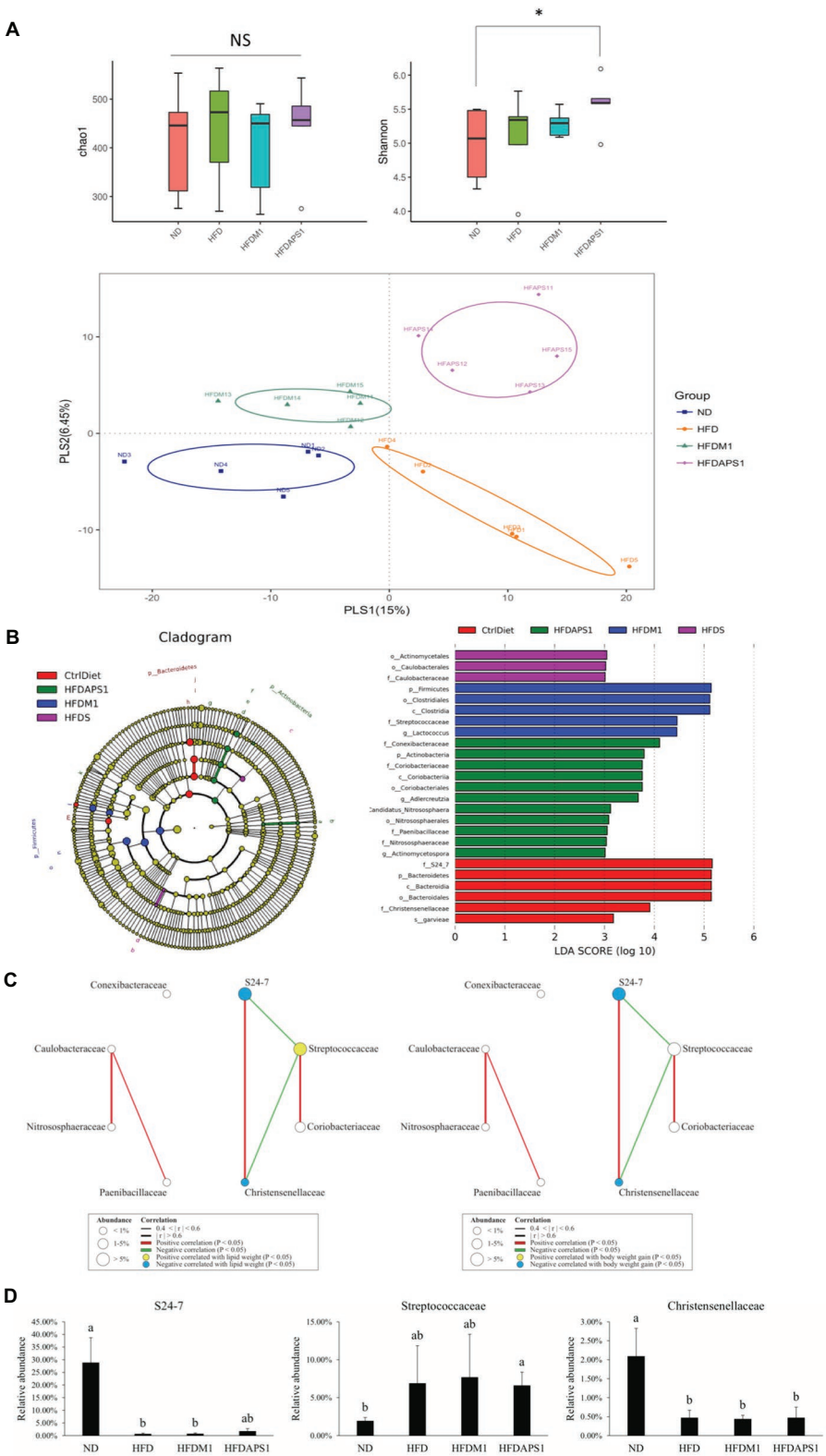

FIGURE 6 | Effects of M1 and APS1 on manipulation of gut microbiota. **(A)** Alpha diversity of Chao1 richness index and Shannon's diversity index and beta-diversity of supervised partial least squares-discriminant analysis (PLS-DA); **(B)** taxonomic cladograms derived from linear discriminant analysis effect size (LEfSe) analysis; bacterial networks co-occurring families of taxonomic cladograms correlating with **(C)** lipid weight and body weight gain; and **(D)** the relative abundance of

(*Continued*)

FIGURE 6 | specific bacteria at the family level of taxonomic cladograms. LEfSe was used to compare the abundances of all detected bacterial taxa among four groups. The differentially abundant taxa shown in the histogram are significantly different by the Kruskal-Wallis test and have an linear discriminant analysis (LDA) score of greater than 3. $n = 5$ per group. Networks of co-occurring families showed associations among ND, HFD, HFDM1 and HFDAPS1. Circles symbols represent bacterial families positive (yellow) or negative (blue) correlated with body weight gain. The edges represent the strength of positive (green) or negative (red) correlations among the families. The data are expressed as the mean ± SEM. Labeled means without a common superscript letter differ. Values of p was calculated by KruskaleWallis test, $*p < 0.05$.

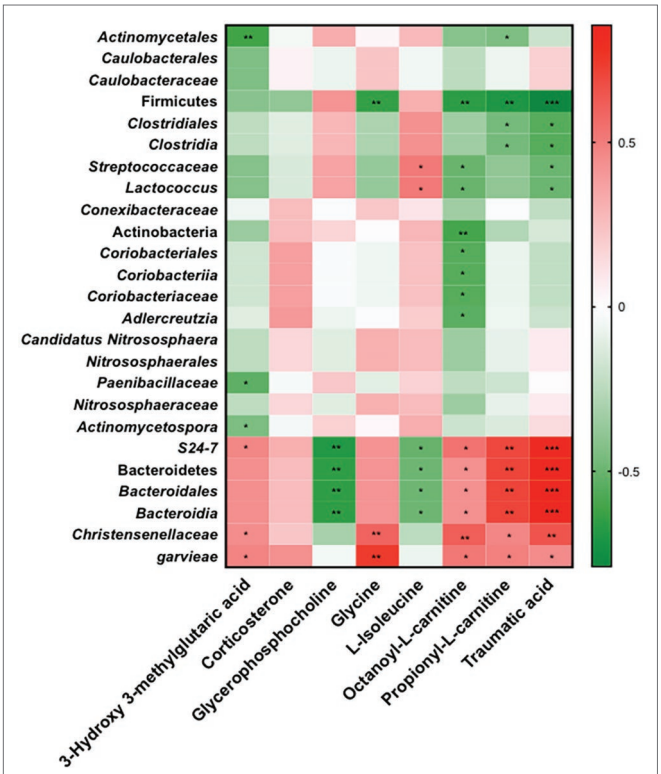

FIGURE 7 | Spearman's correlations of relative abundance of 25 LEfSe selected taxa with serum metabolites significantly modified in four groups. Red to green scale denote positive to negative associations. Spearman's correlations were employed in agreement with data distribution and verified by Kruskal-Wallis test. $*p < 0.05$, $**p < 0.01$, $***p < 0.0001$ following the Spearman's correlations.

The results of the Shannon diversity index and PLS-DA were consistent with previous findings. We further identified the key microorganisms associated with M1 and APS1 intervention, and ultimately, leading to the obese and lean animals. After analysis by LEfSe and Spearman's correlations, two families, *S24_7*, and *Christensenellaceae*, biomarkers in the ND group, were negatively correlated with body weight gain and lipid weight. Both families have been reported to be associated with lean animals (Zhang et al., 2009; Serino et al., 2012; Lin et al., 2016a; Chen et al., 2018b; Peters et al., 2018), which were reduced in the HFDM1 and enriched in the HFDAPS1. The family *Streptococcaceae*, which was in abundance in obese animals (Peters et al., 2018), was abundant in the HFDM1 and reduced in the HFDAPS1. The recently studied also observed that *Christensenella minuta* and its close relatives in the *Christensenellaceae* family were the most heritable bacteria. People with higher amounts of the gut bacteria *C. minuta* tended to be leaner (Goodrich et al., 2014). Additionally, some members of the *S24_7* family could be differentiated by their degree of IgA labeling, indicating that *S24_7* might be targeted by the innate immune system (Ormerod et al., 2016).

Alternation of metabolites profile has been regarded as an indicator to physiological conditions, reflecting the changes of gut microbiota composition (Chen et al., 2019). In the present study, eight key metabolites in serum associated with M1 and APS1 interventions were identified by the non-targeted metabolomic profiling. HMG could effectively lower serum cholesterol (Lupien et al., 1979) and prevent hypertriglyceridemia in rats (Yousufzai and Siddiqi, 1977). PLC and OLC are essential substrates for energy expenditure. PLC is an SCFA esterified to carnitine that plays an important role in fatty acid oxidation and energy expenditure (Mingorance et al., 2012). OLC, which promotes free fatty acids (FFAs) or acyl-CoA being able to move across the inner mitochondrial membrane, has a vital role in fatty acid metabolism (Reuter and Evans, 2012). Isoleucine, a branched-chain amino acid (BCAA), suppressed the development of NAFLD among obese youth by reducing the ability of insulin on hepatic glucose production in adiposity (Perng et al., 2014; Butte et al., 2015; Tricò et al., 2017). GPCs could increase growth hormone secretion and hepatic fat oxidation, resulting in increased serum FFA levels in young adults (Kawamura et al., 2012). GPCs are also considered sensitive indicators for obesity-related diseases such as cardiovascular disease (CVD) in adults (Syme et al., 2016). After further analysis by Spearman's correlations, we demonstrated that the family *Streptococcaceae* with an obese animal was positively correlated with L-isoleucine, and negatively corrected with OLC and traumatic acid, providing a possible link between *Streptococcaceae* and the development of obesity. Conversely, the families *S24_7* and *Christensenellaceae* were negatively correlated with GPC and L-isoleucine and positively corrected with HMG, glycine, OLC, PLC, and traumatic acid, contributing to the connection between these two families and leanness.

Besides the key serum metabolites, SCFAs also showed distinct actions relevant to various gut incretins, hormones, and energy homeostasis (Rosenbaum et al., 2015). Oral administration of butyrate significantly increases plasma levels of the GIP, glucagon-like peptide-1 (GLP-1), PYY, insulin, and amylin, which would have net effects of slowing digestion and nutrient intestinal transit, promoting satiety, and increasing plasma insulin. Acetate is reported to increase leptin release by fat cells. Butyric acid and propionate increase G-protein-mediated secretion of PYY and GLP-1 in the gut, and rates of lipolysis and lipogenesis in fat cells

(Fujishima et al., 2012; Kimura et al., 2014). In the present study, oral administration of APS1 promoted the SCFAs production and downregulated the expressions of resistin and leptin in the intestine. This finding suggests that SCFAs were modulated by APS1-manipulated gut microbiota and further modulated the production of SCFAs to regulate the expression of the gut hormone, thereby controlling host appetite through the gut-brain axis. For M1 intervention, downregulating the expression of resistin, PP, and leptin in the intestine was also observed, indicating that the obese inducing effect of *L. kefiranofaciens* M1 is not due to increasing appetite. This result is paralleled with our previous finding in daily food intake.

Finally, by reviewing papers and our previous data, M1 and APS1 could exert effects on the gut microbiota through the following mechanisms. (1) M1 and APS1 could directly affect gut microbial colonization through inhibitory/promoting effects. Both strains could produce lactic acid and certain SCFAs, which were identified earlier as a key factor affecting microbiota. SCFAs could also interact with the host, contributing to reducing oxygen concentrations and creating a less favorable environment for pathogen growth (Rivera-Chávez et al., 2016). Effect of other metabolic byproducts produced by both strains on the gut microbiota still needs to be further investigated. (2) M1 and APS1 could also impact the gut microbiota indirectly by manipulating the immune system, which in turn influences the colonizing microbiota. Both strains have been reported to interact with immune cells through toll-like receptor (TLR) and modify the T helper (Th1,Th2) or T regulatory cytokines (Hong et al., 2010; Lin et al., 2016b), which plays crucial roles in host defense against colonization of certain microorganisms (Pickard et al., 2017). (3) Additionally, in our early study, *L. kefiranofaciens* could form biofilm (Wang et al., 2012), which might be related to quorum sensing system to increase the cell density against harsh environment. Quorum sensing is a communication mechanism between bacteria to control specific processes, such as biofilm formation, production of secondary metabolites and stress adaptation mechanisms. Gram-positive bacteria have been reported to synthesize small autoinducing peptides (AIPs) as distinct signaling molecules to mediate quorum sensing (Spangler et al., 2019).

CONCLUSIONS

In the present study, we show that interventions involving *L. kefiranofaciens* M1 and *L. mali* APS1 with HFD affect adipogenesis, lipogenesis, and inflammation by regulating the expression of metabolites, and that this is achieved by manipulating microbiota. Administration of *L. kefiranofaciens* M1 and *L. mali* APS1 with HFD had different influences on the abundances of specific families, *Streptococcaceae*, *S24_7*, and *Christensenellaceae* in gut microbiota, which further diversifies the specific serum metabolites, GPC, L-isoleucine, HMG, glycine, OLC, PLC, and traumatic acid. The different levels of these metabolites could contribute to lean and obese subjects by regulating the metabolic pathways involved in adipogenesis, lipogenesis, lipid metabolism, and energy expenditure. SCFAs were also modified by APS1-manipulated gut microbiota to regulate the expression of gut hormones, thereby controlling host appetite through the gut-brain axis. Additionally, the M1 and APS1 interventions regulated low-grade inflammation and macrophages in adipose tissue, leading to obese-related proinflammatory macrophages and leanness-related noninflammatory macrophages, respectively. This study highlights the importance of specific probiotic interventions affecting leanness and obesity of the subjects under HFD, achieved by modulating the tripartite relationship among the host, microbiota, and metabolites.

DATA AVAILABILITY STATEMENT

The original contributions presented in the study are publicly available. This data can be found at the NCBI under accession number PRJNA634807.

ETHICS STATEMENT

The animal study was reviewed and approved by Institutional Animal Care and Use Committee of Livestock Research Institute, Council of Agriculture, Taiwan (Approval No: LRI IACUC 106-32).

AUTHOR CONTRIBUTIONS

Y-CL drafted and prepared the initial article. Y-CL and Y-TC conducted a research and investigation process, performing the experiments and data collection. K-YL conducted the formal analysis on statistical techniques to analyze study data. M-JC were involved in the management and coordination responsibility for the research activity planning and execution. Y-CL prepared the published work by those from the original research group, specifically critical review and revision of pre-publication stages. All authors contributed to the article and approved the submitted version.

FUNDING

This project was funded by the Ministry of Science and Technology in Taiwan (grant number MOST 104-2313-B-002-043-MY3).

ACKNOWLEDGMENTS

The authors would like to thank Dr. Yu-Lun Kuo at BIOTOOLS Co., Ltd. in Taiwan for kindly supporting analysis of NGS data.

REFERENCES

Amabebe, E., Robert, F. O., Agbalalah, T., and Orubu, E. S. F. (2020). Microbial dysbiosis-induced obesity: role of gut microbiota in homeostasis of energy metabolism. *Br. J. Nutr.* 123, 1127–1137. doi: 10.1017/S0007114520000380

Aoki, R., Kamikado, K., Suda, W., Takii, H., Mikami, Y., Suganuma, N., et al. (2017). A proliferative probiotic *Bifidobacterium* strain in the gut ameliorates progression of metabolic disorders via microbiota modulation and acetate elevation. *Sci. Rep.* 7:43522. doi: 10.1038/srep43522

Bäckhed, F., Ding, H., Wang, T., Hooper, L. V., Koh, G. Y., Nagy, A., et al. (2004). The gut microbiota as an environmental factor that regulates fat storage. *Proc. Natl. Acad. Sci. U. S. A.* 101, 15718–15723. doi: 10.1073/pnas.0407076101

Benton, H. P., Wong, D. M., Trauger, S. A., and Siuzdak, G. (2008). XCMS2: processing tandem mass spectrometry data for metabolite identification and structural characterization. *Anal. Chem.* 80, 6382–6389. doi: 10.1021/ac800795f

Breasson, L., Becattini, B., Sardi, C., Molinaro, A., Zani, F., Marone, R., et al. (2017). PI3Kγ activity in leukocytes promotes adipose tissue inflammation and early-onset insulin resistance during obesity. *Sci. Signal.* 10:eaaf2969. doi: 10.1126/scisignal.aaf2969

Butte, N. F., Liu, Y., Zakeri, I. F., Mohney, R. P., Mehta, N., Voruganti, V. S., et al. (2015). Global metabolomic profiling targeting childhood obesity in the Hispanic population. *Am. J. Clin. Nutr.* 102, 256–267. doi: 10.3945/ajcn.115.111872

Cano, P. G., Santacruz, A., Trejo, F. M., and Sanz, Y. (2013). *Bifidobacterium* CECT 7765 improves metabolic and immunological alterations associated with obesity in high-fat diet-fed mice. *Obesity* 21, 2310–2321. doi: 10.1002/oby.20330

Chang, C. J., Lin, C. S., Lu, C. C., Martel, J., Ko, Y. F., Ojcius, D. M., et al. (2015). *Ganoderma lucidum* reduces obesity in mice by modulating the composition of the gut microbiota. *Nat. Commun.* 6:7489. doi: 10.1038/ncomms8489

Chen, Y. P., Hsiao, P. J., Hong, W. S., Dai, T. Y., and Chen, M. J. (2012). *Lactobacillus kefiranofaciens* M1 isolated from milk kefir grains ameliorates experimental colitis in-vitro and in-vivo. *J. Dairy Sci.* 95, 63–74. doi: 10.3168/jds.2011-4696

Chen, Y. T., Lin, Y. C., Lin, J. S., Yang, N. S., and Chen, M. J. (2018a). Sugary kefir strain *Lactobacillus mali* APS1 ameliorated hepatic steatosis by regulation of SIRT-1/Nrf-2 and gut microbiota in rats. *Mol. Nutr. Food Res.* 62:e1700903. doi: 10.1002/mnfr.201700903

Chen, H. C., Wang, S. Y., and Chen, M. J. (2008). Microbiological study of lactic acid bacteria in kefir grains by culture-dependent and culture-independent methods. *Food Microbiol.* 25, 492–501. doi: 10.1016/j.fm.2008.01.003

Chen, M. X., Wang, S. Y., Kuo, C. H., and Tsai, I. L. (2019). Metabolome analysis for investigating host-gut microbiota interactions. *J. Formos. Med. Assoc.* 118, S10–S22. doi: 10.1016/j.jfma.2018.09.007

Chen, Y. T., Yang, N. S., Lin, Y. C., Ho, S. T., Li, K. Y., Lin, J. S., et al. (2018b). A combination of *Lactobacillus mali* APS1 and dieting improved the efficacy of obesity treatment via manipulating gut microbiome in mice. *Sci. Rep.* 8:6153. doi: 10.1038/s41598-018-23844-y

Cheng, M. C., Tsai, T. Y., and Pan, T. M. (2015). Anti-obesity activity of the water extract of *Lactobacillus paracasei subsp. paracasei* NTU 101 fermented soy milk products. *Food Funct.* 6, 3522–3530. doi: 10.1039/C5FO00531K

Choi, J., Kim, K. J., Koh, E. J., and Lee, B. Y. (2018). *Gelidium elegans* extract ameliorates type 2 diabetes via regulation of MAPK and PI3K/Akt signaling. *Nutrients* 10:51. doi: 10.3390/nu10010051

Clarke, G., Stilling, R. M., Kennedy, P. J., Stanton, C., Cryan, J. F., and Dinan, T. G. (2014). Minireview: gut microbiota: the neglected endocrine organ. *Mol. Endocrinol.* 28, 1221–1238. doi: 10.1210/me.2014-1108

Crovesy, L., Masterson, D., and Rosado, E. L. (2020). Profile of the gut microbiota of adults with obesity: a systematic review. *Eur. J. Clin. Nutr.* 2020, 1–12. doi: 10.1038/s41430-020-0607-6

Fujishima, Y., Maeda, N., Inoue, K., Kashine, S., Nishizawa, H., Hirata, A., et al. (2012). Efficacy of liraglutide, a glucagon-like peptide-1 (GLP-1) analogue, on body weight, eating behavior, and glycemic control, in Japanese obese type 2 diabetes. *Cardiovasc. Diabetol.* 11:107. doi: 10.1186/1475-2840-11-107

Goodrich, J. K., Waters, J. L., Poole, A. C., Sutter, J. L., Koren, O., Blekhman, R., et al. (2014). Human genetics shape the gut microbiome. *Cell* 159, 789–799. doi: 10.1016/j.cell.2014.09.053

Gross, B., Pawlak, M., Lefebvre, P., and Staels, B. (2017). PPARs in obesity-induced T2DM, dyslipidaemia and NAFLD. *Nat. Rev. Endocrinol.* 13, 36–49. doi: 10.1038/nrendo.2016.135

Hall, A. B., Tolonen, A. C., and Xavier, R. J. (2017). Human genetic variation and the gut microbiome in disease. *Nat. Rev. Genet.* 18, 690–699. doi: 10.1038/nrg.2017.63

Hill, C., Guarner, F., Reid, G., Gibson, G. R., Merenstein, D. J., Pot, B., et al. (2014). The International Scientific Association for probiotics and prebiotics consensus statement on the scope and appropriate use of the term probiotic. *Nat. Rev. Gastroenterol. Hepatol.* 11, 506–514. doi: 10.1038/nrgastro.2014.66

Ho, T. J., Kuo, C. H., Wang, S. Y., Chen, G. Y., and Tseng, Y. J. (2013). True ion pick (TIPick): a denoising and peak picking algorithm to extract ion signals from liquid chromatography/mass spectrometry data. *J. Mass Spectrom.* 48, 234–242. doi: 10.1002/jms.3154

Holmes, E., Kinross, J., Gibson, G. R., Burcelin, R., Jia, W., Pettersson, S., et al. (2012). Therapeutic modulation of microbiota-host metabolic interactions. *Sci. Transl. Med.* 4:137rv136. doi: 10.1126/scitranslmed.3004244

Honda, K., Moto, M., Uchida, N., He, F., and Hashizume, N. (2012). Anti-diabetic effects of lactic acid bacteria in normal and type 2 diabetic mice. *J. Clin. Biochem. Nutr.* 51, 96–101. doi: 10.3164/jcbn.11-07

Hong, W. S., Chen, Y. P., and Chen, M. J. (2010). The antiallergic effect of Kefir *Lactobacilli*. *J. Food Sci.* 75, H244–H253. doi: 10.1111/j.1750-3841.2010.01787.x

Hong, W. S., Chen, H. C., Chen, Y. P., and Chen, M. J. (2009). Effects of kefir supernatant and lactic acid bacteria isolated from kefir grain on cytokine production by macrophage. *Int. Dairy J.* 19, 244–251. doi: 10.1016/j.idairyj.2008.10.010

Hong, W. S., Chen, Y. P., Dai, T. Y., Huang, I. N., and Chen, M. J. (2011). Effect of heat-inactivated kefir-isolated *Lactobacillus kefiranofaciens* M1 on preventing an allergic airway response in mice. *J. Agric. Food Chem.* 59, 9022–9031. doi: 10.1021/jf201913x

Huttenhower, C., Gevers, D., Knight, R., Abubucker, S., Badger, J. H., Chinwalla, A. T., et al. (2012). Structure, function and diversity of the healthy human microbiome. *Nature* 486, 207–214. doi: 10.1038/nature11234

John, G. K., Wang, L., Nanavati, J., Twose, C., Singh, R., and Mullin, G. (2018). Dietary alteration of the gut microbiome and its impact on weight and fat mass: a systematic review and meta-analysis. *Genes* 9:167. doi: 10.3390/genes9030167

Kamada, N., Seo, S. -U., Chen, G. Y., and Núñez, G. (2013). Role of the gut microbiota in immunity and inflammatory disease. *Nat. Rev. Immunol.* 13, 321–335. doi: 10.1038/nri3430

Karimi, G., Sabran, M. R., Jamaluddin, R., Parvaneh, K., Mohtaruddin, N., Ahmad, Z., et al. (2015). The anti-obesity effects of *Lactobacillus casei* strain Shirota versus Orlistat on high fat diet-induced obese rats. *Food Nutr. Res.* 59, 1–9. doi: 10.3402/fnr.v%v.29273

Kawamura, T., Okubo, T., Sato, K., Fujita, S., Goto, K., Hamaoka, T., et al. (2012). Glycerophosphocholine enhances growth hormone secretion and fat oxidation in young adults. *Nutrition* 28, 1122–1126. doi: 10.1016/j.nut.2012.02.011

Kimura, I., Inoue, D., Hirano, K., and Tsujimoto, G. (2014). The SCFA receptor GPR43 and energy metabolism. *Front. Endocrinol.* 5:85. doi: 10.3389/fendo.2014.00085

Kitade, H., Sawamoto, K., Nagashimada, M., Inoue, H., Yamamoto, Y., Sai, Y., et al. (2012). CCR5 plays a critical role in obesity-induced adipose tissue inflammation and insulin resistance by regulating both macrophage recruitment and M1/M2 status. *Diabetes* 61, 1680–1690. doi: 10.2337/db11-1506

Le Chatelier, E., Nielsen, T., Qin, J., Prifti, E., Hildebrand, F., Falony, G., et al. (2013). Richness of human gut microbiome correlates with metabolic markers. *Nature* 500, 541–546. doi: 10.1038/nature12506

Li, X., Wang, N., Yin, B., Fang, D., Jiang, T., Fang, S., et al. (2016). Effects of *Lactobacillus plantarum* CCFM0236 on hyperglycaemia and insulin resistance in high-fat and streptozotocin-induced type 2 diabetic mice. *J. Appl. Microbiol.* 121, 1727–1736. doi: 10.1111/jam.13276

Lin, H., An, Y., Hao, F., Wang, Y., and Tang, H. (2016a). Correlations of fecal metabonomic and microbiomic changes induced by high-fat diet in the pre-obesity state. *Sci. Rep.* 6:21618. doi: 10.1038/srep21618

Lin, Y. C., Chen, Y. T., Hsieh, H. H., and Chen, M. J. (2016b). Effect of *Lactobacillus mali* APS1 and *L. kefiranofaciens* M1 on obesity and glucose homeostasis in diet-induced obese mice. *J. Funct. Foods* 23, 580–589. doi: 10.1016/j.jff.2016.03.015

Lu, Y., Fan, C., Li, P., Lu, Y., Chang, X., and Qi, K. (2016). Short chain fatty acids prevent high-fat-diet-induced obesity in mice by regulating G protein-

coupled receptors and gut microbiota. *Sci. Rep.* 6:37589. doi: 10.1038/srep37589

Lumeng, C. N., Bodzin, J. L., and Saltiel, A. R. (2007). Obesity induces a phenotypic switch in adipose tissue macrophage polarization. *J. Clin. Invest.* 117, 175–184. doi: 10.1172/JCI29881

Lupien, P. J., Moorjani, S., Brun, D., and Bielmann, P. (1979). Effects of 3-hydroxy-3-methylglutaric acid on plasma and low-density lipoprotein cholesterol levels in familial hypercholesterolemia. *J. Clin. Pharmacol.* 19, 120–126. doi: 10.1002/j.1552-4604.1979.tb02469.x

Mack, I., Cuntz, U., Grämer, C., Niedermaier, S., Pohl, C., Schwiertz, A., et al. (2016). Weight gain in anorexia nervosa does not ameliorate the faecal microbiota, branched chain fatty acid profiles, and gastrointestinal complaints. *Sci. Rep.* 6:26752. doi: 10.1038/srep26752

Malaisé, Y., Menard, S., Cartier, C., Gaultier, E., Lasserre, F., Lencina, C., et al. (2017). Gut dysbiosis and impairment of immune system homeostasis in perinatally-exposed mice to bisphenol A precede obese phenotype development. *Sci. Rep.* 7, 1–12. doi: 10.1038/s41598-017-15196-w

Maruvada, P., Leone, V., Kaplan, L. M., and Chang, E. B. (2017). The human microbiome and obesity: moving beyond associations. *Cell Host Microbe* 22, 589–599. doi: 10.1016/j.chom.2017.10.005

Mehrpouya-Bahrami, P., Chitrala, K. N., Ganewatta, M. S., Tang, C., Murphy, E. A., Enos, R. T., et al. (2017). Blockade of CB1 cannabinoid receptor alters gut microbiota and attenuates inflammation and diet-induced obesity. *Sci. Rep.* 7:15645. doi: 10.1038/s41598-017-15154-6

Mingorance, C., Duluc, L., Chalopin, M., Simard, G., Ducluzeau, P. -H., Herrera, M. D., et al. (2012). Propionyl-L-carnitine corrects metabolic and cardiovascular alterations in diet-induced obese mice and improves liver respiratory chain activity. *PLoS One* 7:e34268. doi: 10.1371/journal.pone.0034268

Moseti, D., Regassa, A., and Kim, W. -K. (2016). Molecular regulation of adipogenesis and potential anti-adipogenic bioactive molecules. *Int. J. Mol. Sci.* 17:124. doi: 10.3390/ijms17010124

Nagpal, R., Newman, T. M., Wang, S., Jain, S., Lovato, J. F., and Yadav, H. (2018). Obesity-linked gut microbiome dysbiosis associated with derangements in gut permeability and intestinal cellular homeostasis independent of diet. *J. Diabetes Res.* 2018:3462092. doi: 10.1155/2018/3462092

Nishimura, S., Nagasaki, M., Okudaira, S., Aoki, J., Ohmori, T., Ohkawa, R., et al. (2014). ENPP2 contributes to adipose tissue expansion in diet-induced obesity. *Diabetes* 63, 4154–4164. doi: 10.2337/db13-1694

Niso-Santano, M., Malik, S. A., Pietrocola, F., Bravo-San Pedro, J. M., Mariño, G., Cianfanelli, V., et al. (2015). Unsaturated fatty acids induce non-canonical autophagy. *EMBO J.* 34, 1025–1041. doi: 10.15252/embj.201489363

Ormerod, K. L., Wood, D. L. A., Lachner, N., Gellatly, S. L., Daly, J. N., Parsons, J. D., et al. (2016). Genomic characterization of the uncultured *Bacteroidales* family S24-7 inhabiting the guts of homeothermic animals. *Microbiome* 4:36. doi: 10.1186/s40168-016-0181-2

Parekh, P. J., Balart, L. A., and Johnson, D. A. (2015). The influence of the gut microbiome on obesity, metabolic syndrome and gastrointestinal disease. *Clin. Transl. Gastroenterol.* 6:e91. doi: 10.1038/ctg.2015.16

Perng, W., Gillman, M. W., Fleisch, A. F., Michalek, R. D., Watkins, S. M., Isganaitis, E., et al. (2014). Metabolomic profiles and childhood obesity. *Obesity* 22, 2570–2578. doi: 10.1002/oby.20901

Peters, B. A., Shapiro, J. A., Church, T. R., Miller, G., Trinh-Shevrin, C., Yuen, E., et al. (2018). A taxonomic signature of obesity in a large study of American adults. *Sci. Rep.* 8:9749. doi: 10.1038/s41598-018-28126-1

Pickard, J. M., Zeng, M. Y., Caruso, R., and Núñez, G. (2017). Gut microbiota: role in pathogen colonization, immune responses and inflammatory disease. *Immunol. Rev.* 279, 70–89. doi: 10.1111/imr.12567

Pindjakova, J., Sartini, C., Lo Re, O., Rappa, F., Coupe, B., Lelouvier, B., et al. (2017). Gut dysbiosis and adaptive immune response in diet-induced obesity vs. systemic inflammation. *Front. Microbiol.* 8, 1–19. doi: 10.3389/fmicb.2017.01157

Reilly, S. M., and Saltiel, A. R. (2017). Adapting to obesity with adipose tissue inflammation. *Nat. Rev. Endocrinol.* 13, 633–643. doi: 10.1038/nrendo.2017.90

Reuter, S. E., and Evans, A. M. (2012). Carnitine and Acylcarnitines. *Clin. Pharmacokinet.* 51, 553–572. doi: 10.1007/BF03261931

Rivera-Chávez, F., Zhang, L. F., Faber, F., Lopez, C. A., Byndloss, M. X., Olsan, E. E., et al. (2016). Depletion of butyrate-producing *Clostridia* from the gut microbiota drives an aerobic luminal expansion of *Salmonella*. *Cell Host Microbe* 19, 443–454. doi: 10.1016/j.chom.2016.03.004

Rosenbaum, M., Knight, R., and Leibel, R. L. (2015). The gut microbiota in human energy homeostasis and obesity. *Trends Endocrinol. Metab.* 26, 493–501. doi: 10.1016/j.tem.2015.07.002

Serino, M., Luche, E., Gres, S., Baylac, A., Bergé, M., Cenac, C., et al. (2012). Metabolic adaptation to a high-fat diet is associated with a change in the gut microbiota. *Gut* 61, 543–553. doi: 10.1136/gutjnl-2011-301012

Shoelson, S. E., Herrero, L., and Naaz, A. (2007). Obesity, inflammation, and insulin resistance. *Gastroenterology* 132, 2169–2180. doi: 10.1053/j.gastro.2007.03.059

Spangler, J. R., Dean, S. N., Leary, D. H., and Walper, S. A. (2019). Response of *Lactobacillus plantarum* WCFS1 to the gram-negative pathogen-associated quorum sensing molecule N-3-oxododecanoyl homoserine lactone. *Front. Microbiol.* 10:715. doi: 10.3389/fmicb.2019.00715

Syme, C., Czajkowski, S., Shin, J., Abrahamowicz, M., Leonard, G., Perron, M., et al. (2016). Glycerophosphocholine metabolites and cardiovascular disease risk factors in adolescents. *Circulation* 134, 1629–1636. doi: 10.1161/CIRCULATIONAHA.116.022993

Tilg, H., Zmora, N., Adolph, T. E., and Elinav, E. (2020). The intestinal microbiota fuelling metabolic inflammation. *Nat. Rev. Immunol.* 20, 40–54. doi: 10.1038/s41577-019-0198-4

Tricò, D., Prinsen, H., Giannini, C., de Graaf, R., Juchem, C., Li, F., et al. (2017). Elevated a-hydroxybutyrate and branched-chain amino acid levels predict deterioration of glycemic control in adolescents. *J. Clin. Endocrinol. Metab.* 102, 2473–2481. doi: 10.1210/jc.2017-00475

Wang, S. Y., Chen, K. N., Lo, Y. M., Chiang, M. L., Chen, H. C., Liu, J. R., et al. (2012). Investigation of microorganisms involved in biosynthesis of the kefir grain. *Food Microbiol.* 32, 274–285. doi: 10.1016/j.fm.2012.07.001

Wang, Y., Devkota, S., Musch, M. W., Jabri, B., Nagler, C., Antonopoulos, D. A., et al. (2010). Regional mucosa-associated microbiota determine physiological expression of TLR2 and TLR4 in murine colon. *PLoS One* 5:e13607. doi: 10.1371/journal.pone.0013607

Wang, S. Y., Kuo, C. H., and Tseng, Y. J. (2013). Batch normalizer: a fast total abundance regression calibration method to simultaneously adjust batch and injection order effects in liquid chromatography/time-of-flight mass spectrometry-based metabolomics data and comparison with current calibration methods. *Anal. Chem.* 85, 1037–1046. doi: 10.1021/ac302877x

Wilkins, L. J., Monga, M., and Miller, A. W. (2019). Defining dysbiosis for a cluster of chronic diseases. *Sci. Rep.* 9, 1–10. doi: 10.1038/s41598-019-49452-y

Yadav, H., Lee, J. H., Lloyd, J., Walter, P., and Rane, S. G. (2013). Beneficial metabolic effects of a probiotic via butyrate-induced GLP-1 hormone secretion. *J. Biol. Chem.* 288, 25088–25097. doi: 10.1074/jbc.M113.452516

Yan, F., and Zheng, X. (2017). Anthocyanin-rich mulberry fruit improves insulin resistance and protects hepatocytes against oxidative stress during hyperglycemia by regulating AMPK/ACC/mTOR pathway. *J. Funct. Foods* 30, 270–281. doi: 10.1016/j.jff.2017.01.027

Yousufzai, S. Y. K., and Siddiqi, M. (1977). Serum and liver lipid responses to 3-hydroxy-3-methylglutaric acid in rats on different carbohydrate diets. *Lipids* 12, 262–266. doi: 10.1007/BF02533344

Zeng, Z., Luo, J., Zuo, F., Zhang, Y., Ma, H., and Chen, S. (2016). Screening for potential novel probiotic *Lactobacillus* strains based on high dipeptidyl peptidase IV and α-glucosidase inhibitory activity. *J. Funct. Foods* 20, 486–495. doi: 10.1016/j.jff.2015.11.030

Zhang, H., DiBaise, J. K., Zuccolo, A., Kudrna, D., Braidotti, M., Yu, Y., et al. (2009). Human gut microbiota in obesity and after gastric bypass. *Proc. Natl. Acad. Sci. U. S. A.* 106, 2365–2370. doi: 10.1073/pnas.0812600106

Zhang, Z., Tang, H., Chen, P., Xie, H., and Tao, Y. (2019). Demystifying the manipulation of host immunity, metabolism, and extraintestinal tumors by the gut microbiome. *Signal Transduct. Target. Ther.* 4:41. doi: 10.1038/s41392-019-0074-5

Conflict of Interest: The authors declare that the research was conducted in the absence of any commercial or financial relationships that could be construed as a potential conflict of interest.

Copyright © 2020 Lin, Chen, Li and Chen. This is an open-access article distributed under the terms of the Creative Commons Attribution License (CC BY). The use, distribution or reproduction in other forums is permitted, provided the original author(s) and the copyright owner(s) are credited and that the original publication in this journal is cited, in accordance with accepted academic practice. No use, distribution or reproduction is permitted which does not comply with these terms.

frontiers in Microbiology

ORIGINAL RESEARCH
published: 28 July 2020
doi: 10.3389/fmicb.2020.01604

High-Fat Diet Affects Heavy Metal Accumulation and Toxicity to Mice Liver and Kidney Probably via Gut Microbiota

Ting Liu[1†], Xue Liang[1†], Chao Lei[1], Qinhong Huang[2], Weiqi Song[3], Rong Fang[1], Chen Li[1], Xiaomei Li[1], Hui Mo[4], Ning Sun[1,5], Haoran Lv[1]* and Zhihua Liu[1]**

[1] Guangzhou Key Laboratory of Enhanced Recovery after Abdominal Surgery, The Fifth Affiliated Hospital of Guangzhou Medical University, Guangzhou, China, [2] The First Affiliated Hospital of Guangzhou Medical University, Guangzhou, China, [3] Department of Public Health, Guangzhou Medical University, Guangzhou, China, [4] The Public Laboratory, South China Botanical Garden, Chinese Academy of Sciences, Guangzhou, China, [5] Research Institute of Chinese Medicine Sciences, Guangdong Pharmaceutical University, Guangzhou, China

Previous studies proved that heavy metals could increase the risk of disease by acting on the gut microbiota. Meanwhile, gut microbiota played important roles in detoxifying heavy metals. However, the response of gut microbiota to heavy metals and which microbes dominated this detoxification processes are still unclear. This study investigated the difference of high-fat-diet (HFD) and normal-diet (ND) gut microbiota and their response to and detoxification effects on arsenic (As), cadmium (Cd), and lead (Pb) exposure. Results showed that gut microbiota of ND and HFD was significantly different and responded to As, Pb, and Cd exposure differently, too. When exposed to 100 ppm As, Cd, or Pb, HFD-fed mice accumulated more heavy metals in the liver and kidney along with more severe functional damage than ND-fed mice, indicated by a more dramatic increase of alanine aminotransferase (ALT) and aspartate aminotransferase (AST) activities and urinary total protein (TPU), urinary uric acid (UUA), and urinary creatinine (Ucrea) content. Among ND gut microbiota, relative abundance of *Bacteroides*, *Lactobacillus*, *Butyricimonas*, and *Dorea* was significantly increased by arsenic (As) exposure; relative abundance of *Faecoccus* and *Lactobacillus* was significantly increased by Cd exposure; relative abundance of *Desulfovibrio*, *Plasmodium*, and *Roseburia* were significantly increased by Pb exposure. However, among HFD gut microbiota, those microbes were not significantly changed. Bivariate association analysis found weak positive correlations between content of fecal excreted heavy metals and richness of total fecal microbiota as well as abundance of some of the heavy metal-enriched microbes. Our study concluded that HFD increased disease risk of heavy metal exposure probably via its gut microbiota which excreted less heavy metal through feces.

Keywords: high-fat diet, heavy metal, gut microbiota, arsenic, cadmium, lead

OPEN ACCESS

Edited by:
Bruno Lamas, INRA UMR 1331 Toxicologie Alimentaire, France

Reviewed by:
Sandrine Ellero-Simatos, Institut National de la Recherche Agronomique (INRA), France
Pragyanshu Khare, National Institute of Pharmaceutical Education and Research, India

***Correspondence:**
Zhihua Liu
liuzhihualzh@hotmail.com; liuzhihua@gzhmu.edu.cn
Haoran Lv
lvhaoran2006@sina.com
Ning Sun
ning.sun@connect.polyu.hk

[†] These authors have contributed equally to this work

Specialty section:
This article was submitted to Food Microbiology, a section of the journal Frontiers in Microbiology

Received: *24 December 2019*
Accepted: *18 June 2020*
Published: *28 July 2020*

Citation:
Liu T, Liang X, Lei C, Huang Q, Song W, Fang R, Li C, Li X, Mo H, Sun N, Lv H and Liu Z (2020) High-Fat Diet Affects Heavy Metal Accumulation and Toxicity to Mice Liver and Kidney Probably via Gut Microbiota. Front. Microbiol. 11:1604. doi: 10.3389/fmicb.2020.01604

INTRODUCTION

Environmental toxin exposure is a global health problem in the 21st century. Heavy metals are one of the most harmful environmental toxins, which are widely found in polluted air, water, and soil. Heavy metals enter and accumulate gradually in the human body through diet uptake. Numerous studies have shown that heavy metal pollution is widely spread in animal and plant products, aquatic products, and various processed foods all over the world (Dadar et al., 2016; Liu et al., 2016; Wijayawardena et al., 2016). Heavy metals that enter the human body through chronic exposure are very difficult to metabolize or decompose, so they accumulate in all tissues and organs over the years and exert chronic damage to the body when they reach a certain threshold (Raehsler et al., 2018). Epidemiological investigations have shown that heavy metals can be detected in the blood, urine, hair, and nails of healthy and diseased people and that the content is correlated with severity of respiration diseases (Wu et al., 2018), cardiovascular diseases (Lamas et al., 2016), neurodegeneration (Bjorklund et al., 2018a; Ghazala et al., 2018; Iqbal et al., 2018) diseases, autism spectrum disorder (Bjorklund et al., 2018b), and obesity (Park et al., 2017; Shao et al., 2017; Wang et al., 2018). Great efforts have been made to reduce heavy metal pollution, but these efforts often have very limited effects (Bisanz et al., 2014). So it is an urgent requirement to explore new methods to reduce their health risks.

Gut microbiota are the most important microecosystem in the human body, which chemically modifies dietary compounds, industrial compounds, pollutants, and drugs, thereby affecting their disease risk, bioavailability, toxicity, and efficacy. However, how gut microbiota metabolize these substances and their impact on human health are still unclear (Koppel et al., 2017). The mechanism of how gut microbiota detoxify heavy metals was rarely reported. More Cd or Pb was detected in the blood and organs such as liver, kidney, and spleen in germ-free mice compared to specific pathogen-free mice after drinking water containing inorganic Cd or Pb for 6 weeks (Breton et al., 2013a,b), indicating that the gut microbiota of SPF mice prevented heavy metals from entering the bloodstream through the gastrointestinal tract and accumulating in target organs. Feces from rat could transfer methylmercury into inorganic mercury, which was less toxic and easier to excrete (Rowland et al., 1978). When rat gut microbiota was eliminated by antibiotics, methylmercury accumulated more, and neurotoxic symptoms became more serious (Rowland et al., 1980). Studies have reported the presence of genes in intestinal microbes related to heavy metal metabolism. Mercury-resistant gene operons were discovered in gram-negative bacteria in primate fecal microbiota (Liebert et al., 1997). Deep excavation of human microbiome data revealed that there were symbiotic microbes in the gastrointestinal tract containing all known genes encoding arsenic-sensing and regulating proteins (Isokpehi et al., 2014). Together, these data implied that the gut microbiota could detoxify heavy metals through absorption, metabolism, sequestration, and excretion. However, response of gut microbiota to heavy metals and which microbes dominated this detoxification processes were still unclear.

Gut microbiota are modified by heredity and various environmental factors, among which diet is the major determinant (Thomas et al., 2017). High-fat diet (HFD) is a common problem worldwide, and the gut dysbiosis caused by HFD is closely related to the incidence of various diseases including obesity, diabetes, cardiovascular disease, and tumor (Cordain et al., 2005). Epidemiological studies have shown that obese people, the majority of which have HFD, accumulate more heavy metals in their bodies than do healthy people (Park et al., 2017; Shao et al., 2017; Wang et al., 2018). We propose that gut microbiota of HFD might have weaker ability to eliminate or detoxify heavy metals than gut microbiota of normal diet (ND). This study investigated the difference of gut microbiota between HFD- and ND-fed mice and their detoxification effects on As, Cd, and Pb exposure. Efforts were made to find characteristics of gut microbiota that have a positive correlation with heavy metals that are excreted more in feces, accumulated less, and damaged the liver and kidney more mildly as well as specific microbes that tolerated heavy metals and may have roles in detoxifying As, Cd, and Pb.

RESULTS

Diet Effects on Liver Function Damage Upon Heavy Metal Exposure

To determine the impact of dietary patterns on mice's response to heavy metal exposure, we first analyzed activity of blood alanine aminotransferase (ALT) and aspartate aminotransferase (AST), the two primary indicators of liver function in plasma samples. Higher activities of ALT or AST indicate more severe liver damage. Arsenic (As), Cd, or Pb was used to treat both ND- and HFD-fed mice. Results showed that consuming HFD versus ND led to higher activity of AST and ALT and that heavy metals further increased the activity of AST and ALT. So HFD-fed mice exposed to heavy metals had the highest AST and ALT activities among all the groups (**Figures 1A–F**). In ND-fed mice, only AST upon As exposure and ALT upon Cd exposure increased significantly ($P < 0.05$) (**Figures 1B,C**), while in HFD-fed mice, AST upon As exposure (**Figure 1B**), ALT and AST upon Cd exposure (**Figures 1C,D**), and ALT upon Pb exposure (**Figure 1E**) increased significantly. Together, these results indicated a possibility that compared to ND, HFD increased liver damage caused by As, Cd, and Pb exposure.

Diet Effects on Kidney Functional Damage Upon Heavy Metal Exposure

To further determine whether HFD would increase kidney damage of heavy metals, we analyzed urine total protein (TPU), urinary creatinine (UCrea), and urinary uric acid (UUA) contents, the three main indicators of kidney function, with higher contents indicating a heavier functional damage. Results showed that consuming HFD versus ND led to higher content of TPU, UCrea, and UUA and that heavy metals further increased content of TPU, UCrea, and UUA with mostly more increase in HFD- versus ND-fed mice (**Figures 2A–I**). Meanwhile,

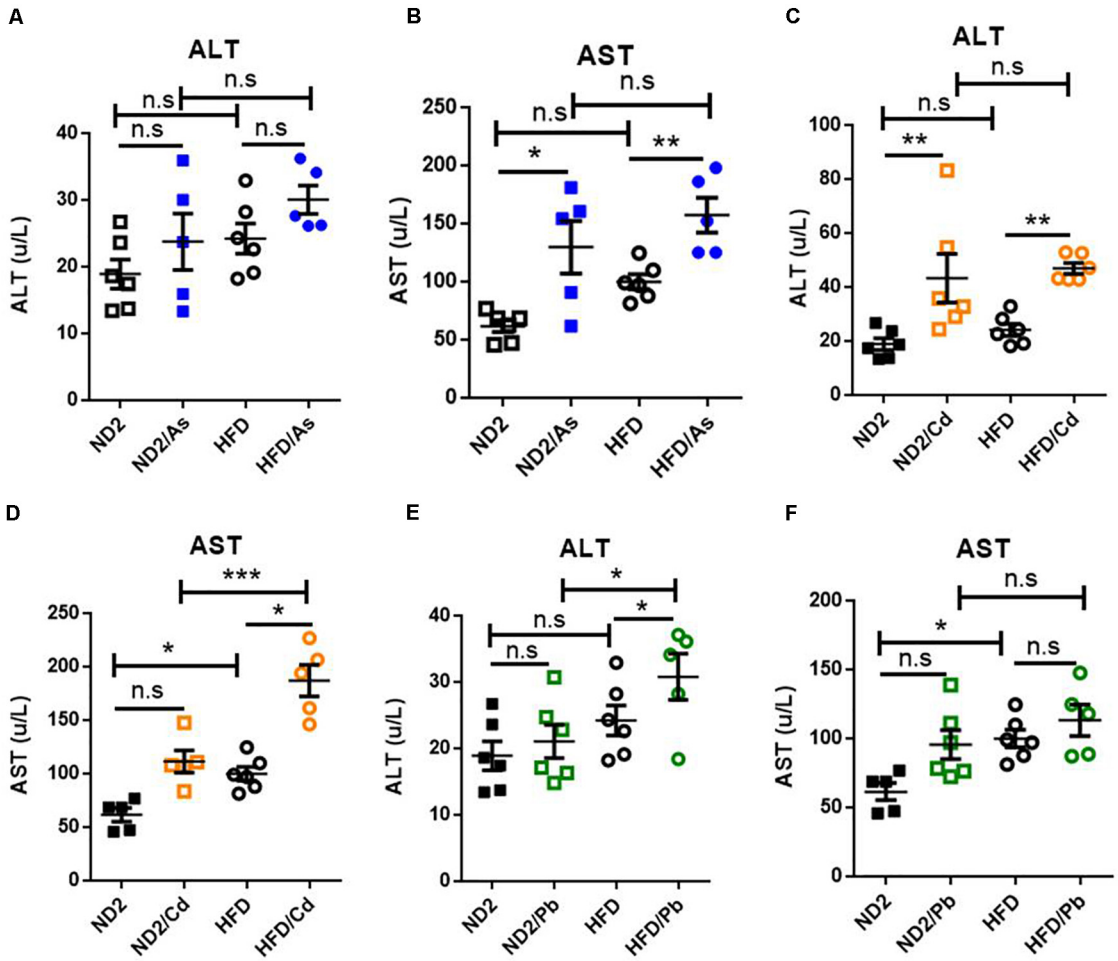

FIGURE 1 | Diet effects on liver function damage upon heavy metal exposure. **(A–F)** ND- and HFD-fed mice were exposed to 100 ppm As, Cd, or Pd for 10 weeks (n = 6 for each group). Plasma was collected and analyzed for AST and ALT activities on the day of killing. Data were expressed as mean ± SEM. Statistics according to two-way ANOVAs and Bonferroni *post hoc* tests. n.s. not significant; $^{*}P < 0.05$; $^{**}P < 0.01$; $^{***}P < 0.001$. ALT, alanine aminotransferase; AST, aspartate aminotransferase.

in ND-fed mice, only UCrea and UUA upon As exposure increased significantly (**Figures 2B,C**), while in HFD-fed mice, all three indicators increased significantly upon As exposure (**Figures 2A–C**), TPU and UUA increased significantly upon Cd exposure (**Figures 2D,F**), and TPU and UUA increased significantly upon Pb exposure (**Figures 2G,I**). Those results implied a trend that HFD increased kidney damage caused by As, Cd, and Pb exposure.

Diet Effects on Heavy Metal Accumulation in Liver and Kidney and Elimination in Feces

To examine the impact of diet on the accumulation of heavy metals in mice, the As, Cd, and Pb content in livers, kidneys, and fecal samples was investigated in ND- and HFD-fed mice exposed to As, Cd, or Pb (**Figures 3A–I**). As expected, upon As, Cd, or Pb exposure, these heavy metals accumulated significantly more in livers and kidneys in HFD-fed mice than in ND-fed mice when the background accumulation in ND- and HFD-fed mice with no heavy metal treatment had no significant difference or was even lower (**Figures 3A,B,D,E,G,H**). Interestingly, upon As, Cd, or Pb exposure, these heavy metals were excreted significantly less through feces in HFD-fed mice compared to ND-fed mice while their background content in feces of mice with no heavy metal treatment had no significant difference (**Figures 3C,F,G**). These data implied that higher accumulation of heavy metals in organs of HFD-fed mice might result from less fecal excretion.

Diet Effects on Total Gut Microbiota Disturbance Upon As, Cd, or Pb Exposure

Since different dietary patterns shape unique gut microbiota profiles, to explore whether gut microbiota played a role in explaining the different harmful effects of heavy metals on ND- and HFD-fed mice, we analyzed the difference of microbiota in fecal samples of ND- and HFD-fed

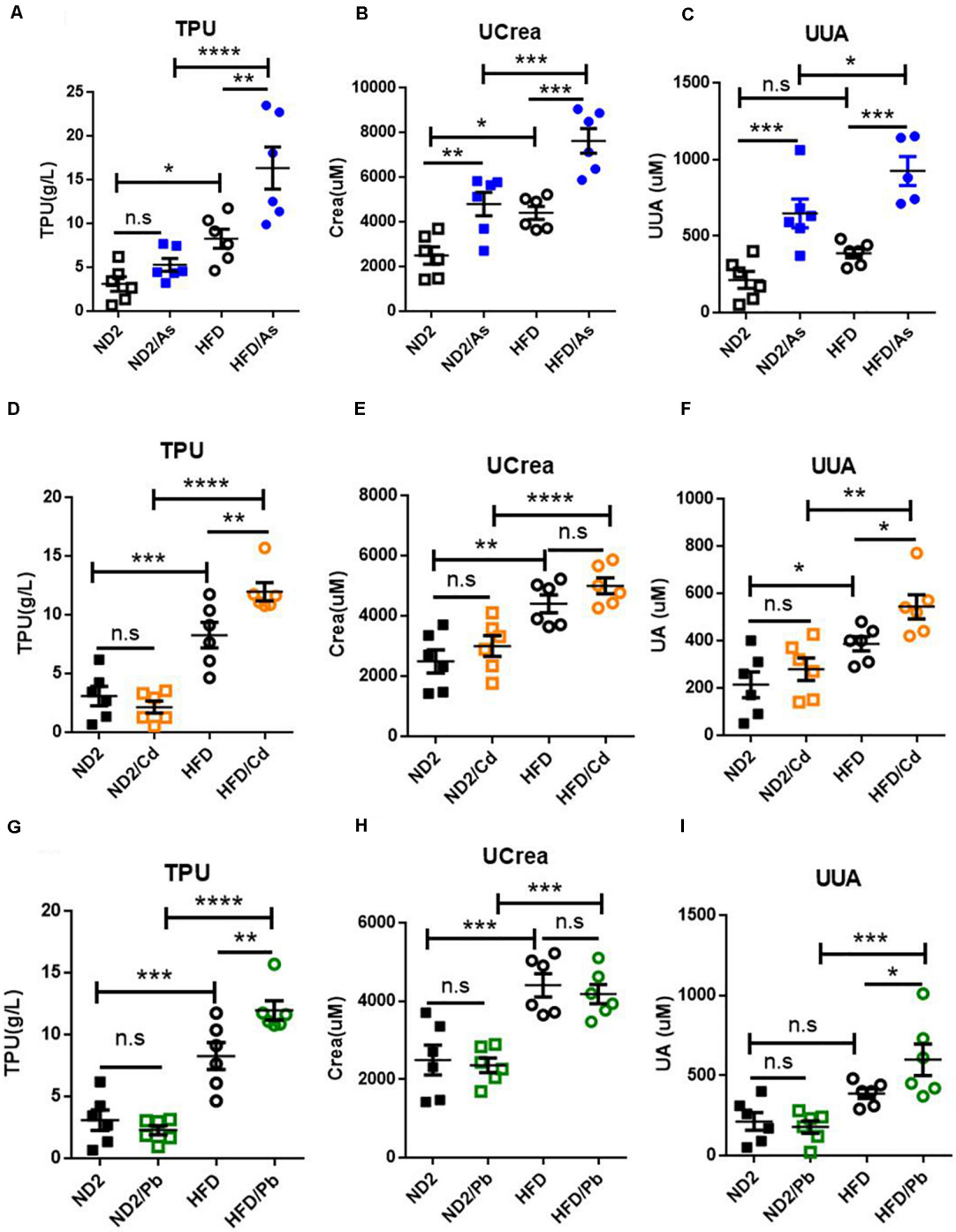

FIGURE 2 | Diet effects on kidney function damage upon heavy metal exposure. **(A–I)** ND- and HFD-fed mice were exposed to 100 ppm As, Cd, or Pd for 10 weeks (n = 6 for each group). Urine was collected and analyzed for total protein, uric acid, and creatinine contents on the day of sampling. Data were expressed as mean ± SEM. Statistics according to two-way ANOVAs and Bonferroni *post hoc* tests. n.s. not significant; *$P < 0.05$; **$P < 0.01$; ***$P < 0.001$; ***$P < 0.0001$. TPU, urinary total protein; UUA, urinary uric acid; Ucrea, urinary creatinine.

mice. A phylogenetic tree was made to summarize the observed alterations in relative abundance of microbial taxa (**Supplementary Figure S1**). It showed that there was a significant difference between gut microbiota of ND- and HFD-fed mice, which may respond differently to heavy metals.

As expected, the gut microbiota of ND- and HFD-fed mice respond differently to heavy metals. Principal coordinate

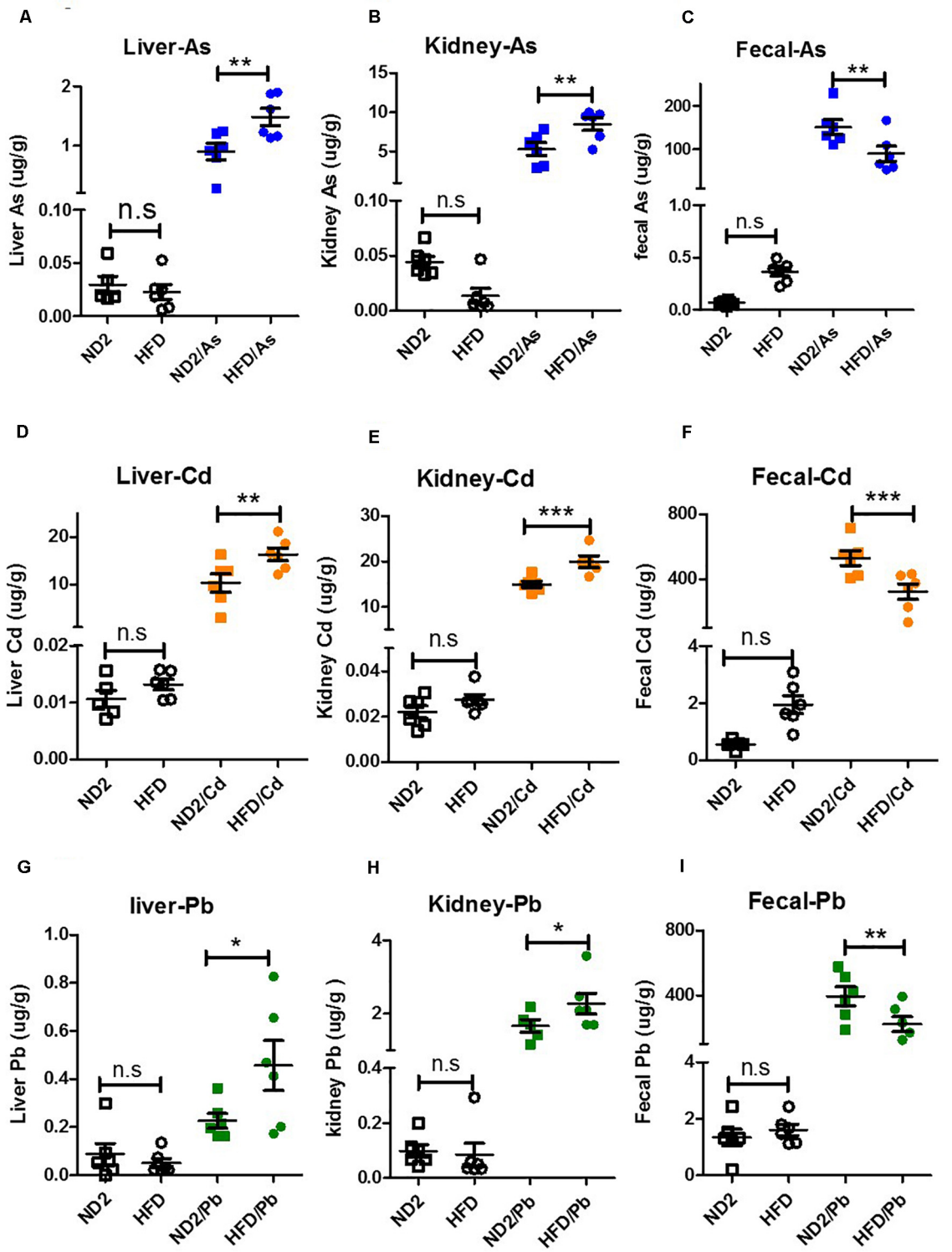

FIGURE 3 | Diet effects on heavy metal accumulation in the liver and kidney and elimination in feces. ND- and HFD-fed mice were exposed to 100 ppm As, Cd, or Pd for 10 weeks (n = 6 for each group). Feces, liver, and kidney were collected for As, Cd, or Pb content analysis. **(A,B)** Bioaccumulation of As in the liver/kidney of ND- and HFD-fed mice upon As exposure. **(C)** As content in feces of ND- and HFD-fed mice upon As exposure. **(D,E)** Bioaccumulation of Cd in the liver/kidney of ND- and HFD-fed mice upon Cd exposure. **(F)** Cd content in feces of ND- and HFD-fed mice upon Cd exposure. **(G,H)** Bioaccumulation of Pb in the liver/kidney of ND- and HFD-fed mice upon Pb exposure. **(I)** Pb content in feces of ND- and HFD-fed mice upon Pb exposure. Data were expressed as mean ± SEM. Statistics according to two-way ANOVAs and Bonferroni *post hoc* tests. n.s. not significant; $^{*}P < 0.05$; $^{**}P < 0.01$; $^{***}P < 0.001$.

component analysis (PCA) based on an unweighted UniFrac analysis showed that the gut microbiota of both ND- and HFD-fed mice changed upon As, Cd, or Pb exposure. However, the HFD microbiota changed more than the ND microbiota (**Figures 4A–C**). Arsenic (As), Cd, or Pb exposure reduced microbiota abundance based on operational taxonomic unit (OTU) number (**Figures 4D–F**) and microbial diversity based on the Chao1 index (**Figures 4G–I**) in both ND- and HFD-fed mice; however, there was more reduction in microbiota abundance and diversity in HFD- than in ND-fed mice. Generally, these data indicated that gut microbiota of HFD-fed mice suffered more disturbance upon As, Cd, or Pb exposure.

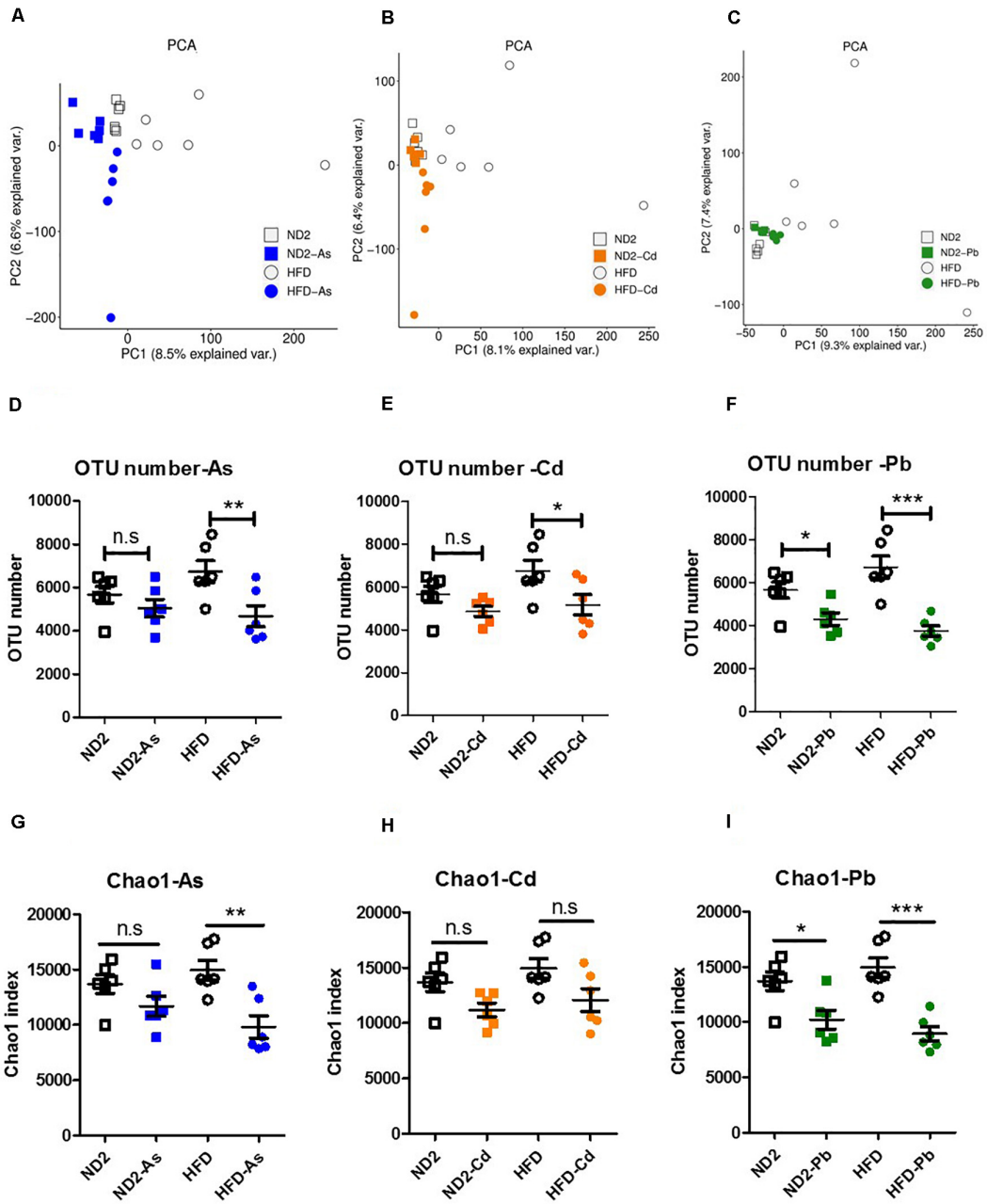

FIGURE 4 | Diet effects on gut microbiota disturbance upon As, Cd, or Pb exposure. ND- and HFD-fed mice were exposed to 100 ppm As, Cd, or Pd for 10 weeks (n = 6 for each group). Cecum feces was collected for gut microbiota analysis by 16S rRNA gene sequencing. **(A–C)** Principal coordinate analysis (PCA) based on an unweighted UniFrac analysis of the intestinal microbial composition where samples of ND-/HFD-fed mice upon As, Cd, or Pb exposure are highlighted with different colors. The position and distance of data points indicate the degree of similarity in terms of both presence and relative abundance of bacterial taxonomies. **(D–F)** Number of observed OTUs. Data (mean + SEM) represent 16S rRNA gene 454-pyrosequencing analysis of intestinal microbiota of mice. **(G–I)** Chao1 index of microbial diversity. Statistics according to two-way ANOVAs and Bonferroni *post hoc* tests. n.s. not significant; $^{*}P < 0.05$; $^{**}P < 0.01$; $^{***}P < 0.001$.

Diet Effects on Specific Gut Microbiota Genus Upon As, Cd, or Pb Exposure

To further find specific microbiota that were changed by heavy metals and which one(s) may confer detoxification effects, we analyzed the abundance change of gut microbiota at all taxon levels by arsenic (As), Cd, or Pb treatment in both ND- and HFD-fed mice (**Supplementary Figures S2–S7**). Specific gut microbiota genus that was changed significantly by As, Cd, or Pb treatment was summarized in **Supplementary Table S2**. Interestingly, among all the specific microbiota genera that were changed by heavy metals, a few increased significantly in the microbiota of ND- but not HFD-fed mice. Upon arsenic (As) exposure, *Bacteroides*, *Butyricimonas*, *Dorea*, and *Lactobacillus* increased significantly in the microbiota of ND- but not HFD-fed mice (**Figures 5A–D**). Upon Cd exposure, *Coprococcus* and *Lactobacillus* increased significantly in microbiota of ND- but not HFD-fed mice (**Figures 5E,F**). Upon Pb exposure, *Desulfovibrio*, *Prevotella*, and *Roseburia* increased significantly in microbiota of ND- but not HFD-fed mice (**Figures 5G–I**). These gut microbiota genera that were enriched by heavy metals in ND-fed mice that suffered less toxicity and accumulation might be candidate microbes with detoxification ability.

Correlation Between Fecal As, Cd, and Pb Content and Abundance of Total Gut Microbiota and Specific Microbiota Genus

To further evaluate the possible detoxification role of the above gut microbiota genera that were enriched by heavy metals in ND-fed mice, we analyzed the correlation between the abundance of these specific microbiota genera as well as the abundance of total gut microbiota and content of fecal heavy metals, based on an assumption that gut microbiota especially those specifically enriched microbiota genera might help to excrete heavy metals with feces, which results in less heavy metal accumulation and organ damage. Results showed that the total microbe abundance and fecal As, Cd, and Pb concentrations were positively correlated, among which microbe abundance of As-exposed mice and their fecal As were significantly positively correlated (**Figures 6A–C**). Weak positive correlations were also found between arsenic (As)-enriched *Bacteroides* and *Lactobacillus* and fecal As content (**Figures 6D,E**), Cd-enriched *Coprococcus* and *Lactobacillus* and fecal Cd content (**Figures 6F,G**), and Pb-enriched *Roseburia* and fecal Pb content (**Figure 6H**). These results implied a causal link between those microbes and heavy metal detoxification.

DISCUSSION

It is widely accepted that diet is the most important determinant of gut microbiota (Lynch and Hsiao, 2019). Studies have confirmed that gut microbiota played roles in heavy metal-caused diseases (Ba et al., 2017; Kim et al., 2017). Tinkov et al. (2018) proposed a causal link between Cd exposure, gut microbiota, and diseases: Cd exposure acted on the gut microbiota and intestines, resulting in increased intestinal barrier permeability, local intestinal inflammation, changes in intestinal microbiota, and their metabolic functions, which led to bacterial translocation, increased lipopolysaccharides and endotoxins, and eventually the risk of infectious diseases. Moreover, metabolic disorders and systemic inflammation would act on target organs such as adipose tissue, liver, kidney, cardiovascular system, and brain, which would increase the risk of corresponding diseases (Tinkov et al., 2018). Here, we report that HFD affects heavy metal toxicity and accumulation in mice liver and kidney and report its relationship to gut microbiota. Results showed that when exposed to heavy metals, there was more heavy metal accumulation in the liver and kidney of HFD- versus ND-fed mice and organ function damage increased more in HFD-fed compared to ND-fed mice. It is probably because of their distinct gut microbiota: HFD microbiota suffered more disturbances when exposed to heavy metals. Some microbes that could respond to heavy metals and enrich them in ND-fed mice did not respond or cannot enrich as much in HFD-fed mice. The abundance of overall microbiota and some of these specific microbes had a positive correlation with the content of fecal heavy metals, suggesting that the gut microbiota especially the specific microbes might play a role in heavy metal detoxification probably via absorption and fecal excretion.

A few literatures reported changes of gut microbiota caused by heavy metal exposure (reviewed by Gillois et al., 2018). There were no consistent results about microbiota changes in each study at the taxa level of species, genus, family, order, or even phylum, which may result from differences in dosage of the heavy metals, exposure time, physiological feature of experimental animals, and most importantly, the food composition of the diet (Tinkov et al., 2018). Anyhow, different intestinal microbes responded differently to heavy metal stresses, and their maximum tolerated concentrations and sorption properties were different (Riley and Mee, 1982; Sizentsov et al., 2019). Our *in vivo* experiments in mice showed that under 100 ppm As, Cd, or Pb, most gut microbes were tolerant without abundance change while a few were sensitive indicated by a decrease in abundance (**Supplementary Figures S2–S7** and **Supplementary Table S2**), implying that some intestinal microbes might not respond to stresses from specific heavy metals. Moreover, we found that the same heavy metal caused mostly the same change of the same microbes in both ND and HFD. For example, under arsenic exposure, *Dorea*, *Lactobacillus*, and *Bacteroides* all increased while *Allobaculum*, *Akkermansia*, and *Bilophila* all decreased in both ND- and HFD-fed mice; however, a few microbes such as *Butyricimonas*, *Adlercreutzia*, and *Prevotella* showed opposite changes in ND- and HFD-fed mice. This may be due to the mutual promotion or inhibition of individual microbes in a complex microbiota ecosystem, which affects their response to stress.

It is worth noting that in five out of six heavy metal treatment groups, *Lactobacillus* was significantly increased, and *Akkermansia* was significantly decreased, regardless of feeding diet (**Supplementary Table S2**). *Lactobacillus* abundance was positively correlated with fecal discharge of both As and Cd. With an estimated >200 species presently, *Lactobacillus* is

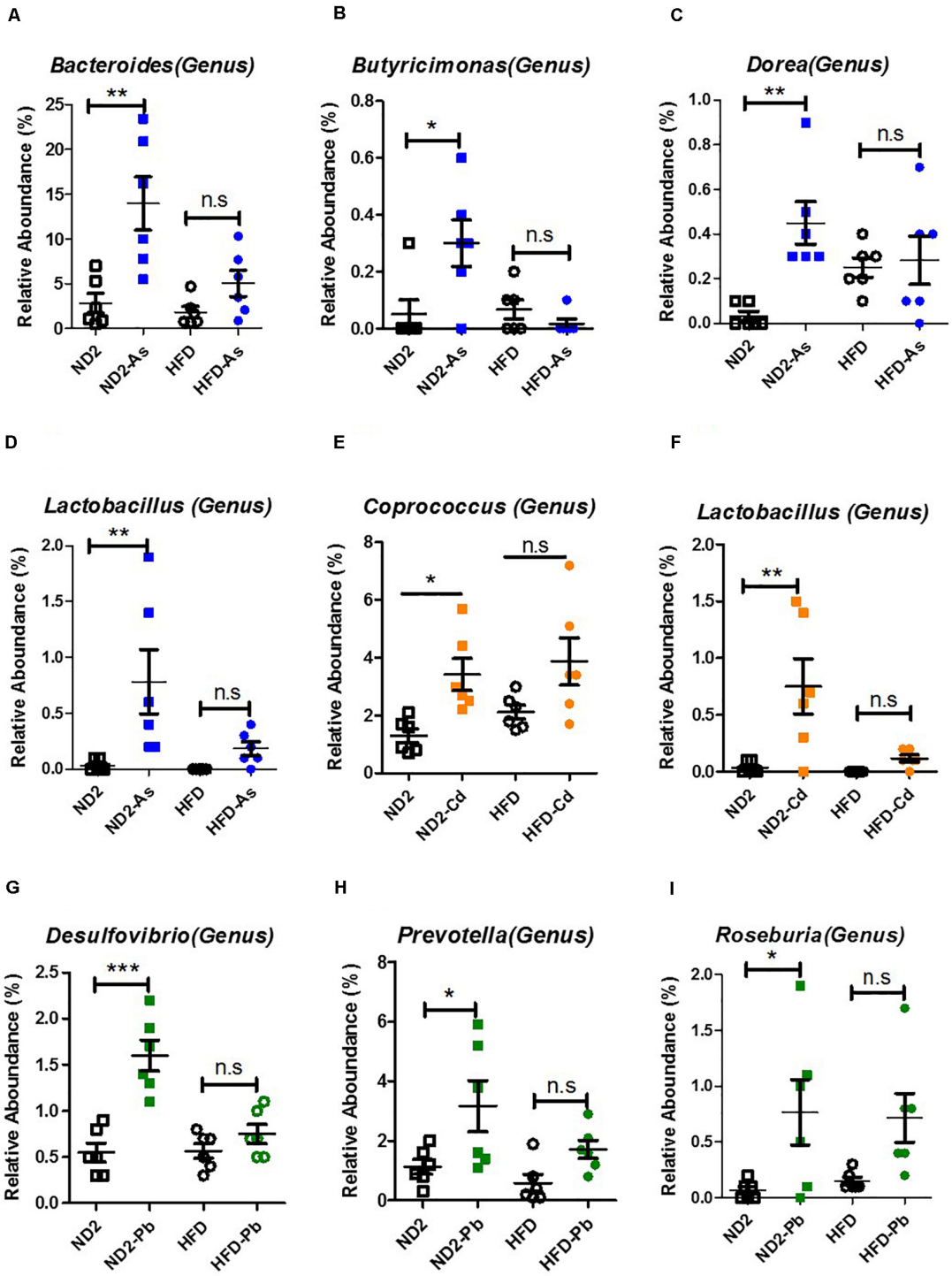

FIGURE 5 | Microbial genus enriched significantly by heavy metals primarily in ND-fed mice. ND- and HFD-fed mice were exposed to 100 ppm As, Cd, or Pd for 10 weeks (n = 6 for each group). Cecum feces was collected for gut microbiota analysis by 16S rRNA gene sequencing. **(A)** *Bacteroides* in the Bacteroidetes phylum, Bacteroidia class, Bacteroidales order, Bacteroidaceae family. **(B)** *Butyricimonas* in the Bacteroidetes phylum, Bacteroidia class, Bacteroidales order, Odoribacteracea family. **(C)** *Dorea*, **(E)** *Coprococcus*, and **(I)** *Roseburia* in Firmicutes phylum, Clostridia class, Clostridiales order, Lachnospiraceae family. **(D,F)** *Lactobacillus salivarius* in the Firmicutes phylum, Bacilli class, Lactobacillales order, Lactobacillaceae family. **(G)** *Desulfovibrio* in Proteobacteria phylum, Deltaproteobacteria class, Desulfovibrionales order, Desulfovibrionaceae family. **(H)** *Prevotella* in Bacteroidetes phylum, Bacteroidia class, Bacteroidales order, Prevotellaceae family. Data are expressed as mean ± SEM. Statistics according to two-way ANOVAs and Bonferroni *post hoc* tests. n.s. not significant; $^{*}P < 0.05$; $^{**}P < 0.01$; $^{***}P < 0.001$.

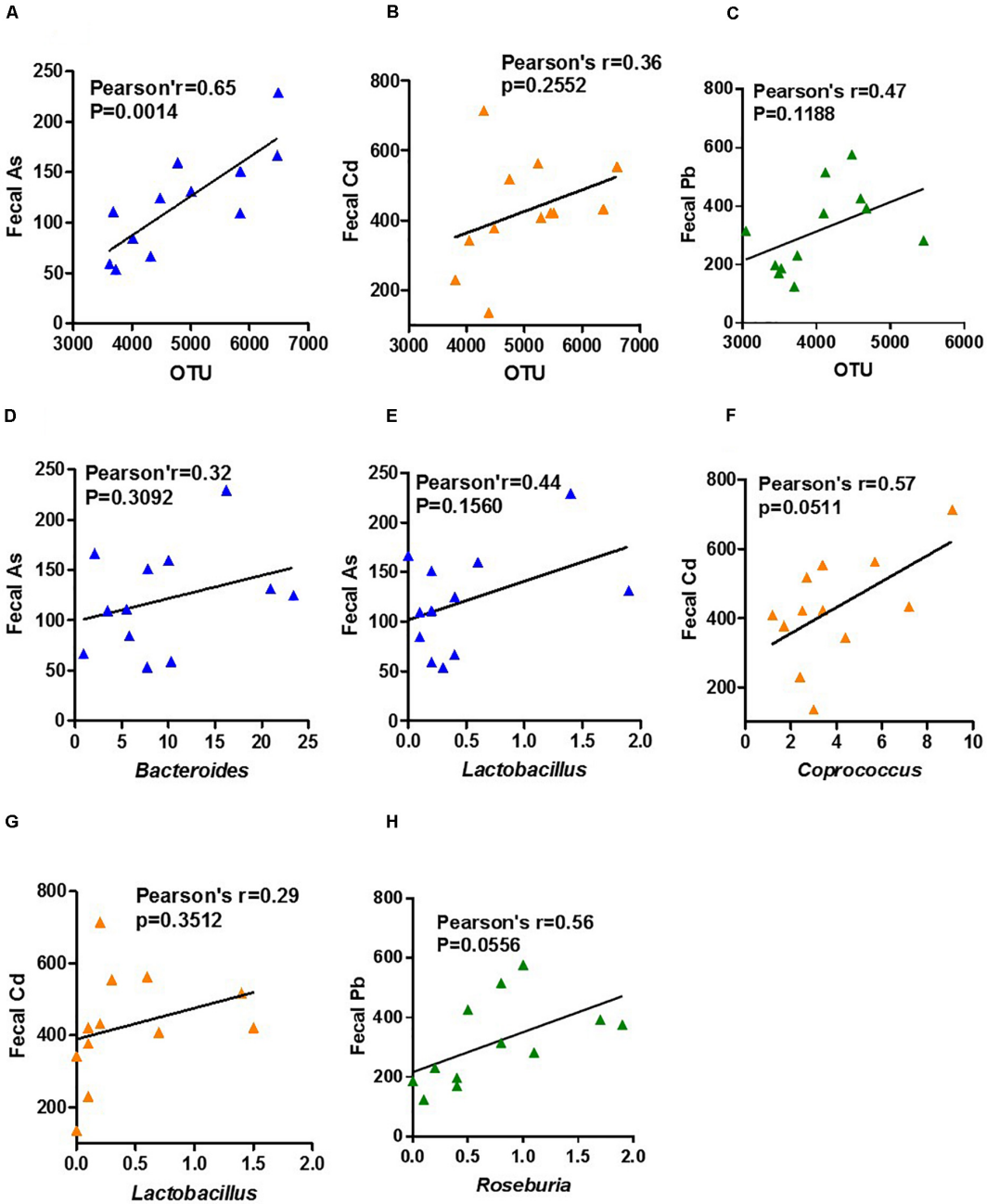

FIGURE 6 | Correlation between fecal As, Cd, and Pb content and gut microbiota abundance of total and specific microbiota genera. Data of ND- and HFD-fed mice upon As, Cd, or Pb exposure were used for Pearson's correlation analysis. Bivariate scatterplots between **(A)** fecal As and total microbiota abundance of As-exposed mice, **(B)** fecal Cd and total microbiota abundance of Cd-exposed mice, **(C)** fecal Pb and total microbiota abundance of Pb exposed mice, fecal As and *Bacteroides* **(D)** and *Lactobacillus* **(E)** abundance of As-exposed mice, fecal Cd and *Coprococcus* **(F)** and *Lactobacillus* **(G)** abundance of Cd-exposed mice, and **(H)** fecal Pb and *Roseburia* abundance of Pb-exposed mice.

well known for its ability to modulate the microbiota in the host gastrointestinal tract, conferring beneficial effects in health (Holzapfel and Wood, 2014; Yeo et al., 2018). Our study proposed that *Lactobacillus* might also have function in heavy metal detoxification. The decrease in *Akkermansia* had been shown in various disease conditions such as obesity and inflammatory bowel disease (Naito et al., 2018). Our study indicated that its decrease might also be related to the risk of disease caused by heavy metal exposure.

Several other gut microbes including *Bacteroides*, *Coprococcus*, and *Roseburia* were enriched by heavy metals and were also positively correlated with heavy metal content in feces.

Genomic and subsequent proteomic analyses for *Bacteroides thetaiotaomicron* and *Bacteroides fragilis* have found multiple pump systems to get rid of toxic substances (Wexler, 2007). *Roseburia* spp. were commensal bacteria producing short-chain fatty acids and could serve as markers of human health (Tamanai-Shacoori et al., 2017). Although their correlations were weak, they provided candidates for future screening for heavy metal detoxification. Certainly, the roles and mechanisms of these intestinal microbes in detoxifying heavy metals and reducing their toxicity to the host still needed to be verified by *in vivo* single-strain replenishment experiments. Since with sequence of 16S rRNA V3/V4, we could not annotate gut microbes accurately to species level, it was expected that full-length sequence could screen out intestinal microbes at the species level that respond to heavy metals in future studies; then proper strains could be used for experimental verification, and the detoxification mechanism has to go after these efforts.

Health risks of heavy metal exposure could be reduced by interventions targeting gut microbiota. Cd-exposed rats when fed with probiotics *Lactobacillus plantarum* and *Bacillus coagulans* showed reduced Cd accumulation in the liver and kidney, as well as reduced serum alanine transaminase and glutamic transaminase activities and creatinine and urea concentrations, suggesting a reduction in Cd toxicity (Jafarpour et al., 2017). In rats exposed to Cd, the abundance of lactic acid bacteria in fecal microbiota was positively correlated with fecal Cd content and negatively correlated with the serum Cd content, indicating that the probiotics might absorb Cd and exclude it (Djurasevic et al., 2017). A randomized open-label pilot study in heavy metal-contaminated areas showed that supplementation of *Lactobacillus rhamnosus* resulted in significantly lower levels of mercury (Hg) and arsenic (As) in the blood of pregnant women than in the control group (Bisanz et al., 2014), suggesting that interventions targeting gut microbiota in specific populations may reduce the health risks of heavy metals. Our study showed that different diets affected accumulation of heavy metal and damage of liver and kidney after heavy metal exposure. It is reasonable to test the possibilities that health risk of heavy metal exposure might be reduced through dietary interventions targeting gut microbiota.

MATERIALS AND METHODS

Mice

Animal experiments were approved and performed in accordance with the guidelines of the Laboratory Animal Center of Guangzhou Medical University (animal protocol number: 2019-634). Eight-week-old male C57BL/6 mice were purchased from Guangdong Medical Laboratory Animal Center (GDMLAC) and kept under controlled temperature and light conditions (25°C, 12-h light–dark cycle), with free access to food and water. Mice were randomly divided into eight groups containing six animals each and housed in groups of three animals per cage. Four groups of mice were fed with ND (13.5% of energy from fat; D12450; GDMLAC, China) and the other four groups with HFD (45% of energy from fat; D12451; GDMLAC, China). The formula of the diet was shown in **Supplementary Table S1**. Each group of ND-/HFD-fed mice was given 0/100 ppm As ($NaAsO_2$, Merck), Cd ($CdCl_2.5H_2O$, Macklin), or Pd ($PbCl_2$, Macklin) in drinking water for 10 weeks.

At week 10, urine and fecal samples were taken. Fecal samples were dried in an oven at 65°C for 24–30 h until the weight became constant. The weight of dried fecal sample was recorded. Animals were fasted for 12 h before killing. Mice were deeply anesthetized with 1% pentobarbital sodium (50 mg/kg BW), and whole blood was withdrawn through the ventral aorta in tubes containing anticoagulant KEDTA. The kidney and liver were removed and weighed. Feces in the cecum was squeezed out. Organ and cecum content samples were immersed in liquid nitrogen and stored at −80°C for further analysis.

Liver Function Analysis

Whole blood was withdrawn through the ventral aorta in tubes containing anticoagulant K2EDTA. Blood was centrifuged at 500 *g* for 5 min, and supernatants (plasma) were collected. Two biomarkers of liver function, activity of ALT and AST, were determined on the day of sampling by commercial ELISA kits: ALT (Cat #05850797190, Roche Diagnostics, United States) and AST (Cat #05850819190, Roche Diagnostics, United States), according to the manufacturer's instructions.

Kidney Function Analysis

Three biomarkers of kidney function, TPU, UUA, and Ucrea, were determined on the day of sampling by commercial ELISA kits: total protein (Cat #051718190, Roche Diagnostics, United States), uric acid (Cat #05171857190, Roche Diagnostics, United States), and creatinine (Cat #06407137190, Roche Diagnostics, United States) according to the manufacturer's instructions.

Gut Microbiota Analysis

Cecal microbiota DNA was extracted using a Stool DNA Kit (Guangzhou IGE Biotechnology, China) and applied to amplification of V3–V4 regions of 16S rDNA. Cecal microbiota composition was assessed using Illumina 2500 sequencing of 16S rDNA amplicon and QIIME-based microbiota analysis. High-quality reads for bioinformatics analysis were selected, and all of the effective reads from all samples were clustered into OTUs based on 99% sequence similarity according to QIIMEU clust. OTUs were annotated through the RDP Classifier (Version 2.2), with a confidence cutoff of 0.8 according to the Green Gene database, and the composition and abundance information of each sample at different classification levels were statistically summarized. Based on the OTU information from each sample, PCA was applied via R to examine the similarity between different samples; α-diversity analyses were performed via the R package phyloseq v.1.19.1 and vegan 2.4.2 packets to calculate the diversity index.

Heavy Metal Analysis

Dried fecal samples and frozen liver and kidney were digested with 6 ml 65% HNO_3 (Merck Darmstadt, Germany) at

25°C overnight and further digested by a microwave sample preparation system (Multiwave 3000, Anton Paar, Austria). After digestion, the solutions were diluted with ultrapure water to a final volume of 50 ml. As, Pb, and Cd were measured by inductively coupled plasma mass spectrometry (7700×, Agilent, Japan) according to Sanchez Lopez et al. (2003).

Statistical Analysis

Required sample sizes were calculated to obtain a power of 0.8, based on the results of similar, previous studies and preliminary data from our own laboratory. Statistical analysis was performed using GraphPad Prism Version 7.0. Unless otherwise indicated, data were analyzed by two-way (heavy metals × diet) repeated-measures ANOVA, followed by Bonferroni *post hoc* tests. All data were presented as mean ± SD. *P*-values < 0.05 were considered significant ($^{*}P < 0.05$, $^{**}P < 0.01$, $^{***}P < 0.001$). Graphs were generated using the software GraphPad Prism 7.0. All significant *post hoc* test results are depicted in the figures. Bivariate associations between fecal heavy metal content and the whole and genus-level gut microbiota abundance were assessed using Pearson's correlation.

CONCLUSION

Gut microbiota could detoxify environment toxins through absorption and/or metabolic conversion (Koppel et al., 2017). Intervention targeting gut microbiota to reduce health risks of heavy metals was expected to be safe and cost-effective (Bisanz et al., 2014). To explore the responses of the gut microbiota upon heavy metal stress, exploiting the strains with the potential to detoxify heavy metals and clarifying the detoxification mechanism were the premise of the method. Our study showed that when exposed to 100 ppm As, Cd, or Pb, HFD-fed mice accumulated more heavy metals in the liver and kidney along with more severe function damage than did ND-fed mice, which might result from lower abundance and diversity of HFD microbiota, especially specific gut microbes that might be involved in this detoxification process. Therefore, the health risk of heavy metal exposure might be reduced through dietary interventions targeting gut microbiota. Arsenic-enriched *Bacteroides* and *Lactobacillus*, cadmium-enriched *Coprococcus* and *Lactobacillus*, and lead-enriched *Roseburia* were positively correlated with As, Cd, or Pb content in stools, respectively, and accumulated less in organs, suggesting that these might be the microbes with the potential to detoxify heavy metals. However, the role of these intestinal microbes in detoxifying heavy metals still needs to be verified by future *in vivo* single-strain replenishment experiments.

DATA AVAILABILITY STATEMENT

The datasets generated for this study can be found in the Sequence Read Archive (SRA), PRJNA596575.

ETHICS STATEMENT

The animal study was reviewed and approved by the Committee Review of Animal Experiments in Guangzhou Medical University (Document no. 2019-634).

AUTHOR CONTRIBUTIONS

TL, XL, ZL, and HL conceived and designed the experiments. TL, CLe, QH, CLi, XL, HM, and RF carried out the experiments. TL and WS participated in analyzing the data. TL and NS drafted the manuscript. All authors read and approved the final version of the manuscript.

FUNDING

This work was supported by the Natural Science Foundation of Guangdong Province (NSFG) (project nos. 2018A030310168 and 2020A151501910) to TL and NS, the National Natural Science Foundation of China (NSFC) (project no. 81703333) to NS, and the Industry-University-Research Cooperation Foundation of Guangdong Science and Technology Department (IUCF-GSTD) (grant no. 2017A090905038) to HL. Guangzhou Key Laboratory Fund (grant no. 201905010004).

ACKNOWLEDGMENTS

The authors would like to thank Mr. Yubin Zhou (from Guangzhou IGE Biotechnology Ltd.) for the kind assistance with microbiota sequencing and analysis. The authors also appreciate Prof. Yongqin Li (from South China Botanical Garden, Chinese Academy of Sciences) for giving valuable suggestions and proofreading this manuscript.

SUPPLEMENTARY MATERIAL

The Supplementary Material for this article can be found online at: https://www.frontiersin.org/articles/10.3389/fmicb.2020.01604/full#supplementary-material

FIGURE S1 | HFD changes relative abundance of most intestinal microbial taxa. Cecum fecal of ND- and HFD-fed mice ($n = 6$ for each group) was collected for gut microbiota analysis by 16S rRNA gene sequencing. Phylogenetic tree created manually showing specific differences in intestinal microbial community at different taxonomic levels between ND and HFD-fed mice. Nodes represent taxa, and the size of each node represents its relative abundance. The color red indicates an increase, blue indicates a decrease, and black indicates no change of relative abundance in HFD compared with ND fed mice. The fully colored nodes indicate the statistically significant difference ($P < 0.05$) and the hollow nodes indicate the statistically non-significant difference by unpaired two-tailed student's *t*-test.

FIGURE S2 | As exposure changes relative abundance of specific intestinal microbial taxa in ND-fed mice. ND-fed mice were exposed to 100 ppm As for 10 weeks ($n = 6$ for each group). Cecum fecal was collected for gut microbiota analysis by 16S rRNA gene sequencing. Phylogenetic tree created manually showing specific differences in intestinal microbial community at different taxonomic levels between As exposure and control mice. Nodes represent taxa, and the size of each node represents its relative abundance. The color red

indicates an increase, blue indicates a decrease, and black indicates no change of relative abundance in As exposure compared with control mice. The full color of the nodes indicates the statistically significant difference and the hollow nodes indicate the statistically non-significant difference by unpaired two-tailed student's *t*-test.

FIGURE S3 | As exposure changes relative abundance of specific intestinal microbial taxa in HFD-fed mice. HFD-fed mice were exposed to 100 ppm As for 10 weeks (n = 6 for each group). Cecum fecal was collected for gut microbiota analysis by 16S rRNA gene sequencing. Phylogenetic tree created manually showing specific differences in intestinal microbial community at different taxonomic levels between As exposure and control mice. Nodes represent taxa, and the size of each node represents its relative abundance. The color red indicates an increase, blue indicates a decrease, and black indicates no change of relative abundance in As exposure compared with control mice. The full color of the nodes indicates the statistically significant difference and the hollow nodes indicate the statistically non-significant difference by unpaired two-tailed student's *t*-test.

FIGURE S4 | Cd exposure changes relative abundance of specific intestinal microbial taxa in ND-fed mice. ND-fed mice were exposed to 100 ppm Cd for 10 weeks (n = 6 for each group). Cecum fecal was collected for gut microbiota analysis by 16S rRNA gene sequencing. Phylogenetic tree created manually showing specific differences in intestinal microbial community at different taxonomic levels between Cd exposure and control mice. Nodes represent taxa, and the size of each node represents its relative abundance. The color red indicates an increase, blue indicates a decrease, and black indicates no change of relative abundance in Cd exposure compared with control mice. The full color of the nodes indicates the statistically significant difference and the hollow nodes indicate the statistically non-significant difference by unpaired two-tailed student's *t*-test.

FIGURE S5 | Cd exposure changes relative abundance of specific intestinal microbial taxa in HFD-fed mice. HFD-fed mice were exposed to 100 ppm Cd for 10 weeks (n = 6 for each group). Cecum fecal was collected for gut microbiota analysis by 16S rRNA gene sequencing. Phylogenetic tree created manually showing specific differences in intestinal microbial community at different taxonomic levels between Cd exposure and control mice. Nodes represent taxa, and the size of each node represents its relative abundance. The color red indicates an increase, blue indicates a decrease, and black indicates no change of relative abundance in Cd exposure compared with control mice. The full color of the nodes indicates the statistically significant difference and the hollow nodes indicate the statistically non-significant difference by unpaired two-tailed student's *t*-test.

FIGURE S6 | Pb exposure changes relative abundance of specific intestinal microbial taxa in ND-fed mice. ND-fed mice were exposed to 100 ppm Pb for 10 weeks (n = 6 for each group). Cecum fecal was collected for gut microbiota analysis by 16S rRNA gene sequencing. Phylogenetic tree created manually showing specific differences in intestinal microbial community at different taxonomic levels between Pb exposure and control mice. Nodes represent taxa, and the size of each node represents its relative abundance. The color red indicates an increase, blue indicates a decrease, and black indicates no change of relative abundance in Pb exposure compared with control mice. The full color of the nodes indicates the statistically significant difference and the hollow nodes indicate the statistically non-significant difference by unpaired two-tailed student's *t*-test.

FIGURE S7 | Pd exposure changes relative abundance of specific intestinal microbial taxa in HFD-fed mice. HFD-fed mice were exposed to 100 ppm Pb for 10 weeks (n = 6 for each group). Cecum fecal was collected for gut microbiota analysis by 16S rRNA gene sequencing. Phylogenetic tree created manually showing specific differences in intestinal microbial community at different taxonomic levels between Pb exposure and control mice. Nodes represent taxa, and the size of each node represents its relative abundance. The color red indicates an increase, blue indicates a decrease, and black indicates no change of relative abundance in Pb exposure compared with control mice. The full color of the nodes indicates the statistically significant difference and the hollow nodes indicate the statistically non-significant difference by unpaired two-tailed student's *t*-test.

TABLE S1 | Diet for Mice.

TABLE S2 | Summary of microbiota changed by heavy metals.

REFERENCES

Ba, Q., Li, M., Chen, P., Huang, C., Duan, X., Lu, L., et al. (2017). Sex-dependent effects of cadmium exposure in early life on gut microbiota and fat accumulation in mice. *Environ. Health Perspect.* 125, 437–446. doi: 10.1289/EHP360

Bisanz, J. E., Enos, M. K., Mwanga, J. R., Changalucha, J., Burton, J. P., Gloor, G. B., et al. (2014). Randomized open-label pilot study of the influence of probiotics and the gut microbiome on toxic metal levels in Tanzanian pregnant women and school children. *MBio* 5:e01580-14. doi: 10.1128/mBio.01580-14

Bjorklund, G., Skalny, A. V., Rahman, M. M., Dadar, M., Yassa, H. A., Aaseth, J., et al. (2018a). Toxic metal (loid)-based pollutants and their possible role in autism spectrum disorder. *Environ. Res.* 166, 234–250. doi: 10.1016/j.envres.2018.05.020

Bjorklund, G., Stejskal, V., Urbina, M. A., Dadar, M., Chirumbolo, S., and Mutter, J. (2018b). Metals and Parkinson's disease: mechanisms and biochemical processes. *Curr. Med. Chem.* 25, 2198–2214. doi: 10.2174/0929867325666171129124616

Breton, J., Daniel, C., Dewulf, J., Pothion, S., Froux, N., Sauty, M., et al. (2013a). Gut microbiota limits heavy metals burden caused by chronic oral exposure. *Toxicol. Lett.* 222, 132–138. doi: 10.1016/j.toxlet.2013.07.021

Breton, J., Massart, S., Vandamme, P., De Brandt, E., Pot, B., and Foligne, B. (2013b). Ecotoxicology inside the gut: impact of heavy metals on the mouse microbiome. *BMC Pharmacol. Toxicol.* 14:62. doi: 10.1186/2050-6511-14-62

Cordain, L., Eaton, S. B., Sebastian, A., Mann, N., Lindeberg, S., Watkins, B. A., et al. (2005). Origins and evolution of the Western diet: health implications for the 21st century. *Am. J. Clin. Nutr.* 81, 341–354. doi: 10.1093/ajcn.81.2.341

Dadar, M., Adel, M., Ferrante, M., NasrollahzadehSaravi, H., Copat, C., and Oliveri Conti, G. (2016). Potential risk assessment of trace metals accumulation in food, water and edible tissue of rainbow trout (*Oncorhynchus mykiss*) farmed in Haraz River, northern Iran. *Toxin Rev.* 35, 141–146. doi: 10.1080/15569543.2016.1217023

Djurasevic, S., Jama, A., Jasnic, N., Vujovic, P., Jovanovic, M., Mitic-Culafic, D., et al. (2017). The protective effects of probiotic bacteria on cadmium toxicity in rats. *J. Med. Food* 20, 189–196. doi: 10.1089/jmf.2016.0090

Ghazala, I., Wahid, Z., Abdul, M., and Ahmed, T. (2018). Elevated heavy metals levels in cognitively impaired patients from Pakistan. *Environ. Toxicol. Pharmacol.* 60, 100–109. doi: 10.1016/j.etap.2018.04.011

Gillois, K., Leveque, M., Theodorou, V., Robert, H., and Mercier-Bonin, M. (2018). Mucus: an underestimated gut target for environmental pollutants and food additives. *Microorganisms* 6:53. doi: 10.3390/microorganisms6020053

Holzapfel, W. H., and Wood, B. J. B. (2014). "Introduction to the LAB," in *Lactic AcidBacteria – Biodiversity and Taxonomy*, eds W. H. Holzapfel and B. J. B. Wood (Hoboken, NJ: John Wiley & Sons Ltd), 1–12.

Iqbal, G., Zada, W., Mannan, A., and Ahmed, T. (2018). Elevated heavy metals levels in cognitively impaired patients from Pakistan. *Environ. Toxicol. Pharmacol.* 60, 100–109. doi: 10.1016/j.etap.2018.04.011

Isokpehi, R. D., Udensi, U. K., Simmons, S. S., Hollman, A. L., Cain, A. E., Olofinsae, S. A., et al. (2014). Evaluative profiling of arsenic sensing and regulatory systems in the human microbiome project genomes. *Microbiol. Insights* 7, 25–34. doi: 10.4137/mbi.s18076

Jafarpour, D., Shekarforoush, S. S., Ghaisari, H. R., Nazifi, S., Sajedianfard, J., and Eskandari, M. H. (2017). Protective effects of synbiotic diets of *Bacillus coagulans*, *Lactobacillus plantarum* and inulin against acute cadmium toxicity in rats. *BMC Complement Altern. Med.* 17:291. doi: 10.1186/s12906-017-1803-3

Kim, E., Lembert, M. M., and Opiyo, S. (2017). Differential role of oxidative stress pathways and microbiota in thedevelopment of allergen specific IgE following chronic ingestion of low doses ofcadmium. *J. Immunol.* 198(1 Suppl.), 194.5.

Koppel, N., Maini Rekdal, V., and Balskus, E. P. (2017). Chemical transformation of xenobiotics by the human gut microbiota. *Science* 356, 1246–1257. doi: 10.1126/science.aag2770

Lamas, G. A., Navas-Acien, A., Mark, D. B., and Lee, K. L. (2016). Heavy metals, cardiovascular disease, and the unexpected benefits of chelation therapy. *J. Am. Coll. Cardiol.* 67, 2411–2418. doi: 10.1016/j.jacc.2016.02.066

Liebert, C. A., Wireman, J., Smith, T., and Summers, A. O. (1997). Phylogeny of mercury resistance (mer) operons of gram-negative bacteria isolated from the fecal flora of primates. *Appl. Environ. Microbiol.* 63, 1066–1076. doi: 10.1128/aem.63.3.1066-1076.1997

Liu, T., Yang, M., Han, Z., and Ow, D. (2016). Rooftop production of leafy vegetables can be profitable and less contaminated than farm grown vegetables. *Agron. Sustain. Dev.* 36, 36–41. doi: 10.1007/s13593-016-0378-6

Lynch, J. B., and Hsiao, E. Y. (2019). Microbiomes as sources of emergent host phenotypes. *Science* 365, 1405–1409. doi: 10.1126/science.aay0240

Naito, Y., Uchiyama, K., and Takagi, T. (2018). A next-generation beneficial microbe: *Akkermansia muciniphila*. *J. Clin. Biochem. Nutr.* 63, 33–35. doi: 10.3164/jcbn.18-57

Park, S. S., Skaar, D. A., Jirtle, R. L., and Hoyo, C. (2017). Epigenetics, obesity and early-life cadmium or lead exposure. *Epigenomics* 9, 57–75. doi: 10.2217/epi-2016-0047

Raehsler, S. L., Choung, R. S., Marietta, E. V., and Murray, J. A. (2018). Accumulation of heavy metals in people on a gluten-free diet. *Clin. Gastroenterol. Hepatol.* 16, 244–251. doi: 10.1016/j.cgh.2017.01.034

Riley, T. V., and Mee, B. J. (1982). Susceptibility of *Bacteroides* spp. to heavy metals. *Antimicrob. Agents Chemother.* 22, 889–892. doi: 10.1128/aac.22.5.889

Rowland, I. R., Davies, M. J., and Evans, J. G. (1980). The effect of the gastrointestinal flora on tissue content of mercury and organomercurial neurotoxicity in rats given methylmercuric chloride. *Dev. Toxicol. Environ. Sci.* 8, 79–82.

Rowland, I. R., Davies, M. J., and Grasso, P. (1978). Metabolism of methylmercuric chloride by the gastro-intestinal flora of the rat. *Xenobiotica* 8, 37–43. doi: 10.3109/00498257809060381

Sanchez Lopez, F. J., Gil Garcia, M. D., Sanchez Morito, N. P., and Martinez Vidal, J. L. (2003). Determination of heavy metals in crayfish by ICP-MSwith a microwave-assisted digestion treatment. *Ecotoxicol. Environ. Saf.* 54, 223–228. doi: 10.1016/S0147-6513(02)00050-7

Shao, W., Liu, Q., He, X., Liu, H., Gu, A., and Jiang, Z. (2017). Association between level of urinary trace heavy metals and obesity among children aged 6-19 years: NHANES 1999-2011. *Environ. Sci. Pollut. Res. Int.* 24, 11573–11581. doi: 10.1007/s11356-017-8803-1

Sizentsov, A., Sizentsov, Y., Kvan, O., Salnikova, E., and Salnikova, V. (2019). A study on heavy metal sorption properties of intestinal microbiota in vitro. *EDP Sciences* 79, 1–4. doi: 10.1051/e3sconf/20197903021

Tamanai-Shacoori, Z., Smida, I., Bousarghin, L., Loreal, O., Meuric, V., Fong, S. B., et al. (2017). Roseburia spp.: a marker of health? *Future Microbiol.* 12, 157–170. doi: 10.2217/fmb-2016-0130

Thomas, S., Izard, J., Walsh, E., Batich, K., Chongsathidkiet, P., Clarke, G., et al. (2017). The host microbiome regulates and maintains human health: a primer and perspective for non-microbiologists. *Cancer Res.* 77, 1783–1812. doi: 10.1158/0008-5472.can-16-2929

Tinkov, A. A., Gritsenko, V. A., Skalnaya, M. G., Cherkasov, S. V., Aaseth, J., and Skalny, A. V. (2018). Gut as a target for cadmium toxicity. *Environ. Pollut.* 235, 429–434. doi: 10.1016/j.envpol.2017.12.114

Wang, X., Mukherjee, B., and Park, S. K. (2018). Associations of cumulative exposure to heavy metal mixtures with obesity and its comorbidities among U.S. adults in NHANES 2003-2014. *Environ. Int.* 121(Pt 1), 683–694. doi: 10.1016/j.envint.2018.09.035

Wexler, H. M. (2007). *Bacteroides*: the good, the bad, and the nitty-gritty. *Clin. Microbiol. Rev.* 20, 593–621. doi: 10.1128/CMR.00008-07

Wijayawardena, M. A. A., Megharaj, M., and Naidu, R. (2016). "Exposure, toxicity, health impacts and bioavailability of heavy metal mixtures," in *Advances in Agronomy*, Vol. 138, ed. D. L. Sparks (London: Academic Press), 175–234. doi: 10.1016/bs.agron.2016.03.002

Wu, K. G., Chang, C. Y., Yen, C. Y., and Lai, C. C. (2018). Associations between environmental heavy metal exposure and childhood asthma: a population-based study. *J. Microbiol. Immunol. Infect.* 52, 352–362. doi: 10.1016/j.jmii.2018.08.001

Yeo, S., Shin, H. S., Lee, H. W., Hong, D., Park, H., Holzapfel, W., et al. (2018). Determination of optimized growth medium and cryoprotective additives to enhance the growth and survival of *Lactobacillus salivarius*. *J. Microbiol. Biotechnol.* 28, 718–731. doi: 10.4014/jmb.1801.01059

Conflict of Interest: The authors declare that the research was conducted in the absence of any commercial or financial relationships that could be construed as a potential conflict of interest.

Copyright © 2020 Liu, Liang, Lei, Huang, Song, Fang, Li, Li, Mo, Sun, Lv and Liu. This is an open-access article distributed under the terms of the Creative Commons Attribution License (CC BY). The use, distribution or reproduction in other forums is permitted, provided the original author(s) and the copyright owner(s) are credited and that the original publication in this journal is cited, in accordance with accepted academic practice. No use, distribution or reproduction is permitted which does not comply with these terms.

frontiers in Microbiology

MINI REVIEW
published: 25 September 2020
doi: 10.3389/fmicb.2020.556729

Separating the Empirical Wheat From the Pseudoscientific Chaff: A Critical Review of the Literature Surrounding Glyphosate, Dysbiosis and Wheat-Sensitivity

Jacqueline A. Barnett[1] *and Deanna L. Gibson*[1,2]*

[1] Department of Biology, The University of British Columbia, Kelowna, BC, Canada, [2] Department of Medicine, Faculty of Medicine, The University of British Columbia, Kelowna, BC, Canada

OPEN ACCESS

Edited by:
Ana Rivas,
University of Granada, Spain

Reviewed by:
Aymé Spor,
INRA UMR1347 Agroécologie, France
Uri Gophna,
Tel Aviv University, Israel

***Correspondence:**
Deanna L. Gibson
Deanna.Gibson@ubc.ca

Specialty section:
This article was submitted to Food Microbiology, a section of the journal Frontiers in Microbiology

Received: *28 April 2020*
Accepted: *24 August 2020*
Published: *25 September 2020*

Citation:
Barnett JA and Gibson DL (2020) Separating the Empirical Wheat From the Pseudoscientific Chaff: A Critical Review of the Literature Surrounding Glyphosate, Dysbiosis and Wheat-Sensitivity. Front. Microbiol. 11:556729. doi: 10.3389/fmicb.2020.556729

The prevalence of digestive disorders has increased globally, as countries have adopted a more "Westernized" diet pattern. A Western diet, characterized as high in fat and refined carbohydrates, can also be defined as a product of increased technology and industrialization. Modern farmers rely on agrochemicals to meet the needs of a growing population, and these chemicals have shifted the Western diet's chemical composition. While the number of individuals choosing to live a wheat-free lifestyle without a celiac disease diagnosis has increased, clinical trials have shown that gluten from wheat is not responsible for causing symptoms in healthy individuals suggesting that something else is inducing symptoms. The herbicide, glyphosate, is applied to wheat crops before harvest to encourage ripening resulting in higher glyphosate residues in commercial wheat products within North America. Glyphosate inhibits the shikimate pathway, a pathway exclusive to plants and bacteria. Glyphosate's effect on dysbiosis was not considered when making safety recommendations. Here, we evaluate the literature surrounding glyphosate's effects on the gut microbiome and conclude that glyphosate residues on food could cause dysbiosis, given that opportunistic pathogens are more resistant to glyphosate compared to commensal bacteria. However, research on glyphosate's effects on the microbiome suffers from numerous methodological weaknesses, and these limitations make it impossible to draw any definitive conclusions regarding glyphosate's influence on health through alterations in the gut microbiome. In this review, we critically evaluate the evidence currently known and discuss recommendations for future studies.

Keywords: gut microbiome, dysbiosis, glyphosate, Roundup, crop-desiccation, mental health, wheat intolerance, non-celiac gluten sensitivity

DIGESTIVE DISEASES AND CROP DESICCATION

Digestive disorders cost North Americans an estimated $154 billion annually in healthcare costs and lost productivity (Fedorak et al., 2012; Peery et al., 2019). Canada has the highest incidence of digestive diseases in the world, with two-thirds of Canadians suffering from a gastrointestinal condition within a given year (Fedorak et al., 2012). Some of these disorders are chronic inflammatory conditions, including inflammatory bowel disease and celiac disease. However, many digestive disorders plaguing North Americans are non-specific, eluding diagnosis based on any one set of criteria. Over the past decade, North America has seen a growing increase in the number of individuals choosing to live a wheat-free lifestyle in the absence of a celiac disease diagnosis (**Figure 1A**). When surveyed, individuals who abstain from wheat-based foods report experiencing less gastrointestinal discomfort and improved digestive health, reduced inflammation, reduced joint pain, and improved mental health (Health Canada, 2014). Often, individuals attribute the act of going *gluten*-free to their improved health and wellbeing (Niland and Cash, 2018). However, double-blind, randomized clinical trials have implicitly shown that gluten from wheat is not responsible for symptoms in non-celiac and otherwise healthy individuals (Croall et al., 2019). Is it possible that agricultural practices we have embraced in the past two decades are responsible for this dramatic increase in wheat-sensitivity?

One agricultural practice that gained popularity during the 1990s is the desiccation of crops, including wheat. Desiccation refers to the process of applying a chemical to a plant before harvest to kill vegetation. Desiccation corrects for uneven growth and is common in regions where the growing season is short and damp. Cereal grains, including wheat, are particularly prone to uneven ripening resulting in an increased prevalence of desiccation (**Figure 1B**). Glyphosate is a systemic desiccant with broad-spectrum herbicidal action taking weeks to dry crops. However, glyphosate has the added benefit of controlling green weeds and therefore is one of the most commonly used commercial desiccants.

Some European countries, including Italy, have banned the use of glyphosate pre-harvest while others, including France and Germany, plan to ban its use entirely by 2023. North America is one of the most prolific glyphosate users, with over 25 million kilograms purchased annually in Canada (Health Canada, 2012), and over 36 million kilograms applied annually in the United States (Benbrook, 2016). Routine monitoring of 3,188 food-items collected by the Canadian Food Inspection Agency (CFIA) found that 29.7% of items surveyed contained glyphosate residues (Canadian Food Inspection Agency, 2017). Data collected by the CFIA also revealed that pre-harvest application of glyphosate on wheat crops is leading to higher glyphosate residues within the Canadian food supply. Of the 3,188 samples tested, 869 were grain products. In total, 36.6% of the grain-based products tested contained glyphosate residues, and 3.9% contained residues over the maximum limit currently set for cereal crops (Canadian Food Inspection Agency, 2017). To understand the possible implications of these findings and how glyphosate might influence human health, one must first understand its underlying mechanism of action.

GLYPHOSATE TARGETS TYPES OF BACTERIA PRESENT IN THE GUT MICROBIOME

Glyphosate exhibits its herbicidal action through inhibition of the shikimate pathway, a seven-step metabolic pathway where carbon skeletons from carbohydrate metabolism are converted to chorismate. Glyphosate acts as a competitive inhibitor of the enzyme 5-enolpyruvylshikimate-3-phosphate synthase (EPSPS), preventing the synthesis of chorismate. Chorismate is vital for many plant functions, including aromatic amino acid, hormone, and vitamin synthesis. Mammals do not possess the shikimate pathway or any of the enzymes, which is why glyphosate was considered to be non-toxic to humans. However, recent studies have highlighted the potential cytotoxic and carcinogenic effects of glyphosate both *in vivo* and *in vitro* (Van Bruggen et al., 2018). In addition to direct toxicity, it is possible that glyphosate could influence health through secondary means via the gut microbiome, which harbors trillions of microorganisms living as a functional ecosystem. The shikimate pathway is essential for bacterial survival that some organisms have developed glyphosate resistance. Class I EPSPS enzymes are found within all plants and bacteria and are highly sensitive to the effects of glyphosate (Molin, 1998). Class II enzymes have been characterized in a subset of bacteria and are more common in pathogenic species, including *Staphylococcus aureus* and *Streptococcus pneumonia* (Sutton et al., 2016). In the absence of Class II enzymes, some bacteria, including *Escherichia coli*, have developed mutations that mitigate the harmful effects of glyphosate (Cao et al., 2012) and these advantageous mutations appear to be more common in pathogenic isolates (Bote et al., 2019). Commensal bacteria appear to be more susceptible to glyphosate, as they are more likely to possess glyphosate-sensitive Class I EPSPS enzymes than potentially pathogenic bacteria, thereby promoting dysbiosis (**Figure 2A**). Literature often describes gut dysbiosis as an overabundance of opportunistic pathogens, including *E. coli* and *S. aureus*, and this imbalance is associated with increased inflammation (Sannasiddappa et al., 2011; Kittana et al., 2018), obesity (Gao et al., 2015) and altered behavior (Jang et al., 2018). In essence, symptoms that individuals report a reduction in when eliminating wheat from their diet.

When determining glyphosate's toxicity, the highest level that does not produce harmful effects is referred to as the no-observed-effect-level (NOEL) (Reyna, 1985). The acceptable daily intake (ADI) is the amount of glyphosate that can be ingested daily without discernible health risk; (Reyna, 1985) and is determined by dividing the NOEL by a safety factor (commonly 100) (Renwick, 1993). However, different governing bodies may err on the side of caution and use a higher safety factor, leading to an array of ADI values globally. For instance, the Environmental Protection Agency (EPA), the acting executive agency of the United States, has the highest ADI for glyphosate

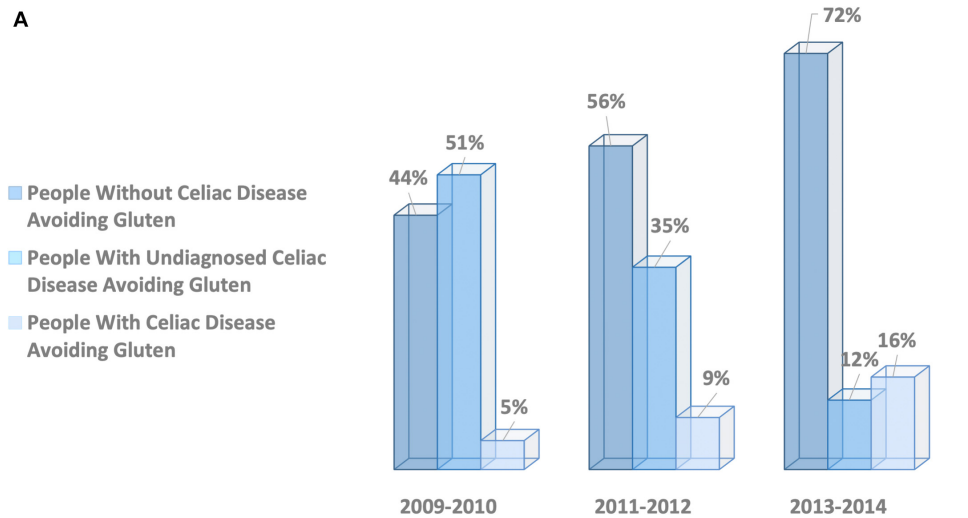

B

	WHEAT	CORN	SOY	CANOLA	OAT
KILOGRAMS OF AI APPLIED PER YEAR	3.9 MILLION	28.8 MILLION	46 MILLION	227,000	45,000
MAXIMUM RESIDUE LIMIT IN NORTH AMERICA	5MG/KG	3MG/KG	N/A	20MG/KG	15MG/KG
AMOUNT CONSUMED BY CANADIANS EVERY YEAR	66.8 KG	2.5 KG	1.7 KG	4.5KG	<1 KG

FIGURE 1 | (A) Over the past decade, more North Americans are choosing to exclude wheat from their diet, citing health benefits in the absence of a celiac disease diagnosis. North America has seen a growing increase in the number of individuals adopting a gluten-free diet in the absence of a celiac disease diagnosis. Data obtained from the National Health and Nutrition Examination Survey. Data presented as percentage of respondents (Choung et al., 2017). **(B)** Summary of maximum residue limits allowed for glyphosate on the five most consumed food crops in North America (Health Canada, 2015).

globally, currently set at 1.75 mg/kg body weight/day (Mao et al., 2018). For comparison, the ADI established by Europe and Canada is 0.5 mg and 0.3 mg/kg body weight/day (Nielsen et al., 2018), respectively. However, only direct glyphosate toxicity was considered when determining the NOEL. Alarmingly, glyphosate's influence over health through secondary means, such as the gut microbiome, was never considered. Given that the gut microbiome is critical for our overall health and disease susceptibility, glyphosate residues on wheat may contribute to dysbiosis, thereby affecting our overall health. To understand the secondary effects of glyphosate on human health through dysbiosis, we reviewed the literature and critically evaluated the evidence surrounding glyphosate's effects on the gut microbiome. Given the magnitude of the EPA dose compared to other countries, any study using a dose higher than the EPA's ADI will be referred to as "high-dose."

GLYPHOSATE EXPOSURE INDUCES GUT DYSBIOSIS

All bacteria contain glyphosate-sensitive Class I EPSPS enzymes; however, the degree to which bacteria succumb to its effect differs considerably. Opportunistic pathogens in the gut, are more likely to contain Class II EPSPS enzymes that are resistant to glyphosate. Studies using high-dose glyphosate exposure drives dysbiosis increasing opportunistic pathogens, including members of the phyla Fusobacteria (Tang et al., 2020).

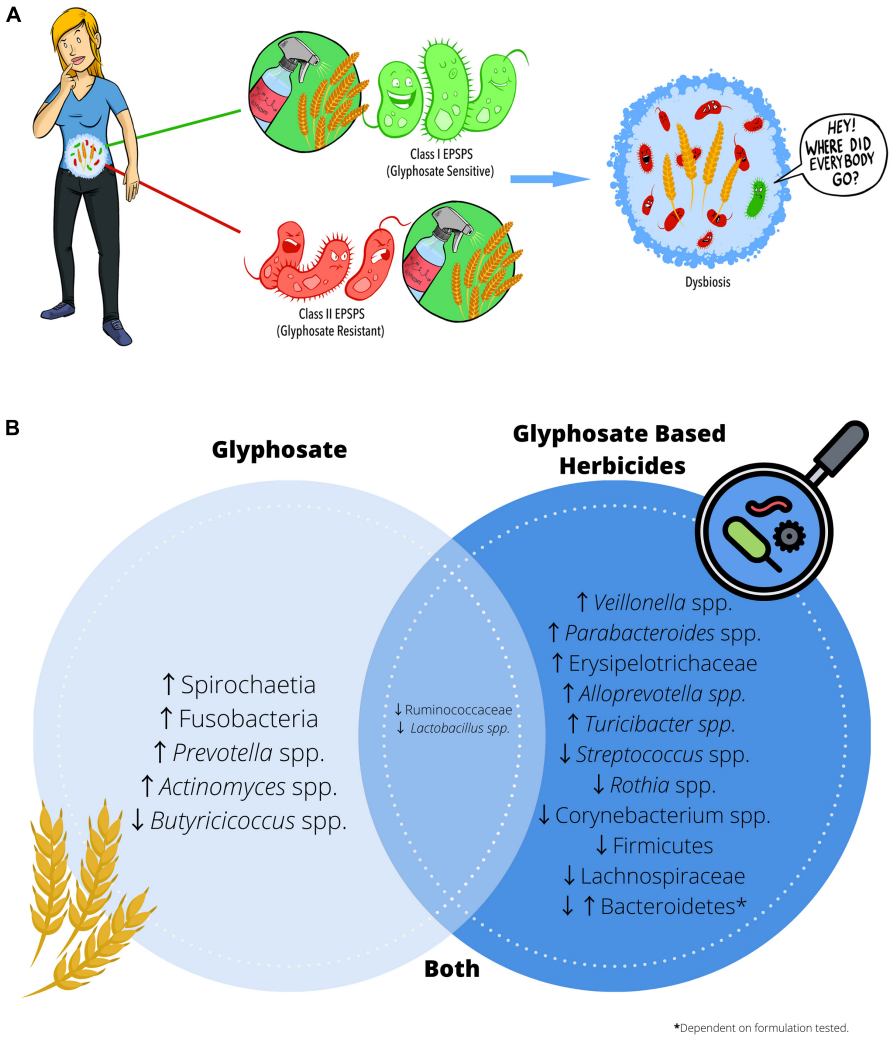

FIGURE 2 | Glyphosate residues present on food may cause intestinal dysbiosis. **(A)** Glyphosate exhibits its herbicidal action through inhibition of the shikimate pathway enzyme EPSPS. Class I EPSPS are sensitive to the effects of glyphosate and are found in all plants and bacteria. However, glyphosate resistant EPSPS (Class II) appear to be more prevalent in opportunistic pathogens and may contribute to dysbiosis. **(B)** Summary of the alterations in microbial composition reported in the literature when administering either glyphosate or glyphosate-based herbicides.

The phylum Fusobacteria contains both commensal organisms and pathogenic species; however, an increased abundance of Fusobacteria has been associated with the development of colorectal cancer (Park et al., 2016). High-dose glyphosate exposure has also been correlated with increases in other bacterial groups, including *Prevotella* spp. and *Actinomyces* spp. (Mao et al., 2018). An increased abundance of rod-shaped bacteria including, *Prevotella* spp. (Lerner et al., 2017), and *Actinomyces* spp. (Ou et al., 2009) is a potential risk factor in celiac disease development in susceptible individuals. These findings suggest that high-dose glyphosate exposure may promote opportunistic pathogen expansion in the gut microbiome.

The extinction of commensal bacteria also contributes to gut dysbiosis. Indeed, animal studies examining the impact of glyphosate on the microbiome at doses ranging from 5 mg–500 mg/kg body weight/day have shown that glyphosate decreases bacterial species commonly hypothesized to be beneficial, including *Lactobacillus* spp. (Mao et al., 2018) and *Butyricicoccus* spp. (Dechartres et al., 2019). *Lactobacillus* spp. constitutes a significant component of the human microbiota in several sites throughout the digestive tract, including stomach, duodenum and jejunum (Walter, 2008). *Lactobacillus* spp. tend to exhibit a mutualistic relationship with humans by protecting against pathogenic infections in exchange for nutrients from their human host. As its name implies, members of the genus *Butyricicoccus* spp. are significant producers of the short-chain fatty acid butyrate, which is essential in the maintenance of gastrointestinal health through inhibition of pro-inflammatory pathways and the reduction of oxidative stress within the colon (Canani et al., 2011). Butyrate is also the primary energy source of colonic epithelial cells, and adequate levels aid in maintaining barrier function (Konig et al., 2016). A failure

to maintain barrier function homeostasis has been implicated in chronic inflammation (Canani et al., 2011; Konig et al., 2016), and high-dose glyphosate exposure causes higher levels of pro-inflammatory cytokines including IL-1β, IL-6 and TNF-α in addition to increased transcription of mitogen-activated protein (MAP) kinase and nuclear factor kappa-light-chain-enhancer of activated B cells (NF-kB) within the small intestine (Mao et al., 2018). In addition to increasing inflammation and oxidative stress, reduced butyrate levels influence intestinal motility (Walter, 2008), which has been associated with a host of digestive symptoms including abdominal pain, diarrhea and reflux (Martinucci et al., 2014). While these studies suggest that glyphosate alone may induce dysbiosis, in practice, crops are sprayed with glyphosate-based herbicides (GBH), which contain many additives in addition to glyphosate. These additives, alone or combined with glyphosate, could have differential effects on bacterial communities present within the gut.

COMMERCIAL HERBICIDE ADJUVANTS FURTHER DRIVE DYSBIOSIS

The literature has shown that some bacterial communities that are resistant to glyphosate exposure are less able to withstand commercial herbicide exposure. Indeed, glyphosate and GBH share some similarities, like decreases in *Lactobacillus spp*. (Mao et al., 2018; Tang et al., 2020). However, the differences in microbial composition observed with GBH exposure are dependent on the formulation tested. For example, exposure to the herbicide R Grand Travaux Plus® results in a significant increase in the Bacteroidetes phyla (Lozano et al., 2018). Whereas exposure to the glyphosate-based herbicide Roundup® resulted in a significant *decrease* in Bacteroidetes (Aitbali et al., 2018). Bacteroidetes are considered one of the most stable phyla of the gastrointestinal bacteriome, and they serve a broad range of metabolic functions for their host. A reduction in Bacteroidetes has been shown to be associated with obesity (Koliada et al., 2017), whereas an overabundance has been associated with irritable bowel syndrome (Pittayanon et al., 2019). There were other notable differences observed between commercial formulations. Exposure to Roundup 3Plus® resulted in significant decreases in Lachnospiraceae and increased Erysipelotrichaceae (Dechartres et al., 2019). Lachnospiraceae has been shown to be protective against colon cancer in humans through its production of butyric acid (Meehan and Beiko, 2014). In contrast, the increased abundance of Erysipelotrichaceae has been implicated in the development of colon cancer (Kaakoush, 2015). These findings suggest that herbicide adjuvants may induce alterations to the gut microbiome and may have a synergistic effect when used in combination with glyphosate. However, it is essential to note that the range of doses examined varied considerably, with some studies using relatively small amounts [50 ng/L (Lozano et al., 2018)] to enormous doses [500 mg/kg body weight (Tang et al., 2020)] to elicit a response. An interesting theme in the literature is that the deleterious effects of both glyphosate and GBH do not appear to be dose-dependent. To truly understand the potential implications of glyphosate exposure on the gut microbiome and human health, it is vital to examine doses that have been previously deemed safe for human exposure.

PRE AND POST-NATAL GLYPHOSATE AND GLYPHOSATE-BASED HERBICIDE EXPOSURE MAY INFLUENCE EARLY MICROBIOME DEVELOPMENT

Early-life exposure to EPA approved levels of glyphosate or GBH, results in significant changes to the developing neonatal microbiome in a mouse model (Mao et al., 2018). While pregnant dams exposed to glyphosate or the herbicide Roundup® did not display dysbiosis, pups exposed during gestation and throughout weaning showed altered gut microbiome diversity, including reductions in *Lactobacillus* and an increase in Bacteroidetes (*Prevotella* spp.) (Mao et al., 2018). Pups exposed to Roundup® also had alterations to other communities, including a reduction in *Streptococcus* spp., and *Rothia* spp., and increases in *Veillonella* spp., as well as *Parabacteroides* spp., (Mao et al., 2018) again highlighting the possible additive effects of GBH formulations. Given the neonatal gut microbiome plays such a critical role in immune development and tolerance (Mazmanian and Round, 2009) the dysbiosis caused by glyphosate could have catastrophic consequences for immunity. Indeed, subspecies of the *Rothia* genus have been identified as playing a critical role in the degradation of gluten within the mouth and upper gastrointestinal tract (Zamakhchari et al., 2011). Gluten proteins are difficult to digest by mammalian proteolytic enzymes and recent studies have highlighted microorganism derived enzymes which aid in breaking down these proteins (Zamakhchari et al., 2011). *Rothia* spp., contain not only the enzymes necessary for protein degradation but also have enzymes that target the immunogenic epitopes that play a crucial role in celiac disease (Zamakhchari et al., 2011). These findings suggest that exposure to glyphosate, either alone or in a commercial preparation, at doses previously deemed safe for human health, may have profound effects on microbiome development and may be an environmental trigger in the development of celiac disease.

GLYPHOSATE AND GLYPHOSATE-BASED HERBICIDE EXPOSURE MAY ALTER BEHAVIOR THROUGH CHANGES IN THE GUT MICROBIOME

While there are many consequences to glyphosate-induced dysbiosis, one of the more pressing effects may be on our mental health. Recent studies show that dysbiosis can affect the gut-brain axis (Carabotti et al., 2015) a bidirectional communication system between the central nervous system and the gastrointestinal tract (Martinucci et al., 2014). Exposure to Roundup 3Plus® during pregnancy significantly increased the abundance of *Turicibacter* spp., (Dechartres et al., 2019) which, in combination with Clostridiaceae, plays a critical role in the modulation of gut-derived serotonin (Reigstad et al., 2015).

Serotonin is a monoamine neurotransmitter that elicits effects locally within the gastrointestinal tract regulating intestinal movements and secretion (Reigstad et al., 2015). Serotonin is also a key neurotransmitter in the gut-brain-microbiome axis (O'Mahony et al., 2015) and the intricate crosstalk between the gut microbiome and altered serotonergic neurotransmission have implications for mood and behavior (Fung et al., 2019). Indeed, pregnant dams exposed to either glyphosate alone or the herbicide Roundup 3Plus®, displayed altered licking behavior toward their pups and abnormal brain pathology (Dechartres et al., 2019). Exposure to Roundup® is associated with increased anxiety and depression-like behaviors in mice, correlated with decreases in *Corynebacterium* spp., Firmicutes (*Lactobacillus* spp.) and Bacteroidetes (Aitbali et al., 2018). Research focused on the gut-brain-microbiome axis is in its infancy, and much remains unknown in this rapidly developing field. However, given that mood disorders are often comorbidities associated with digestive diseases, understanding the implications ubiquitous environmental toxins, including glyphosate, may have on the gut microbiome and behavior is of vital importance.

SHEAFING IT TOGETHER

Over the past two decades, there has been a dramatic increase in the number of individuals reporting beneficial health effects when eliminating wheat from their diets. Exposure to glyphosate alone or through the administration of herbicide appears to promote gut dysbiosis through a reduction in commensal bacteria species, including *Lactobacillus* spp., (Aitbali et al., 2018; Mao et al., 2018; Tang et al., 2020) and butyrate-producing bacteria (Dechartres et al., 2019) and an increase in opportunistic pathogens (Mao et al., 2018; Dechartres et al., 2019; Tang et al., 2020). This imbalance may be due to the presence of glyphosate-resistant class II EPSPS enzymes which appear to be more common in opportunistic pathogens. However, the sequence of class II EPSPS enzymes appear to be unique to the particular strain they are isolated from (i.e., CP4 EPSPS, Ab EPSPS) and many Class II enzymes remain uncharacterized. The dysbiosis induced by glyphosate appears to favor several disease phenotypes including inflammation, (Kittana et al., 2018; Tang et al., 2020) reflux-disease, (Martinucci et al., 2014) obesity (Koliada et al., 2017) and colon cancer, (Park et al., 2016) and may be an important environmental trigger in the etiology of celiac disease through alterations in gluten-neutralizing bacteria (Mao et al., 2018) or the over-abundance of rod-shaped bacteria (Ou et al., 2009; Lerner et al., 2017). The effects of glyphosate on the gut microbiome can have systemic consequences through modulation of the serotonergic system which may have implications for behavior and could play a role in the development of mood disorders including anxiety and depression (Aitbali et al., 2018). Glyphosate may also have ramifications for early microbiome development when exposed both pre and postnatally (Mao et al., 2018).

While the current review focused on the agricultural practice of desiccating wheat, it should be noted that many crops, including legumes, corn, and soy, have been shown to contain high glyphosate residues due to desiccation and the advancement of glyphosate-resistant crops. Eliminating wheat from one's diet does not guarantee the elimination of glyphosate exposure. However, wheat products have been shown in independent testing to contain higher residues post-processing (Canadian Food Inspection Agency, 2017) and make up a significant portion of the average North American's dietary glyphosate exposure. Future studies examining other popular diet patterns, including gluten-free, ketogenic, paleo and the Mediterranean diet pattern, may offer unique insight with regards to dietary glyphosate exposure.

Research surrounding glyphosate's effect on the gut microbiome has yielded conflicting results, with studies suggesting glyphosate has a limited impact on the gut microbiome (Nielsen et al., 2018) and others claiming it has extensive, detrimental effects (Aitbali et al., 2018; Lozano et al., 2018; Mao et al., 2018; Dechartres et al., 2019; Tang et al., 2020). How can there be so much variation in the data? Research examining glyphosate's impact on gut health has primarily suffered from two major methodological flaws. First, dose matters – too much of anything, whether it be water or aspirin – has the potential to be detrimental to one's health. Research surrounding glyphosate's effects on gut health often use exaggeratedly high doses compared to what the average North American is exposed to through diet. Some studies promote the ADI as a physiologically relevant dose, however most ADI's for glyphosate are much higher than what the average individual is exposed to through diet alone. Future studies examining dietary levels of glyphosate exposure on the gut microbiome are warranted to determine the actual risk of glyphosate induced dysbiosis. The second weakness has to do with the formulation. While glyphosate is the active ingredient, food crops are desiccated with GBH, which contain compounds in addition to glyphosate. Complicating matters further is the fact that most GBH are proprietary and their ingredients and the relative percentages are unknown. This ambiguity poses a significant challenge for researchers as they do not know what they're working with, the amount present and the synergistic effects of these chemicals when combined. Additionally, crops are often treated with a proverbial "cocktail" of agrochemicals, including other herbicides, in addition to glyphosate and GBH. The cytotoxic effects of glyphosate appear to increase when combined with other herbicides, including Paraquat (Gunatilake et al., 2019). This synergistic phenomenon suggests that relatively low glyphosate residues within our food supply could have serious consequences when combined with other commonly used agrochemicals. Moreover, this synergistic phenomenon has never been studied on the composition of the gut microbiome.

Arguably, the best way to determine the effect of desiccated crops on the microbiome would be to examine the effects of consuming commercially available desiccated and non-desiccated crops on the microbiome composition. The duration of the experimental intervention may also have profound implications for microbial diversity. The studies included in the current review had exposure durations ranging from 2 weeks (Nielsen et al., 2018) to 2 years (Lozano et al., 2018) with the former reporting no significant alterations to the composition of the microbiome, even at doses of 25 mg/kg body weight/day (Nielsen et al., 2018). Often, the first foods introduced to infants

are wheat and grain-based and, in the absence of intolerance, we continue eating wheat-based foods for the duration of our lives, meaning chronic glyphosate exposure throughout life. Studies have even suggested that certain taxa present within the gut microbiome are heritable (Goodrich et al., 2014; Beaumont et al., 2016) signifying that the effects of glyphosate exposure could be inherited and even compounded over time. Long term, multi-generational animal studies utilizing appropriate dietary exposure levels are necessary for determining the *actual* implications for human health. Furthermore, studies conducted examining the effects of glyphosate on the gut microbiome have only explored healthy populations. In many conditions, including inflammatory bowel disease and celiac disease, there is a combination of environmental and biological factors that culminate in the etiology of disease. Additionally, all studies included in this review are rodent studies. While mice are an invaluable tool in microbiome research, there are some dissimilarities in the composition of the gastrointestinal tract and mouse microbiome compared to that of a human. Future correlative studies examining the microbial composition of pesticide workers or individuals consuming a predominantly organic diet may shed light on the actual risk posed to humans. However, given how ubiquitous glyphosate is within the North American landscape, it would likely be impossible to find a true glyphosate-free control for comparison.

CONCLUSION

Glyphosate exposure, either through active ingredient alone or commercial herbicide formulations, has the potential to induce dysbiosis by creating an imbalance between commensal members of the gastrointestinal microbiome and opportunistic pathogens. Glyphosate may be a critical environmental trigger in the etiology of several disease states associated with dysbiosis, including celiac disease, inflammatory bowel disease and irritable bowel syndrome. Glyphosate exposure may also have consequences for mental health, including anxiety and depression, through alterations in the gut microbiome. However, the research surrounding glyphosate's effects on the gut microbiome also suffers from numerous methodological weaknesses including artificially high-doses, insufficient duration, proprietary ingredients and an over reliance on animal models. Future long-term studies examining physiologically relevant doses in both healthy and genetically susceptible populations are warranted to determine the real risk posed to human health.

AUTHOR CONTRIBUTIONS

JB critically reviewed and summarized all literature, drafted the figures and the manuscript. DG conceived of the study with insights from JB, provided oversight, supervised the project, and critically evaluated the manuscript. JB and DG edited the manuscript and approved the final version. Both authors contributed to the article and approved the submitted version.

FUNDING

JB is funded by a PGS-D from the Natural Sciences and Engineering Research Council (NSERC.) DG is funded by Crohn's and Colitis Canada, NSERC and the Michael Smith Foundation for Health Research.

ACKNOWLEDGMENTS

We thank Dr. M. Hart for thoughtful discussions and ideas contributing to this project and Kevin Fraser for the artwork featured in **Figure 2A**.

REFERENCES

Aitbali, Y., Ba-M'hamed, S., Elhidar, N., Nafis, A., Soraa, N., and Bennis, M. (2018). Glyphosate based herbicide exposure affects gut microbiota, anxiety anddepression-like behaviors in mice. *Neurotoxicol. Teratol.* 67, 44–49. doi: 10.1016/j.ntt.2018.04.002

Beaumont, M., Goodrich, J. K., Jackson, M. A., Yet, I., Davenport, E. R., Vieira-Silva, S., et al. (2016). Heritable components of the human fecal microbiomeare associated with visceral fat. *Genome Biol.* 17:189. doi: 10.1186/s13059-016-1052-7

Benbrook, C. M. (2016). Trends in glyphosate herbicide use in the united states andglobally. *Environ. Sci. Eur.* 28, 1–15. doi: 10.1186/s12302-0160070-0

Bote, K., Pöppe, J., Merle, R., Makarova, O., and Roesler, U. (2019). Minimum inhibitoryconcentration of glyphosate and of a glyphosate-containing herbicide formulationfor *Escherichia coli* isolates - differences between pathogenic and non-pathogenicisolates and between host species. *Front. Microbiol.* 10:932. doi: 10.3389/fmicb.2019.00932

Canadian Food Inspection Agency (2017). *Safeguarding with Science: GlyphosateTestingin 2015-2016*. Ottawa: Canadian Food Inspection Agency.

Canani, R. B., Costanzo, M. D., Leone, L., Pedata, M., Meli, R., and Calignano, A. (2011). Potential beneficial effects of butyrate inintestinal and extraintestinal diseases. *World J. Gastroenterol.* 17, 1519–1528. doi: 10.3748/wjg.v17.i12.1519

Cao, G., Liu, Y., Zhang, S., Yang, X., Chen, R., Zhang, Y., et al. (2012). A novel5 enolpyruvylshikimate-3-phosphate synthase shows high glyphosate tolerance in *Escherichia coli* and tobacco plants. *PLoS One* 7:e38718. doi: 10.1371/journal.pone.0038718

Carabotti, M., Scirocco, A., Maselli, M. A., and Severi, C. (2015). The gut-brain axis:Interactions between enteric microbiota, central and enteric nervous systems. *Ann. Gastroenterol.* 28, 203–209.

Choung, R. S., Unalp-Arida, A., Ruhl, C. E., Brantner, T. L., Everhart, J. E., and Murray, J. A. (2017). Less hidden celiac disease but increased gluten avoidance withouta diagnosis inthe united states: findings from the national health and nutritionexamination surveys from 2009 to 2014. *Mayo Clin. Proc.* 92:30. doi: 10.1016/j.mayocp.2016.10.012

Croall, I. D., Aziz, I., Trott, N., Tosi, P., Hoggard, N., and Sanders, D. S. (2019). Glutendoes not induce gastrointestinal symptoms in healthy volunteers: a double-blindrandomized placebo trial. *Gastroenterology* 157, 881–883. doi: 10.1053/j.gastro.2019.05.015

Dechartres, J., Pawluski, J. L., Gueguen, M., Jablaoui, A., Maguin, E., Rhimi, M., et al. (2019). Glyphosate and glyphosate-based herbicide exposureduring the peripartum period affects maternal brain plasticity, maternal behaviourand microbiome. *J. Neuroendocrinol.* 31:e12731. doi: 10.1111/jne.12731

Fedorak, R. N., Switzer, C. M., and Bridges, R. J. (2012). Canadian digestive healthfoundation public impact series. *Can. J. Gastroenterol.* 26, 350–352. doi: 10.1155/2012/384787

Fung, T. C., Vuong, H. E., Luna, C. D. G., Pronovost, G. N., Aleksandrova, A. A., Riley, N. G., et al. (2019). Intestinal serotonin and fluoxetine exposuremodulate bacterial colonization in the gut. *Nat. Microbiol.* 4:20642073. doi: 10.1038/s41564-019-0540-4

Gao, X., Jia, R., Xie, L., Kuang, L., Feng, L., and Wan, C. (2015). Obesity in school-agedchildren andits correlation with gut *E.coli* and bifidobacteria: a case-controlstudy. *BMC Pediatr.* 15:64. doi: 10.1186/s12887-015-0384-x

Goodrich, J. K., Waters, J. L., Poole, A. C., Sutter, J. L., Koren, O., Blekhman, R., et al. (2014). Human genetics shape the gut microbiome. *Cell* 159:789799. doi: 10.1016/j.cell.2014.09.053

Gunatilake, S., Seneff, S., and Orlando, L. (2019). Glyphosate's synergistic toxicity incombination with other factors as a cause of chronic kidney disease of unknownorigin. *Int. J. Environ. Res. Public Health* 16:2734. doi: 10.3390/ijerph16152734

Health Canada (2015). *Maximum Residue Limits for Pesticides Database*. Available online at: https://pr-rp.hcsc.gc.ca/mrl-lrm/index-eng.php.

Health Canada (2012). *Pest Control Products Sales Report for 2012*. Ottawa, ON: Health Canada.

Health Canada (2014). *"Gluten Free" Claims in the Marketplace*. Ottawa, ON: Health Canada.

Jang, H., Lee, K., Lee, H., and Kim, D. (2018). Immobilization stress-induced *Escherichia coli* causes anxiety by inducing NF-κB activation through gut microbiotadisturbance. *Sci. Rep.* 8, 13897–13914. doi: 10.1038/s41598-018-31764-0

Kaakoush, N. O. (2015). Insights into the role of erysipelotrichaceae in the humanhost. *Front. Cell. Infect. Microbiol.* 5:84. doi: 10.3389/fcimb.2015.00084

Kittana, H., Gomes-Neto, J. C., Heck, K., Geis, A. L., Segura Muñoz, R. R., Cody, L. A., et al. (2018). Commensal *Escherichia coli* strains can promoteintestinal inflammation via differential interleukin-6 production. *Front. Inimmunol.* 9:2318. doi: 10.3389/fimmu.2018.02318

Koliada, A., Syzenko, G., Moseiko, V., Budovska, L., Puchkov, K., Perederiy, V., et al. (2017). Association between body mass index andFirmicutes/Bacteroidetes ratio in an adult ukrainian population. *BMC Microbiol.* 17:120. doi: 10.1186/s12866-017-1027-1

Konig, J., Wells, J., Cani, P. D., Garcia-Rodenas, C. L., MacDonald, T., Mercenier, A., et al. (2016). Institutionen för medicinska vetenskaper. Human intestinal barrierfunction in health anddisease. *Clin. Transl. Gastroenterol.* 7:e196. doi: 10.1038/ctg.2016.54

Lerner, A., Arleevskaya, M., Schmiedl, A., and Matthias, T. (2017). Microbes and virusesare bugging the gut in celiac disease. are they friends or foes?. *Front. Microbiol.* 8:1392. doi: 10.3389/fmicb.2017.01392

Lozano, V. L., Defarge, N., Rocque, L., Mesnage, R., Hennequin, D., Cassier, R., et al. (2018). Sex-dependent impact of roundup on the rat gutmicrobiome. *Toxicol. Rep.* 5, 96–107. doi: 10.1016/j.toxrep.2017.12.005

Mao, Q., Manservisi, F., Panzacchi, S., Mandrioli, D., Menghetti, I., Vornoli, A., et al. (2018). Theramazzini institute 13-week pilot study on glyphosate and roundup administered at human equivalent dose to sprague dawley rats: effects on themicrobiome. *Environ. Health* 17:5012. doi: 10.1186/s12940-018-0394-x

Martinucci, I., De Bortoli, N., Savarino, E., Franchi, R., Bertani, L., Urbano, M. T., et al. (2014). p.10.26 distal and proximal esophageal impedance basal valuesin patients with nonerosive reflux disease and functional heartburn. *Digest. Liver Dis.* 46:S93. doi: 10.1016/S1590-8658(14)60275-9

Mazmanian, S. K., and Round, J. L. (2009). The gut microbiota shapes intestinal immuneresponses during health and disease. *Nat. Rev. Immunol.* 9:600. doi: 10.1038/nri2614

Meehan, C. J., and Beiko, R. G. (2014). A phylogenomic view of ecological specializationin thelachnospiraceae, a family of digestive tract-associated bacteria. *Genome Biol. Evol.* 6, 703–713. doi: 10.1093/gbe/evu050

Molin, W. T. (1998). Glyphosate, a unique global herbicide. *Weed Technol.* 12:564565. doi: 10.1017/S0890037X0004433X

Nielsen, L. N., Roager, H. M., Casas, M. E., Frandsen, H. L., Gosewinkel, U., Bester, K., et al. (2018). Glyphosate has limited short-term effects on commensalbacterial community composition in the gut environment due to sufficientaromatic amino acid levels. *Environ. Pollut.* 233, 364–376. doi: 10.1016/j.envpol.2017.10.016

Niland, B., and Cash, B. D. (2018). Health benefits and adverse effects of a gluten-free dietin non-celiac disease patients. *Gastroenterol. Hepatol.* 14, 82–91.

O'Mahony, S. M., Clarke, G., Borre, Y. E., Dinan, T. G., and Cryan, J. F. (2015). Serotonin, tryptophan metabolism and the brain-gut-microbiomeaxis. *Behav. Brain Res.* 277, 32–48. doi: 10.1016/j.bbr.2014.07.027

Ou, G., Hedberg, M., Hörstedt, P., Baranov, V., Forsberg, G., and Drobni, M. (2009). Proximal small intestinal microbiota and identification of rod-shapedbacteria associated with childhood celiac disease. *Am. J. Gastroenterol.* 104, 3058–3067. doi: 10.1038/ajg.2009.524

Park, C. H., Han, D. S., Oh, Y., Lee, A., Lee, Y., and Eun, C. S. (2016). Role offusobacteria in the serrated pathway of colorectal carcinogenesis. *Sci. Rep.* 6:25271. doi: 10.1038/srep25271

Peery, A. F., Crockett, S. D., Murphy, C. C., Lund, J. L., Dellon, E. S., Williams, J. L., et al. (2019). Burden and cost of gastrointestinal, liver, and pancreaticdiseases in the united states: update 2018. *Gastroenterology* 156, 254.e11–272.e11. doi: 10.1053/j.gastro.2018.08.063

Pittayanon, R., Lau, J. T., Yuan, Y., Leontiadis, G. I., Tse, F., Surette, M., et al. (2019). Gutmicrobiota in patients with irritable bowel Syndrome—Asystematic review. *Gastroenterology* 157, 97–108. doi: 10.1053/j.gastro.2019.03.049

Reigstad, C. S., Salmonson, C. E., Rainey, J. F. III, Szurszewski, J. H., Linden, D. R., Sonnenburg, J. L., et al. (2015). Gut microbes promote colonicserotonin production through an effect of short-chain fatty acids onenterochromaffin cells. *FASEB J.* 29, 1395–1403. doi: 10.1096/fj.14259598

Renwick, A. G. (1993). Data-derived safety factors for the evaluation of food additivesand environmental contaminants. *Food Additives Contaminants* 10:275. doi: 10.1080/02652039309374152

Reyna, M. (1985). *Twelve-Month Study of Glyphosate Administered by Gelatin Capsule to Beagledogs*. Unpublished Report no. 830116, project no. ML-83-13, submittedto U.S.Environmental Protection Agency by Monsanto Company EnvironmentalHealth. Reregistration Eligibility Decision (RED) Glyphosate; EPA-738-F-93011. Washington, DC: U. S. Environmental Protection Agency.

Sannasiddappa, T. H., Costabile, A., Gibson, G. R., and Clarke, S. R. (2011). The influenceof staphylococcus aureus on gut microbial ecology in an in vitro continuousculture humancolonicmodel system. *PLoS One* 6:e23227. doi: 10.1371/journal.pone.0023227

Sutton, K. A., Breen, J., Russo, T. A., Schultz, L. W., and Umland, T. C. (2016). Crystal structure of 5-enolpyruvylshikimate-3-phosphate (EPSP)synthase from the ESKAPE pathogen *Acinetobacter baumannii*. *Acta Crystallogr. Sect. F* 72, 179–187. doi: 10.1107/S2053230X16001114

Tang, Q., Tang, J., Ren, X., and Li, C. (2020). Glyphosate exposure induces inflammatoryresponses in the small intestine and alters gut microbial composition inrats. *Environ. Pollut.* 261:114129. doi: 10.1016/j.envpol.2020.114129

Van Bruggen, A. H. C., He, M. M., Shin, K., Mai, V., Jeong, K. C., Finckh, M. R., et al. (2018). Environmental and health effects of the herbicideglyphosate. *Sci. Total Environ.* 616-617, 255–268. doi: 10.1016/j.scitotenv.2017.10.309

Walter, J. (2008). Ecological role of lactobacilli in the gastrointestinal tract: implicationsfor fundamental and biomedical research. *Appl. Environ. Microbiol.* 74, 4985–4996. doi: 10.1128/aem.00753-08

Zamakhchari, M., Wei, G., Dewhirst, F., Lee, J., Schuppan, D., Oppenheim, F. G., et al. (2011). Identification of rothia bacteria as gluten-degradingnatural colonizers of the upper gastro-intestinal tract. *PLoS One* 6:e24455. doi: 10.1371/journal.pone.0024455

Conflict of Interest: The authors declare that the research was conducted in the absence of any commercial or financial relationships that could be construed as a potential conflict of interest.

Copyright © 2020 Barnett and Gibson. This is an open-access article distributed under the terms of the Creative Commons Attribution License (CC BY). The use, distribution or reproduction in other forums is permitted, provided the original author(s) and the copyright owner(s) are credited and that the original publication in this journal is cited, in accordance with accepted academic practice. No use, distribution or reproduction is permitted which does not comply with these terms.

frontiers in Microbiology

REVIEW
published: 30 November 2020
doi: 10.3389/fmicb.2020.578007

Endobolome, a New Concept for Determining the Influence of Microbiota Disrupting Chemicals (MDC) in Relation to Specific Endocrine Pathogenesis

Margarita Aguilera[1,2], Yolanda Gálvez-Ontiveros[3] and Ana Rivas[2,3]*

[1] Department of Microbiology, Faculty of Pharmacy, University of Granada, Granada, Spain, [2] Instituto de Investigación Biosanitaria ibs.GRANADA, Granada, Spain, [3] Department of Nutrition and Food Science, Faculty of Pharmacy, University of Granada, Granada, Spain

OPEN ACCESS

Edited by:
Katia Sivieri,
São Paulo State University, Brazil

Reviewed by:
Nico Jehmlich,
Helmholtz Centre for Environmental Research (UFZ), Germany
Natasa Golic,
University of Belgrade, Serbia

***Correspondence:**
Yolanda Gálvez-Ontiveros
yolandagalvez@ugr.es

Specialty section:
This article was submitted to Microbial Symbioses, a section of the journal Frontiers in Microbiology

Received: *01 July 2020*
Accepted: *04 November 2020*
Published: *30 November 2020*

Citation:
Aguilera M, Gálvez-Ontiveros Y and Rivas A (2020) Endobolome, a New Concept for Determining the Influence of Microbiota Disrupting Chemicals (MDC) in Relation to Specific Endocrine Pathogenesis. Front. Microbiol. 11:578007. doi: 10.3389/fmicb.2020.578007

Endogenous steroid hormones and Endocrine Disrupting Chemicals (EDC) interact with gut microbiota through different pathways. We suggest the use of the term "endobolome" when referring to the group of gut microbiota genes and pathways involved in the metabolism of steroid hormones and EDC. States of dysbiosis and reduced diversity of the gut microbiota may impact and modify the endobolome resulting at long-term in the development of certain pathophysiological conditions. The endobolome might play a central role in the gut microbiota as seen by the amount of potentially endobolome-mediated diseases and thereby it can be considered an useful diagnostic tool and therapeutic target for future functional research strategies that envisage the use of next generation of probiotics. In addition, we propose that EDC and other xenobiotics that alter the gut microbial composition and its metabolic capacities should be categorized into a subgroup termed "microbiota disrupting chemicals" (MDC). This will help to distinguish the role of contaminants from other microbiota natural modifiers such as those contained or released from diet, environment, physical activity and stress. These MDC might have the ability to promote specific changes in the microbiota that can ultimately result in common intestinal and chronic or long-term systemic diseases in the host. The risk of developing certain disorders associated with gut microbiota changes should be established by determining both the effects of the MDC on gut microbiota and the impact of microbiota changes on chemicals metabolism and host susceptibility. In any case, further animal controlled experiments, clinical trials and large epidemiological studies are required in order to establish the concatenated impact of the MDC-microbiota-host health axis.

Keywords: microbiota, endocrine disrupting chemicals, endobolome, hormones, endocrine pathogenesis, microbiota disrupting chemicals

INTRODUCTION

The effects of the bidirectional between steroid hormones and gut microbiota on the development of diseases have been recently reported (Kwa et al., 2016; Bajer et al., 2017). Hormones can have an impact on the composition and metabolism of the microbiota. In turn, the gut microbiome is highly involved in hormone homeostasis through a number of possible mechanisms. The concept "microgenderome" refers to the role of sex differences in gut microbiota in relation to the incidence and comorbidity of certain diseases (Mulak et al., 2014). An interesting example of gut microbiome/hormones interactions is the role of sex in type 1 diabetes found in a non-obese diabetic mouse model that revealed that exposure of female mice to androgens protected them from the disease (Fox, 1992; Markle et al., 2013), which suggests the role played by sex-specific interactions in disease development. The way this modulation affects hormone metabolism, physiology, and pathophysiology is still unclear. The gut microbiome can also modify hormone levels in the host by participating in hormone biotransformation. A key triad of sex hormones, host genotypic and phenotypic responses, and gut microbiome has been proposed (Rosenfeld, 2017).

Previous research works have dealt with the effects of diet, exercise and antibiotic use on host gut microbiome (Munyaka et al., 2014; Murphy et al., 2015; Xu and Knight, 2015; Zhang and Yang, 2016; Singh et al., 2017), but the effects of exposure to exogenous chemicals on the microbiota have been poorly investigated (Hu et al., 2016). Among these environmental contaminants, the Endocrine Disrupting Chemicals (EDC) have been recently defined by the Endocrine Society as: "an exogenous [non-natural] chemical, or mixture of chemicals, that interferes with any aspect of hormone action" (Zoeller et al., 2016). This interference with the endocrine system may result in biological, physical and metabolic disturbances in humans. EDC can bioaccumulate up the food chain and in the environment and that have been detected in humans worldwide. These chemicals include dioxins, pesticides, pyrethroids, polychlorinated biphenyls (PCBs), flame retardants and, antibacterial such as triclosan (García-Mayor et al., 2012; Darbre, 2017; Galvez-Ontiveros et al., 2020), plant derived compounds found such as phytoestrogens and plasticizers such as phthalates and bisphenol A (BPA). Exposure to EDC might result in marked disturbances in the gut microbiome, which in turn lead to widespread disruptions in several host systems and damage of the commensal bacteria in the host gut (Rosenfeld, 2017). However, the association between misbalanced microbiota diversity or dysbiosis and possible biological mechanisms responsible for the development of certain diseases in different environmental exposure settings remains largely unknown (Hu et al., 2016).

The term "estrobolome" was previously used to describe the gut microbiota genes involved in the synthesis of estrogen-metabolizing enzymes (Plottel and Blaser, 2011). We now suggest the use of the term "endobolome" when referring to the group of gut microbiota genes and pathways involved not only in the synthesis of estrogens, but also in the metabolism of other steroid hormones and endocrine disruptor chemicals. States of dysbiosis and reduced diversity of the gut microbiota may impact and modify the endobolome resulting at long-term in the development of certain pathophysiological conditions. The reduction in the diversity of microbial communities' composition and inflammation could decrease the enzymatic activity which, sequentially, decreases the metabolization of hormones and EDC into their modified, active or inactive and circulating metabolites. This reduced availability of circulating hormones and EDC results in changes in hormone receptor activation, which may lead to the development of disorders related to demonstrated hormone deficiencies such as obesity, metabolic syndrome, and cardiovascular and related cognitive dysfunctions. Conversely, endobolome can also stimulate the production of gut microbial enzymes which leads to an increase in circulating hormones which, in turn, increase the risk of diseases related with high serum levels of hormones such as sex-hormone driven cancers.

The relevance of the crosstalk between EDC, hormones and gut microbiota warrants a review of the current information available on the interactions of these chemical disruptors with sex steroid hormones and gut microbiota as well on the role played by these interactions in the development of hormone-related diseases.

ESTROBOLOME	ENDOBOLOME
It described the gut microbiota genes involved in the synthesis of estrogen-metabolizing enzymes (Plottel and Blaser, 2011).	New term to compile the group of gut microbiota genes, pathways and enzymes involved not only in the synthesis of estrogens, but also in the metabolism of other steroid hormones and endocrine disruptor chemicals in cohesion with their impact onto human health/disease balance.

NATURAL HORMONE-GUT MICROBIOME AXIS

Sex-related differences in gut microbome have been found in human and mice experimental models. These differences show a greater alpha diversity in the gut microbiome of women (Falony et al., 2016), and lower abundance of *Clostridia*, *Methanobrevibacter,* and *Desulfovibrio* in men (Falony et al., 2016). As in humans, a larger alpha diversity was found in female mice and a higher relative abundance of *Bacteroidetes* in males (Yurkovetskiy et al., 2013; Kozik et al., 2017).

There is evidence supporting the idea that sex-dependent differences in gut microbiome composition are related to sex steroid hormones (**Table 1**). In this respect, some studies have shown that gut microbiome in women differs from that of men after puberty and that gonadectomy results in disturbances in the microbiome or dysbiosis. For instance, during infancy there were no differences in the microbiota between fraternal twins of the same or different sex. Moreover, in different- or same-sex fraternal twins no differences in gut microbiota were found during childhood, but after puberty significant structural differences in gut microbiome were found in different-sex fraternal twins in comparison with same-sex twins (Yatsunenko et al., 2012). Similar sex-dependent changes were observed in rodent models after puberty (Markle et al., 2013; Yurkovetskiy et al., 2013) and after gonadectomy

TABLE 1 | Studies linking natural hormones, the related diseases and the effects on the microbiota.

References	Animal model	Microbiota location	Dysbiosis/Related condition	Microbiota changes
Studies in animals				
Yuan et al. (2018)	C57BL6 mice	Gut	• Endometriosis induced the dysbiosis.	• Increased *Firmicutes/Bacteroidetes* ratio. • Increased *Bifidobacterium* (phylum *Actionobacteria*).
Bailey and Coe (2002)	Female rhesus monkeys	Gut	• Endometriosis is associated with an altered profile of intestinal microbiota.	• Decreased Lactobacilli. • Increased Gram-negative aerobic and facultative anaerobic bacteria.
Markle et al. (2013)	Diabetic and non-obese diabetic mice	Gut	• Childhood T1D may induce dysbiosis.	• Commensal colonization resulted in increased serum levels of testosterone and protected non-obese diabetic males from T1D. • In young females, the transfer of gut microbiota from adult males resulted in microbiota changes, with increased testosterone and metabolic changes, decreased inflammation of pancreatic islets and autoantibody production, and protection against T1D.
Guo et al. (2016)	Female Sprague-Dawley rats with PCOS	Gut	• PCOS may significantly alter the gut microbiome.	• Decreased *Lactobacillus, Ruminococcus*, and *Clostridium* and increased *Prevotella* were found in PCOS females. For *Bifidobacterium, Escherichia coli, Enterococcus*, and *Bacteroides* there was no significant differences between PCOS females and the control group. • Gut dysbiosis was related to sex hormone levels, estrous cycles and morphological changes in the ovaries.
Kelley et al. (2016)	Female C57BL/6N mice with PCOS	Gut	• PCOS may significantly alter the gut microbiome.	• A significant decrease in the overall species composition and phylogenetic diversity of the gut microbiota, particularly in the relative abundance of *Bacteroidetes* and *Firmicutes*, was observed.
Studies in humans				
Banerjee et al. (2017)	Women	Tumor ovarian tissue and non-tumor ovarian tissue	• Altered microbiome in ovarian tumor tissue.	• Increased *Proteobacteria* and *Firmicutes*. • Decreased *Bacteroidetes, Actinobacteria, Chlamydiae, Fusobacteria, Spirochaetes* and *Tenericutes*. • *Retroviridae, Hepadnaviridae, Papillomaviridae, Flaviviridae, Polyomaviridae* and *Herpesviridae* abound in > 50% of cancer samples. • *Pneumocystis*, *Acremonium, Cladophialophora*, *Malassezia,* and *Microsporidia Pleistophora* were significantly detected in all the ovarian cancer samples screened//in 100% of tumor samples examined.
Sfanos et al. (2018)	Men	Gut	• Prostate cancer hormonal therapy may alter the gut microbiota.	• Decreased alpha diversity in the gut microbiota of prostate cancer patients. • A significant increase in *Akkermansia muciniphila*, *Ruminococcaceae* spp., and *Lachnospiraceae* spp., was found in the fecal samples of prostate cancer patients undergoing oral ATT. Additionally, a significant decrease in the number of sequencing reads belonging to families such as *Brevibacteriaceae*, *Erysipelotrichaceae*, and *Streptococcaceae* was also observed.
Golombos et al. (2018)	Men	Gut	• An alteration of gut microbiota was observed in men with prostate cancer.	• Increased *Bacteriodes massiliensis* in prostate cancer patients versus controls. • Increased *Faecalibacterium prausnitzii* and *Eubacterium rectale* in controls versus prostate cancer patients.
Liu et al. (2017)	Women	Gut	• Disturbances in the gut microbiota of both obese and non-obese women with PCOS compared to non-obese controls.	• Decreased bacterial alpha diversity, increased LPS-producing bacteria, and decreased spore-forming bacteria species. • Increased *Bacteroides* and *Escherichia/Shigella* and decreased *Akkermensia* in obese women with PCOS.
Fuhrman et al. (2014)	Women	Gut	• Higher gut microbiota diversity was found in women with a high hydroxylated estrogens metabolites/parental estrogens ratio in urine.	• The relative abundances of the *Clostridia* class, including the *Clostridiales* order and the *Ruminococcaceae* family, were directly associated with the ratio of metabolites to parental estrogens, while the *Bacteroides* genus was inversely associated with this ratio.

T1D: type 1 diabetes; PCOS: polycystic ovary syndrome; ATT: axis-targeted therapies.

with a reduction in alpha diversity in ovariectomized mice and rats (Moreno-Indias et al., 2016; Choi et al., 2017). Ovariectomized mice showed decreased *Bacteroidetes* and increased *Firmicutes* versus controls (Choi et al., 2017). In male mice reduced *Bacteroidetes* and *Ruminococcaceae* were observed after gonadectomy compared to controls (Harada et al., 2016; Org et al., 2016). Future investigations should examine acute versus long-term effects of gonadectomy (with or without hormone replacement) in rodents and in other species of mammals.

Microbiota, environmental and pathogenic bacteria have the capacity to metabolize steroid hormones and their related metabolites (Garcia-Gomez et al., 2013). Adlercreutz et al. (1984) showed that disturbances in the gut microbiota secondary to antibiotic therapy resulted in an increase in fecal estrogens in women, which suggests the involvement of microbiota in estrogen levels. Lombardi et al. (1978) demonstrated that fecal microbiota may metabolize parent estrogens and their metabolites. Fuhrman et al. (2014) demonstrated that high estrogen metabolites/parent estrogens ratios related to increased microbiota diversity in healthy postmenopausal women. In a mouse model, Markle et al. (2013) showed that early-life changes in gut microbiome result in increased testosterone and metabolic changes that can suppress autoimmune diseases in genetically high-risk animals while preserving fertility.

Gut microbiota can affect circulating levels of hormone metabolites by deconjugation of the conjugated forms secreted in bile and they can be subsequently reabsorbed through the mucosal wall. Fuhrman et al. (2014) showed that estriol, a hydroxylated estradiol metabolite, enters the enterohepatic circulation, and that urinary and fecal levels of estriol and parent estrogens are altered after antibiotic administration. They also suggest that gut microbiota may differentially affect total hormone levels as the association between total hormone and microbiota diversity, which seemed to be stronger for metabolites than for parent hormones. Lastly, they found higher gut microbiota diversity in women with higher levels of hydroxylated estrogen metabolites.

Shin et al. (2019) conducted a study in 31 men and 26 women and reported that sex steroid hormone levels are correlated with gut microbial diversity and composition. In men, they observed that testosterone levels were associated with increased *Acinetobacter*, *Dorea*, *Ruminococcus*, and *Megamonas*. In women, high estrogen levels were associated with increased *Bacteroidetes* and decreased *Firmicutes* phyla. Lastly, a strong association was found between *Slackia* and *Butyricimonas* and estradiol levels.

The essential role played by gut bacteria in hormone metabolism was described decades ago (Janssen and Kersten, 2015). Gut colonization by bacteria in germ-free mice resulted in the regularization of the estrous cycle in females and increased sperm counts in males, which in turn led to the repair of fertility and reproductive capacities (Shimizu et al., 1998). In a cross-sectional study conducted by Fuhrman et al. (2014) that included 60 healthy postmenopausal women, the authors examined the relationship between the composition and diversity of microbiome, assessed trough 16S rRNA gene sequencing, with measurements of urinary levels of estrogens and their metabolites. Authors found a significant correlation between microbiota diversity and the estrogen metabolites/parent estrogens ratio in urine. Moreover, this ratio increased with increased microbial phylogenetic diversity. These findings support the hypothesis that differences in estrogen levels and their metabolism significantly correlate with alterations in gut microbial diversity.

All these studies compiled above revealed significant evidence of hormonal regulation of the microbe-controlling mechanisms, supporting sex differences in microbiota, in addition to sex-specific responses to the same microbiota. The relationship between microbiota, hormones and metabolism seems multi-directional. Collectively, these studies indicate that upcoming investigations into the composition and function of the microbiota must carry on dividing data for sex-differential interactions to understand these complex connections more entirely.

HORMONE-GUT MICROBIOME AXIS

Multidirectional relationships between microbiota, hormones and metabolism. Hormones exert regulation of the microbe-controlling mechanisms, supporting sex differences in microbiota, as well as sex-specific responses to the same microbiota.

The determination of the endobolome experimental parameters may serve as potential biomarkers of certain diseases (**Figure 1**). For example, the determination of β-glucuronidases may help in the identification of some specific bacterial species and, as mentioned above, this enzyme might potentially increase the intestinal reabsorption of endogenous hormones and EDC. Microbial β-glucuronidases will process endogenous molecules like β-glucuronides of hormones and exogenous β-glucuronides from the diet by enabling these compounds to bind to hormone receptors and subsequently produce their physiological effects (Baker et al., 2017). Phytoestrogens also exert their activity via mechanisms involving hormonal receptors. As mentioned above, increased estrogen metabolites correlate with increased microbiota diversity versus parent hormones in fecal samples (Fuhrman et al., 2014). Additionally, a higher parent hormones/hormone metabolites ratio correlates with an increased risk of breast cancer (Samavat and Kurzer, 2015), obesity and other metabolic diseases (Chen and Madak-Erdogan, 2016).

Interestingly, androgens also play a central role in sexual physiology, and disturbances in their action are associated with the development of different conditions in both men and women. Collden et al. (2019) demonstrated that glucuronidases produced by the cecal microbiota can degrade the high content of testosterone and dihydrotestosterone found in the small intestine. The high content of free or unconjugated dihydrotestosterone found in the colon of healthy young mice of both sexes and men suggests that gut microbiota might be involved in the metabolism of intestinal androgens and can therefore affect the risk of

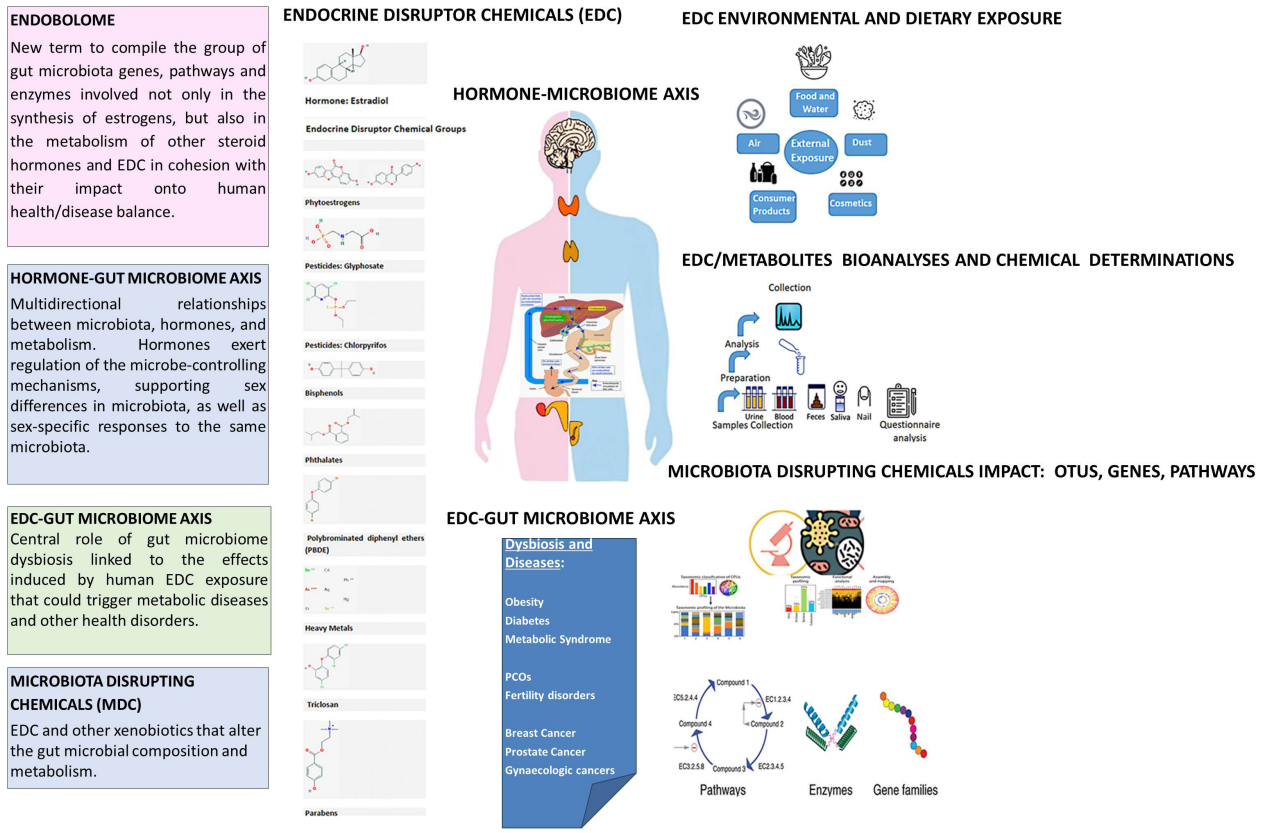

FIGURE 1 | Endobolome: multiproxy approach to determine the influence of microbiota disrupting chemicals (MDC) in relation to specific endocrine pathogenesis.

androgen-related diseases in the distal intestine and probably also in remote anatomical sites.

Identification of the bacterial genes in the gut microbiota that encode enzymes responsible for the biotransformation of endogenous steroids could explain potential interactions between gut microbiome, host and the development of certain diseases. *In vitro* studies have shown the capacity of gut microbiota to the biotransformation of steroids. In this respect, Ervin et al. (2019) conducted the first *in vitro* study to determine the capacity of 35 β-glucuronidases of human gut to reactivate estrone-3-glucuronide and estradiol-17-glucuronide to their parent compounds. This supports the idea that the estrobolome is a complex series of processes that occur in the gastrointestinal tract of mammals and the probably involves different enzymes, including distinct types of β-glucuronidases. Ridlon et al. (2013) showed that *Clostridium scindens* may transform primary bile acids to toxic secondary acids, and remove the two-carbon side chain of glucocorticoids transforming them into androgens. Doden et al. (2019) demonstrated that 20 β-hydroxysteroid dehydrogenase from *Bifidobacterium adolescentis* can reduce host glucocorticoids and thereby serve as potential probiotics for the management of androgen-related conditions.

Another possible mechanism of interaction between EDC, endogenous sex steroid hormones and gut microbiota is that dysbiosis caused by EDC and hormone imbalance levels may increase the permeability of the intestinal mucosa barrier in the host. This would allow pathogens, LPS, toxins and metabolites to enter the circulatory system thereby promoting chronic low-grade systemic inflammation in the host, even targeting organs like the brain (Fuhrman et al., 2014; Pickard et al., 2017).

Another potential mechanism involves the capacity of gut microbiota to metabolize EDC and host hormones to produce novel hormone receptor ligands (Schug et al., 2011). Additionally, the microbiota may be modified in order to generate lower-affinity hormones with endocrine functions but with a reduced risk of developing hormone-responsive diseases like breast cancer (Chen K. L. A. et al., 2018). It has been showed in a mouse model that the status of hormone receptors such as estrogen receptor β may alter microbiota composition and this microbiota behaves differently to changes from diet complexity, promoting Proteobacteria enrichment (Mulak et al., 2014). This suggests that sex hormones have the capacity to mediate and modulate growth, metabolism, and virulence of bacterial pathogens.

Bringing together all these findings allow us to validate the theory that the endobolome implies a multidimensional set of processes on-going inside the gastrointestinal tract that possible involves many enzymes and pathways. The capacity of microbes to control hormones and of hormones to modify microbial diversity must be considered in future studies. Furthermore, it is possible that in complex microbial communities the functions

of hormone control could be diverse between different members of the community. The detection of crucial microbial enzymes in biodegradation might support to find microbial hormone degradation routes and biomarkers of hormones metabolism by a microbial community.

Moreover, we suggest that the gut may act a reservoir for hormone metabolites that could exert effect locally and possibly in the distance in systemic homeostasis and the development of disease. Hormones and microbiota could exert their activity separately for the development of disorders and diseases; however, recent studies have shown that hormones and microbiota may function together in conditions related to hormone hypersecretion or deficiency (Tetel et al., 2018). However, the way certain hormones alter the microbiome to confer normal metabolic phenotypes or how microbial hormone metabolites act as ligands binding to hormone receptors to mediate metabolic functions (Fukui et al., 2018).

The communication between gut microbiota and hormones guides to biological modifications through a diversity of tissues ranging from neuronal development to reproductive health. When dysibiosis occurs, these physiological responses are altered and contribute to development of disease. Polycystic ovary syndrome (PCOS) is a chronic metabolic disease in reproductive-aged women with prevalence between 3 and 26% and whose pathogenesis is currently unknown. A novel hypothesis suggests that microbiota dysbiosis may promote the production of androgens in the ovaries which results in disordered folliculogenesis triggered by a chronic inflammatory response and insulin resistance (Tremellen and Pearce, 2012). Kelley et al. (2016) found in a letrozole (a non-steroidal aromatase inhibitor) induced PCOS murine model that treatment with letrozole significantly changed the gut microbiome composition in a time-dependent manner with a reduction in overall species and phylogenetic richness. Guo et al. (2016) transplanted fecal microbiota from healthy rats to letrozole-induced PCOS mice and found that transplantation resulted in normalization of the estrous cycles and the ovarian morphology. These findings suggest the association between sex hormone levels, estrous cycles, ovarian morphology and gut microbiota composition. Another murine model study showed that transplantation of male cecal microbiota to females led to increased testosterone levels, compared with unmanipulated control females and female mice transplanted with female cecal microbiota (Markle et al., 2013). Liu et al. (2017) conducted a study in 33 PCOS patients and found that gut dysbiosis correlated with the disease. The authors also reported an increase in the relative abundance of *Bacteroides*, *Escherichia*/*Shigella,* and *Streptococcus* in PCOS individuals, a negative correlation between these bacterial species and ghrelin levels, and a positive correlation with testosterone and body mass index (BMI). Lastly, decreased abundances of *Akkermansia* and *Ruminococcus* in PCOS, with a negative correlation of these species and body-weight, sex-hormone, and brain–gut peptides. Summarizing, human microbiota seems to play a key role in endocrine and reproductive system disorders. Moreover, microbiota reproductive dysbiosis have started to be treated by probiotics using typical species from genus *Lactobacillus* (Lopez-Moreno and Aguilera, 2020). Some *Bifidobacteria* seems modulate sex hormone levels in patients with PCOS through the gut–brain axis (Zhang et al., 2019).

The prostate is an estrogen and androgen target tissue and estrogens have been shown to promote growth and differentiation of prostate, potentially leading to the development of prostate cancer. Recent studies indicate that gut microbial species leading to increased serum levels of estrogens may increase the risk of prostate cancer (Nelles et al., 2011). Androgens are involved in the growth and survival of normal prostate cells and in the development of prostate cancer, with androgen suppression therapy being a usual treatment for this type of cancer. However, although most patients with advanced metastatic prostate cancer respond to androgen deprivation, the tumors eventually become androgen-independent (Feldman and Feldman, 2001; Porter et al., 2018). The capacity of gut microbiome to alter androgen levels may result in depletion, less effective androgen suppression therapy. Sfanos et al. (2018) found a distinct microbial composition in patients undergoing oral androgen suppression therapy versus patients not treated with this therapy. Treated patients also showed an increase in the bacterial metabolic pathways that stimulate androgen synthesis. In addition, significant differences were found in the gut microbial composition between prostate cancer patients and patients with benign lesions (Golombos et al., 2018). Similarly, Magri et al. (2018) considered prostatitis as a systemic diseases correlating with alterations of specific microbiota or seminal dysbiosis.

The relation between the gut microbiome and the development of gynecologic cancers remains unclear (Mert et al., 2018), but there is growing evidence of the role played by changes in microbiome in an increased risk of these types of cancers. It is plausible that all these factors can lead to cancer by modifying the microbiota and its interaction with host DNA or just simply by triggering inflammatory reactions. Some possible mechanisms related to this increased risk are the capacity of the microbiota to interact with the host DNA and to promote chronic inflammation. As for epithelial ovarian cancer patients, Banerjee et al. (2017) found a distinct gut microbiota composition versus controls. *Retroviridae* and human papilloma virus as well as *Proteobacteria* and *Firmicutes* were found in ovarian cancer patients versus controls (Mitra et al., 2016). In agreement with this hypotheses, probiotic microorganisms are been investigating recently by their antigenotoxic potential effects (Janosch et al., 2019).

Breast cancer has also been related with disturbances in the microbiota. In this respect, it has been reported a decreased gut microbial diversity and a different composition in postmenopausal women with breast cancer versus controls (Zhu et al., 2018). Lahiji et al. (2020) analyzed recently the effect of symbiotic on glycemic profile and sex hormones in overweight and obese breast cancer survivors following a weight-loss diet through a randomized controlled trial. However, Jones et al. (2019) did not found any correlation between fecal microbiota and breast density on the mammograms.

As with gut microbiota, the enteroendocrine cells found in the gastrointestinal tract can alter the microbial composition having an effect on the intestinal health patterns of estrogen metabolism

used as markers of breast cancer risk in postmenopausal women have been correlated with gut microbiota diversity and composition (Kwa et al., 2016).

Estrogens promote the growth and proliferation of epithelial cells in the mammary gland and in the reproductive system and are thereby associated with proliferative conditions like endometrial cancer and endometriosis. Several authors have suggested an association between gut microbiota alterations and development of endometriosis (Ata et al., 2019). Bailey and Coe (2002) supported this equivalent idea association in a rhesus monkey model. In addition, in a murine model Yuan et al. (2018) reported a distinct composition of gut microbiota 42 days after endometriosis induction.

Taking together all this data shown that commensal microbiota of the host could be implicated in gender bias existing in numerous diseases. The capacity of the gut microbiome in controlling hormone levels allow to have stimulating therapeutics applications in different diseases, taken into account a sex-tailored therapeutic approach.

Efficacy and safety of current hormone replacement therapies might be improved by combining probiotics with the hormones that work independently or synergistically to provide a more holistic treatment approach against hormonal disease (De Franciscis et al., 2019). Lastly, it has been suggested that probiotic bacteria administered in combination with hormone replacement therapy may increase the efficacy of hormone replacement and attenuate the side effects that can arise from its use, therefore providing a more comprehensive treatment of hormonal diseases. Next generation probiotics will explore the function in this area of knowledge (Ejtahed and Hasani-Ranjbar, 2019). The response to therapeutic alteration of the microbiota using prebiotics, live biotherapeutics or fecal transplant therapy is likewise probable to be dissimilar in males and females, although this has not been specifically studied to date.

The studies compiled revealed significant evidence of sex-specific communities, the role of sexual maturation producing changes to microbial communities, and proof that microbial communities could have a key function by modulating hormonal and metabolic pathways. Results highlight the need to examine sex-specificity in microbial composition and function.

ENDOCRINE DISRUPTORS-GUT MICROBIOME AXIS

The role played by human exposure to EDC in the development of diseases such as breast cancer, diabetes, obesity and some neurobehavioral disorders is widely known (Andujar et al., 2019). These diseases have also been related to gut dysbiosis, which suggests the central role of gut microbiome in the effects induced by EDC exposure in human metabolism (Galvez-Ontiveros et al., 2020). It can therefore be suggested that the exposure to EDC may result in alterations in the gut microbiome which may ultimately affect human health. In a bidirectional interaction, microbiota can metabolize EDC to biologically active or inactive forms, and EDC may induce the proliferation and growth of certain bacteria. These EDC-induced changes in the gut microbiota may lead to disturbances in different host systems. However, it remains unclear if EDC-induced metabolic disruptions in the host occur before the changes in the microbiome or if the EDC-induced microbiome changes result in metabolic disruptions (Rosenfeld, 2017).

The gastrointestinal tract is the main route of entry for EDC; however, their absorption through the intestinal wall is low and they are transported by the peristaltic movement to the distal small intestine and caecum where microbial flora is more abundant and they can be directly metabolized by the microbiota thereby increasing or decreasing their toxicity to the host. Part of the disruptors is taken to the liver by the portal circulation where they are conjugated. These conjugated forms can be excreted in the bile entering the small intestine where microbiota tend to deconjugate them therefore restoring the original compound or producing new toxic metabolites. EDC can also affect the composition and metabolic activity of gut microbiota, which in turn may result in a disrupted activity of EDC metabolites or in the toxicity of other contaminants metabolized by the gut microbiota (Claus et al., 2017). Data from animal models suggest that the alterations in gut microbiota not only affect the levels of microbial enzymes, but also the levels of hepatic enzymes in the host (Snedeker and Hay, 2012). In addition, exposure to EDC could alter gut microbiota functions.

The gut microbiota has the capacity to transform non-EDC in active compounds. For example, Van de Wiele et al. (2005) reported that colonic microbiota can metabolize polyaromatic hydrocarbons into 1-hydroxy pyrene and 7-hydroxybenzo[a]pyrene, biologically active estrogen metabolites, while the gastrointestinal digestion of these xenobiotics did not produce estrogen metabolites. This finding suggests that the colonic microbial communities have the capacity to transform parent compounds directly into active metabolites.

The hypothesis that exposure to EDC may result in alterations of the gut microbial composition has not yet been extensively explored. In this scenario, the microbiota and their products may act as mediators of the effects caused by these contaminants, which will eventually lead to the development of disorders and diseases. Several EDC have been shown to promote dysbiosis or to inhibit bacterial growth in *in vitro* and in *in vivo* models (Galvez-Ontiveros et al., 2020). Dysbiosis has been associated with intestinal and non-intestinal disorders which have been in turn related to EDC exposure. This would be consistent with the idea that EDC exposure may have an impact on the normal gut microbiota colonization, which will ultimately affect host physiology and health. These EDC-induced alterations of the gut microbiota composition may represent an underestimated mechanism of interfering with human health.

MICROBIOTA DISRUPTING CHEMICALS (MDC)

We propose that EDC and other xenobiotics that alter the gut microbial composition and metabolism should be categorized into a subgroup termed "microbiota disrupting chemicals" (MDC). This will help to distinguish the role of contaminants

from other microbiota disruptors such as diet, environment, physical activity and stress. These MDC might have the ability to promote changes in the microbiota that can ultimately result in intestinal, hormonal and chronic or long-term systemic diseases in the host as illustrated in **Figure 1**.

Below we summarize the best known and studied by now MDC and their effects on the microbiota.

EDC-GUT MICROBIOME AXIS

Central role of gut microbiome dysbiosis linked to the effects induced by human EDC exposure that could trigger metabolic diseases and other health disorders.

MICROBIOTA DISRUPTING CHEMICALS (MDC)

EDC and other xenobiotics that alter the gut microbial composition and metabolism.

Pesticides

Several studies have revealed the central role played by gut microbiota in the toxicity of pesticides, with important implications for environmental, animal and human health (Yuan et al., 2019; **Table 2**). Glyphosate and chlorpyrifos, the most widely used herbicide and pesticide, respectively, exhibit endocrine disrupting activity. Human exposure occurs mainly through diet and drinking water (Gillezeau et al., 2019). They have been reported to interfere with gut microbial communities and enteroendocrine cells (Li et al., 2019). Mucosal-associated invariant T-cells (MAIT) are activated by bacterial-derived metabolites from riboflavin and folic acid biosynthesis. Mendler et al. (2020) investigated the effects of chlorpyrifos and glyphosate on the regulation of MAIT activity but gut microbiota and found that exposure to these pesticides results in disturbances in the gut microbial communities studied, thereby promoting a pro-inflammatory immune response.

In a fish model, chlorpyrifos led to disorders in the hepatic lipid metabolism linked to oxidative stress in the gut and dysbiosis (Wang et al., 2019). In a murine model, Liang et al. observed that chlorpyrifos induced changes in the gut microbiota which resulted in an increased risk of obesity and insulin resistance (Liang et al., 2019). They also found that this pesticide can disrupt the integrity of the intestinal barrier, leading to the entry of lipopolysaccharides into the bloodstream ultimately resulting in low-grade inflammation.

Using 16 S rRNA gene sequencing in a rat model, Tang et al. (2020) observed that glyphosate exposure led to a significant increase in α-diversity and changes in gut microbiota composition with decreased relative abundance of Firmicutes and Lactobacillus and enrichment of potentially bacterial pathogens. *Firmicutes* produces butyrate as a byproduct of fermentation. It has been reported that butyrate-producing bacteria play a role in intestinal epithelial barrier maintenance (Canani et al., 2011). Rueda-Ruzafa et al. (2019) showed that glyphosate-mediated inactivation of 5-enolpyruvylshikimate-3-phosphate synthase from intestinal microbiota results in dysbiosis which in turn led to alterations in central nervous system causing emotional, neurological and neurodegenerative disorders.

In a rat model, Li et al. (2019) investigated the effects of chronic exposure to chlorpyrifos on serum hormone levels, pro-inflammatory cytokines and gut microbiota and found that exposure significantly decreased levels of luteinizing hormone, follicle stimulating hormone and testosterone and change gut microbiota composition. The affected bacteria included short-chain fatty acid-producers, which stimulate the hypothalamic-pituitary-adrenal axis and the immune response, and increase the permeability of the gut barrier.

Diazinon, an organophosphate pesticide with estrogenic activity (Manabe et al., 2006) has shown to alter the structure of the gut microbiome community, functional metagenome, and their associated metabolic profiles in a sex-related manner in murine models (Gao et al., 2017a). Gao et al. (2017a) suggest that diazinon neurotoxicity and its sex-dependent effects are related to the pesticide-induced alterations of the gut microbiome and its functions. The same authors (Gao et al., 2017b) investigated the effects of diazinon exposure by determination the gut bacterial metatranscriptome. They demonstrated that diazinon has the capacity to regulate quorum sensing, a system used to regulate bacterial population density and composition, and more importantly, their functional genes. Lastly, they also found that diazinon exposure results in the activation of stress response pathways and in disruptions of energy metabolism of gut bacteria.

Organochlorine pesticides with endocrine disrupting capacity have been also related with alterations in gut microbiota. Dichlorodiphenyldichloroethylene (DDE) exposure of 3-week-old male Sprague Dawley rats led to an increase of fat and body weight, dysregulation of glucose homeostasis, and promoted dysbiosis as suggested by a higher *Firmicutes/Bacteroidetes* ratio, resulting in disruptions in energy harvesting. DDE also resulted in alterations in the lipid metabolome profile with high plasma concentrations of phosphatidylcholine, phosphatidylserine, hosphatidylethanolamine, and triacylglycerol. The presence of these lipid metabolites was significantly associated with changes in microbiota composition (Liang et al., 2008).

Bisphenol and Phthalates

Bisphenol A (BPA) is an environmental contaminant with endocrine disrupting activity widely used in the manufacture of polycarbonate plastics and epoxy resins and is released in large volumes into the environment. Phthalates are used in many household products and in food packaging acting as binding products and plasticizers. Human exposure to these contaminants occurs mainly through the diet, as they leech from plastic packaging, water, dust and to lesser extent from skin contact (Larsson et al., 2017). Both endocrine disrupters have shown to affect gut microbiota composition and function in animal models (**Table 3**). In a mouse model, DeLuca et al. (2018) found that BPA has the capacity to promote colonic inflammation and alter the levels of tryptophan and other microbiota metabolites derived from aromatic amino acids related to autoimmune diseases, specifically to inflammatory bowel conditions. In a mouse model, Lai et al. (2016) used 16S rRNA gene sequencing of cecal microbiota to demonstrate that BPA exposure through diet may result in alterations of gut microbiota composition and function, promoting the growth of *Proteobacteria*, a marker of dysbiosis, that has been associated to different disorders such as metabolic syndrome and inflammatory bowel disease (Zhang et al., 2006). Increased

TABLE 2 | Studies linking exposure to pesticides and gut microbiota changes.

References	Animal model	Pesticide dose	Microbiota changes	Health effects
***In vitro* studies**				
Mendler et al. (2020)	Humans	CPF (50–200μM) or GLP (75–300 mg/L)	• The growth of *E. coli, Bifidobacterium adolescentis* and *Lactobacillus reuteri* was not inhibited.	• *E. coli* activated a significantly higher number of MAIT cells to produce TNFα and IFNγ after exposure to CPF. However, *B. adolescentis* and *L. reuteri* did not induce activation of MAIT cells *per se* after exposure to CPF or GLP. • *E. coli* decreased riboflavin production after exposure to CPF. In contrast, folate production by *E. coli* was significantly increased after exposure to CPF. • GLP exposure resulted in MAIT cell activation by *E. coli*, but exposure did not affect vitamin production. • Exposure to CPF and, to a lesser extent, GLP, can result in bacterial metabolism changes, with imbalances in the levels of activation/inhibition of bacterial metabolites that could have an impact on the inflammatory immune responses.
Studies in animals				
Wang et al. (2019)	Zebrafish	CPF (30, 100, and 300 μg/L)	• Significant decrease in γ-*Proteobacteria*.	• CPF induces oxidative stress. • Exposure to CPF could induce liver disorders of glucose and lipid metabolism in adult zebrafish.
Liang et al. (2019)	C57Bl/6 and CD-1 mice	CPF (5 mg/kg)	• Decreased *Bacteroidetes* phyla. • Increased *Proteobacteria* phyla.	• Exposure to CPF resulted in disrupted integrity of the intestinal barrier, which increases the entry of lipopolysaccharides into the body and lastly low-grade inflammation. • Increased fat mass. • Decreased insulin sensitivity.
Tang et al. (2020)	Male Sprague Dawley rats	GLP (0, 5, 50, and 500 mg/kg)	• Decreased *Firmicutes* phylum and *Lactobacillus* genus. • Increased pathogenic bacteria *Clostridium botulinum*.	• GLP exposure decreased the villus height/crypt depth ratio in the duodenum and jejunum which is associated to decreased digestive and absorptive capacity. • Decreased activity of antioxidant enzymes • GLP exposure promotes the production of proinflammatory factors (IL-1β, IL-6, TNF-α, MAPK3, NF-κB and Caspase-3).
Li et al. (2019)	Male Wistar rats	CPF (0.3 mg/kg)	• Increased relative abundances of *Streptococcus*, *Ruminiclostridium*, and *norank_f_Coriobacteriaceae* in adult rats exposed to CPF. • Reduced relative abundances of *Corynebacterium_1, Psychrobacter, Facklamia, norank_f__Peptococcaceae, Oligella, Brevibacterium, Catabacter, Dietzia, Atopostipe*s and *Ignavigranum* in newly weaned rats exposed to CPF.	• Decreased concentrations of luteinizing hormone, follicle-stimulating hormone, and testosterone were found in rats exposed to CPF and fed normal-fat diet. The counteracted effect of the high-fat diet was also found in intestinal hormones and pro-inflammatory cytokines. • TNF-α were found in newly weaned rats exposed to CPF, whereas only peptide YY, ghrelin and IL-6 increased significantly in rats exposed in adulthood.
Gao et al. (2017a)	C57BL/6 mice	Diazinon (4 mg/L)	• Decrease in several genera of the *Lachnospiraceae* family in exposed male and female mice. • High prevalence of pathogenic bacteria (*Burkholderiales* and *Erysipelotrichaceae_Coprobacillus*) was only found in exposed male mice. As well as increased *Bacteroidetes* phylum and decreased *Firmicutes*. • *Lachnospiraceae, Ruminococcaceae, Clostridiaceae* and *Erysipelotrichaceae* decreased in female mice.	• Tryptophanase was significantly downregulated in male mice but not in females. • Glycine was decreased in male mice, but not in females. • Exposure to diazinon resulted in disturbances of bile acid metabolism in both male and female mice, but the patterns and involved metabolites were sex dependent. Lithocholic acid and cholesterol increased in males. Lithocholic acid also increased in females, but with decreased cholesterol.
Gao et al. (2017b)	C57BL/6 mice	Diazinon (4 mg/L)	• Intestinal dysbiosis was observed in the previous study (Gao et al., 2017a).	• Altered quorum sensing mechanisms. • Increased motility and genes related to sporulation. • Activation of stress response pathways. • Impaired metabolic homeostasis of carbohydrates, fatty acids, and amino acids.

CPF, chlorpyrifos; GLP, glyphosate; MAIT cell, Mucosal-associated invariant T-Cell; TNFα, tumor necrosis factor-α; IFNγ, interferon-γ.

TABLE 3 | Studies linking exposure to bisphenol and phthalate and gut microbiota changes.

References	Animal model	BPA or phtalates dose	Microbiota changes	Health effects
***In vitro* studies**				
Lei et al. (2019)	C57BL/6J mice	DEHP (10 or 100μM)	• Increased abundance of *Lactobacillus* and *Parabacteroides*. • Decreased abundance of *Fluviicola* and *Enterococcus*.	• Exposed cultured microbiota increased the production of metabolites typically associated with fermentation of sugar and amino acid residues. • Among the metabolites detected are potentially toxic compounds derived from aromatic amino acid. Metabolites normally found in low concentrations in the intestine of healthy individuals but in high concentrations in developmental disorders were also detected [3-phenylpropionic acid and 3- (3-hydroxyphenyl) propionic acid are precursors of 3- (3 -hydroxyphenyl) -3 hydroxypropionic].
Studies in animals				
DeLuca et al. (2018)	C57BL/6 mice	BPA (50 μg/kg)	_	• Exacerbation of colon inflammation in animals with dextran sulfate sodium-induced colitis. • Reduction of fecal tryptophan and aromatic amino acids.
Lai et al. (2016)	CD-1 mice	BPA (BPA content in contaminated diet)	• Increased phylum *Proteobacteria* and Helicobacteraceae family. • Decreased *Firmicutes* and *Clostridia.*	• Absorption of BPA in the diet affects gut microbial composition, which relates with increased risk of metabolic disorders and inflammatory bowel disease.
Javurek et al. (2016)	California mice	BPA (50 mg/kg)	• Exposure to BPA in P0 females resulted in increased Mogibacteriaceae, *Sutterella* spp. and Clostridiales. BPA exposure of F1 females resulted in increased *Bifidobacterium* and the family Mogibacteriaceae. • In P0 males exposure led to increased abundance of *Mollicutes* and *Prevotellaceae* and increased. *Akkermansia* and *Methanobrevibacter* in F1 males	• BPA binds to and activates the estrogen receptors. • Many bacterial genera associated to EDC exposure are also found in several diseases such as inflammatory bowel disease, metabolic disorders, and colorectal cancer.
Malaise et al. (2017)	Mice	BPA (50 μg/kg)	• Decreased bifidobacteria and *Clostridium. butyricum* and *Clostridium Cluster XIVa*.	• Obesogenic impact of early and intrauterine exposure to BPA. • Glucose intolerance and decreased insulin sensitivity were observed in young and adult mice perinatally exposed to BPA. • Perinatal BPA exposure may also result in a loss of intestinal barrier.
Chen et al. (2018a)	Zefrafish	BPA (0, 2, and 20 μg/L)	• BPA exposure in male fish resulted in increased abundance of *Actinobacteria* at 13.9% ($P < 0.001$), *Hyphomicrobium*, and *Lawsonia*. • Single BPA exposure in female fish resulted in increased abundance of *Actinobacteria* to 15.7% ($P < 0.001$) and *Hyphomicrobium*.	• Exposure to 2 μg/L BPA resulted in decreased body weight in male fish versus controls, also in a significant reduction of the condition factor, and decreased intestinal levels of serotonin. • No significant differences in body length, body weight, or condition factor were observed in female fish. Single exposure to BPA resulted in significantly higher intestinal levels of serotonin versus controls. • Decreased levels of intestinal IL1β were observed in males versus significantly higher levels in females.

(Continued)

TABLE 3 | Continued

References	Animal model	BPA or phtalates dose	Microbiota changes	Health effects
Xu et al. (2019)	Mice	BPA (30 or 300 μg/kg)	• Exposure to low BPA dose resulted in increased *Bacteroidetes* in non-obese diabetic female mice. Exposure to high dose increased unclassified bacteria from *Rikenellacaea* and decreased unclassified bacteria from *Bacteroidales* and *Lactobacillus*. • Sub-acute exposure in males resulted in an increase in bacteria classified as other at the phylum level was significantly increased from the low dose, while *Tenericutes* was significantly decreased in both BPA doses of exposure. At the genus level, exposure to high BPA dose increased *Odoribacter* and unclassified *Campylobacterales* and decreased *Anaeroplasma* and *Camplybacter*, while *Lactobacillus* was decreased at low BPA dose.	• BPA accelerated the development of T1D in female mice, but delayed the development of the disease in males. • The gut microbiome profile was consistently pro-inflammatory in females, but males had an overall decrease in anti-inflammatory and pro-inflammatory gut microbes.
Lei et al. (2019)	C57BL/6J mice	DEHP (1 or 10 mg/kg)	• Increased *Lachnoclostridum* abundance. • Decreased *Akkermansia, Odoribacter* and *Clostridium sensu stricto.*	• Diethylhexyl phthalate promoted p-cresol production but inhibited butyrate synthesis. • Exposure to diethylhexyl phthalate could be involved in neurodevelopmental disorders associated with dysbiosis.
Adamovsky et al. (2020)	Zebrafish	DEHP (3mg/kg)	• Diethylhexyl phthalate exposure increased *Bacteroidiales* and *Gammaproteobacteria* and decreased *Verrucomicrobiae* in males and females. • In males the abundance of *Fusobacteria* and *Betaproteobacteria* increased and *Saccharibacteria* decreased.	• Exposure in males negatively affected several membrane transport proteins, organic anion transporting polypeptides encoded by *slc* genes. • Altered metabolites detected by intestinal and immune Th cells.
Wang et al. (2020)	Sprague-Dawley and Wistar rats, BALB/c and C57BL/6J mice.	DEHP (0, 300, 1,000, and 3,000 mg/kg)	• Sprague-Dawley rats showed an increase in the Firmicutes/Bacteroidetes ratio and in the abundance of *Proteobacteria.* • In C57LB/6J mice Proteobacteria and *Actinobacteria* showed a downward trend. *Tenericutes* showed only a significant increase in cecal content. At the genus level, a decreased abundance of *Prevotella, Lachnospiraceae,* and *Desulfovibrio* was found. • In BALB/c mice only *Bacteroides* decreased, while Runimococcaceae and Rikenellaceae showed a significant increase. • Wistar rats showed increased abundance of *Adlercreutzia,* Eubacateriaceae and *Roseburia*, and a decrease of *Coprococcus,* Dehalobacteiaceae.	• Sprague-Dawley rats were more sensitive to exposure to DEHP with more severe organic damage, the highest Th1 inflammatory response and highest increase in body weight. Liver index increased in the medium and high dose groups. IL-2, IFN-γ, and TNF-α increased significantly and testosterone decreased. • In mice, only C57LB/6J mice exposed to high dose showed a higher liver index. Alanine aminotransferase, aspartate aminotransferase, alkalinephosphatase levels increased markedly in the highest dose group. • In Wistar rats, exposure to DEHP induced only a significant increase of alanineaminotransferase in the low and medium dose groups. • In BALB/c mice testosterone concentration decreased.
Studies in humans				
Yang et al. (2019)	Newborns	DEHP exposure in through medical treatment	• Firmicutes/Bacteroidetes ratios changed significantly. • *Bifidobacterium longum, Rothia* spp. and *Veillonella* decreased.	• *Rothia* and *Veillonella* abundance has been associated with a lower incidence of asthma. • Early exposure to diethylhexyl phthalate can alter the immune response in adulthood.

BPA, bisphenol A; DEHP, Diethylhexylphthalate; TNF-α, tumor necrosis factor-α; IFNγ, interferon-γ, T1D, type 1 diabetes.

Helicobacteraceae and decreased *Firmicutes* and *Clostridia* populations were observed in BPA-fed mice. In a mouse model, Javurek et al. (2016) used 16s rRNA sequencing to show that BPA exposure, especially during development, results in generational and sex-related changes in the gut microbiome. Exposure to BPA induced in the parents and their offspring the growth of bacteria related to an increased risk of inflammatory bowel disease (IBD), metabolic disorders, and colorectal cancer. Also, in a murine model, Malaise et al. (2017) observed that perinatal exposure to BPA promoted disturbances in gut microbiota and immune system through a decrease in the Th1/Th17 cell frequencies in the lamina propria as well as an increase of Th1 andTh17 responses in the spleen. These early-life alterations are associated with impaired glucose sensitivity and IgA secretion into feces, and a drop of fecal *bifidobacteria* versus non-exposed mice.

Chen et al. (2018a) found that simultaneous exposure to titanium dioxide nanoparticles and BPA in zebrafish resulted in growth and gut microbiota alterations including loss of the mucosal barrier integrity and increased inflammation and oxidative stress. In addition, the changes in gut microbiota were sex- and concentration-dependent. The authors also found a correlation between zebrafish body weight and abundances of *Bacteroides*, which was also closely associated with the genera *Anaerococcus*, *Finegoldia*, and *Peptoniphilus*. They also reported that BPA at low concentrations interacts antagonistically with titanium dioxide but BPA at higher concentrations interacts synergistically. Lai et al. (2016) found that dietary BPA exposure in mice resulted in changes in gut microbiota structure similar to those found in mice on high-fat and high-sucrose diets. Xu et al. (2019) described that the effects of BPA-exposure on type 1 diabetes (T1D) in non-obese diabetic mice and found that were sex- age-dependent with changes in gut microbiota and inflammation being the main mechanisms disease worsening in juvenile exposure, while decreased inflammation resulted in attenuated T1D in perinatally exposed females.

In a mouse model Lei et al. (2019) showed that exposure to diethylhexylphthalate (DEP), a chemical associated with neurodevelopmental disorders, led to changes in gut microbial structure and metabolite profile. These changes in the microbiota may activate the production of *p*-cresol, a potentially toxic metabolite that has also been correlated with neurodevelopmental disorders. Recently, Adamovsky et al. (2020) showed that DEP exposure results in alterations in the microbiome-gut-immune axis which promotes adverse effects of DEHP on the host by altering metabolites sensed by both intestinal and immune T-cells. Wang et al. (2020) postulate that the differences in the toxicity of DEP on different strains and species of rodents are related to the distinctive DEP-induced changes in gut. Lastly, Yang et al. (2019) investigated whether phthalate exposure in newborns through medical treatment that required intravenous infusions had an impact on gut microbiota composition and diversity and found that this type of exposure caused gut dysbiosis, with decreased *Rothia* sp. and *Bifidobacterium longum*. The authors conclude that early-life exposure to DEP alters gut microbiota in newborns and may result in disruptions of immune responses later in life.

Metals

Many heavy metals have shown endocrine disrupting properties, and human exposure occurs through diet and water, inhalation of polluted air, smoking and dermal absorption (Sabra et al., 2017). The effects of metal exposure on the gut microbiota have been studied in various species including mice, rats, chickens, fish, and humans in adulthood (**Table 4**).

Recent works have described the effects of metals on microbiota including the paper by Zhou et al. (2020) reported that subchronic exposure to mercury in chickens caused dysbiosis and altered microbial growth and development, which may ultimately led to metabolic disorders. Zhao et al. (2020) showed that mercury exposure in mice resulted in alterations in microbial growth and development, metabolic disorders, and promoted apoptosis in mice. Gut dysbiosis was associated with increased abundance of *Coprococcus*, *Oscillospira* and *Helicobacter* and reduced *Lgnatzschineria*, *Salinicoccus,* and *Bacillus*.

Ruan et al. (2019) reported that high exposure to copper and mercury in female mice led to histopathological lesions and changed the diversity of the cecal microbiota. In an amphibian model, Zheng et al. (2020) investigated the effects of exposure to copper, cadmium and chrome on the gut microbiota and found that at the phylum level, copper exposure increased *Proteobacteria*, that has been described to be associated with metabolic diseases (Rizzatti et al., 2017). Copper, cadmium and chrome exposure significantly increased *Bacteroidetes* that is implicated in the protein metabolism and in the complex cycling of carbon (He et al., 2018). Lastly, exposure to copper and cadmium resulted in a reduction of Fusobacteria. The abundance of Fusobacteria is negatively related to the incidence of infectious and diseases producing tissue necrosis (Knutie et al., 2018).

Zhang et al. (2020) found that exposure to cadmium in crustacean *P. clarkii* resulted in histological changes in the intestines and alteration of the richness, diversity, and composition of its gut microbiota with changes in the relative abundances of *Firmicutes, Proteobacteria, Bacteroidetes, Fusobacteria*, and *Actinobacteria*. Yan et al. (2020) investigated the toxicity of environmentally relevant concentrations of metals and microplastics on the gut bacteria and gonadal development in medaka fish and found significant changes in gut microbiota. The authors also reported that the exposure to metals increased the diversity and abundance of intestinal microbiota, in particular of *Proteobacteria*. In an epidemiologic study Shao and Zhu (2020) found that long-term exposure to arsenic, cadmium, copper, lead and zinc increased the relative abundances of *Lachnospiraceae, Eubacterium eligens, Ruminococcaceae UGG-014, Erysipelotrichaceae UCG-003, Tyzzerella 3, Bacteroides, Slackia*, and *Roseburia* and decreased *Prevotella*. The authors also reported that these changes in the microbiota were sex-dependent. Richardson et al. (2018) reported that the microbiota can be used as a pre-clinical marker of exposure to specific heavy metals. They described significant changes in the gut microbial composition in rats after exposure to high doses of chromium and cobalt, and dose-dependent changes after exposure to arsenic, cadmium and nickel.

There are few studies that examine the effects of metal exposure in human microbiota. In this respect,

TABLE 4 | Studies linking exposure to metals and gut microbiota changes.

References	Animal model	Metal dose	Microbiota changes	Health effects
Studies in animals				
Zhou et al. (2020)	Chickens	Mercuric chloride (250 mg/L)	• At the phylum level, at 30 days there was an increase in the abundance of Proteobacteria and Tenericutes phyla, while Tenericutes phylum increased significantly at 60 days.	• Exposure to mercury reduced body weight. • Possible induction of metabolic disorders (carbohydrate, terpenoids and polyketides, and xenobiotics).
Zhao et al. (2020)	Kunming mice	Mercuric chloride (0 and 80 mg/L)	• Increased abundance *Coprococcus, Oscillospira,* and *Helicobacter*. • Decreased *Lgnatzschineria, Salinicoccus,* and *Bacillus*.	• Increased body weight and glucose levels. • Intestinal injury. • Significantly increased expression of pro-apoptotic genes (Bax, JNK, ASK1, caspase3, and TNF-α), and significantly decreased expression of the anti-apoptotic gene Bcl-2.
Ruan et al. (2019)	Female Kunming mice	Cu and Hg	Decreased abundance of *Rikenella*, *Jeotgailcoccus* and decreased abundance of *Staphylococcus*. *Corynebacterium* increased significantly in mice exposed to Cu. • Decreased abundance of *Sporosarcina, Jeotgailcoccus* and decreased abundance of *Staphylococcus* in the Hg and Cu+Hg groups. *Anaeroplasm* increased significantly in the Cu+Hg group.	• Increased thickness of muscularis internal and externa. • Widened submucosa. • Reduction of goblet cells. • Necrosis of enterocytes. • Decreased height of intestinal villi.
Zheng et al. (2020)	*B. gargarizans tadpoles*	Cu (32 and 64 μg/L), Cr (104 and 416 μg/L), Cd (100 and 200 μg/L), NO_3 -N (20 and 100 mg/L).	Exposure to NO_3 -N, Cd, and Cu increased the abundance of *Proteobacteria*. • Exposures to Cu, Cd, Cr, NO_3 –N increased the abundance of *Bacteroidetes*. • Exposure to Cu and Cd decreased the abundance of *Fusobacteria*.	• Exposure to NO_3 -N increased the risk of developing metabolic disorders, various diseases, and adaptation to the environment.
Zhang et al. (2020)	*P. clarkii* crayfish	Cd (0, 2, 5, and 10 mg/L)	Firmicutes, Proteobacteria, Bacteroidetes, and Fusobacteria were the predominant phyla in the gut microbiota after exposure to Cd.	• Exposure to Cd could induce histological intestinal damage.
Yan et al. (2020)	*O. melastigma*	Pb (50 μg/L), Cd (10 μg/L), and Zn (100 μg/L)	Increased abundance of Firmicutes *(Lachnoclostridium-10,* Ruminococcaceae and *Lactobacillus*), *Proteobacteria (Burkholderiales and Pseudomonas),* and *Bacteroidetes* were observed in females treated with Pb, Cd, and Zn. • The gut microbiota of adult males was more sensitive to exposure to Pb, Cd, and Zn than that of females. Exposure in males led to increased abundances of Aurantimonadaceae*, Rhizobium, Rhizobiaceae, Paracoccus, Methylobacterium, Methylobacteriaceae,* and Aurantimonadacea.	• Poor quality of the eggs was observed after exposure.
Richardson et al. (2018)	Sprague-Dawley rats	As (15, 22, or 31 mg/kg), Cd (35, 54, or 85 mg/kg), Co (27, 47, or 82 mg/kg), Cr (44, 62, or 88 mg/kg), Ni (177, 232, or 300 mg/kg)	Exposure to metals resulted in disturbed gut microbiota composition, but the specific taxa affected were not consistent. • The *Proteobacteria* phylum (Enterobactericeae) increased in abundance in response to exposure to high doses of As and Ni.	–

(Continued)

TABLE 4 | Continued

References	Animal model	Metal dose	Microbiota changes	Health effects
Studies in humans				
Shao and Zhu (2020)	Adults	As, Cd, Cu, Pb, Znc (environmental exposure)	Chronic exposure to As, Cd, Cu, Pb, and Zn resulted in disturbances of gut microbiotas in inhabitants of contaminated areas, particularly men. Increased Lachnospiraceae, *Eubacterium elegns*, Ruminococcaceae *UGG-014*, Erysipelotrichaceae *UCG-003, Tyzzerella 3, Bacteroides, Slackia, Italic, and Roseburia*. • Decrease in *Prevotella*.	–
Eggers et al. (2019)	Adults	Pb (environmental exposure)	Increases in microbial α-diversity and richness were associated with higher concentrations of Pb in urine. Proteobacteria abundance increaseds.	–

Cu, copper; Hg, mercury; Cr, chromium; Cd, cadmium; NO_3 –N, nitrate ion; Pb, lead; Zn, zinc; As, arsenic; Co, cobalt; Ni, nickel.

Eggers et al. (2019) examined the association between lead concentration in urine and gut composition in adults and found that increased lead levels were correlated with increased α-diversity and richness. In addition, differences in *Proteobacteria*, including members of *Burkholderiales*, as well as in β-diversity were significantly associated ($p = 0.003$) with differences in lead levels in urine.

Triclosan, Parabens

Triclosan (TCS) is a well-known EDC added to many consumer products intended to reduce or prevent bacterial contamination (Halden et al., 2017). Parabens are widely used as preservatives in cosmetics, personal care products, drugs, and foods (Quiros-Alcala et al., 2018). Triclosan and parabens have been showed to alter microbiota in different studies (**Table 5**). Hu et al. (2016) examined the effect of low-dose exposure to DEP, methylparaben (MPB), TCS and the effect of simultaneous exposure (MIX) in the gut bacterial composition in adolescent rats and found an increased relative abundance of *Bacteroidetes* (*Prevotella*) and reduced relative abundance of *Firmicutes* (*Bacilli*) in exposed rats versus controls. The authors also found an increased abundance of *Elusimicrobia* in rats exposed simultaneously to DEP and MPB, increased *Betaproteobacteria* in simultaneous exposure to MPB and MIX, and *Deltaproteobacteria* in TCS-exposed rats. Surprisingly, these differences in gut bacterial composition decreased diminished by adulthood despite continued exposure, suggesting that environmental exposure to these chemicals during adolescence has a strongest effect on the gut microbiome. They also observed that exposure during adolescence, especially to DEP and MPB, led to a slight but consistent reduction in the bodyweight, consistent with the reduced *Firmicutes/Bacteroidetes* ratio found in exposed adolescent rats. It has been reported that the gut microbiota of obese animals and humans shows a higher *Firmicutes*/*Bacteroidetes* ratio compared with normal-weight individuals, suggesting this ratio as a biomarker. However, the actual evidence of this association is not convincing (Magne et al., 2020).

In a zebrafish model Gaulke et al. (2016) found that TCS exposure resulted in alterations in the composition and ecological dynamics of gut microbial communities. TCS exposure was also related to rapid changes in microbiome structure and diversity, with disturbance of *Enterobacteriaceae*. TCS-induced changes in gut microbiota have also been found in other animal models, including fathead minnows (Narrowe et al., 2015), rats (Hu et al., 2016), and mice (Gao et al., 2017; Yang et al., 2018).

In contrast, only few studies have investigated the effects of TCS exposure on the gut microbiota in humans. Bever et al. (2018) found that fecal microbiota diversity in infants exposed to triclosan through to breast milk was different from that found in infant fed milk with non-detectable levels of TCS. In addition, higher relative abundance of genus *Dermabacter* was observed in children exposed to breast milk containing TCS. Ribado et al. (2017) reported that chronic exposure to TCS through toothpaste increased the relative abundance of broadly antibiotic-resistant *Proteobacteria* species in adults and in children with high TCS levels in urine.

TABLE 5 | Studies linking exposure to triclosan and parabens and microbiome changes.

References	Animal model	Triclosan and Paraben dose	Microbiota changes	Health effects
Studies in animals				
Gaulke et al. (2016)	Zebrafish	TCS (100 μg/g)	• Exposure to TCS led to a slight reduction in diversity, with significant decreases in α-diversity between days 4 and 7 in exposed fish. • Reduced abundance of *Enterobacteriaceae* and increased abundance of *Pseudomonas*.	–
Narrowe et al. (2015)	Fathead minnow	TCS (100 and 1,000 ng/L)	• Increase in α-diversity associated with TCS exposure.	• Exposure to TCS may induce long-term effects on the host organism.
Hu et al. (2016)	Sprague-Dawley rats	MPB (0.105 mg/kg) and TCS (0.05 mg/kg)	• The abundance of *Bacteroidetes* (*Prevotella*) and *Elusimicrobia* increases in both groups. • Firmicutes (*Bacilli*) abundance decreased in both groups. • Betaproteobacteria abundance increased in the group exposed to MPB. • Deltaproteobacteria increased in the group exposed to TCS.	• A subtle but constant reduction in body weight was observed in the young rats.
Yang et al. (2018)	C57BL/6 male mice	TCS (5–80 mg/kg)	• Beneficial bacteria like *Bifidobacterium* were reduced.	• Exposure to TCS led to low-grade colon inflammation and colitis and increased risk of colon cancer related to the presence of colitis.
Gao et al. (2017)	C57BL/6 mice	TCS (2 mg/L)	• After 4 weeks of exposure, α-diversity increased but it subsequently decreased after 9 weeks of exposure.	• The bacterial genes involved in stress response showed significant enrichment after exposure to TCS. • High enrichment of metal resistome in the gut microbiota, which is related to a reduced effectiveness of infection treatment.
Studies in humans				
Bever et al. (2018)	Infants	TCS (exposure through breast milk)	• Significant increases in the genus *Dermabacter*, order Rhodospirillales, and family Rhodospirillaceae were found in babies exposed to TCS through breast milk.	–
Ribado et al. (2017)	Infants and their mothers	TCS (environmental exposure and through breast milk)	• Enrichment of the phylum *Proteobacteria* in mothers exposed to TCS-containing toothpaste. • Enrichment of *Proteobacteria* in infants with higher TCS levels.	–

TCS, triclosan; MPB, methylparaben.

TABLE 6 | Studies linking exposure to polybrominated diphenyl ethers and microbiota changes.

References	Animal model	PBDE dose	Microbiota changes	Health effects
Studies in animals				
Chen et al. (2018b)	Zebrafish	PBDE mixture (DE-71) (5 ng/L)	• Higher relative abundance of Firmicutes and Bacteroidetes in the gut of male fish, but a lower Firmicutes/Bacteroidetes ratio was observed. • DE-71 led to decreased Bacteroidetes in the gut of female fish with a higher Firmicutes/Bacteroidetes ratio. • *Mycoplasma, Ruminiclostridium*, *unclassified* Firmicutes *sensu stricto* and *Fusobacterium* were not detected in the gut of male and female fish.	• In males, an alteration in intestinal health was observed due to exposure to DE-71, which led to disruptions of the neural signaling, of the integrity of the epithelial barrier, inflammatory response, oxidative stress and antioxidant capacity, as well as disruptions of the detoxifying capacity. • In females, the physiological activities of the intestine remained unchanged.
Wang et al. (2018)	Mice	PBDE-47 (0, 0.002 and 0.2 mg/kg)	• Exposure resulted in decreased abundance of *Bacteroidetes* and *Proteobacteria* and in an increase of *Actinobacteria* at the phylum level. • Exposure resulted in increased abundance of *Candidatus_Saccharimonas, Ruminococcaceae_UCG-013, Staphylococcus, Gemella, Eubacterium_nodatum_group, Corynebacterium_1* and *Paenalcaligenesen* and in a decrease in the abundance of *Turicibacter* and *Anaerotruncus* at the genus level.	• High fat diet-induced obesity increased as a result of the exposure to BDE-47. • Steatosis of the liver, disturbances in glucose homeostasis, metabolic dysfunction, and altered levels of gene mRNAs involved in lipid metabolism were found in mice fed high-fat diet and exposed BDE-47.
Li et al. (2017)	Male C57BL/6 mice	PBDE-47 (10–100 μmol/kg) and PBDE-99 (10–100 μmol/kg)	_	• Absence of gut microbiome increased PBDE-99-mediated upregulation of many genes involved in drug metabolism and it also affected hydroxylation of PBDEs. • Exposure to PBDE increased unconjugated bile acids in multiple bio-compartments in a gut microbiota-dependent manner.
Studies in humans				
Laue et al. (2019)	Children	PBDE-47, PBDE-99, PBDE-100, PBDE-153 (environmental exposure)	• Exposure to PBDE-99 was associated with a decrease in uncultured bacteria within the Ruminococcaceae *NK4A214* group and exposure to PBDE-47 led to differences in *Ruminococcus 2*.	_

PBDEs: Polybrominated diphenyl ethers; DE-71: PBDE mixture; PBDE-47: 2, 2′, 4, 4′-tetrabromodiphenil ether; PBDE-99: 2, 2′, 4, 4′, 5-pentabromodiphenil ether; PBDE-100: 2,2′,4,4′,6-pentabromodiphenyl ether; PBDE-153: 2,2′,4,4′,5,5′-Hexabromodiphenyl ether.

Polybrominated Diphenyl Ethers (PBDEs)

PBDEs are environmentally persistent chemicals widely used as flame retardants (Poston and Saha, 2019) that have been shown to alter microbiota (**Table 6**). In a zebrafish model, Chen et al. (2018b) showed that exposure to environmentally realistic concentrations of PBDEs resulted in alterations in the gut microbial community in a sex-dependent manner, significantly affecting zebrafish health. Wang et al. (2018) found that perinatal exposure to bromodiphenyl ether (BDE-47) in an obese rat model led to obesity, hepatic steatosis, and dysfunctional glucose homeostasis and metabolism. The authors also reported that exposure to BDE-47 led to changes in gut microbiota diversity and composition, and microbial metabolism. These exposure-related changes were stronger in mice on a high-fat diet. These findings suggest that early life exposure to BDE-47 at low doses of may stimulate obesity and the development of metabolic dysfunction.

Li et al. (2017) investigated whether exposure to PBDEs is associated with dysbiosis in standard and germ-free mice and reported that PBDE exposure resulted in a significant decrease in the alpha diversity of gut microbiome and modulated 45 bacterial species with increased *Akkermansia muciniphila* and Erysipelotrichaceae *Allobaculum* spp., which have shown antiinflammatory and antiobesity capacity. Lastly, they also found that PBDE exposure increased the amount of unconjugated bile acids in a gut microbiota-dependent manner.

Laue et al. (2019) compared the effects of PBDE perinatal exposure on the gut microbiome profiles with the effects of exposure in mid-childhood. Higher PBDE concentrations were related to lower abundances of uncultured bacteria in the *Ruminococcaceae NK4A214* group and with variable abundances of *Ruminococcus 2* species. These changes at the taxon-level did not lead to differences in within- or between-subject diversity. Lastly, exposures at delivery were not linked to differences in taxa.

CONCLUSION

Endogenous steroid hormones and EDC interact with gut microbiota through different pathways: (i) they could be directly metabolized by the gut microbiota after ingestion or after being conjugated in the liver, and (ii) they can interfere with the composition and/or metabolic activity of the gut microbiota. Both interactions may have an effect in host health. We propose that toxicological studies should consider the changes in the gut microbiota related to contaminant exposure and term the chemicals having an effect on gut microbiota as "microbiota disrupting chemicals." The risk of developing certain disorders associated with gut microbiota changes should be established by determining both the effects of the MDC on gut microbiota and the impact of microbiota changes on chemicals metabolism and host susceptibility.

Gut microbiota composition used in combination with the determination of serum, urinary and fecal levels of estrogens can be used as susceptibility or risk biomarkers for disease. Profiling of the gut microbiome could be taken a step further by performing metagenomic analysis to determine the levels of genes encoding β-glucuronidases and other enzymes involved in hormone metabolism in the context of hormone-related diseases. Novel hormone modulation methods involving modifications of the microbiome or control of hormone and EDC exposure may be very effective and provide an alternative to current treatments of hormone-dependent disorders. Additionally, the therapeutic effects of bacteria on the endobolome, which cluster biosynthetic and metabolic arsenal for estrogens, steroid hormones and/or endocrine disruptor chemicals, should also be considered for the design and development of biotherapeutic products. The endobolome plays a central role in the gut microbiota as seen by the amount of potentially endobolome-mediated diseases and thereby it can be considered an attractive diagnostic tool and therapeutic target for future research strategies that envisage the use of next generation of probiotics.

In any case, further animal controlled experiments, clinical trials and large epidemiological studies are required in order to establish the concatenated impact of the microbial disrupting chemical-microbiota-host health axis.

AUTHOR CONTRIBUTIONS

MA and AR: conceptualization. MA, AR, and YG-O: methodology, writing – original draft preparation, review, and editing. All authors have read and agreed to the published version of the manuscript.

FUNDING

This work was carried out within the frame of GP/EFSA/ENCO/380 2018/03/G04: OBEMIRISK: Knowledge platform for assessing the risk of Bisphenols on gut microbiota and its role in obesogenic phenotype: looking for biomarkers. This research was also funded by Spanish State Research Agency (SRA) EIN2019-103431, EIN2019-103082 and Proyecto cofinanciado FEDER-Consejería de Salud y Familias, Junta de Andalucía PE-0250-2019.

ACKNOWLEDGMENTS

The results presented in this article constitute part of YG-O doctoral thesis, performed in the Nutrition and Food Sciences Doctorate Program of the University of Granada.

REFERENCES

Adamovsky, O., Buerger, A. N., Vespalcova, H., Sohag, S. R., Hanlon, A. T., Ginn, P. E., et al. (2020). Evaluation of microbiome-host relationships in the Zebrafish gastrointestinal system reveals adaptive immunity is a target of bis(2-ethylhexyl) Phthalate (DEHP) Exposure. *Environ. Sci. Technol.* 54, 5719–5728. doi: 10.1021/acs.est.0c00628

Adlercreutz, H., Pulkkinen, M. O., Hamalainen, E. K., and Korpela, J. T. (1984). Studies on the role of intestinal bacteria in metabolism of synthetic and natural steroid-hormones. *J. Steroid Biochem. Mol. Biol.* 20, 217–229. doi: 10.1016/0022-4731(84)90208-5

Andujar, N., Galvez-Ontiveros, Y., Zafra-Gomez, A., Rodrigo, L., Alvarez-Cubero, M. J., Aguilera, M., et al. (2019). Bisphenol a analogues in food and their hormonal and obesogenic effects: a review. *Nutrients* 11:2136. doi: 10.3390/nu11092136

Ata, B., Yildiz, S., Turkgeldi, E., Perez-Brocal, V., Dinleyici, E. C., Moya, A., et al. (2019). The Endobiota study: comparison of vaginal, cervical and gut microbiota between women with stage 3/4 endometriosis and healthy controls. *Sci. Rep.* 9:2204. doi: 10.1038/s41598-019-39700-6

Bailey, M. T., and Coe, C. L. (2002). Endometriosis is associated with an altered profile of intestinal microflora in female rhesus monkeys. *Hum. Reprod.* 17, 1704–1708. doi: 10.1093/humrep/17.7.1704

Bajer, L., Kverka, M., Kostovcik, M., Macinga, P., Dvorak, J., Stehlikova, Z., et al. (2017). Distinct gut microbiota profiles in patients with primary sclerosing cholangitis and ulcerative colitis. *World J. Gastroenterol.* 23, 4548–4558. doi: 10.3748/wjg.v23.i25.4548

Baker, J. M., Al-Nakkash, L., and Herbst-Kralovetz, M. M. (2017). Estrogen gut microbiome axis: physiological and clinical implications. *Maturitas* 103, 45–53. doi: 10.1016/j.maturitas.2017.06.025

Banerjee, S., Tian, T., Wei, Z., Shih, N., Feldman, M. D., Alwine, J. C., et al. (2017). The ovarian cancer oncobiome. *Oncotarget* 8, 36225–36245. doi: 10.18632/oncotarget.16717

Bever, C. S., Rand, A. A., Nording, M., Taft, D., Kalanetra, K. M., Mills, D. A., et al. (2018). Effects of triclosan in breast milk on the infant fecal microbiome. *Chemosphere* 203, 467–473. doi: 10.1016/j.chemosphere.2018.03.186

Canani, R. B., Costanzo, M. D., Leone, L., Pedata, M., Meli, R., and Calignano, A. (2011). Potential beneficial effects of butyrate in intestinal and extraintestinal diseases. *World J. Gastroenterol.* 17, 1519–1528. doi: 10.3748/wjg.v17.i12.1519

Chen, K. L., and Madak-Erdogan, Z. (2016). Estrogen and microbiota crosstalk: Should we pay attention? *Trends Endocrinol. Metab.* 27, 752–755. doi: 10.1016/j.tem.2016.08.001

Chen, K. L. A., Liu, X., Zhao, Y. C., Hieronymi, K., Rossi, G., Auvil, L. S., et al. (2018). Long-term administration of conjugated estrogen and bazedoxifene decreased murine fecal beta-glucuronidase activity without impacting overall microbiome community. *Sci. Rep.* 8:8166. doi: 10.1038/s41598-018-26506-1

Chen, L., Guo, Y., Hu, C., Lam, P. K. S., Lam, J. C. W., and Zhou, B. (2018a). Dysbiosis of gut microbiota by chronic coexposure to titanium dioxide nanoparticles and bisphenol A: implications for host health in zebrafish. *Environ. Pollut.* 234, 307–317. doi: 10.1016/j.envpol.2017.11.074

Chen, L., Hu, C., Lai, N. L., Zhang, W., Hua, J., Lam, P. K. S., et al. (2018b). Acute exposure to PBDEs at an environmentally realistic concentration causes abrupt changes in the gut microbiota and host health of zebrafish. *Environ. Pollut.* 240, 17–26. doi: 10.1016/j.envpol.2018.04.062

Choi, S., Hwang, Y., Shin, M., and Yi, H. (2017). Difference in the gut microbiome between ovariectomy-induced obesity and diet-induced obesity. *J. Microbiol. Biotechnol.* 27, 2228–2236. doi: 10.4014/jmb.1710.10001

Claus, S., Guillou, H., and Ellero-Simatos, S. (2017). The gut microbiota: a major player in the toxicity of environmental pollutants? *NPJ Biofilms Microbiomes* 3:17001. doi: 10.1038/npjbiofilms.2017.1

Collden, H., Landin, A., Wallenius, V., Elebring, E., Fandriks, L., Nilsson, M. E., et al. (2019). The gut microbiota is a major regulator of androgen metabolism in intestinal contents. *Am. J. Physiol. Endocrinol. Metab.* 317, E1182–E1192. doi: 10.1152/ajpendo.00338.2019

Darbre, P. D. (2017). Endocrine disruptors and obesity. *Curr. Obes. Rep.* 6, 18–27. doi: 10.1007/s13679-017-0240-4

De Franciscis, P., Colacurci, N., Riemma, G., Conte, A., Pittana, E., Guida, M., et al. (2019). A nutraceutical approach to menopausal complaints. *Medicina* 55:544. doi: 10.3390/medicina55090544

DeLuca, J. A. A., Allred, K. F., Menon, R., Riordan, R., Weeks, B. R., Jayaraman, A., et al. (2018). Bisphenol-A alters microbiota metabolites derived from aromatic amino acids and worsens disease activity during colitis. *Exp. Biol. Med.* 243, 864–875. doi: 10.1177/1535370218782139

Doden, H., Pollet, R., Mythen, S., Wawrzak, Z., Devendran, S., Cann, I., et al. (2019). Structural and biochemical characterization of 20β-hydroxysteroid dehydrogenase from Bifidobacterium adolescentis strain L2-32. *J. Biol. Chem.* 294, 12040–12053. doi: 10.1074/jbc.RA119.009390

Eggers, S., Safdar, N., Sethi, A. K., Suen, G., Peppard, P. E., Kates, A. E., et al. (2019). Urinary lead concentration and composition of the adult gut microbiota in a cross-sectional population-based sample. *Environ. Int.* 133:105122. doi: 10.1016/j.envint.2019.105122

Ejtahed, H., and Hasani-Ranjbar, S. (2019). Neuromodulatory effect of microbiome on gut-brain axis; new target for obesity drugs. *J. Diabetes Metab. Disord.* 18, 263–265. doi: 10.1007/s40200-019-00384-4

Ervin, S., Li, H., Lim, L., Roberts, L., Liang, X., Mani, S., et al. (2019). Gut microbial β-glucuronidases reactivate estrogens as components of the estrobolome that reactivate estrogens. *J. Biol. Chem.* 294, 18586–18599. doi: 10.1074/jbc.RA119.010950

Falony, G., Joossens, M., Vieira-Silva, S., Wang, J., Darzi, Y., Faust, K., et al. (2016). Population-level analysis of gut microbiome variation. *Science* 352, 560–564. doi: 10.1126/science.aad3503

Feldman, B. J., and Feldman, D. (2001). The development of androgen-independent prostate cancer. *Nat. Rev. Cancer* 1, 34–45. doi: 10.1038/35094009

Fox, H. S. (1992). Androgen treatment prevents diabetes in nonobese diabetic mice. *J. Exp. Med.* 175, 1409–1412. doi: 10.1084/jem.175.5.1409

Fuhrman, B. J., Feigelson, H. S., Flores, R., Gail, M. H., Xu, X., Ravel, J., et al. (2014). Associations of the fecal microbiome with urinary estrogens and estrogen metabolites in postmenopausal women. *J. Clin. Endocrinol. Metab.* 99, 4632–4640. doi: 10.1210/jc.2014-2222

Fukui, H., Xu, X., and Miwa, H. (2018). Role of gut microbiota-gut hormone axis in the pathophysiology of functional gastrointestinal disorders. *J. Neurogastroenterol. Motil.* 24, 367–386. doi: 10.5056/jnm18071

Galvez-Ontiveros, Y., Paez, S., Monteagudo, C., and Rivas, A. (2020). Endocrine disruptors in food: impact on gut microbiota and metabolic diseases. *Nutrients* 12:1158. doi: 10.3390/nu12041158

Gao, B., Bian, X., Mahbub, R., and Lu, K. (2017a). Sex-specific effects of organophosphate diazinon on the gut microbiome and its metabolic functions. *Environ. Health Perspect.* 125, 198–206. doi: 10.1289/EHP202

Gao, B., Bian, X., Chi, L., Tu, P., Ru, H., and Lu, K. (2017b). Organophosphate diazinon altered quorum sensing, cell motility, stress response, and carbohydrate metabolism of gut microbiome. *Toxicol. Sci.* 157, 354–364. doi: 10.1093/toxsci/kfx053

Gao, B., Tu, P., Bian, X., Chi, L., Ru, H., and Lu, K. (2017). Profound perturbation induced by triclosan exposure in mouse gut microbiome: a less resilient microbial community with elevated antibiotic and metal resistomes. *BMC Pharmacol. Toxicol.* 18:46. doi: 10.1186/s40360-017-0150-9

Garcia-Gomez, E., Gonzalez-Pedrajo, B., and Camacho-Arroyo, I. (2013). Role of Sex Steroid Hormones in Bacterial-Host Interactions. *Biomed. Res. Int.* 2013:928290. doi: 10.1155/2013/928290

García-Mayor, R. V., Larrañaga Vidal, A., Docet Caamaño, M. F., and Lafuente Giménez, A. (2012). Disruptores endocrinos y obesidad: obesógenos. *Endocrinol. Nutr.* 59, 261–267. doi: 10.1016/j.endonu.2011.11.008

Gaulke, C. A., Barton, C. L., Proffitt, S., Tanguay, R. L., and Sharpton, T. J. (2016). Triclosan exposure is associated with rapid restructuring of the microbiome in adult zebrafish. *PLoS One* 11:e0154632. doi: 10.1371/journal.pone.0154632

Gillezeau, C., Alpert, N., Joshi, P., and Taioli, E. (2019). Urinary dialkylphosphate metabolite levels in US adults-national health and nutrition examination survey 1999-2008. *Int. J. Environ. Res. Public Health* 16:4605. doi: 10.3390/ijerph16234605

Golombos, D. M., Ayangbesan, A., O'Malley, P., Lewicki, P., Barlow, L., Barbieri, C. E., et al. (2018). The role of gut microbiome in the pathogenesis of prostate cancer: a prospective, pilot study. *Urology* 111, 122–128. doi: 10.1016/j.urology.2017.08.039

Guo, Y., Qi, Y., Yang, X., Zhao, L., Wen, S., Liu, Y., et al. (2016). Association between polycystic ovary syndrome and gut microbiota. *PLoS One* 11:e0153196. doi: 10.1371/journal.pone.0153196

Halden, R. U., Lindeman, A. E., Aiello, A. E., Andrews, D., Arnold, W. A., Fair, P., et al. (2017). The florence statement on Triclosan and Triclocarban. *Environ. Health Perspect.* 125:064501. doi: 10.1289/EHP1788

Harada, N., Hanaoka, R., Horiuchi, H., Kitakaze, T., Mitani, T., Inui, H., et al. (2016). Castration influences intestinal microflora and induces abdominal obesity in high-fat diet-fed mice. *Sci. Rep.* 6:23001. doi: 10.1038/srep23001

He, F., Zhai, J., Zhang, L., Liu, D., Ma, Y., Rong, K., et al. (2018). Variations in gut microbiota and fecal metabolic phenotype associated with fenbendazole and ivermectin tablets by 16s rRNA gene sequencing and lc/ms-based metabolomics in amur tiger. *Biochem. Biophys. Res. Commun.* 499, 447–453. doi: 10.1016/j.bbrc.2018.03.158

Hu, J., Raikhel, V., Gopalakrishnan, K., Fernandez-Hernandez, H., Lambertini, L., Manservisi, F., et al. (2016). Effect of postnatal low-dose exposure to environmental chemicals on the gut microbiome in a rodent model. *Microbiome* 4:26. doi: 10.1186/s40168-016-0173-2

Janosch, D., Dubbert, S., Eiteljoerge, K., Diehl, B. W. K., Sonnenborn, U., Passchier, L. V., et al. (2019). Anti-genotoxic and anti-mutagenic activity of *Escherichia coli* Nissle 1917 as assessed by *in vitro* tests. *Benef. Microbes* 10, 449–461. doi: 10.3920/BM2018.0113

Janssen, A. W. F., and Kersten, S. (2015). The role of the gut microbiota in metabolic health. *FASEB J.* 29, 3111–3123. doi: 10.1096/fj.14-269514

Javurek, A. B., Spollen, W. G., Johnson, S. A., Bivens, N. J., Bromert, K. H., Givan, S. A., et al. (2016). Effects of exposure to bisphenol A and ethinyl estradiol on the gut microbiota of parents and their offspring in a rodent model. *Gut Microbes* 7, 471–485. doi: 10.1080/19490976.2016.1234657

Jones, G. S., Feigelson, H. S., Falk, R. T., Hua, X., Ravel, J., Yu, G., et al. (2019). Mammographic breast density and its association with urinary estrogens and the fecal microbiota in postmenopausal women. *PLoS One* 14:e0216114. doi: 10.1371/journal.pone.0216114

Kelley, S. T., Skarra, D. V., Rivera, A. J., and Thackray, V. G. (2016). The gut microbiome is altered in a letrozole-induced mouse model of polycystic ovary syndrome. *PLoS One* 11:e0146509. doi: 10.1371/journal.pone.0146509

Knutie, S. A., Gabor, C., Kohl, K. D., and Rohr, J. R. (2018). Do host-associated gut microbiota mediate the effect of an herbicide on disease risk in frogs? *J. Anim. Ecol.* 87, 489–499. doi: 10.1111/1365-2656.12769

Kozik, A. J., Nakatsu, C. H., Chun, H., and Jones-Hall, Y. L. (2017). Age, sex, and TNF associated differences in the gut microbiota of mice and their impact on acute TNBS colitis. *Exp. Mol. Pathol.* 103, 311–319. doi: 10.1016/j.yexmp.2017.11.014

Kwa, M., Plottel, C. S., Blaser, M. J., and Adams, S. (2016). The intestinal microbiome and estrogen receptor-positive female breast cancer. *J. Natl. Cancer Inst.* 108:djw029. doi: 10.1093/jnci/djw029

Lahiji, M. R., Najafi, S., Janani, L., Yazdani, B., Razmpoosh, E., and Zarrati, M. (2020). The effect of synbiotic on glycemic profile and sex hormones in overweight and obese breast cancer survivors following a weight-loss diet: a randomized, triple-blind, controlled trial. *Clin. Nutr.* doi: 10.1016/j.clnu.2020.05.043 [Epub ahead of print].

Lai, K., Chung, Y., Li, R., Wan, H., and Wong, C. K. (2016). Bisphenol A alters gut microbiome: comparative metagenomics analysis. *Environ. Pollut.* 218, 923–930. doi: 10.1016/j.envpol.2016.08.039

Larsson, K., Lindh, C. H., Jonsson, B. A. G., Giovanoulis, G., Bibi, M., Bottai, M., et al. (2017). Phthalates, non-phthalate plasticizers and bisphenols in Swedish preschool dust in relation to children's exposure. *Environ. Int.* 102, 114–124. doi: 10.1016/j.envint.2017.02.006

Laue, H. E., Brennan, K. J. M., Gillet, V., Abdelouahab, N., Coull, B. A., Weisskopf, M. G., et al. (2019). Associations of prenatal exposure to polybrominated diphenyl ethers and polychlorinated biphenyls with long-term gut microbiome structure: a pilot study. *Environ. Epidemiol.* 3:e039. doi: 10.1097/EE9.0000000000000039

Lei, M., Menon, R., Manteiga, S., Alden, N., Hunt, C., Alaniz, R. C., et al. (2019). Environmental Chemical Diethylhexyl Phthalate Alters Intestinal Microbiota Community Structure and Metabolite Profile in Mice. *mSystems* 4:e00724-19. doi: 10.1128/mSystems.00724-19

Li, C. Y., Lee, S., Cade, S., Kuo, L., Schultz, I. R., Bhatt, D. K., et al. (2017). Novel interactions between gut microbiome and host drug-processing genes modify the hepatic metabolism of the environmental chemicals Polybrominated Diphenyl Ethers. *Drug Metab. Dispos.* 45, 1197–1214. doi: 10.1124/dmd.117.077024

Li, J., Fang, B., Pang, G., Zhang, M., and Ren, F. (2019). Age- and diet-specific effects of chronic exposure to chlorpyrifos on hormones, inflammation and gut microbiota in rats. *Pestic. Biochem. Physiol.* 159, 68–79. doi: 10.1016/j.pestbp.2019.05.018

Liang, X. M., Hu, Y. F., Yu, H. G., and Yang, K. D. (2008). [Effects of p,p '-DDE and beta-BHC on the apoptosis of Sertoli cells *in vitro*]. *Zhonghua Yu Fang Yi Xue Za Zhi* 42, 648–652.

Liang, Y., Zhan, J., Liu, D., Luo, M., Han, J., Liu, X., et al. (2019). Organophosphorus pesticide chlorpyrifos intake promotes obesity and insulin resistance through impacting gut and gut microbiota. *Microbiome* 7:19. doi: 10.1186/s40168-019-0635-4

Liu, R., Zhang, C., Shi, Y., Zhang, F., Li, L., Wang, X., et al. (2017). Dysbiosis of gut microbiota associated with clinical parameters in polycystic ovary syndrome. *Front. Microbiol.* 8:324. doi: 10.3389/fmicb.2017.00324

Lombardi, P., Goldin, B., Boutin, E., and Gorbach, S. L. (1978). Metabolism of androgens and estrogens by human fecal microorganisms. *J. Steroid Biochem. Mol. Biol.* 9, 795–801. doi: 10.1016/0022-4731(78)90203-0

Lopez-Moreno, A., and Aguilera, M. (2020). Probiotics dietary supplementation for modulating endocrine and fertility microbiota dysbiosis. *Nutrients* 12:757. doi: 10.3390/nu12030757

Magne, F., Gotteland, M., Gauthier, L., Zazueta, A., Pesoa, S., Navarrete, P., et al. (2020). The firmicutes/bacteroidetes ratio: a relevant marker of gut dysbiosis in obese patients? *Nutrients* 12:1474. doi: 10.3390/nu12051474

Magri, V., Boltri, M., Cai, T., Colombo, R., Cuzzocrea, S., De Visschere, P., et al. (2018). Multidisciplinary approach to prostatitis. *Arch. Ital. Urol. Nefrol. Androl.* 90, 227–248. doi: 10.4081/aiua.2018.4.227

Malaise, Y., Menard, S., Cartier, C., Gaultier, E., Lasserre, F., Lencina, C., et al. (2017). Gut dysbiosis and impairment of immune system homeostasis in perinatally-exposed mice to Bisphenol A precede obese phenotype development. *Sci. Rep.* 7:14472. doi: 10.1038/s41598-017-15196-w

Manabe, M., Kanda, S., Fukunaga, K., Tsubura, A., and Nishiyama, T. (2006). Evaluation of the estrogenic activities of some pesticides and their combinations using MtT/Se cell proliferation assay. *Int. J. Hyg. Environ. Health* 209, 413–421. doi: 10.1016/j.ijheh.2006.04.004

Markle, J. G. M., Frank, D. N., Mortin-Toth, S., Robertson, C. E., Feazel, L. M., Rolle-Kampczyk, U., et al. (2013). Sex differences in the gut microbiome drive hormone-dependent regulation of autoimmunity. *Science* 339, 1084–1088. doi: 10.1126/science.1233521

Mendler, A., Geier, F., Haange, S., Pierzchalski, A., Krause, J. L., Nijenhuis, I., et al. (2020). Mucosal-associated invariant T-Cell (MAIT) activation is altered by chlorpyrifos- and glyphosate-treated commensal gut bacteria. *J. Immunotoxicol.* 17, 10–20. doi: 10.1080/1547691X.2019.1706672

Mert, I., Walther-Antonio, M., and Mariani, A. (2018). Case for a role of the microbiome in gynecologic cancers: clinician's perspective. *J. Obstet. Gynaecol. Res.* 44, 1693–1704. doi: 10.1111/jog.13701

Mitra, A., MacIntyre, D. A., Marchesi, J. R., Lee, Y. S., Bennett, P. R., and Kyrgiou, M. (2016). The vaginal microbiota, human papillomavirus infection and cervical intraepithelial neoplasia: What do we know and where are we going next? *Microbiome* 4:58. doi: 10.1186/s40168-016-0203-0

Moreno-Indias, I., Sanchez-Alcoholado, L., Sanchez-Garrido, M. A., Martin-Nunez, G. M., Perez-Jimenez, F., Tena-Sempere, M., et al. (2016). Neonatal androgen exposure causes persistent gut microbiota dysbiosis related to metabolic disease in adult female rats. *Endocrinology* 157, 4888–4898. doi: 10.1210/en.2016-1317

Mulak, A., Tache, Y., and Larauche, M. (2014). Sex hormones in the modulation of irritable bowel syndrome. *World J. Gastroenterol.* 20, 2433–2448. doi: 10.3748/wjg.v20.i10.2433

Munyaka, P. M., Khafipour, E., and Ghia, J. (2014). External influence of early childhood establishment of gut microbiota and subsequent health implications. *Front. Pediatr.* 2:109. doi: 10.3389/fped.2014.00109

Murphy, E. A., Velazquez, K. T., and Herbert, K. M. (2015). Influence of high-fat diet on gut microbiota: a driving force for chronic disease risk. *Curr. Opin. Clin. Nutr. Metab. Care* 18, 515–520. doi: 10.1097/MCO.0000000000000209

Narrowe, A. B., Albuthi-Lantz, M., Smith, E. P., Bower, K. J., Roane, T. M., Vajda, A. M., et al. (2015). Perturbation and restoration of the fathead minnow gut microbiome after low-level triclosan exposure. *Microbiome* 3:6. doi: 10.1186/s40168-015-0069-6

Nelles, J. L., Hu, W., and Prins, G. S. (2011). Estrogen action and prostate cancer. *Expert Rev. Endocrinol. Metabol.* 6, 437–451. doi: 10.1586/EEM.11.20

Org, E., Mehrabian, M., Parks, B. W., Shipkova, P., Liu, X., Drake, T. A., et al. (2016). Sex differences and hormonal effects on gut microbiota composition in mice. *Gut Microbes* 7, 313–322. doi: 10.1080/19490976.2016.1203502

Pickard, J. M., Zeng, M. Y., Caruso, R., and Nunez, G. (2017). Gut microbiota: role in pathogen colonization, immune responses, and inflammatory disease. *Immunol. Rev.* 279, 70–89. doi: 10.1111/imr.12567

Plottel, C. S., and Blaser, M. J. (2011). Microbiome and malignancy. *Cell Host Microbe* 10, 324–335. doi: 10.1016/j.chom.2011.10.003

Porter, C. M., Shrestha, E., Peiffer, L. B., and Sfanos, K. S. (2018). The microbiome in prostate inflammation and prostate cancer. *Prostate Cancer Prostatic. Dis.* 21, 345–354. doi: 10.1038/s41391-018-0041-1

Poston, R. G., and Saha, R. N. (2019). Epigenetic effects of polybrominated diphenyl ethers on human health. *Int. J. Environ. Res. Public Health* 16:2703. doi: 10.3390/ijerph16152703

Quiros-Alcala, L., Buckley, J. P., and Boyle, M. (2018). Parabens and measures of adiposity among adults and children from the US general population: NHANES 2007-2014. *Int. J. Hyg. Environ. Health* 221, 652–660. doi: 10.1016/j.ijheh.2018.03.006

Ribado, J. V., Ley, C., Haggerty, T. D., Tkachenko, E., Bhatt, A. S., and Parsonnet, J. (2017). Household triclosan and triclocarban effects on the infant and maternal microbiome. *EMBO Mol. Med.* 9, 1732–1741. doi: 10.15252/emmm.201707882

Richardson, J. B., Dancy, B. C. R., Horton, C. L., Lee, Y. S., Madejczyk, M. S., Xu, Z. Z., et al. (2018). Exposure to toxic metals triggers unique responses from the rat gut microbiota. *Sci. Rep.* 8:6578. doi: 10.1038/s41598-018-24931-w

Ridlon, J. M., Ikegawa, S., Alves, J. M. P., Zhou, B., Kobayashi, A., Iida, T., et al. (2013). Clostridium scindens: a human gut microbe with a high potential to convert glucocorticoids into androgens. *J. Lipid Res.* 54, 2437–2449. doi: 10.1194/jlr.M038869

Rizzatti, G., Lopetuso, L. R., Gibiino, G., Binda, C., and Gasbarrini, A. (2017). *Proteobacteria*: a common factor in human diseases. *Biomed. Res. Int.* 2017:9351507. doi: 10.1155/2017/9351507

Rosenfeld, C. S. (2017). Gut dysbiosis in animals due to environmental chemical exposures. *Front. Cell. Infect. Microbiol.* 7:396. doi: 10.3389/fcimb.2017.00396

Ruan, Y., Wu, C., Guo, X., Xu, Z., Xing, C., Cao, H., et al. (2019). High doses of copper and mercury changed cecal microbiota in female mice. *Biol. Trace Elem. Res.* 189, 134–144. doi: 10.1007/s12011-018-1456-1

Rueda-Ruzafa, L., Cruz, F., Roman, P., and Cardona, D. (2019). Gut microbiota and neurological effects of glyphosate. *Neurotoxicology* 75, 1–8. doi: 10.1016/j.neuro.2019.08.006

Sabra, S., Malmqvist, E., Saborit, A., Gratacos, E., and Gomez-Roig, M. D. (2017). Heavy metals exposure levels and their correlation with different clinical forms of fetal growth restriction. *PLoS One* 12:e0185645. doi: 10.1371/journal.pone.0185645

Samavat, H., and Kurzer, M. S. (2015). Estrogen metabolism and breast cancer. *Cancer Lett.* 356, 231–243. doi: 10.1016/j.canlet.2014.04.018

Schug, T. T., Janesick, A., Blumberg, B., and Heindel, J. J. (2011). Endocrine disrupting chemicals and disease susceptibility. *J. Steroid Biochem. Mol. Biol.* 127, 204–215. doi: 10.1016/j.jsbmb.2011.08.007

Sfanos, K. S., Markowski, M. C., Peiffer, L. B., Ernst, S. E., White, J. R., Pienta, K. J., et al. (2018). Compositional differences in gastrointestinal microbiota in prostate cancer patients treated with androgen axis-targeted therapies. *Prostate Cancer Prostatic. Dis.* 21, 539–548. doi: 10.1038/s41391-018-0061-x

Shao, M., and Zhu, Y. (2020). Long-term metal exposure changes gut microbiota of residents surrounding a mining and smelting area. *Sci. Rep.* 10:4453. doi: 10.1038/s41598-020-61143-7

Shimizu, K., Muranaka, Y., Fujimura, R., Ishida, H., Tazume, S., and Shimamura, T. (1998). Normalization of reproductive function in germfree mice following bacterial contamination. *Exp. Anim.* 47, 151–158. doi: 10.1538/expanim.47.151

Shin, J., Park, Y., Sim, M., Kim, S., Joung, H., and Shin, D. (2019). Serum level of sex steroid hormone is associated with diversity and profiles of human gut microbiome. *Res. Microbiol.* 170, 192–201. doi: 10.1016/j.resmic.2019.03.003

Singh, R. K., Chang, H., Yan, D., Lee, K. M., Ucmak, D., Wong, K., et al. (2017). Influence of diet on the gut microbiome and implications for human health. *J. Transl. Med.* 15:73. doi: 10.1186/s12967-017-1175-y

Snedeker, S., and Hay, A. (2012). Do interactions between gut ecology and environmental chemicals contribute to obesity and diabetes? *Environ. Health Perspect.* 120, 332–339. doi: 10.1289/ehp.1104204

Tang, Q., Tang, J., Ren, X., and Li, C. (2020). Glyphosate exposure induces inflammatory responses in the small intestine and alters gut microbial composition in rats. *Environ. Pollut.* 261:114129. doi: 10.1016/j.envpol.2020.114129

Tetel, M. J., de Vries, G. J., Melcangi, R. C., Panzica, G., and O'Mahony, S. M. (2018). Steroids, stress and the gut microbiome-brain axis. *J. Neuroendocrinol.* 30, e12548. doi: 10.1111/jne.12548

Tremellen, K., and Pearce, K. (2012). Dysbiosis of Gut Microbiota (DOGMA) - A novel theory for the development of Polycystic Ovarian Syndrome. *Med. Hypotheses* 79, 104–112. doi: 10.1016/j.mehy.2012.04.016

Van de Wiele, T., Vanhaecke, L., Boeckaert, C., Peru, K., Headley, J., Verstraete, W., et al. (2005). Human colon microbiota transform polycyclic aromatic hydrocarbons to estrogenic metabolites. *Environ. Health Perspect.* 113, 6–10. doi: 10.1289/ehp.7259

Wang, D., Yan, J., Teng, M., Yan, S., Zhou, Z., and Zhu, W. (2018). In utero and lactational exposure to BDE-47 promotes obesity development in mouse offspring fed a high-fat diet: impaired lipid metabolism and intestinal dysbiosis. *Arch. Toxicol.* 92, 1847–1860. doi: 10.1007/s00204-018-2177-0

Wang, G., Chen, Q., Tian, P., Wang, L., Li, X., Lee, Y., et al. (2020). Gut microbiota dysbiosis might be responsible to different toxicity caused by Di-(2-ethylhexyl) phthalate exposure in murine rodents. *Environ. Pollut.* 261, 114164. doi: 10.1016/j.envpol.2020.114164

Wang, X., Shen, M., Zhou, J., and Jin, Y. (2019). Chlorpyrifos disturbs hepatic metabolism associated with oxidative stress and gut microbiota dysbiosis in adult zebrafish. *Comp. Biochem. Physiol. C Toxicol. Pharmacol.* 216, 19–28. doi: 10.1016/j.cbpc.2018.11.010

Xu, J., Huang, G., Nagy, T., Teng, Q., and Guo, T. L. (2019). Sex-dependent effects of bisphenol A on type 1 diabetes development in non-obese diabetic (n.d.) mice. *Arch. Toxicol.* 93, 997–1008. doi: 10.1007/s00204-018-2379-5

Xu, Z., and Knight, R. (2015). Dietary effects on human gut microbiome diversity. *Br. J. Nutr.* 113, S1–S5. doi: 10.1017/S0007114514004127

Yan, W., Hamid, N., Deng, S., Jia, P., and Pei, D. (2020). Individual and combined toxicogenetic effects of microplastics and heavy metals (Cd, Pb, and Zn) perturb gut microbiota homeostasis and gonadal development in marine medaka (Oryzias melastigma). *J. Hazard Mater.* 397, 122795. doi: 10.1016/j.jhazmat.2020.122795

Yang, H., Wang, W., Romano, K. A., Gu, M., Sanidad, K. Z., Kim, D., et al. (2018). A common antimicrobial additive increases colonic inflammation and colitis-associated colon tumorigenesis in mice. *Sci. Transl. Med.* 10:eaan4116. doi: 10.1126/scitranslmed.aan4116

Yang, Y., Yang, Y. S. H., Lin, I., Chen, Y., Lin, H., Wu, C., et al. (2019). Phthalate exposure alters gut microbiota composition and IgM vaccine response in human newborns. *Food Chem. Toxicol.* 132:110700. doi: 10.1016/j.fct.2019.110700

Yatsunenko, T., Rey, F. E., Manary, M. J., Trehan, I., Dominguez-Bello, M. G., Contreras, M., et al. (2012). Human gut microbiome viewed across age and geography. *Nature* 486, 222–227. doi: 10.1038/nature11053

Yuan, M., Li, D., Zhang, Z., Sun, H., An, M., and Wang, G. (2018). Endometriosis induces gut microbiota alterations in mice. *Hum. Reprod.* 33, 607–616. doi: 10.1093/humrep/dex372

Yuan, X., Pan, Z., Jin, C., Ni, Y., Fu, Z., and Jin, Y. (2019). Gut microbiota: an underestimated and unintended recipient for pesticide-induced toxicity. *Chemosphere* 227, 425–434. doi: 10.1016/j.chemosphere.2019.04.088

Yurkovetskiy, L., Burrows, M., Khan, A. A., Graham, L., Volchkov, P., Becker, L., et al. (2013). Gender Bias in Autoimmunity Is Influenced by Microbiota. *Immunity* 39, 400–412. doi: 10.1016/j.immuni.2013.08.013

Zhang, J., Sun, Z., Jiang, S., Bai, X., Ma, C., Peng, Q., et al. (2019). Probiotic Bifidobacterium lactis V9 Regulates the Secretion of Sex Hormones in Polycystic Ovary Syndrome Patients through the Gut-Brain Axis. *mSystems* 4:e00017-19. doi: 10.1128/mSystems.00017-19

Zhang, L., Day, A., McKenzie, G., and Mitchell, H. (2006). Nongastric *Helicobacter* Species detected in the intestinal tract of children. *J. Clin. Microbiol.* 44, 2276–2279. doi: 10.1128/JCM.02017-05

Zhang, M., and Yang, X. (2016). Effects of a high fat diet on intestinal microbiota and gastrointestinal diseases. *World J. Gastroenterol.* 22, 8905–8909. doi: 10.3748/wjg.v22.i40.8905

Zhang, Y., Li, Z., Kholodkevich, S., Sharov, A., Chen, C., Feng, Y., et al. (2020). Effects of cadmium on intestinal histology and microbiota in freshwater crayfish (Procambarus clarkii). *Chemosphere* 242:125105. doi: 10.1016/j.chemosphere.2019.125105

Zhao, Y., Zhou, C., Wu, C., Guo, X., Hu, G., Wu, Q., et al. (2020). Subchronic oral mercury caused intestinal injury and changed gut microbiota in mice. *Sci. Total Environ.* 721:137639. doi: 10.1016/j.scitotenv.2020.137639

Zheng, R., Chen, X., Ren, C., Teng, Y., Shen, Y., Wu, M., et al. (2020). Comparison of the characteristics of intestinal microbiota response in Bufo gargarizans tadpolesxposure to the different environmental chemicals (Cu, Cr, Cd and NO3-N). *Chemosphere* 247, 125925. doi: 10.1016/j.chemosphere.2020.125925

Zhou, C., Xu, P., Huang, C., Liu, G., Chen, S., Hu, G., et al. (2020). Effects of subchronic exposure of mercuric chloride on intestinal histology and microbiota in the cecum of chicken. *Ecotoxicol. Environ. Saf.* 188:109920. doi: 10.1016/j.ecoenv.2019.109920

Zhu, J., Liao, M., Yao, Z., Liang, W., Li, Q., Liu, J., et al. (2018). Breast cancer in postmenopausal women is associated with an altered gut metagenome. *Microbiome* 6:136. doi: 10.1186/s40168-018-0515-3

Zoeller, R. T., Bergman, A., Becher, G., Bjerregaard, P., Bomman, R., Brandt, I., et al. (2016). The path forward on endocrine disruptors requires focus on the basics. *Toxicol. Sci.* 149:272. doi: 10.1093/toxsci/kfv255

Conflict of Interest: The authors declare that the research was conducted in the absence of any commercial or financial relationships that could be construed as a potential conflict of interest.

Copyright © 2020 Aguilera, Gálvez-Ontiveros and Rivas. This is an open-access article distributed under the terms of the Creative Commons Attribution License (CC BY). The use, distribution or reproduction in other forums is permitted, provided the original author(s) and the copyright owner(s) are credited and that the original publication in this journal is cited, in accordance with accepted academic practice. No use, distribution or reproduction is permitted which does not comply with these terms.

frontiers in Physiology

ORIGINAL RESEARCH
published: 18 January 2021
doi: 10.3389/fphys.2020.577237

Acacetin Ameliorates Experimental Colitis in Mice via Inhibiting Macrophage Inflammatory Response and Regulating the Composition of Gut Microbiota

Junyu Ren[1†], Bei Yue[1†], Hao Wang[1†], Beibei Zhang[1], Xiaoping Luo[1], Zhilun Yu[1], Jing Zhang[1], Yijing Ren[1], Sridhar Mani[2], Zhengtao Wang[1] and Wei Dou[1*]*

[1] The MOE key Laboratory of Standardization of Chinese Medicines, Shanghai Key Laboratory of Compound Chinese Medicines, and the SATCM key Laboratory of New Resources and Quality Evaluation of Chinese Medicines, Institute of Chinese Materia Medica, Shanghai University of Traditional Chinese Medicine (SHUTCM), Shanghai, China, [2] Department of Medicine and Genetics, Albert Einstein College of Medicine, The Bronx, NY, United States

OPEN ACCESS

Edited by:
Margarita Aguilera,
University of Granada, Spain

Reviewed by:
Karen Yvonne Stokes,
Louisiana State University Health Shreveport, United States
Naoki Asano,
Tohoku University, Japan

***Correspondence:**
Zhengtao Wang
ztwang@shutcm.edu.cn;
wzhengtao@yahoo.com
Wei Dou
douwei123456@126.com

[†] These authors have contributed equally to this work

Specialty section:
This article was submitted to Gastrointestinal Sciences, a section of the journal Frontiers in Physiology

Received: 29 June 2020
Accepted: 28 December 2020
Published: 18 January 2021

Citation:
Ren J, Yue B, Wang H, Zhang B, Luo X, Yu Z, Zhang J, Ren Y, Mani S, Wang Z and Dou W (2021) Acacetin Ameliorates Experimental Colitis in Mice via Inhibiting Macrophage Inflammatory Response and Regulating the Composition of Gut Microbiota. Front. Physiol. 11:577237. doi: 10.3389/fphys.2020.577237

Acacetin, a natural dietary flavonoid abundantly found in acacia honey and citrus fruits, reportedly exerts several biological effects, such as anti-tumor, anti-inflammatory, and anti-oxidative effects. However, the effects of acacetin on intestinal inflammation remain unclear. We sought to investigate whether acacetin ameliorates inflammatory bowel disease (IBD) in mice with dextran sulfate sodium (DSS)-induced ulcerative colitis (UC). Our results suggest that acacetin alleviates the clinical symptoms of DSS-induced colitis, as determined by body weight loss, diarrhea, colon shortening, inflammatory infiltration, and histological injury. Further studies showed that acacetin remarkably inhibited both the macrophage inflammatory response *in vitro* and levels of inflammatory mediators in mice with colitis. In addition, some features of the gut microbiota were disordered in mice with DSS-induced colitis, as evidenced by a significant reduction in microbiota diversity and a marked shift in bacterial profiles. However, acacetin treatment improved this imbalance and restored gut microbiota to levels that were similar to those in normal mice. In conclusion, our work presents evidence that acacetin attenuates DSS-induced colitis in mice, at least in part, by inhibiting inflammation and regulating the intestinal microbiota.

Keywords: ulcerative colitis, gut microbiota, inflammatory mediators, dextran sulfate sodium, acacetin

INTRODUCTION

Ulcerative colitis (UC) is a major form of inflammatory bowel disease (IBD), characterized by continuous and diffuse inflammatory lesions of the colorectal mucosa. The original distribution of UC included European and American countries. However, with the development of global industrialization, as well as changing lifestyles and the living environment, UC has gradually become a common disease worldwide. In developing countries with large populations, the incidence of UC increases each year, which causes considerable mental stress and brings an economic burden to the affected patients (Kaplan, 2015; Ananthakrishnan et al., 2018). Abdominal

pain, diarrhea and mucopurulent bloody stools are the main clinical manifestations of UC, which usually first affects the rectum and then spreads to the whole colon (Sun B. et al., 2018). The etiology of UC is unclear and it is thought to be influenced by a combination of several factors, such as genetic susceptibility, impaired intestinal integrity, dysfunctional immune responses, and environmental pathogens (Zhang et al., 2014; Ramos and Papadakis, 2019). Several treatments have been developed for UC, including glucocorticoids, sulfasalazine, and immunosuppressive drugs (Hu et al., 2019). However, the clinical application of these drugs in long-term treatment is limited by their adverse effects and the high recurrence rates observed, which necessitates the development of novel therapies or complementary and alternative medicine for IBD.

In the past few decades, an increasing number of studies have suggested that alterations in the composition of gut microbiota can play key roles in the pathogenesis of UC. Patients with UC are often characterized by a damaged intestinal mucosal barrier, reduced microbial diversity, and disrupted balance of "harmful" and "protective" bacteria in the intestine (Kostic et al., 2014; Kiely et al., 2018). In particular, the composition of three major bacterial phyla in the gut microbiota are reportedly disturbed in patients with UC, as manifested by a reduced proportion of Firmicutes and Bacteroidetes, and an increased proportion of Proteobacteria (Smits et al., 2013; Matsuoka and Kanai, 2015). The transplantation of fecal bacteria and probiotic therapy in patients with UC are reportedly effective therapeutic approaches, and have shown promising outcomes in clinical practice (Zuo and Ng, 2018; Burrello et al., 2019; Khan et al., 2019). Furthermore, the disturbance of intestinal flora may serve as a major factor in the development of UC. Disordered gut microbiota may damage the intestinal barrier, promote intestinal permeability, activate the immune system, and ultimately contribute to the occurrence and progression of UC (Ott, 2004; Kostic et al., 2014; Kiely et al., 2018).

Epidemiological evidence suggests that increased dietary intake of flavonoid-rich fruits and vegetables is associated with a lower risk of IBD (Hu et al., 2019). Flavonoid compounds comprise a large family of hydroxylated polyphenolic molecules that are abundant in plants and have potential therapeutic potency in IBD (Salaritabar et al., 2017). Acacetin (5,7-dihydroxy-4'-methoxyflavone), a flavone widely recognized as an important bioactive constituent of acacia honey and citrus fruits, reportedly exerts protective effects on the gastrointestinal tract (Zhang et al., 2017; Yin et al., 2019). Acacetin can be isolated from the *Saussurea involucrata* plant (Liou et al., 2017), damiana (*Turnera diffusa*), and black locust (*Robinia pseudoacacia*) (Punia et al., 2017; Prasad et al., 2020). In addition, acacetin reportedly has various pharmacological activities, including antioxidant, anti-inflammatory, and anti-tumor activities (Xiao et al., 2019). However, its effects in UC and the associated underlying mechanisms remain unknown. In this study, we present evidence that acacetin could relieve UC-associated symptoms in mice, and show that the attenuated effects were mediated, at least in part, by inhibiting the macrophage inflammatory response and regulating the composition of gut microbiota.

MATERIALS AND METHODS

Bone marrow-derived macrophages (BMDMs) culture and treatment, and immunohistochemical staining assay details are mentioned in Supplemental Methods.

Materials

Acacetin ($C_{16}H_{12}O_5$, molecular weight: 284.26, high-performance liquid chromatography purity ≥98%) was purchased from Chengdu Biopurify Phytochemicals Ltd. Dextran sulfate sodium (DSS) (molecular mass, 36–50 kDa) was purchased from MP Biochemical (Irvine, CA, United States). RAW264.7 mouse macrophage cells were purchased from the American Type Culture Collection (ATCC, Manassas, VA, United States). Dulbecco's modified Eagle's medium (DMEM), 100 U/ml penicillin/streptomycin and fetal bovine serum (FBS) were purchased from Gibco BRL (Grand Island, NY, United States). Diethylpyrocarbonate-treated water, lipopolysaccharide (LPS), dimethyl sulfoxide, paraformaldehyde, and diaminobenzidine were obtained from Sigma-Aldrich (Shanghai, China). The enhanced chemiluminescence (ECL) detection kit was obtained from Millipore (Billerica, MA, United States). Rabbit antibodies to inducible nitric oxide synthase (iNOS) (#13120), cyclooxygenase-2 (COX-2) (#12282), tumor necrosis factor alpha (TNF-α) (#3707S), and β-actin (#4970) were obtained from Cell Signaling Technology (Danvers, MA, United States). Rabbit antibodies to interleukin 6 (IL-6) (ab83339) were obtained from Abcam (Cambridge, MA, United States). Trizol and the SuperScript II Reverse Transcriptase kit were purchased from Thermo Scientific Inc., (Waltham, MA, United States). The SYBR Premix ExTaq Mix was purchased from Takara Biotechnology (Shiga, Japan). The cell counting kit 8 (CCK-8) assay kit was purchased from Meilun Biological Technology Co., Ltd. All other reagents were obtained from Thermo Fisher Scientific (Waltham, MA, United States).

Mice and DSS-Induced Colitis

Healthy, female C57BL/6 mice (20 ± 2 g), 6–8 weeks old, were purchased from Shanghai Laboratory Animal Center, they were maintained under specific pathogen-free conditions at a fixed temperature range of 23–25°C and relative humidity of 55 ± 10%, with a 12-h light/dark cycle. All mice were allowed to acclimatize for 7 days after arrival and supplied *ad libitum* a standard dry diet and tap water. All animal study protocols were approved and carried out in accordance with the principles of the declaration recommendations of the Animal Experimentation Ethics Committee at Shanghai University of Traditional Chinese Medicine (Animal license key: PZSHUTCM190315022).

As described previously (Dou et al., 2014), the experiment lasted for 9 days. Acute experimental colitis was induced in mice by administering drinking water containing 3.5% (w/vol) DSS for 7 days, while control mice received drinking water only. Acacetin was dissolved in 0.5% methylcellulose at dosages of 50 and 150 mg/kg. Mice were randomly distributed into the following five groups (n = 10 mice per group): Group 1 was treated as vehicle controls, which were administered 100 μL of 0.5% (wt/vol) methylcellulose by oral gavage once per day; Group

2 was the acacetin group, which was administered acacetin at a daily dose of 150 mg/kg throughout the experiment; Group 3 was the DSS group, which was administered 3.5% DSS in the drinking water from day 3 to day 9 and 100 μL of 0.5% (wt/vol) methylcellulose by oral gavage once per day; Groups 4 and 5 received acacetin at doses of 50 and 150 mg/kg/day per body weight, respectively, by oral gavage from day 1 to day 9.

Histological Assessment of Colitis

Mice were monitored and daily records were maintained for changes in body weight, diarrhea, and bloody stools. Mice were sacrificed under anesthesia on day 9, and 4 h after the last gavage. The entire colon was then removed and its length was measured. The distal colon was resected, fixed in 10% formaldehyde overnight, and embedded in paraffin. The paraffin-embedded colon sections were stained with hematoxylin and eosin for histological evaluation. Histological injury was evaluated blindly by a combination of inflammatory cell infiltration (score 0–3) and mucosal damage (score 0–3), as described previously (Zhang et al., 2015).

Fecal Microbiota 16S rRNA Gene Sequencing

Mice feces were collected and stored at −80°C. Total genomic DNA was extracted from fecal samples using the E.Z.N.A.® Soil DNA kit (Omega Bio-tek, GA, United States) according to the manufacturer's protocols. The concentration and quality of DNA were checked using the NanoDrop 2000 UV-Vis spectrophotometer (Thermo Scientific, Wilmington, DE, United States). The V3–V4 regions of the bacterial 16S rRNA were amplified with the universal primers, 338F (5′-ACT CCTACGGGAGGCAGCAG-3′) and 806R (5′-GGACTACH VGGGTWTCTAAT-3′) using a thermocycler PCR system (GeneAmp 9700 ABI, Carlsbad, CA, United States). The protocol included amplification at 95°C for 3 min in the first instance, followed by 27 cycles (denaturation at 95°C for 30 s, annealing at 55°C for 30 s, and elongation at 72°C for 45 s), and a final extension (72°C, 10 min). Sequencing and data analysis were then performed on the Illumina MiSeq platform (Illumina, San Diego, CA, United States) according to the standard protocol of Majorbio Bio-Pharm Technology Co., Ltd (Majorbio, Shanghai, China). Sequence similarities of samples ≥97% were classified as the same operational taxonomic units (OTUs). The taxonomy of each 16S rRNA gene sequence was analyzed via the RDP Classifier algorithm against the Silva (SSU123) 16S rRNA database using a 70% confidence threshold.

Immunoblotting Analysis

Proteins extracted from colon tissues (1–1.5 cm proximal to the anus) and cultured cells were homogenized and lysed in cold radioimmunoprecipitation assay buffer with a suitable concentration of protease and phosphatase inhibitor cocktail tablets. The homogenate was then centrifuged (4°C, 12000 *g*, 15 min) and the supernatant was collected. The total protein concentration was determined via the bicinchoninic acid assay. Total protein (30 mg) from each sample was prepared and separated using either 10% or 12% SDS-PAGE, and subsequently transferred to 0.2 μm polyvinylidene fluoride membranes. Membranes were blocked with 5% (w/v) skim milk for 2 h at 25°C, and incubated overnight with primary antibodies against iNOS, COX-2, IL-6, TNF-α, or β-actin. The membranes were then washed three times with phosphate-buffered saline with Tween® for 10 min. The corresponding HRP-conjugated secondary antibody was added and membranes were further incubated for 1 h. The immunoreactive bands were observed with the aid of an ECL detection reagent and the images of blots were analyzed on a GS-700 imaging densitometer (Bio-Rad, CA, United States). The housekeeping gene, β-actin, was used as an internal control.

Quantitative Real-Time PCR (qPCR) Analysis

All experimental procedures followed the respective kit manufacturer's protocols. Total RNA was extracted from colon samples using the TRIzol reagent. Complementary DNA (cDNA) was reverse transcribed using the SuperScript II Reverse Transcriptase kit and 1.5 μg total RNA from each sample. Primers for the inflammatory mediators and internal reference were as follows: interleukin 1 beta (IL-1β): forward, 5′-ATTGTGGCTGTGGAGAAGAAGA-3′, reverse, 5′-TGAAG GAAAAGAAGGTG-3′; IL-6: forward, 5′-GCCTTCCCTACTTC ACAA-3′, reverse, 5′-ACAACTCTTTTCTCATTTCCAC-3′; iNOS: forward, 5′-GTCCTACACCACACCAAACT-3′, reverse, 5′-ATCTCTGCCTATCCGTCTC-3′; COX-2: forward, 5′-ACAA CAACTCCATCCTCCT-3′, reverse, 5′-GGTATTTCATCTCTCT GCTCTG-3′; TNF-α: forward, 5′-CTCTTCTCATTCCTGCT TGT-3′, reverse, 5′-GTGGTTTGTGAGTGTGAGG-3′; and β-actin: forward, 5′-GGGAAATCGTGCGTGAC-3′, reverse, 5′-AGGCTGGAAAAGAGCCT-3′. The qPCR followed the protocol of the Takara SYBR Green Master Mix Kit and was quantitatively analyzed using the ABI Prism 7900HT Sequence Detection System (Life Technologies, Carlsbad, CA, United States). The internal control was β-actin.

Cell Culture and Cell Viability Assay

The RAW264.7 cells were cultured in Dulbecco's modified Eagle Medium supplemented with 10% fetal bovine serum and a mixture of antibiotics (100 units/mL penicillin and streptomycin) under 5% CO_2 at 37°C. The RAW264.7 cells (2×10^5/well) were seeded in a 96-well plate overnight. Cells were subsequently incubated with a wide dose range of acacetin (0, 5, 10, 15, 20, 25, 30, 35, 40, and 45 μmol/L) for 24 h. Cell viability was determined using a CCK-8 assay kit. A volume of 10 μL of the CCK-8 solution was added to each well, which was then incubated for 30 min at 37°C. Absorbance was measured at 450 nm using a microplate reader.

Measurement of Nitric Oxide (NO) Production

The RAW264.7 cells were seeded in a 96-well plate at a density of 1×10^5 cells/well, and then incubated with different doses of acacetin (0, 5, 10, 15, 20, 25, 30, and 40 μmol/L) for 2 h, prior

to stimulation with LPS (1 μg/mL) for an additional 24 h. The cell culture media were collected and the Griess reagent was used to detect NO production. Absorbance was measured at 540 nm using a microplate reader.

Statistics

All data were presented as the mean ± SEM. Differences between groups were analyzed with one-way analysis of variance using the GraphPad Prism 7 software (GraphPad Software, La Jolla, CA, United States). All p-values < 0.05 (two-sided) were considered significant. All 16S rDNA sequencing data were analyzed on the Majorbio I-Sanger Cloud Platform online (www.i-sanger.com).

RESULTS

Acacetin Ameliorated DSS-Induced Acute Colitis in Mice

The mice with DSS-induced colitis showed significant weight loss and diarrhea, while mice treated with acacetin (50 or 150 mg/kg) showed significantly milder colitis symptoms (**Figures 1A,B**). As with other indexes, such as body weight, diarrhea, and colon length, the length of the colon in the DSS group was significantly shortened compared with the other four groups. After the administration of acacetin (50 or 150 mg/kg), the reduction in colon length was reversed (**Figures 1C,D**). No significant differences in body weight and colon length were observed between the control group and acacetin treatment group (**Figures 1A–D**). In addition, no signs of marked inflammation were observed in the intestines of the control group or acacetin (alone) treatment group, based on macroscopic histopathological analysis. However, intestinal tissue injury was apparent in the colon of the DSS model group, which showed severe epithelial damage, abnormal crypt structures, and extensive neutrophilic infiltration. Acacetin (50 or 150 mg/kg) treatment alleviated the loss of mucosal architecture, ulcerations, and inflammatory infiltration (**Figures 2A,B**). Specifically, acacetin (50 mg/kg) produced the best phenotypes, and the 50 mg/kg acacetin treatment group was thus applied for subsequent experimental analyses. Collectively, these results suggest that acacetin could ameliorate the symptoms of DSS-induced colitis.

Acacetin Inhibited the Production of Inflammatory Mediators in Macrophages

Macrophages are the major source of proinflammatory mediators when inflammation occurs in the intestine (Yan et al., 2018). Therefore, we used RAW264.7 mouse macrophages to evaluate the anti-inflammatory effects of acacetin *in vitro*. We used the CCK-8 kit to test the cytotoxicity of acacetin on RAW264.7 cells. The results showed that acacetin was almost non-cytotoxic at dosages up to 45 μmol/L (**Figure 3A**). The iNOS in macrophages can activate the secretion of NO in inflammatory states (Jiang et al., 2020). Our results show that acacetin treatment can reduce the production of NO, as well as the protein levels of iNOS and COX-2 in LPS-induced RAW267.4 cells in a dose-dependent manner (**Figures 3B–D**). We quantified the mRNA expression of iNOS and COX-2 in LPS-stimulated macrophages. Acacetin treatment was found to attenuate the mRNA levels of iNOS and COX-2 in LPS-induced RAW264.7 cells (**Figure 3E**). In addition, acacetin treatment also decreased the secretion of NO, as well as the protein level of iNOS in IFN-γ and LPS induced bone marrow-derived macrophages (BMDMs) (**Supplementary Figure 1**). Hence, acacetin was able to inhibit the production of inflammatory mediators in RAW264.7 cells and BMDM cells.

Acacetin Decreased Macrophage Infiltration and the Levels of Inflammatory Mediators in Mice With Colitis

To assess the potential innate immune influence of acacetin on DSS-induced colitis, we examined the macrophage infiltration by immunohistochemical staining of the macrophage markers F4/80. We found that the infiltration of macrophages expressing F4/80 in colon tissue was significantly decreased by acacetin treatment compared with colitis mice (**Supplementary Figure 2**). Several studies suggest that COX-2, iNOS, IL-6, and TNF-α are important proinflammatory mediators associated with the acute phase of IBD (Papadakis and Targan, 2000; Neurath, 2014). Therefore, we evaluated the effects of acacetin on the production of inflammatory mediators *in vivo*. As illustrated in **Figure 4A**, the mRNA levels of IL-1β, TNF-α, iNOS, IL-6, and iNOS were markedly increased in mice with DSS-induced colitis. However, acacetin treatment significantly reduced the mRNA expression of inflammatory mediators. On the other hand, immunoblots showed that DSS treatment led to a marked increase in the protein expression of COX-2 and iNOS in colonic tissue. However, the administration of acacetin markedly reduced the expression of COX-2 and iNOS (**Figures 4B,C**). These results suggest that acacetin could reduce the production of inflammatory mediators in mice with DSS-induced colitis.

Acacetin Regulated the Gut Microbiota Composition

To investigate the possible effects of acacetin on DSS-induced changes in the composition of intestinal microbiota, we analyzed fecal samples through 16S rRNA sequencing. The principal component analysis showed a noticeably separate cluster between the DSS group and the control group. A similar phenomenon was observed in comparisons of the DSS group and DSS + acacetin group (**Figures 5A–D**). In addition, acacetin treatment recovered the community diversity and significantly shifted the gut microbiota structure in the PC1 direction in mice with DSS-induced colitis. The Shannon index revealed that DSS treatment resulted in a significant decline in intestinal microbial community diversity, compared with the control or acacetin (alone) treatment groups (**Figure 5B**).

Regarding the distribution of species at the level of the phylum in the bar plot, *Firmicutes*, *Bacteroidetes*, *Epsilonbacteraeota*, *Proteobacteria*, *Deferribacteres*, and *Actinobacteria* were the representative phyla among the fecal samples of each group. In the DSS (alone) treatment group, *Proteobacteria* and *Deferribacteres* were enriched, while *Firmicutes* were

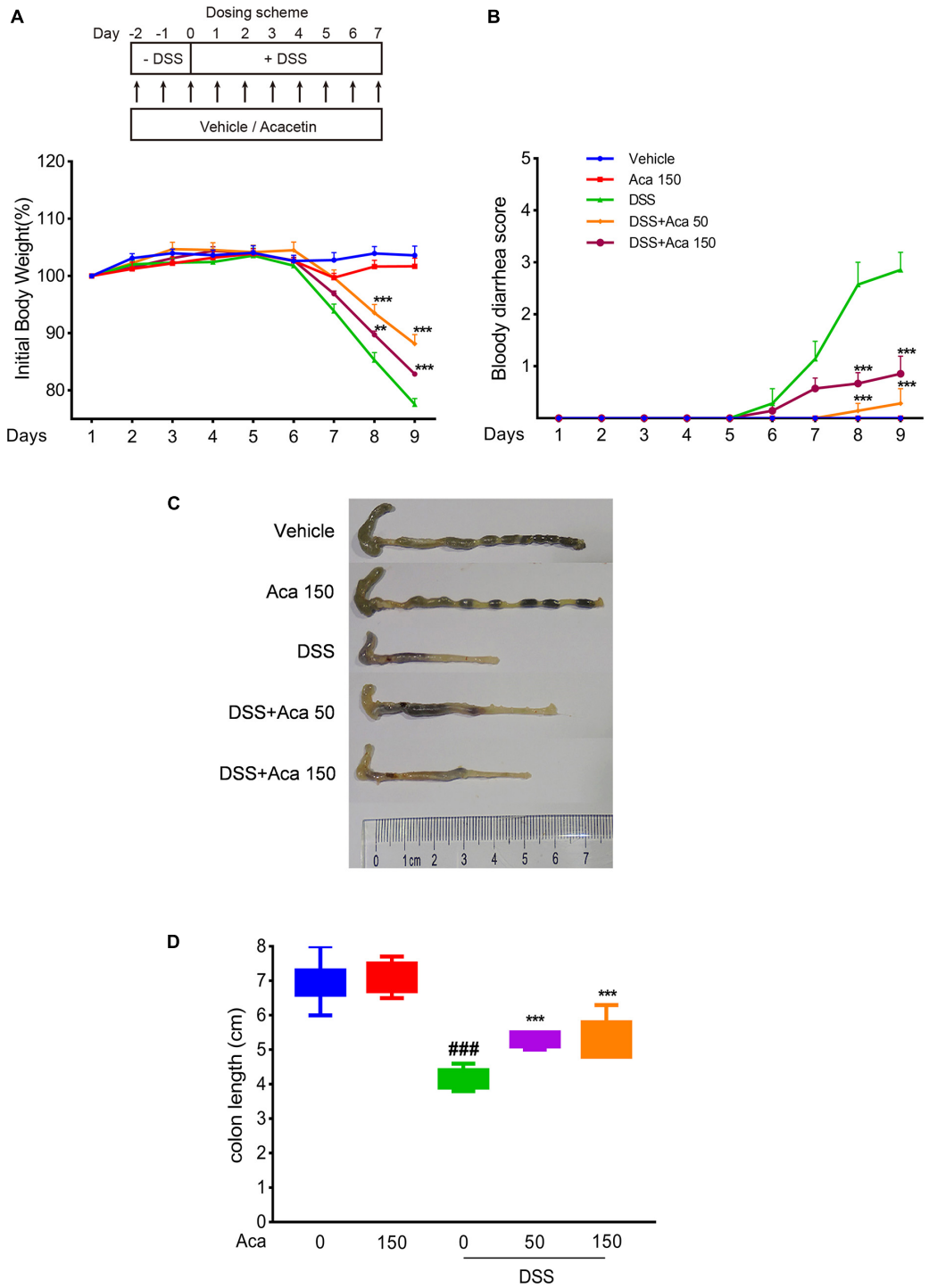

FIGURE 1 | Acacetin ameliorated weight loss, bloody diarrhea, and colon shortening in dextran sulfate sodium (DSS)-treated mice. **(A)** Mice body weight changes after induction of colitis by DSS. The data were plotted as a percentage of the weight at baseline. **(B)** Bloody diarrhea score. The data were plotted as scores for bloody diarrhea following DSS treatment at different time points. Macroscopic observation **(C)** and assessment of colon shortening **(D)** after DSS treatment. Data were expressed as the mean ± SEM (n = 7 mice in each group). $^{**}p < 0.005$, $^{***}p < 0.001$ vs. the DSS group; $^{\#\#\#}p < 0.001$ vs. the vehicle group.

reduced (**Figures 6A,B**). The proportion of the aforementioned microbiota with changed levels was reversed after acacetin treatment (**Figure 6B**). On the other hand, the increased abundance of *Bacteroidaceae*, *Deferribacteraceae*, and *Enterobacteriaceae* in the DSS-treated group was reversed at the level of the phylum after acacetin administration (**Figures 6A,B**).

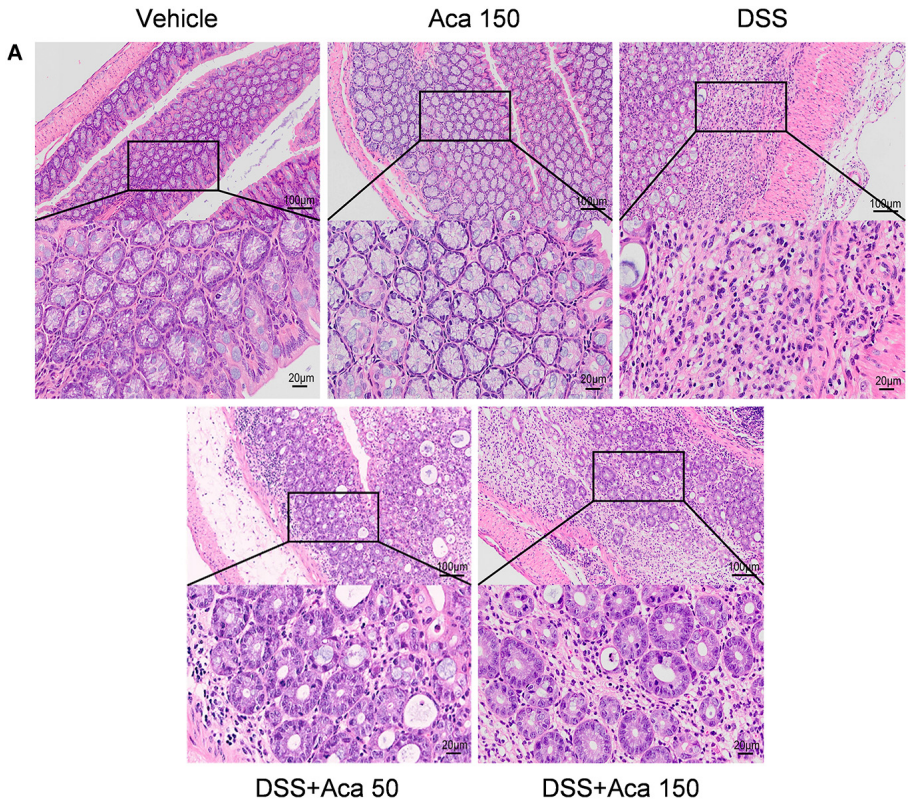

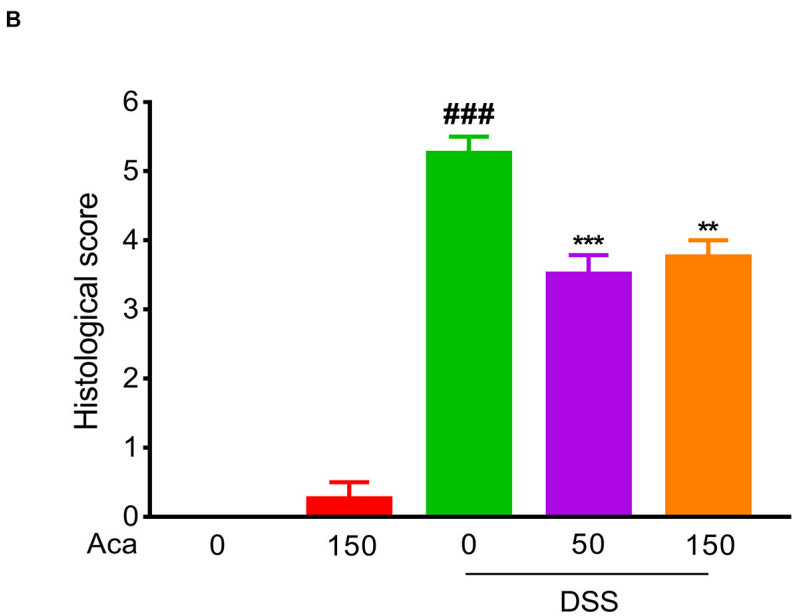

FIGURE 2 | Acacetin ameliorated inflammatory infiltration and histopathological damage in dextran sulfate sodium (DSS)-treated mice. Representative hematoxylin and eosin-stained colon sections **(A)** and histological score **(B)**. The scale bar corresponds to 100 μm or 20 μm. Data were presented as the mean ± SEM (n = 7 mice per group). $^{**}p < 0.01$, $^{***}p < 0.001$ vs. the DSS group; $^{\#\#\#}p < 0.001$ vs. the vehicle group.

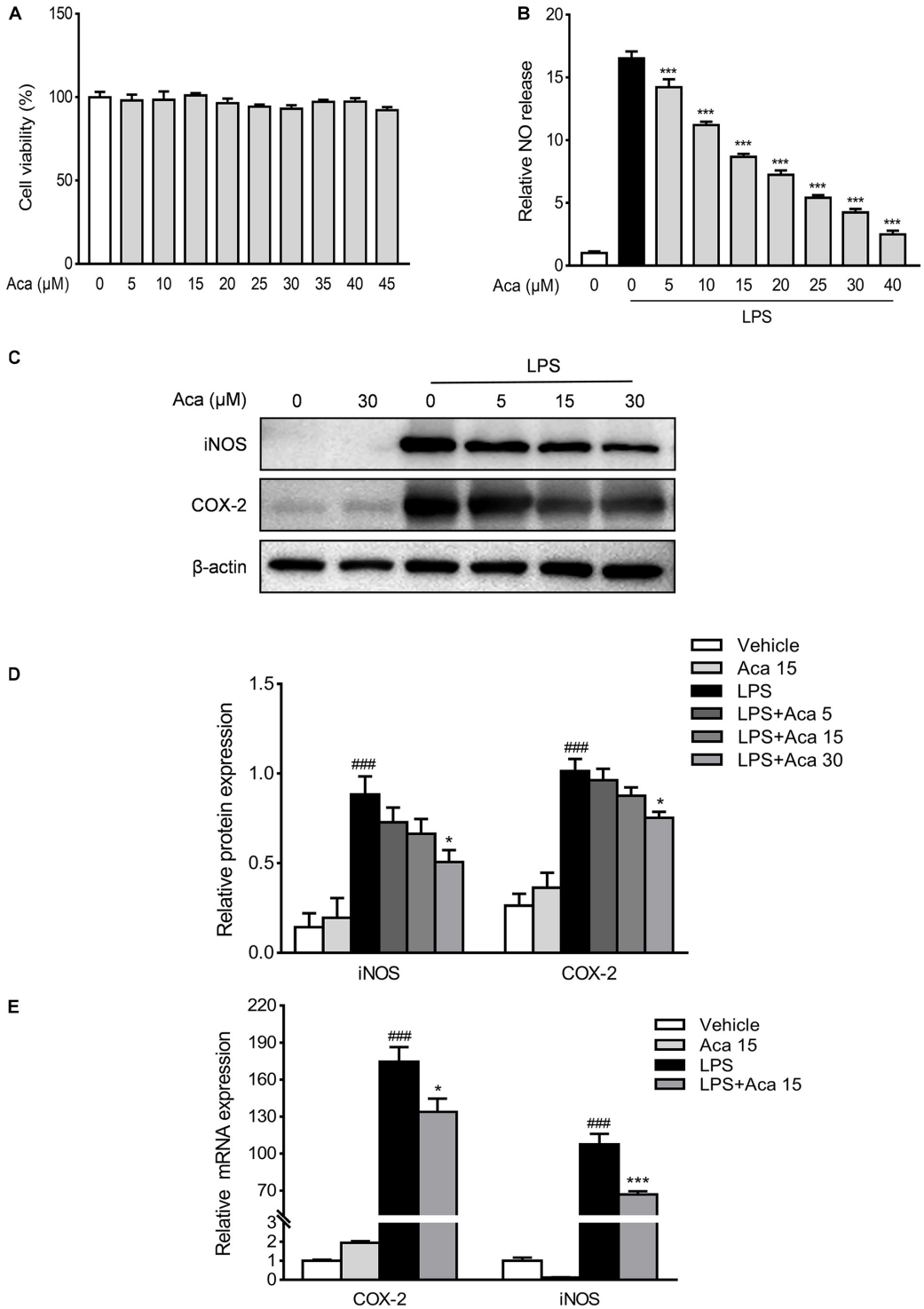

FIGURE 3 | Acacetin inhibited the expression of inflammatory mediators *in vitro*. Effects of acacetin on cell viability **(A)** and the secretion of nitric oxide (NO) **(B)** in lipopolysaccharide (LPS)-induced RAW264.7 cells. **(C)** Protein expression levels of LPS-induced RAW264.7 cells, including inducible nitric oxide synthase (iNOS) and cyclooxygenase-2 (COX-2), were determined by western blot analysis. **(D)** Quantification of protein expression was determined by densitometric analysis of the blots. Expression was normalized to β-actin. **(E)** Effects of acacetin on the expression of proinflammatory mediator mRNA in LPS-induced RAW264.7 cells. The mRNA expression of COX-2 and iNOS were determined by qPCR. All expressions were normalized to β-actin. Data are presented as the mean ± SEM ($n = 3$). $^{*}p < 0.05$, $^{***}p < 0.001$ vs. the DSS group; $^{\#\#\#}p < 0.001$ vs. the vehicle group.

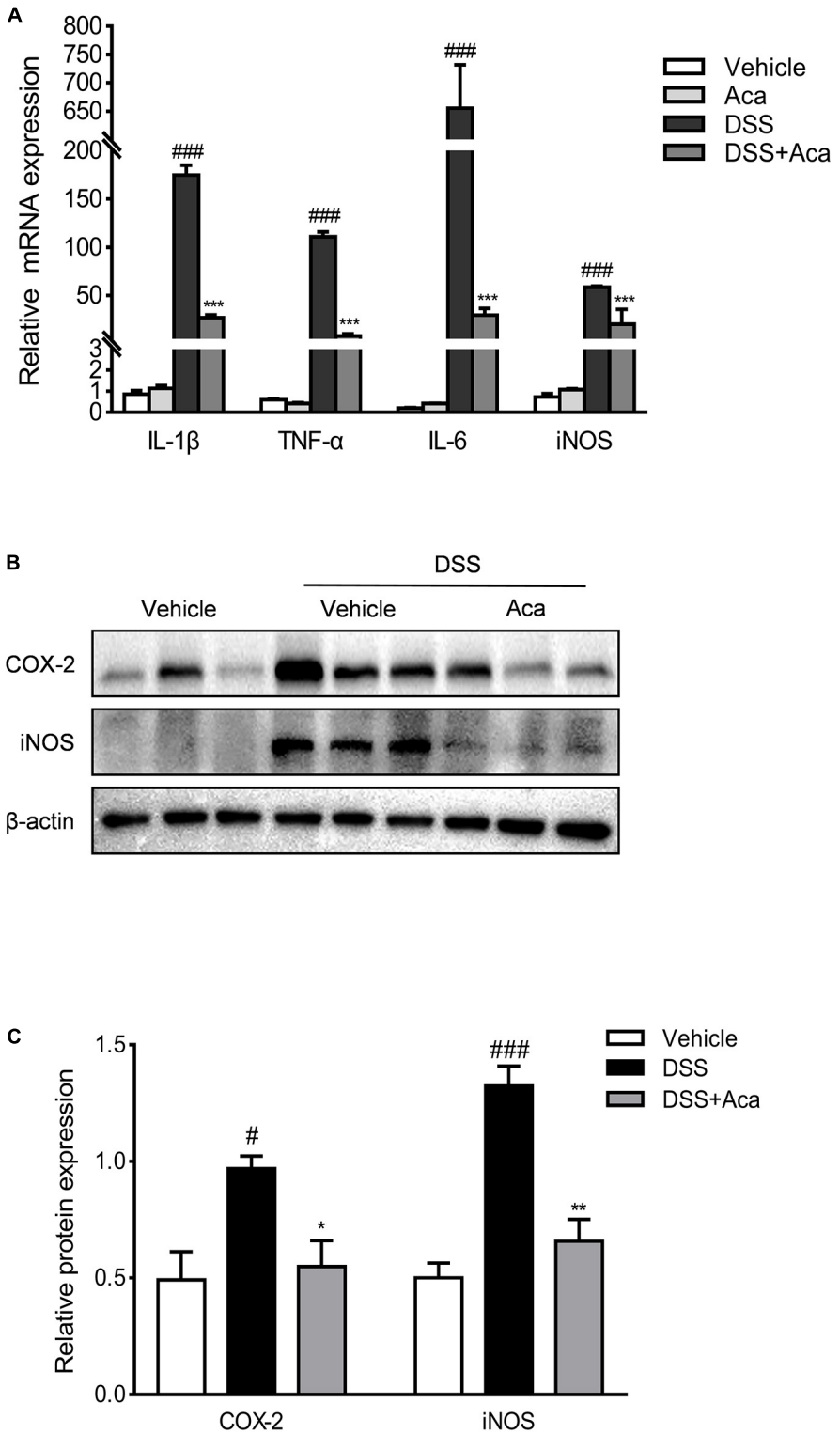

FIGURE 4 | Acacetin inhibited the expression of inflammatory mediators *in vivo*. **(A)** Effects of acacetin on proinflammatory mediator gene expression in colon tissue of dextran sulfate sodium (DSS)-treated mice. The mRNA expression of interleukin 1 beta (IL-1β), tumor necrosis factor alpha (TNF-α), interleukin 6 (IL-6), and inducible nitric oxide synthase (iNOS) in colon samples were determined by qPCR. All expressions were normalized to β-actin. **(B)** Effects of acacetin on the inflammatory mediator protein expression of cyclooxygenase-2 (COX-2) and iNOS in colon tissue of DSS-treated mice. **(C)** Quantification of protein expression was performed by densitometric analysis of the blots. Expression was normalized to β-actin. Data are expressed as the mean ± SEM ($n = 3$). $^{*}p < 0.05$, $^{**}p < 0.005$, $^{***}p < 0.001$ vs. the DSS group; $^{\#}p < 0.05$, $^{\#\#\#}p < 0.001$ vs. the vehicle group.

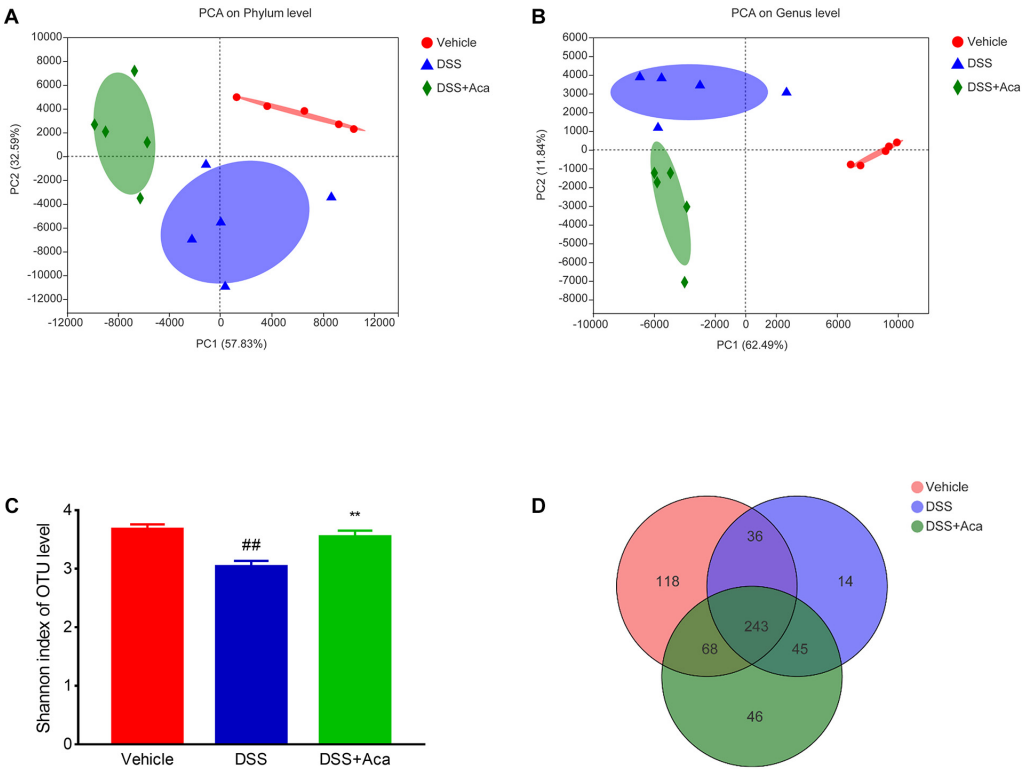

FIGURE 5 | Acacetin regulated the composition of gut microbiota in mice treated with dextran sulfate sodium (DSS). **(A)** Principal component analysis (PCA) graphical results at the phylum level. **(B)** Graphical results of PCA at the genus level. **(C)** Index-group difference test of the Shannon index in sample hierarchical cluster tree, alpha diversity. Student's *t*-test. Classification level: operational taxonomic unit (OTU). Data are presented as the mean (n = 5 mice per group). **(D)** Venn diagram indicates the differential numbers of OTUs in each group. $^{**}p < 0.01$ vs. the DSS group; $^{\#\#}p < 0.01$ vs. the vehicle group.

At the genus level, the DSS-treated group exhibited a proportional increase in the abundances of *Escherichia-Shigella* and *Faecalibaculum*, whereas the abundances of those two genera were reduced after acacetin treatment (**Figures 7A,C**). Furthermore, slight differences in *Family XIII* and *Turicibacter* were noted between the DSS group and the DSS + acacetin group; however, no significant differences were observed (**Figures 7B,C**).

Then we conducted a community heatmap analysis on genus level showing 20 genera with a relatively high abundance (**Figure 8A**). This result is consistent with the showing of bar plot. Circos analysis confirmed the heatmap results (**Figure 8B**). *Escherichia-Shigella* was decreased from 76% to 24% and *Faecalibaculum* from 74 to 22% by acacetin treatment (**Figure 8B**). However, *Turicibacter* was increased, with an abundance of 0.42% in the DSS group and 35% in the DSS + acacetin group (**Figure 8B**).

These results indicate that DSS-induced colitis could disrupt intestinal microbiota homeostasis, while acacetin treatment could reverse this disruption.

DISCUSSION

The pathological mechanism of IBD presently remains to be discovered, and IBD has been listed as a modern refractory disease (Ramos and Papadakis, 2019). Conventional therapeutic drugs may produce various side effects, yield a high recurrence rate, and cannot adequately meet the extensive treatment needs of patients with UC. Hence, exploration of the underlying molecular mechanisms and the discovery and development of optimal therapies for IBD are all crucial (Zhang et al., 2014).

To investigate the etiology and pathogenesis of UC, we established a DSS-induced colitis mouse model, which is the most widely used experimental model for UC (Eichele and Kharbanda, 2017). In this animal model, weight loss, bloody diarrhea, and colon length are critical hallmarks by which the severity of colitis can be evaluated. The administration of acacetin was found to improve these symptoms in mice with DSS-induced colitis. Moreover, the mice treated with acacetin alone showed no abnormalities nor toxic effects compared with those treated with DSS throughout the study. These findings suggest that the administration of acacetin at specific concentrations is relatively safe in mice.

Elevated levels of inflammatory cytokines can serve as disease hallmarks in patients with UC (Ishiguro, 1999). Compelling evidence suggests that cytokines are crucial pathophysiological regulators of the occurrence and development of the inflammatory response of IBD (Strober and Fuss, 2011). Interactions between the TNF family of receptors and their ligands are crucial in immune responses (Zhang et al., 2019). The

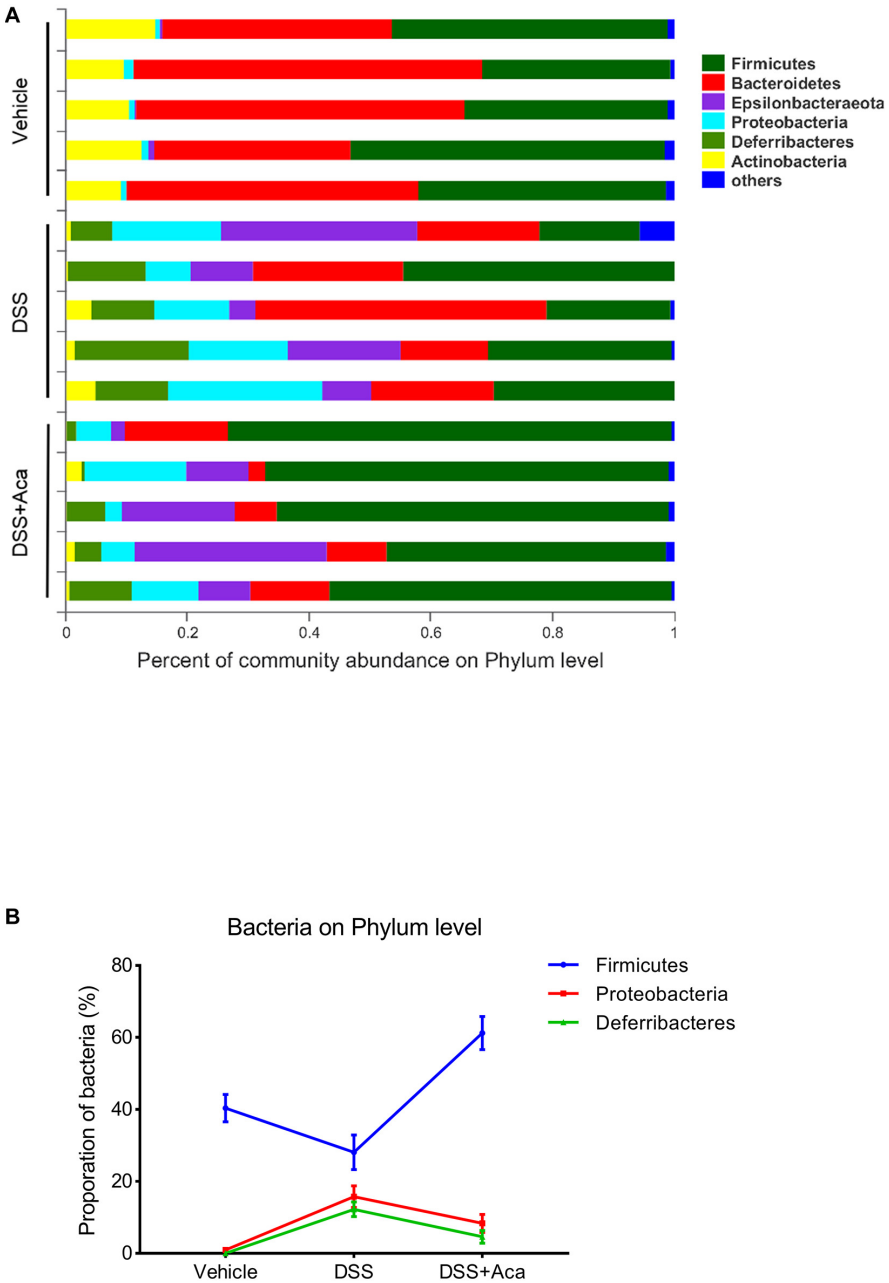

FIGURE 6 | Acacetin regulated the composition and abundance of gut microbiota at the phylum level. **(A)** Proportion of dominant phylum communities in each group of samples. Less than 10% of the phylum communities were merged with others. **(B)** Distribution of the three dominant phyla (Firmicutes, Proteobacteria, and Deferribacteres) in each group. Data are presented as the mean ± SEM (n = 5 mice per group).

progression of inflammation is associated with TNF-α, as it is involved in the recruitment of leukocytes to the inflamed areas (Gupta et al., 2018). Furthermore, IL-6 plays an important role in the development of inflammation by promoting lymphocyte proliferation, which plays a crucial role in the acute stage of the inflammatory response (Mudter and Neurath, 2007). As a key proinflammatory cytokine, IL-1β can accelerate inflammation and initiate antimicrobial immune responses (LaRock et al., 2016; Monajemi et al., 2018). Both iNOS and COX-2 are key inflammatory mediators involved in the incidence of UC (Cox et al., 2005; Sun L. et al., 2018). In the present study, increased production of iNOS, COX-2, IL-6, TNF-α, and IL-1β was observed in mice with DSS-induced colitis. Oral administration of acacetin at 50 mg/kg significantly reduced the production of these proinflammatory mediators.

Macrophages are crucial for raising appropriate immune response against ingested pathogens. Compelling evidence has shown that macrophages are the main source of inflammatory

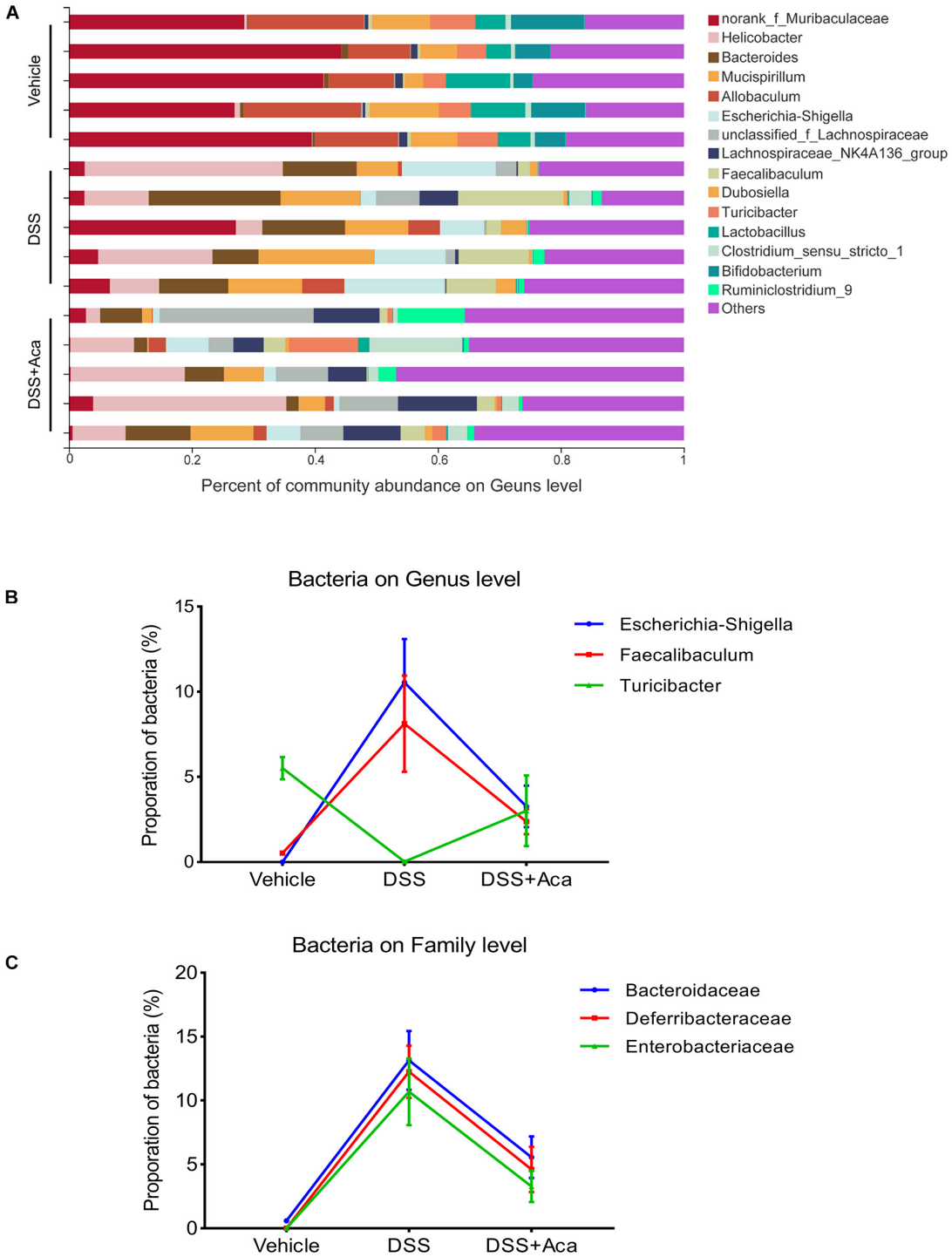

FIGURE 7 | Acacetin regulated the composition and abundance of gut microbiota at the genus level. **(A)** Proportion of dominant genus communities in each group of samples. Less than 5% of the genus communities were merged with others. **(B)** Distribution of the three dominant families (Bacteroidaceae, Deferribacteraceae, and Enterobacteriaceae) in each group. **(C)** Distribution of three dominant genera (*Escherichia-Shigella*, *Faecalibaculum*, and *Turicibacter*) in each group. Data are expressed as the mean ± SEM (n = 5 mice per group).

cytokines during the inflammatory response (Bosma et al., 2016; Jones et al., 2018). Evidence has showed that the reduction of macrophages and inhibition of macrophage response contribute to the therapeutic effect in UC patients (Zeissig et al., 2019). As a colitis model, DSS induces disease symptoms of damaged intestinal epithelial barrier and thereby increases the

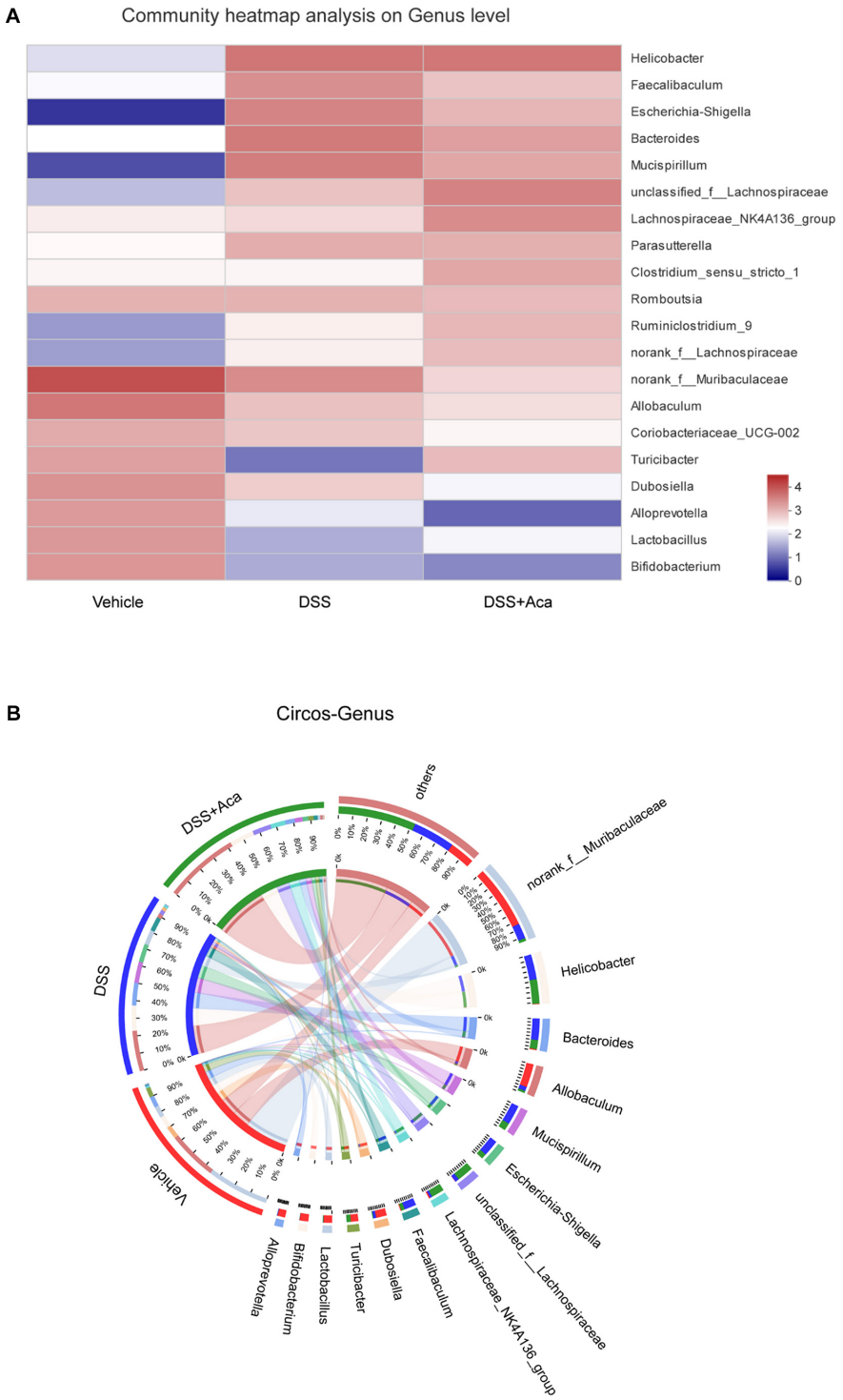

FIGURE 8 | Acacetin regulated the composition and abundance of gut microbiota at the genus level. **(A)** Heatmap comparing expression of different group in 20 genera with a relatively high abundance **(B)** Circos analysis showed the corresponding abundance relationship between different groups and bacterial communities. Data are expressed as the mean ± SEM (n = 5 mice per group).

opportunities that gut lumen contents expose to innate immunity elements (e.g., macrophages) (Eichele and Kharbanda, 2017). Therefore, we further evaluated the anti-inflammatory effects of acacetin *in vitro*. Our results indicate that acacetin can prominently inhibit the levels of NO, iNOS, and COX-2 in LPS-stimulated RAW264.7 murine macrophages, as well as decrease

the secretion of NO and the protein expression of iNOS in IFN-γ and LPS induced BMDM cells, which is consistent with the findings of previous reports (Pan et al., 2006). Notably, acacetin led to significant reduction of macrophage infiltration (labeled by F4/80 +), this results suggest that inhibiting macrophage inflammatory response might contribute to the attenuated effects of acacetin on DSS-induced colitis mice.

Moreover, researchers have gained important insights into gut microbiota composition during intestinal inflammation and have revealed new directions for IBD treatment (Ungaro et al., 2017). Several studies have highlighted that the remarkable changes in gut microbiota composition in patients with UC can cause intestinal inflammation. Severe dysbiosis is mainly manifested in the gut of patients with UC, when there is a reduced abundance of *Firmicutes* and *Bacteroidetes*, and increased abundance of *Proteobacteria* (Lepage et al., 2011; Natividad et al., 2015; Munyaka et al., 2016; Glassner et al., 2020).

Some species at the phylum level (e.g., Proteobacteria) could play a role in the pathogenesis of UC, leading to adhesion and invasion of intestinal epithelial cells, disruption of host defense, stimulation of the inflammatory response, alterations in the structure of intestinal microbiota, and ultimately, promote the onset of UC (Bai et al., 2019). Furthermore, *Escherichia*, which is an IgA-coated bacteria at the genus level, is the dominant pathogen involved in the pathogenesis of UC (Xu et al., 2018). *Escherichia-Shigella*, gram-negative bacteria with an outer LPS membrane, can invade the human colonic epithelium and induce inflammatory responses (Gronbach et al., 2014).

In the present study, the abundances of *Proteobacteria* and *Escherichia-Shigella* were reduced following acacetin treatment in mice with DSS-induced colitis. Moreover, significant alterations were observed in DSS-treated mice, as levels of *Firmicutes* were reduced at the phylum level and those of *Escherichia-Shigella* were increased at the genus level; however, acacetin alleviated these changes. Notably, this results are quite consistent with our previously studied natural compounds, including obacunone and pinocembrin (Luo et al., 2020; Yue et al., 2020). There are also some researches indicate that *Escherichia-Shigella* are positively correlated with high expression of inflammatory cytokines, and many studies have shown its adverse effects in IBD (Zeissig et al., 2019). Collectively, our findings provide evidence of the effects of acacetin in reversing the DSS-induced dysbiosis of intestinal microbiota and changes in community composition.

Indeed, the maintenance of the intestinal health depends on a homeostasis between the microbiota and the innate immune system, and macrophages are the most abundant in the innate immune cells (Sica et al., 2015; Yue et al., 2019). Macrophages can generate varieties of inflammatory cytokines, which further activate innate/adaptive immunity, and therefore get rid of the invading bacteria in intestinal lamina propria (Weber et al., 2009). However, excessive inflammatory response can cause the imbalance of immunity homeostasis and influence the microbial composition, which could exacerbate the intestinal inflammation in turn (Sonnenberg and Hepworth, 2019). Moreover, numbers of studies suggested that both exaggerated inflammatory response and dysbacteriosis are often co-existing in IBD patients (Yao et al., 2019). Hence, both inflammatory response and dysbacteriosis are reciprocal causation in the IBD pathogenesis. Our studies showed the evidence that acacetin could ameliorate intestinal inflammation and regulate dysbacteria. There is a need for research to precisely describe the causal link between inflammatory response and dysbacteriosis. Additionally, the precise mechanism of acacetin in the maintenance of intestinal homeostasis needs further clarification.

CONCLUSION

Overall, these new findings suggest that acacetin could alleviate DSS-induced colitis in mice by inhibiting the macrophage inflammatory response and reversing gut microbiota dysbiosis.

DATA AVAILABILITY STATEMENT

The raw data supporting the conclusions of this article will be made available by the authors, without undue reservation.

ETHICS STATEMENT

The animal study was reviewed and approved by the Animal Experiment Ethics Committee at Shanghai University of Traditional Chinese Medicine (Animal license key: PZSHUTCM190315022).

AUTHOR CONTRIBUTIONS

JR conducted this study and performed the statistical analysis. BY, HW, BZ, XL, ZY, JZ, and YR assisted with the experiments. JR and BY finished the first draft of the manuscript. WD, ZW, and SM read and critically revised the final version of the manuscript. All authors contributed to the article and approved the submitted version.

FUNDING

This work was funded through the National Natural Science Foundation of China (Grant Nos. 81920108033 and 81530096), Natural Science Foundation of Shanghai (Grant No. 20ZR1458000), and National Institutes of Health Grant RO1 CA2222469 (SM).

ACKNOWLEDGMENTS

The authors would like to thank all members of the Shanghai Key Laboratory of Formulated Chinese Medicines.

SUPPLEMENTARY MATERIAL

The Supplementary Material for this article can be found online at: https://www.frontiersin.org/articles/10.3389/fphys.2020.577237/full#supplementary-material

REFERENCES

Ananthakrishnan, A. N., Bernstein, C. N., Iliopoulos, D., Macpherson, A., Neurath, M. F., Ali, R. A. R., et al. (2018). Environmental triggers in IBD: a review of progress and evidence. *Nat. Rev. Gastroenterol. Hepatol.* 15, 39–49. doi: 10.1038/nrgastro.2017.136

Bai, Y., Wang, S., Xu, W., Weng, Y., Zhu, S., Sheng, H., et al. (2019). Cinobufacini ameliorates experimental colitis via modulating the composition of gut microbiota. *PLoS One* 14:e223231. doi: 10.1371/journal.pone.0223231

Bosma, M., Gerling, M., Pasto, J., Georgiadi, A., Graham, E., Shilkova, O., et al. (2016). FNDC4 acts as an anti-inflammatory factor on macrophages and improves colitis in mice. *Nat. Commun.* 7:11314. doi: 10.1038/ncomms11314

Burrello, C., Giuffrè, M. R., Macandog, A. D., Diaz-Basabe, A., Cribiù, F. M., Lopez, G., et al. (2019). Fecal microbiota transplantation controls murine chronic intestinal inflammation by modulating immune cell functions and gut microbiota composition. *Cells* 8:517. doi: 10.3390/cells8060517

Cox, D. G., Crusius, J. B., Peeters, P. H., Bueno-de-Mesquita, H. B., Pena, A. S., and Canzian, F. (2005). Haplotype of prostaglandin synthase 2/cyclooxygenase 2 is involved in the susceptibility to inflammatory bowel disease. *World J. Gastroenterol.* 11, 6003–6008. doi: 10.3748/wjg.v11.i38.6003

Dou, W., Zhang, J., Ren, G., Ding, L., Sun, A., Deng, C., et al. (2014). Mangiferin attenuates the symptoms of dextran sulfate sodium-induced colitis in mice via NF-κB and MAPK signaling inactivation. *Int. Immunopharmacol.* 23, 170–178. doi: 10.1016/j.intimp.2014.08.025

Eichele, D. D., and Kharbanda, K. K. (2017). Dextran sodium sulfate colitis murine model: an indispensable tool for advancing our understanding of inflammatory bowel diseases pathogenesis. *World J. Gastroenterol.* 23, 6016–6029. doi: 10.3748/wjg.v23.i33.6016

Glassner, K. L., Abraham, B. P., and Quigley, E. M. M. (2020). The microbiome and inflammatory bowel disease. *J. Allergy Clin. Immunol.* 145, 16–27. doi: 10.1016/j.jaci.2019.11.003

Gronbach, K., Flade, I., Holst, O., Lindner, B., Ruscheweyh, H. J., Wittmann, A., et al. (2014). Endotoxicity of lipopolysaccharide as a determinant of T-cell-mediated colitis induction in mice. *Gastroenterology* 146, 765–775. doi: 10.1053/j.gastro.2013.11.033

Gupta, R. A., Motiwala, M. N., Mahajan, U. N., and Sabre, S. G. (2018). Protective effect of *Sesbania grandiflora* on acetic acid induced ulcerative colitis in mice by inhibition of TNF-alpha and IL-6. *J. Ethnopharmacol.* 219, 222–232. doi: 10.1016/j.jep.2018.02.043

Hu, L., Wu, C., Zhang, Z., Liu, M., Maruthi Prasad, E., Chen, Y., et al. (2019). Pinocembrin protects against dextran sulfate sodium-induced rats colitis by ameliorating inflammation, improving barrier function and modulating gut microbiota. *Front. Physiol.* 10:908. doi: 10.3389/fphys.2019.00908.jep.2018.02.043

Ishiguro, Y. (1999). Mucosal proinflammatory cytokine production correlates with endoscopic activity of ulcerative colitis. *J. Gastroenterol.* 34, 66–74. doi: 10.1007/s005350050218

Jiang, Y., Xiao, L., Fu, W., Tang, Y., Lertnimitphun, P., Kim, N., et al. (2020). Gaudichaudione H inhibits inflammatory responses in macrophages and dextran sodium sulfate-induced colitis in mice. *Front. Pharmacol.* 10:1561. doi: 10.3389/fphar.2019.01561

Jones, G., Bain, C. C., Fenton, T. M., Kelly, A., Brown, S. L., Ivens, A. C., et al. (2018). Dynamics of colon monocyte and macrophage activation during colitis. *Front. Immunol.* 9:2764. doi: 10.3389/fimmu.2018.02764

Kaplan, G. G. (2015). The global burden of IBD: from 2015 to 2025. *Nat. Rev. Gastroenterol. Hepatol.* 12, 720–727. doi: 10.1038/nrgastro.2015.150

Khan, I., Ullah, N., Zha, L., Bai, Y., Khan, A., Zhao, T., et al. (2019). Alteration of gut microbiota in inflammatory bowel disease (IBD): cause or consequence? IBD treatment targeting the gut microbiome. *Pathogens* 8:126. doi: 10.3390/pathogens8030126

Kiely, C. J., Pavli, P., and O'Brien, C. L. (2018). The role of inflammation in temporal shifts in the inflammatory bowel disease mucosal microbiome. *Gut Microbes* 9, 477–485. doi: 10.1080/19490976.2018.1448742

Kostic, A. D., Xavier, R. J., and Gevers, D. (2014). The microbiome in inflammatory bowel disease: current status and the future ahead. *Gastroenterology* 146, 1489–1499. doi: 10.1053/j.gastro.2014.02.009

LaRock, C. N., Todd, J., LaRock, D. L., Olson, J., O'Donoghue, A. J., Robertson, A. A., et al. (2016). IL-1β is an innate immune sensor of microbial proteolysis. *Sci. Immunol.* 1:eaah3539. doi: 10.1126/sciimmunol.aah3539

Lepage, P., Häsler, R., Spehlmann, M. E., Rehman, A., Zvirbliene, A., Begun, A., et al. (2011). Twin study indicates loss of interaction between microbiota and mucosa of patients with ulcerative colitis. *Gastroenterology* 141, 227–236. doi: 10.1053/j.gastro.2011.04.011

Liou, C., Wu, S., Chen, L., Yeh, K., Chen, C., and Huang, W. (2017). Acacetin from traditionally used saussurea involucrata Kar. et Kir. suppressed adipogenesis in 3T3-L1 adipocytes and attenuated lipid accumulation in obese mice. *Front. Pharmacol.* 8:589. doi: 10.3389/fphar.2017.00589

Luo, X., Yue, B., Yu, Z., Ren, Y., Zhang, J., Ren, J., et al. (2020). Obacunone protects against ulcerative colitis in mice by modulating gut microbiota, attenuating TLR4/NF-κB signaling cascades, and improving disrupted epithelial barriers. *Front Microbiol.* 11:497. doi: 10.3389/fmicb.2020.00497

Matsuoka, K., and Kanai, T. (2015). The gut microbiota and inflammatory bowel disease. *Semin. Immunopathol.* 37, 47–55. doi: 10.1007/s00281-014-0454-4

Monajemi, M., Pang, Y. C. F., Bjornson, S., Menzies, S. C., van Rooijen, N., and Sly, L. M. (2018). Malt1 blocks IL-1β production by macrophages in vitro and limits dextran sodium sulfate-induced intestinal inflammation in vivo. *J. Leukoc. Biol.* 104, 557–572. doi: 10.1002/JLB.3VMA0118-019R

Mudter, J., and Neurath, M. F. (2007). Il-6 signaling in inflammatory bowel disease: pathophysiological role and clinical relevance. *Inflamm. Bowel Dis.* 13, 1016–1023. doi: 10.1002/ibd.20148

Munyaka, P. M., Sepehri, S., Ghia, J. E., and Khafipour, E. (2016). Carrageenan gum and adherent invasive *escherichia coli* in a piglet model of inflammatory bowel disease: impact on intestinal mucosa-associated microbiota. *Front. Microbiol.* 7:462. doi: 10.3389/fmicb.2016.00462

Natividad, J. M., Pinto-Sanchez, M. I., Galipeau, H. J., Jury, J., Jordana, M., Reinisch, W., et al. (2015). ecobiotherapy rich in firmicutes decreases susceptibility to colitis in a humanized gnotobiotic mouse model. *Inflamm. Bowel Dis.* 21, 1883–1893. doi: 10.1097/MIB.0000000000000422

Neurath, M. F. (2014). Cytokines in inflammatory bowel disease. *Nat. Rev. Immunol.* 14, 329–342. doi: 10.1038/nri3661

Ott, S. J. (2004). Reduction in diversity of the colonic mucosa associated bacterial microflora in patients with active inflammatory bowel disease. *Gut* 53, 685–693. doi: 10.1136/gut.2003.025403

Pan, M., Lai, C., Wang, Y., and Ho, C. (2006). Acacetin suppressed LPS-induced up-expression of iNOS and COX-2 in murine macrophages and TPA-induced tumor promotion in mice. *Biochem. Pharmacol.* 72, 1293–1303. doi: 10.1016/j.bcp.2006.07.039

Papadakis, K. A., and Targan, S. R. (2000). Role of cytokines in the pathogenesis of inflammatory bowel disease. *Annu. Rev. Med.* 51, 289–298. doi: 10.1146/annurev.med.51.1.289

Prasad, N., Sharma, J. R., and Yadav, U. C. S. (2020). Induction of growth cessation by acacetin via β-catenin pathway and apoptosis by apoptosis inducing factor activation in colorectal carcinoma cells. *Mol. Biol. Rep.* 47, 987–1001. doi: 10.1007/s11033-019-05191-x

Punia, R., Raina, K., Agarwal, R., and Singh, R. P. (2017). Acacetin enhances the therapeutic efficacy of doxorubicin in non-small-cell lung carcinoma cells. *PLoS One* 12:e182870. doi: 10.1371/journal.pone.0182870

Ramos, G. P., and Papadakis, K. A. (2019). Mechanisms of disease: inflammatory bowel diseases. *Mayo Clin. Proc.* 94, 155–165. doi: 10.1016/j.mayocp.2018.09.013

Salaritabar, A., Darvishi, B., Hadjiakhoondi, F., Manayi, A., Sureda, A., Nabavi, S. F., et al. (2017). Therapeutic potential of flavonoids in inflammatory bowel disease: a comprehensive review. *World J. Gastroenterol.* 23:5097. doi: 10.3748/wjg.v23.i28.5097

Sica, A., Erreni, M., Allavena, P., and Porta, C. (2015). Macrophage polarization in pathology. *Cell Mol. Life Sci.* 72, 4111–4126. doi: 10.1007/s00018-015-1995-y

Smits, L. P., Bouter, K. E., de Vos, W. M., Borody, T. J., and Nieuwdorp, M. (2013). Therapeutic potential of fecal microbiota transplantation. *Gastroenterology* 145, 946–953. doi: 10.1053/j.gastro.2013.08.058

Sonnenberg, G. F., and Hepworth, M. R. (2019). Functional interactions between innate lymphoid cells and adaptive immunity. *Nat. Rev. Immunol.* 19, 599–613. doi: 10.1038/s41577-019-0194-8

Strober, W., and Fuss, I. J. (2011). Proinflammatory cytokines in the pathogenesis of inflammatory bowel diseases. *Gastroenterology* 140, 1756–1767. doi: 10.1053/j.gastro.2011.02.016

Sun, B., Yuan, J., Wang, S., Lin, J., Zhang, W., Shao, J., et al. (2018). Qingchang suppository ameliorates colonic vascular permeability in dextran-sulfate-sodium-induced colitis. *Front. Pharmacol.* 9:1235. doi: 10.3389/fphar.2018.01235

Sun, L., Zhang, H., Gu, C., Guo, S., Li, G., Lian, R., et al. (2018). Protective effect of acacetin on sepsis-induced acute lung injury via its anti-inflammatory and antioxidative activity. *Arch. Pharm. Res.* 41, 1199–1210. doi: 10.1007/s12272-017-0991-1

Ungaro, R., Mehandru, S., Allen, P. B., Peyrin-Biroulet, L., and Colombel, J. (2017). Ulcerative colitis. *Lancet* 389, 1756–1770. doi: 10.1016/S0140-6736(16)32126-2

Weber, B., Saurer, L., and Mueller, C. (2009). Intestinal macrophages: differentiation and involvement in intestinal immunopathologies. *Semin. Immunopathol.* 31, 171–184. doi: 10.1007/s00281-009-0156-5

Xiao, W., Zhou, W., Ma, Q., Cui, W., Mei, Q., and Zhao, X. (2019). Serotonergically dependent antidepressant-like activity on behavior and stress axis responsivity of acacetin. *Pharmacol. Res.* 146:104310. doi: 10.1016/j.phrs.2019.104310

Xu, J., Chen, N., Wu, Z., Song, Y., Zhang, Y., Wu, N., et al. (2018). 5-aminosalicylic acid alters the gut bacterial microbiota in patients with ulcerative colitis. *Front. Microbiol.* 9:1274. doi: 10.3389/fmicb.2018.01274

Yan, Y., Shao, M., Qi, Q., Xu, Y., Yang, X., Zhu, F., et al. (2018). Artemisinin analogue SM934 ameliorates DSS-induced mouse ulcerative colitis via suppressing neutrophils and macrophages. *Acta Pharmacol. Sin.* 39, 1633–1644. doi: 10.1038/aps.2017.185

Yao, D., Dong, M., Dai, C., and Wu, S. (2019). Inflammation and inflammatory cytokine contribute to the initiation and development of ulcerative colitis and its associated cancer. *Inflamm. Bowel Dis.* 25, 1595–1602. doi: 10.1093/ibd/izz149

Yin, J., Ma, Y., Liang, C., Gao, J., Wang, H., and Zhang, L. (2019). A Systematic study of the metabolites of dietary acacetin in vivo and in vitro based on UHPLC-Q-TOF-MS/MS analysis. *J. Agric. Food Chem.* 67, 5530–5543. doi: 10.1021/acs.jafc.9b00330

Yue, B., Luo, X., Yu, Z., Mani, S., Wang, Z., and Dou, W. (2019). Inflammatory bowel disease: a potential result from the collusion between gut microbiota and mucosal immune system. *Microorganisms* 7:440. doi: 10.3390/microorganisms7100440

Yue, B., Ren, J., Yu, Z., Luo, X., Ren, Y., Zhang, J., et al. (2020). Pinocembrin alleviates ulcerative colitis in mice via regulating gut microbiota, supressing TLR4/MD2/NF-κB pathway and promoting intestinal barrier. *Biosci. Rep.* 40, BSR20200986. doi: 10.1042/BSR20200986

Zeissig, S., Rosati, E., Dowds, C. M., Aden, K., Bethge, J., Schulte, B., et al. (2019). Vedolizumab is associated with changes in innate rather than adaptive immunity in patients with inflammatory bowel disease. *Gut* 68, 25–39. doi: 10.1136/gutjnl-2018-316023

Zhang, J., Ding, L., Wang, B., Ren, G., Sun, A., Deng, C., et al. (2015). Notoginsenoside R1 attenuates experimental inflammatory bowel disease via pregnane X receptor activation. *J. Pharmacol. Exp. Ther.* 352, 315–324. doi: 10.1124/jpet.114.218750

Zhang, J., Dou, W., Zhang, E., Sun, A., Ding, L., Wei, X., et al. (2014). Paeoniflorin abrogates DSS-induced colitis via a TLR4-dependent pathway. *Am. J. Physiol. Gastrointest. Liver Physiol.* 306, G27–G36. doi: 10.1152/ajpgi.00465.2012

Zhang, P., Jiao, H., Wang, C., Lin, Y., and You, S. (2019). Chlorogenic acid ameliorates colitis and alters colonic microbiota in a mouse model of dextran sulfate sodium-induced colitis. *Front. Physiol.* 10:325. doi: 10.3389/fphys.2019.00325

Zhang, Q., Zhu, L., Gong, X., Ruan, Y., Yu, J., Jiang, H., et al. (2017). Sulfonation disposition of acacetin: in vitro and in vivo. *J. Agric. Food Chem.* 65, 4921–4931. doi: 10.1021/acs.jafc.7b00854

Zuo, T., and Ng, S. C. (2018). The gut microbiota in the pathogenesis and therapeutics of inflammatory bowel disease. *Front. Microbiol.* 9:2247. doi: 10.3389/fmicb.2018.02247

Conflict of Interest: The authors declare that the research was conducted in the absence of any commercial or financial relationships that could be construed as a potential conflict of interest.

Copyright © 2021 Ren, Yue, Wang, Zhang, Luo, Yu, Zhang, Ren, Mani, Wang and Dou. This is an open-access article distributed under the terms of the Creative Commons Attribution License (CC BY). The use, distribution or reproduction in other forums is permitted, provided the original author(s) and the copyright owner(s) are credited and that the original publication in this journal is cited, in accordance with accepted academic practice. No use, distribution or reproduction is permitted which does not comply with these terms.

frontiers in Microbiology

ORIGINAL RESEARCH
published: 12 February 2021
doi: 10.3389/fmicb.2021.557180

Distinct Changes Occur in the Human Breast Milk Microbiome Between Early and Established Lactation in Breastfeeding Guatemalan Mothers

*Emmanuel Gonzalez[1,2], Nicholas J. B. Brereton[3], Chen Li[4], Lilian Lopez Leyva[4], Noel W. Solomons[5], Luis B. Agellon[5], Marilyn E. Scott[6] and Kristine G. Koski[4]**

[1] Canadian Centre for Computational Genomics (C3G), Department of Human Genetics, McGill University, Montréal, QC, Canada, [2] Microbiome Research Platform, McGill Interdisciplinary Initiative in Infection and Immunity (MI4), Genome Centre, McGill University, Montréal, QC, Canada, [3] Institut de Recherche en Biologie Végétale, Université de Montréal, Montréal, QC, Canada, [4] School of Human Nutrition, McGill University, Ste-Anne de Bellevue, QC, Canada, [5] Center for Studies of Sensory Impairment, Aging and Metabolism (CeSSIAM), Guatemala City, Guatemala, [6] Institute of Parasitology, McGill University, Ste-Anne de Bellevue, QC, Canada

OPEN ACCESS

Edited by:
Ana Rivas, University of Granada, Spain

Reviewed by:
Rosa Del Campo, Ramón y Cajal Institute for Health Research, Spain
Margarita Aguilera, University of Granada, Spain

***Correspondence:**
Kristine G. Koski
kristine.koski@mcgill.ca

Specialty section:
This article was submitted to Food Microbiology, a section of the journal Frontiers in Microbiology

Received: *29 April 2020*
Accepted: *21 January 2021*
Published: *12 February 2021*

Citation:
Gonzalez E, Brereton NJB, Li C, Lopez Leyva L, Solomons NW, Agellon LB, Scott ME and Koski KG (2021) Distinct Changes Occur in the Human Breast Milk Microbiome Between Early and Established Lactation in Breastfeeding Guatemalan Mothers. Front. Microbiol. 12:557180. doi: 10.3389/fmicb.2021.557180

Human breast milk contains a diverse community of bacteria, but as breast milk microbiome studies have largely focused on mothers from high income countries where few women breastfeed to 6 months, the temporal changes in the breast milk microbiome that occur during later lactation stages have not been explored. For this cross-sectional study, microbiota from breast milk samples of *Mam*-Mayan mothers living in eight remote rural communities in the Western Highlands of Guatemala were analyzed. All mothers delivered vaginally and breastfed their infants for 6 months. Breast milk from 76 unrelated mothers was used to compare two lactation stages, either "early" (6–46 days post-partum, $n = 33$) or "late" (109–184 days post-partum, $n = 43$). Breast milk microbial communities were assessed using 16S ribosomal RNA gene sequencing and lactation stages were compared using DESeq2 differential abundance analysis. A total of 1,505 OTUs were identified, including 287 which could be annotated as putative species. Among several maternal factors, lactation stage explained microbiome variance and inertia in ordination with the most significance ($p < 0.001$). Differential abundance analysis identified 137 OTUs as significantly higher in either early or late lactation. These included a general shift from *Staphylococcus* and *Streptococcus* species in early lactation to *Sphingobium* and *Pseudomonas* species in late lactation. Species enriched in early lactation included putative commensal bacteria known to colonize the infant oral and intestinal tracts whereas species enriched in late lactation had a uniform functional trait associated with aromatic compound degradation. Differentially abundant species also included several species which have not previously been reported within breast milk, such as *Janthinobacterium agaricidamnosum*, *Novosphingobium clariflavum*, *Ottowia beijingensis,* and *Flavobacterium cucumis.* These discoveries describe temporal changes to the breast milk microbiome of healthy Guatemalan mothers from early to late

lactation. Collectively, these findings illustrate how studying under-represented human populations might advance our understanding of factors that modulate the human milk microbiome in low and middle income countries (LMIC).

Keywords: 16S rRNA gene, human breast milk, microbiome, lactation stage, metagenomics 16S

INTRODUCTION

Human breast milk is a source of macronutrients and micronutrients essential for infant nutrition (Cunningham et al., 1991; Walker, 2010; Andreas et al., 2015). Research has established that breast milk also provides infants with a continuous source of commensal and potentially beneficial bacteria which can act to inoculate the infant respiratory and gastrointestinal tracts (Fernández et al., 2013; McGuire and McGuire, 2017). Predominant genera commonly reported include *Staphylococcus*, *Streptococcus, Pseudomonas, Cutibacterium (*formally *Propionibacterium*), or *Bifidobacterium* (Jeurink et al., 2012; Fitzstevens et al., 2017). Recently, metagenomic sequencing studies have begun to characterize the diverse bacterial species in breast milk to better understand how this process might be associated with infant and long-term health (Biagi et al., 2017; Ruiz et al., 2019; Sakwinska and Bosco, 2019).

Several maternal factors are thought to modify bacterial communities in human breast milk. One study reported differences in bacteria (observed at the genera level) related to stage of lactation, maternal BMI and mode of delivery (Cabrera-Rubio et al., 2012), but other studies have reported little or no differences in relative abundance of genera due to maternal age, parity, mode of delivery, or infant sex (Urbaniak et al., 2016; Williams et al., 2017). Given the advancements in resolution of microbial barcoding technologies (Knight et al., 2018; Bolyen et al., 2019; Gonzalez et al., 2019), coupled with the need to identify the factors that influence breast milk microbiota (McGuire and McGuire, 2017), the purpose of the study was to determine if human milk microbiota differed by maternal age, BMI, parity, breastfeeding practices and lactation stage. Breast milk samples were collected from unrelated lactating mothers living in the remote Western Highlands of Guatemala during early (6–46 days postpartum) or established lactation (109–184 days postpartum) as previously described (Wren et al., 2015).

MATERIALS AND METHODS

Study Site and Participants

This cross-sectional study was part of collaboration between McGill University and the Center for Studies of Sensory Impairment, Aging and Metabolism (CeSSIAM) in the Republic of Guatemala. Field studies were conducted in eight rural Mam-speaking communities of the San Juan Ostuncalco region in Guatemala (Chomat et al., 2015) between June 2012 and January 2013. Lactating mothers were identified and invited to participate by community health workers. Individuals who had been treated with antibiotics were excluded. All mothers delivered vaginally and breastfed their infants. Samples from participating mothers with infants aged from 6 to 46 (n = 33) and 109–184 (n = 43) days postpartum were used to compare the milk microbiome during early and late lactation. Breastfeeding practices were also compared. Exclusively breastfeeding was defined as infants receiving only breast milk; predominant breastfeeding was defined as infants who breastfed but also received water, most commonly as "agüitas" (*herbal teas),* and mixed breastfeeding was defined as infants who breastfed but were also given solid foods in addition to aguitas (Wren et al., 2015).

Breast Milk Sample Collection

Prior to sample collection, the nipple and areola of the breast were cleaned with 70% ethanol. Breast milk samples were collected during a 3 h time window in the morning from the breast (not recently used for breastfeeding) via full manual expression by a trained midwife. Milk was collected into sterile 60 ml plastic vials and immediately stored on ice. Samples were partitioned into 15 ml tubes at the field laboratory (−30°C) prior to transfer on dry ice to McGill University where they were stored at −80°C (Li et al., 2016).

16S rRNA Gene Amplification, Sequencing, and Bioinformatics

DNA extraction was performed using 1ml of milk with DNeasy Blood and Tissue mini kit from Qiagen according to the manufacturer's protocol by Genomic Quebec Innovation Centre. For PCR, a target region of ∼526 bp based on the *Escherichia coli* 16S rRNA gene covering the V1–V3 was amplified with the primers 27F (3′-AGAGTTTGATCCTGGCTCAG-5′) and 533R (3′-TTACCGCGGCTGCTGGCAC-5′) (Cabrera-Rubio et al., 2012; Mediano et al., 2017; Lackey et al., 2019). Amplification used the following conditions: initial denaturation 94°C for 2 min, denaturation 94°C for 30 s, annealing 58°C for 30 s, extension 72°C for 30 s, final extension 72°C for 7 min, 4°C hold, over 35 cycles. Amplification was conducted by the Genomic Quebec Innovation Centre at McGill University and sequencing was performed using the Illumina MiSeq platform. Reagent controls were below the detection limit used by Genomic Quebec Innovation Centre for quality assurance. The Anchor pipeline (Gonzalez et al., 2019) was used to process amplicon sequences. Briefly, Mothur (Schloss et al., 2009) was used to align and dereplicate sequences before high count OTU selection at a count threshold of 36 across all samples. NCBI 16S rRNA RefSeq, NCBI non-redundant nucleotide, SILVA, and the Ribosomal Database Project (RDP) databases were used to annotate OTUs using BLASTn with criteria of >99% for identity and coverage. When a BLASTn return had 100% identity and coverage hits across multiple database, priority was given to NCBI 16S rRNA

RefSeq due to the high standard of curation. Low counting amplicons (<36 counts) were binned to high-count OTUs at a lower threshold of >98% identity/coverage. Multiple, equally good (highest identity/coverage), annotation was retained and reported. All annotation, and in particular species calls, should be considered putative even when sharing 100% sequence identity to a single species due to database errors.

Alpha diversity of breast milk samples was measured using Shannon and inverse Simpson indices within Phyloseq R package (McMurdie and Holmes, 2013). Beta diversity was estimated based on variation stabilization normalized counts (rlog) using Bray-Curtis dissimilarity and the Constrained Analysis of Principal Coordinates (CAP) ordination method. Dispersion ellipses were drawn using veganCovEllipse function from Vegan package in R (Oksanen et al., 2017). Significant distance was evaluated between the groups using non-parametric analysis of similarities (ANOSIM) on normalized counts based on Bray distances (Vegan package). To characterize differentially abundant taxonomic units between groups of samples, parametric models developed in transcriptomics perform well when applied to microbiome biomarker data (uneven library sizes, sparsity, and sample representativity) (Jonsson et al., 2016; Weiss et al., 2017; Brereton et al., 2019; Gonzalez et al., 2019; Minerbi et al., 2019). DESeq2 procedure (Love et al., 2014a) was used to calculate differentially abundant taxonomic units. Taxonomic units tested with a false discovery rate (FDR or the expected proportion of false positive findings) <0.1 were considered significant (Anders et al., 2013; Love et al., 2014b, 2015; Gonzalez et al., 2019). Pearson's correlation was calculated between rlog normalized OTU counts. Correlation matrices were sorted based on hierarchical clustering of OTUs and represented using R package corrplot (Wei and Simko, 2017).

RESULTS

Characterization of Guatemalan Mothers

Participating mothers were randomly selected from 8 remote *Mam*-Mayan villages in the Western Highlands of Guatemala: Los Romero (28%), Buena Vista (25%), Los Alnonzo (13%), and <10% from each of Espumpujá, Los Lopez, Los Perez, La Unión, and La Esperanza. Population characteristics by lactation stage are summarized in **Table 1**. With regards to breastfeeding practices, 86% exclusively or predominantly breastfed; mixed feeding was more common in late lactation, increasing from 3 to 23.3%; regardless of breastfeeding practice, frequency per 24 h averaged 11 feeds per day, which aligns with current recommendations.

Breast Milk Microbiome Community Differs Between Lactation Stages

Sample extractions yielded significantly different concentrations of total genomic DNA between early and late groups at an average of 11.9 ng μl (±3.2) compared to 3.0 ng μl (±0.6), respectively. A total of 1,505 OTUs were assembled and captured 6,294,781 sequence reads across all 76 breast milk samples. These could be annotated as 287 species (71% of reads), 180 genera and 23 family or higher taxa as well as 1,015 which couldn't be recognized as 99% similar (in both identity and coverage) to any known taxa (termed TrueUnknowns). Of the 287 OTUs annotated as putative species, the average BLASTn return identity was 99.8% including 167 perfect hits (100% identity). At a phyla level, bacteria from Firmicutes, Proteobacteria, Actinobacteria, and Bacteroidetes were most prevalent in comprising 48, 44, 6, and 1% of sequenced

TABLE 1 | Characteristics of Guatemalan mothers at each lactation stage.

	Lactation stages		
	Total mean ± *SD* or % (95% CI)	**Early mean ± *SD* or % (95% CI)**	**Late mean ± *SD* or % (95% CI)**
Region (%)			
Los Alonzo	13.1	18.2	9.3
Buena Vista	25.0	12.1	34.9
Espumpujá	2.6	6.1	0.0
Los López	3.9	9.1	0.0
Los Pérez	9.2	3.0	14.0
Los Romero	27.6	36.4	20.9
La Unión	9.2	6.1	11.6
La Esperanza	9.2	9.1	9.3
Maternal age (years)	23.2 ± 5.8	22.7 ± 5.5	23.6 ± 6.0
Maternal height (cm)	146.7 ± 5.1	146.2 ± 4.7	147.2 ± 5.4
Maternal weight (kg)	50.8 ± 7.6	50.2 ± 6.7	51.2 ± 8.3
Maternal BMI (kg/m^2)	23.5 ± 3.1	23.5 ± 2.8	23.5 ± 3.4
Parity			
Primiparous	49.0	45.0	52.0
Multiparous	51.0	55.0	48.0
Marital status (%)			
Married	25.0	27.0	22.5
United	73.0	73.0	72.5
Single	3.0	0.0	5.0
Education (%)			
No	81.0	85.0	76.0
Primary education or higher	19.0	15.0	24.0
Delivery location and attendant			
Informal sector and midwife	78.0	85.0	73.0
Hospital and formal	22.0	15.0	28.0
Infant feeding practices			
Exclusive	47.4	51.5	44.2
Predominant	38.2	45.5	32.6
Mixed	14.5	3.0	23.3
Breastfeeding First hour	61.0	53.0	68.0
Frequency/24 h	11.9 ± 4.3	11.7 ± 4.7	12.1 ± 4
Infant first food			
Breast	88.0	88.0	87.5
Agüitas	11.0	12.0	10.0
Beverages	1.0	0.0	2.5

amplicons, respectively (**Supplementary File 1**). The most abundant species across all samples were *Streptococcus salivarius* and *Novosphingobium clariflavum* making up 7.54 and 6.22% amplicons, respectively.

Distance-based ordination using sparsity filtered raw count matrix was performed with five different categorical variables; four were dichotomous (lactation stage, parity, BMI, and mother age) and one (breastfeeding practice) was based on three factors (exclusive, predominant, or mixed). Constrained Analysis of Principal Coordinates (CAP) analysis best segregated mothers based on lactation stage (**Figure 1**) and identified significant differences with Monte Carlo permutation testing between sample groups (10,000 permutations) at $p < 0.001$; parity, BMI, mother age and breastfeeding practice were not significant ($p > 0.1$ in all cases). Shannon and Inverse Simpson indices, used to estimate microbiome diversity, were not significantly (t-test $p < 0.05$) higher in late compared to early lactation stage breast milk (**Figure 1**).

In contrast, differential abundance analysis using DESeq2 identified taxa which were significantly different in relative abundance between early and late lactation stages. In total, 137 OTUs were identified as significantly differentially abundant, including 39 which were in higher relative abundance in early stage milk and the remaining 98 higher in late stage milk (**Figure 2** and **Supplementary File 2**). These could be annotated at various taxonomic levels, including: 60 species, 25 genera, 1 family as well as 52 which could not be recognized (TrueUnknowns). A general shift in differential abundance was observed with lower relative abundance in some taxa from Firmicutes in early stage milk which were replaced by taxa from Proteobacteria in late stage milk. This was driven by *Streptococcus* and *Staphylococcus* species present at higher relative abundance within early milk whereas *Sphingomonadaceae* and *Pseudomonas* were higher in late milk, with the majority of differentially abundant species in each respective taxa group being inversely correlated (**Figure 3** and **Supplementary File 1**).

Bacterial Species Associated With Early Lactation

Ten distinct *Staphylococcus* OTUs were identified as having significantly higher relative abundance in early milk, including the species: *S. hominis, S. epidermidis,* and *S. hyicus* (**Figure 2**). The most abundant *Staphylococcus* OTU (Staphylococcus_MS_6) was ambiguous and could represent one or more of the species *S. epidermidis*, *S. haemolyticus,* or *S. hominis*.

Seventeen differentially abundant OTUs with higher abundance in early lactation stage breast milk were identified as putative species within the genus *Streptococcus*. These included *S. mitis*, *S. parasanguinis*, *S. peroris*, *S. pneumoniae*, *S. pseudopneumoniae,* and *S. salivarius* as well as four OTUs which were ambiguous and could represent a number different of species. Beyond *Staphylococcus* and *Streptococcus,* other OTUs representing species identified as significantly higher in relative abundance in early milk included: *Corynebacterium tuberculostearicum, Corynebacterium jeikeiu, Lactobacillus gasseri, Acinetobacter johnsonii, Kocuria palustris,* and *Janthinobacterium agaricidamnosum*.

Bacterial Species Associated With Late Lactation

The general pattern of higher *Staphylococcus* and specific *Streptococcus* species in early milk was also reflected by corresponding significant ($p < 0.05$) inverse correlations with *Sphingobium yanoikuyae*, *Pseudomonas putida*, *Stenotrophomonas maltophilia, Ottowia beijingensis,* and *Comamonas testosteroni*, all of which were significantly differentially abundant with higher relative abundance in late breast milk.

Five distinct *S. yanoikuyae* OTUs and a *S. limneticum* OTU were identified as significantly higher in late milk. The two most abundant OTUs, Sphingobium yanoikuyae_4 and Sphingobium yanoikuyae_5, likely represent distinct strains in sharing 100% identity with *Sphingobium yanoikuyae* S72 and ATCC 51230, respectively, with each strain harboring four identical gene copies. Additionally, a single *Novosphingobium clariflavum* OTU was identified as differentially abundant and higher in late breast milk. The *Novosphingobium clariflavum* OTU was particularly high in abundance in the majority of late breast milk samples and was the most abundant OTU in 51% of late milk samples, representing an average of 25% of raw reads.

Nine *Pseudomonas* OTUs were differentially expressed with eight having higher relative abundance in late milk. These included four *P. putida* and one *P. fulva* OTU as well as three ambiguous OTUs which could be *P. putida*, *P. fulva*, *P. parafulva,* and/or *P. gingeri*. *Stenotrophomonas maltophilia* (closely related to *Pseudomonas*), *Cloacibacterium normanense*, *Flavobacterium cucumis, Ottowia beijingensis* (absent from early milk samples), *Prevotella melaninogenica*, *Veillonella dispar, Actinomyces odontolyticus* as well as the highly abundant *Comamonas testosteroni*, were also each identified as significantly more abundant in late lactation stage breast milk.

A number of poorly characterized OTUs were also identified as having higher relative abundance in late milk. These were dominated by unknown sequences previously observed in samples from oral or saliva microbiome studies, such as: TrueUnknown_ 944 and TrueUnknown_ 978 (97.5% similar *Streptococcus sanguinis* SK1), TrueUnknown_967 and TrueUnknown_980 (98% similar *Prevotella* sp.), TrueUnknown_915 (98% similar *Granulicatella elegans*), as well as the high relative abundance TrueUnknown_926 which was 97% similar to a (challenging to culture) TM7 group bacterium often found in oral samples.

DISCUSSION

General Characteristics

Breast milk supplies a continuous source of bacteria during lactation (Fitzstevens et al., 2017) and there is consensus that this provision inoculates the gastrointestinal tract with commensal or beneficial bacteria (Martín et al., 2004; Ramsay et al., 2004; Moossavi et al., 2019; Williams et al., 2019). However,

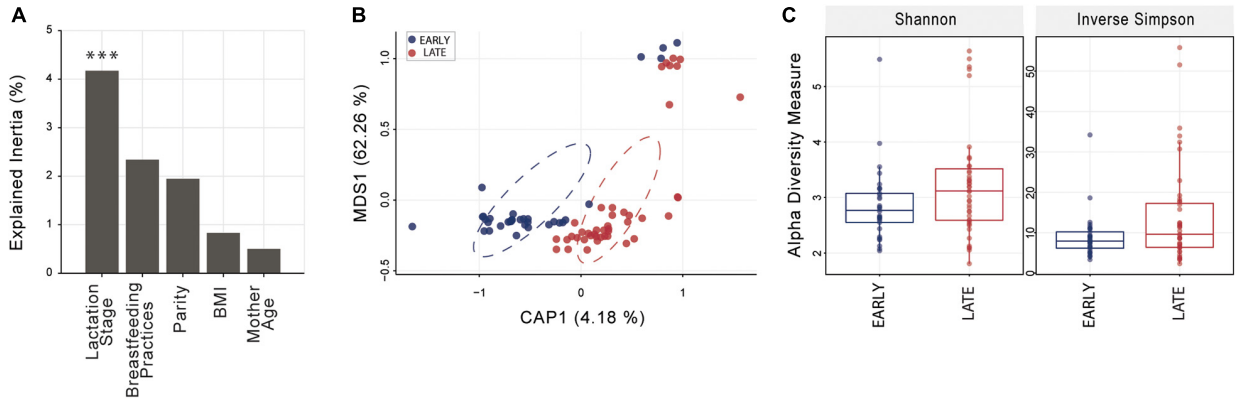

FIGURE 1 | Breast milk community ordination and alpha diversity comparing early and late lactation microbiome. **(A)** Variation explained by the tested variables in constrained ordination (CAP). Significance testing using Monte Carlo permutation test (10,000 permutation; ***$p < 0.001$). **(B)** Lactation stage CAP, circles represent sample density relative to each group. **(C)** Alpha diversity indices were not significantly different (*t*-test, $p > 0.05$) between early ($n = 33$) and late ($n = 43$) lactation groups. See **Supplementary File 1** for an overview of OTU taxonomy.

this milk bacterial community is thought to be influenced by the communities present in other maternal tissues (e.g., skin and the gastrointestinal tract) as well as the infant oral cavity (e.g., "retrograde flow") and the environment (Jost et al., 2014; LaTuga et al., 2014; Rodríguez, 2014). Despite this, the microbiome of breast milk is still poorly understood, and no consensus has been reached on the "core" genera microbiome (Jeurink et al., 2012; Fitzstevens et al., 2017) or if dynamic changes in this bacterial community might occur throughout lactation. In our study, unrelated mothers living in eight remote but distinct communities with little possibility of exchanging microbes among one another were studied. Moreover, this indigenous Guatemalan population was chosen because nearly 100% exclusively or predominantly breastfed for 6 months (Wren et al., 2015), complying with WHO recommendations to actively breastfeed during this period (World Health Organization, 2014). This is considerably higher than the global average of 41% of mothers breastfeeding for 6 months, which falls to as low as 26% in North America (UNICEF, 2018). Importantly, this study population also represented a cohort of mothers who are not from a high-income country, which currently dominates the research field. Thus, this study contributes toward identifying common characteristics and possible biases generated from a shortfall in participant diversity from under-represented communities in breast milk microbiome research.

Early Lactation Stage Breast Milk Is Dominated by Commensal Bacterial Species

Although previous studies have reported differences in the human milk microbiome related to maternal BMI and stage of lactation (Cabrera-Rubio et al., 2012; Williams et al., 2017, 2019; Moossavi et al., 2019), few have characterized the milk microbiome by identifying changes in the relative abundance of putative species. The benefit of high-resolution microbiome analysis at species level is that, although many species remain poorly characterized, the potential for association to established functions is improved when compared to annotation at phyla, family or genera level. Species-level annotation however, even when sequences share 100% 16S rRNA gene fragment similarity to a single species, should be considered as putative as substantial mistakes exist in major repositories (Gonzalez et al., 2019). The two most abundant species identified in higher relative abundance in early lactation stage were the coagulase negative *Staphylococcus hominis* and *Staphylococcus epidermidis* (**Figure 2**), both of which are ubiquitous in humans and have been previously associated with opportunistic pathogenicity (Coates et al., 2014). The higher abundance of *S. hominis* and *S. epidermidis* in early milk is consistent with findings that non-virulent strains of these species are likely early gut pioneers of term infants, and may have the potential to reduce colonization by more virulent species (Soeorg et al., 2017). In our study, it was also interesting to note that although both species are recognized as common skin bacteria and common inhabitants of healthy breast milk environment (Heikkilä and Saris, 2003; Martín et al., 2007), their relative abundance was lower in late milk.

Streptococcus mitis and *Streptococcus salivarius* strains are usually considered commensal, are commonly isolated from milk (Kilian et al., 2014; Delorme et al., 2015; Sørensen et al., 2016) and have been identified as infant oral microbiome inhabitants within the first days after birth (Pearce et al., 1995). The OTUs from both species were generally in higher relative abundance in early milk (**Figure 2**). An exception to this was in *S. mitis*, where two of the six differentially abundant *S. mitis* OTUs (Streptococcus_mitis_9 and Streptococcus_mitis_12) had higher relative abundance in late milk. Interestingly, the most abundant *S. mitis* OTU in early (Streptococcus_mitis_14) and late (Streptococcus_mitis_9) lactation stages share 100% identity to distinct strains, *Strep mitis* RH_12363_08 and *Strep mitis* SK637, respectively. These OTUs, alongside the others identified as significantly varying between early and late lactation stages are most similar to different *S. mitis* phylogenetic sub-clades (**Supplementary File 1**; NCBI Genome Tree report), in line with previously described strain

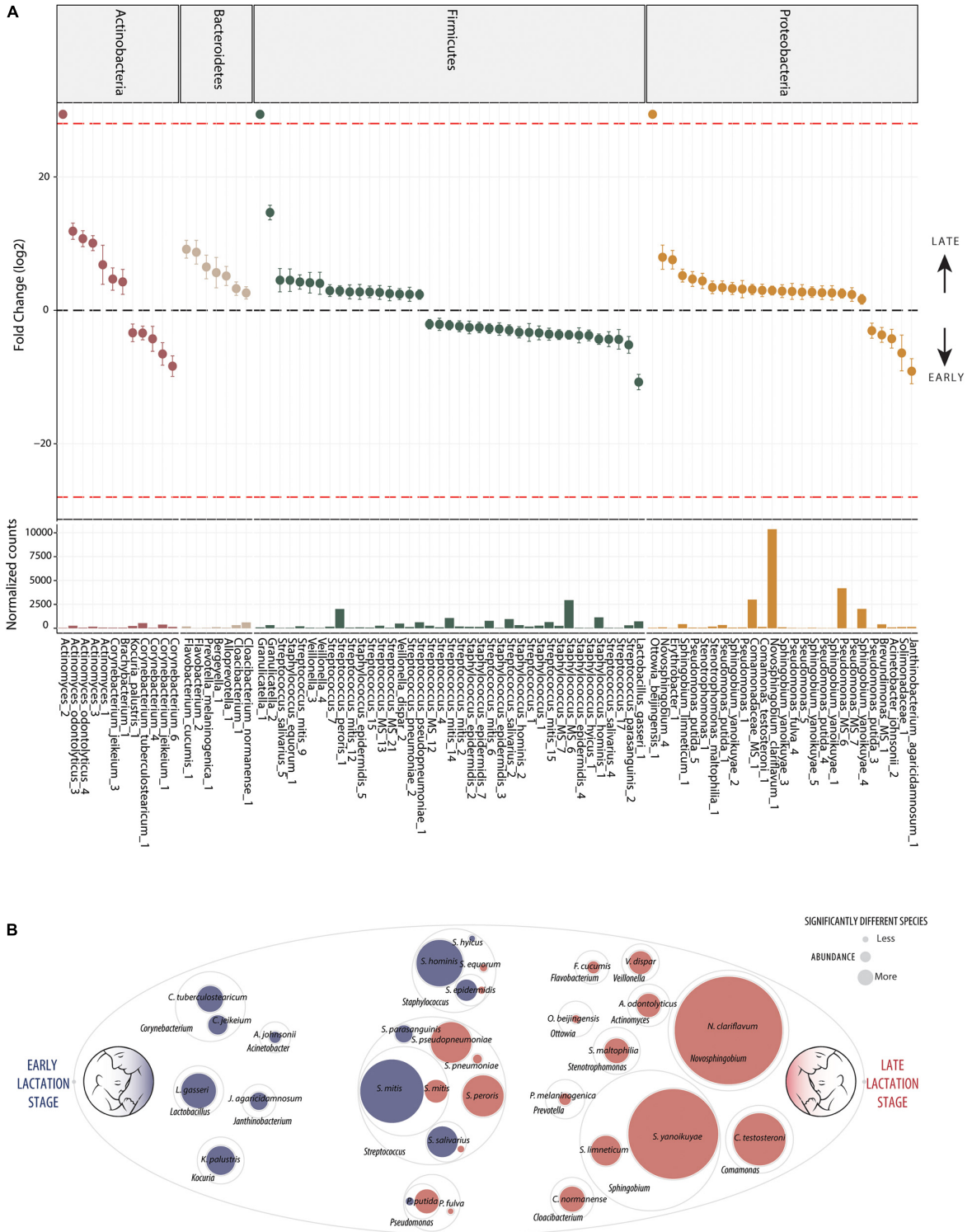

FIGURE 2 | Differentially abundant bacteria associated to lactation stage. Differentially abundant OTUs between the early (n = 33) and late (n = 43) groups. **(A)** Fold change (FC $\log_2$) in relative abundance of significantly different (DESeq2) OTUs between groups and their normalized mean counts. Species are grouped by phylum. The dashed red line indicates "infinite" fold change, where an OTU had detectable counts in samples from only a single group. **(B)** An illustration of species-level differentially abundant bacteria between milk of early (blue) and late (red) lactation stages. Raw abundance is represented. The complete OTU table including relative abundance, annotation, count distribution, blast statistics, alternative database hits, and sequences are provided in **Supplementary File 1**.

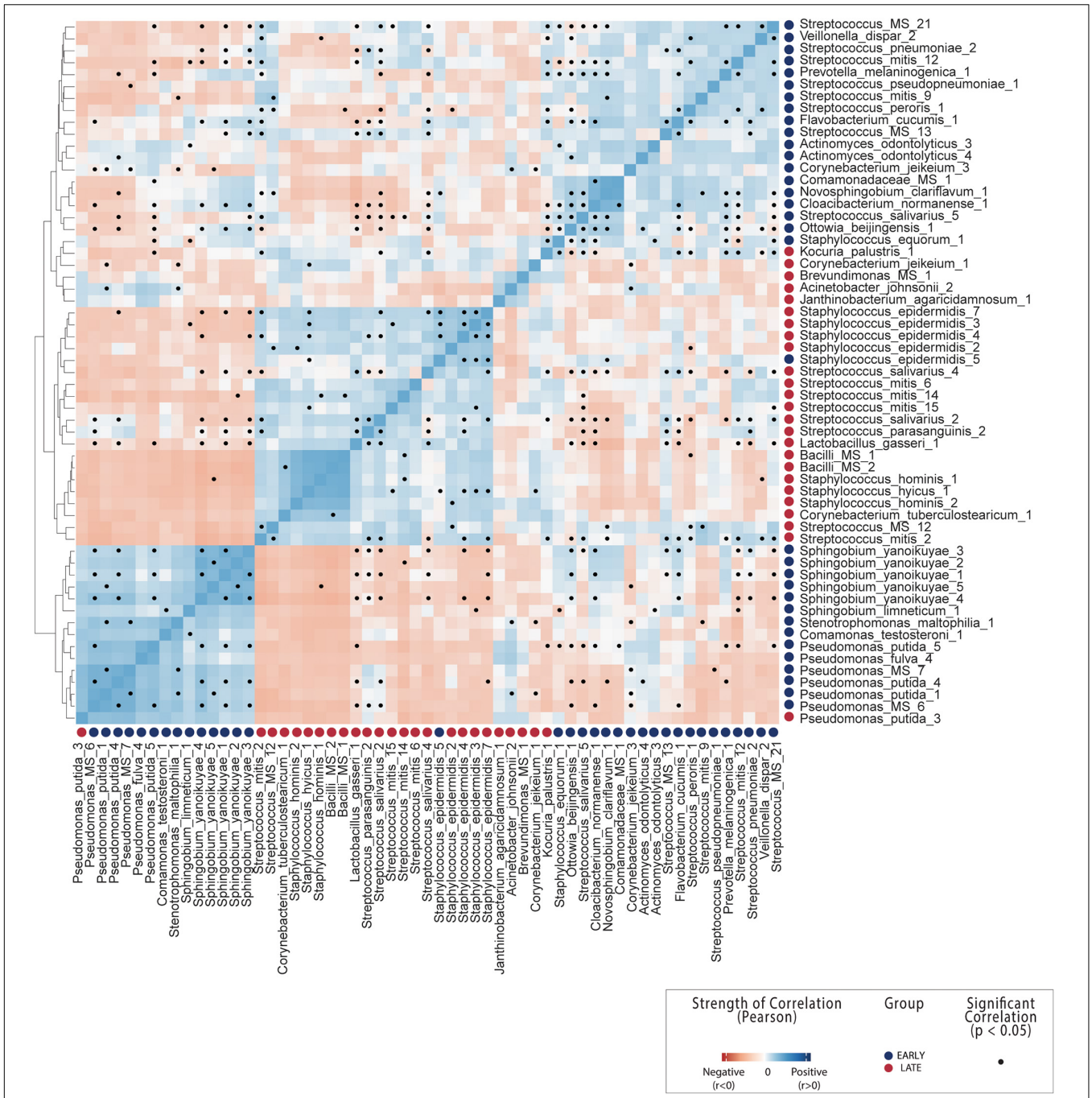

FIGURE 3 | OTU-OTU correlations across all breast milk samples. Count correlation of all OTUs differentially abundant between early and late lactation stages which could be annotated at species level. Colors indicate positive (blue) or negative (red) correlation and black dots indicate significance ($p < 0.05$). See **Supplementary File 1** correlations including non-differentially abundant of OTUs from mothers.

phylogeny (Rasmussen et al., 2016). Although little is known about functional variation between these strains, these results suggest that such variation does exist.

Species from the genus *Corynebacterium* are very commonly isolated from human breast milk and are generally considered commensal in nature (Hunt et al., 2011; McGuire and McGuire, 2017). The two species identified as higher in relative abundance in early milk could be a concern as both *C. tuberculostearicum* (which was first identified as leprosy-derived *Corynebacterium* and *C. jeikeium)* have historically been considered pathogenic (Riegel et al., 1994; Paviour et al., 2002; Hinić et al., 2012), although recent evidence has indicated that these species can be commensal (Damaceno et al., 2017). Similarly, *Acinetobacter johnsonii,* which has been previously, although not commonly,

detected in breast milk and is known to utilize lactate (Bouvet and Grimont, 1986; Delgado et al., 2008), could be a potential health concern as it has been associated with mastitis (Patel et al., 2017). *Kocuria palustris*, first isolated from rhizosphere samples (Kovács et al., 1999), was also unexpected within early breast milk as the species has not previously been reported in breast milk samples; although the genera has been detected in both ruminant and human milk (Jeurink et al., 2012; Li et al., 2017; Lackey et al., 2019).

A number of species characterized as potentially beneficial to infant health were also identified as significantly enriched in early breast milk. *Lactobacillus gasseri* is well characterized as a species with some strains that produce bacteriocins (gassericin A) (Pandey et al., 2013; Mousa et al., 2017) and is widely considered a putative early colonizer of infant guts. It is subsequently heavily marketed as a probiotic due to the potential to provide host resistance to infections from pathogens such as *Listeria monocytogenes* (Kawai et al., 2004; Selle and Klaenhammer, 2013), although evidence of this function *in situ* has not been yet been generated. *L. gasseri* was significantly positively correlated with *S. salivarius* and *S. parasanguinis* here (**Figure 3** and **Supplementary File 1**) and inversely correlated with the *Sphingobium* and *Pseudomonas* species in late milk microbiome. Another species with potential antimicrobial properties in significantly higher relative abundance in early lactation stage breast milk was *Janthinobacterium agaricidamnosum*, which produces an anti-fungal compound (jagaricin) with strong antifungal activity against major human fungal pathogens (Lincoln et al., 1999; Graupner et al., 2012, 2015). Although the species could potentially improve infant biotic resistance, it has not previously been observed in milk and is largely uncharacterized (jagaricin also has hemolytic activity; Fischer et al., 2019).

Species Associated With Late Lactation Stage Breast Milk Have a Common Function

An inverse correlation between bacteria within the phyla Firmicutes and Proteobacteria has recently been observed in human breast milk (Moossavi et al., 2019). The major genera identified here as representing this shift toward Proteobacteria in later lactation (**Figure 2**), *Sphingobium* and *Novosphingobium*, are often found in human breast milk and have been previously identified as highly abundant together with *Pseudomonas* in milk of healthy mothers in a non-marker based metagenomic study (Jiménez et al., 2015). *Sphingobium yanoikuyae*, identified here as significantly higher in relative abundance in late breast milk, is a well-known soil bioremediation species with some strains having polycyclic aromatic hydrocarbons (PAH) degradation activity in the environment (Cunliffe and Kertesz, 2006; Kou et al., 2018) but was first isolated from human clinical samples (Yabuuchi et al., 1990). Recruitment of bacteria with such functionality could be a response to accumulation of xenobiotics such as PAHs and polychlorinated biphenyls, which can accumulate in fatty tissue and breast milk (Dekoning and Karmaus, 2000), although this would not explain association with lactation stage. On the other hand, this species has also been previously observed as associated with nipple aspirate fluid of healthy women in a breast cancer study, where the authors speculated that the PAH degrading activity may provide protection against cancer tumor development (Chan et al., 2016; Parida and Sharma, 2019). Finally, although *N. clariflavum* was very widely distributed throughout samples, the species has yet to be characterized in detail (Zhang et al., 2017) and has never been previously identified in breast milk samples. However, *Novosphingobium* have been isolated from a very wide range of habitats including soils, plants and water, and are known as aromatic hydrocarbon compound degraders expected within soils and rhizospheres contaminated with persistent organic pollutants (Kumar et al., 2017; Wang et al., 2018).

The pattern of hydrocarbon degradation functionality was consistent with the majority of species identified as significantly enriched in late breast milk (**Figure 2**). *Pseudomonas putida* strains are common soil and rhizosphere degraders of persistent organic pollutants which are used for bioremediation as it can metabolize aromatic hydrocarbons as a sole carbon source (Feist and Hegeman, 1969; Dunn and Gunsalus, 1973; Marqués and Ramos, 1993), including caffeine (Summers et al., 2015). While *Pseudomonas* species are commonly observed in metagenomic studies of healthy mothers (Jeurink et al., 2012; Fitzstevens et al., 2017), they are generally considered environmental contamination in human breast milk (Jiménez et al., 2015). The closely related *Stenotrophomonas maltophilia*, which is considered non-lactose fermenting, has previously been identified as an opportunistic pathogen associated with cystic fibrosis, where it can form mixed species biofilm with *Pseudomonas aeruginosa* (Esposito et al., 2017). Given an established capability to cooperatively associate with *P. aeruginosa,* it is interesting to note that the species was significantly correlated in our study with *P. putida* (**Figure 3**).

Consistent with the differential abundance of *Sphingobium yanoikuyae* and *P. putida*, strains of *Stenotrophomonas maltophilia* also have extensive hydrocarbon degradation activity (Singh and Fulekar, 2010; Arulazhagan et al., 2017). The same is true of *Cloacibacterium normanense*, which is often isolated from wastewater and can often grow on oily sludge as its sole carbon source (Cerqueira et al., 2012), and *Comamonas testosteroni*, which has been isolated from cow milk (Quigley et al., 2013) and has strains associated with (eponymously) steroid and broader aromatic hydrocarbon degrading (Kamimura et al., 2010; Horinouchi et al., 2018). *Ottowia beijingensis*, first isolated from phenol degrading consortia in wastewater sludge, and *Flavobacterium cucumis* have not previously been reported in breast milk, to the authors' knowledge, but both have strains with hydrocarbon degradation capability (Al-Mailem et al., 2014; Cao et al., 2014; Fernandez-Gonzalez et al., 2018), consistent with the majority of differentially abundant species significantly enriched in late milk.

Other species significantly enriched in late milk have previously been isolated from an expected common source—the oral cavity, including *Prevotella melaninogenica*, *Veillonella dispar and Actinomyces odontolyticus*. *Actinomyces odontolyticus* is often considered pathogenic and strains have been associated

with infection/mastitis (Hoyles et al., 2001; Bing et al., 2015), but it is also a common oral commensal species which has been observed to increase during puberty (Gusberti et al., 1990). *P. melaninogenica* is a common oral commensal bacteria which has been suggested as transmitted directly from mother to colonize the infant mouth via saliva (Könönen et al., 1994), and has also been suggested for the oral commensal *Granulicatella* (Dewhirst et al., 2010; Gomez and Nelson, 2017). Species such as *V. dispar*, identified here as significantly higher in relative abundance in late milk, has been recently discussed with relevance to infant age (being commonly isolated from the oral cavity) (Tuominen et al., 2018) and strains have been identified in late (3 months postpartum) milk alongside *Granulicatella* (Simpson et al., 2018) and uncharacterized species from the hard to culture TM7 group of bacteria Candidatus saccharibacteria (Cabrera-Rubio et al., 2012). These findings suggest important roles of poorly characterized and unknown bacteria associated to lactation stage, highlighting that a substantial amount is yet to be discovered about breast milk as an ecosystem.

Limitations

Differentially abundant species are presented here based on amplified 16S rRNA gene sequences alone and do not establish viability of bacteria putatively identified. Future research confirming these findings should attempt to isolate species identified using culturing techniques. A concern often raised in milk microbiome studies relates to primer selection, an important limitation in bacterial marker technology. Inconsistency in the perceived "core" genera of bacteria commonly identified in the breast milk of healthy mothers is well captured in the systematic human breast milk microbiome reviews of Jeurink et al. (2012) and Fitzstevens et al. (2017) where most of the major studies report *Staphylococcus*, *Streptococcus, Pseudomonas* and either *Bifidobacterium* or *Cutibacterium* (formally *Propionibacterium*). This observed inconsistency between *Bifidobacterium* and *Cutibacterium* originates from the fundamental limitation of bacterial marker technology that there are no universal primers for the 16S rRNA gene (Klindworth et al., 2013; Gonzalez et al., 2019). Sequence analysis has revealed that the difference between these studies relates to a bias associated with primer selection. Specifically, the primers 27F/533R (utilized in this study), targets the V1-V3 region of the 16S rRNA gene and are often used in breast milk microbiome studies (Cabrera-Rubio et al., 2012; Mediano et al., 2017; Lackey et al., 2019) can successfully amplify the putative "core" breast milk genus *Cutibacterium* (formally *Propionibacterium*) (Hunt et al., 2011; Jost et al., 2013; Jiménez et al., 2015) but cannot amplify species from the putative "core" genus *Bifidobacterium* (Klindworth et al., 2013). Conversely, the other most commonly used primers, the 515F/806R primer pair (V4 region targeting), do amplify species within the genus *Bifidobacterium* but do not amplify species from the genera *Cutibacterium* (Klindworth et al., 2013), although *Bifidobacterium* sp. are often (Moossavi et al., 2019) but not always (Davé et al., 2016; Ramani et al., 2018) identified in breast milk studies when such primers are used. Whole genome shotgun (WGS) approaches can serve to resolve these types of identification bias generated from 16S rRNA primer selection; however, quantitative differential abundance analysis using WGS approaches remains a technical challenge for studies involving high sample numbers and with high bacterial diversity, such as is present within breast milk. Although *Pseudomonas* sp. are normally identified in breast milk of healthy mothers (Martín et al., 2007; Hunt et al., 2011, 2012; Jost et al., 2013; Ward et al., 2013; Jiménez et al., 2015; Urbaniak et al., 2016; McGuire and McGuire, 2017; Moossavi et al., 2019) species from the genera are common in the environment and could represent contamination (Jiménez et al., 2015; Treven et al., 2019), particularly as late breast milk samples had lower average DNA concentrations, although recent evidence suggests *Pseudomonas* presence in breast milk is genuine (Douglas et al., 2020).

CONCLUSION

Evidence is provided of extensive remodeling of the breast milk microbiome across lactation stages in a cohort of healthy unrelated Guatemalan mothers. These include a microbiome shift from specific *Staphylococcus* and *Streptococcus* species at the beginning of lactation toward *Sphingobium* and *Pseudomonas* species at a later stage of lactation. Collectively, the findings reveal that common changes occur in the healthy human breast milk microbiome over the first 6 months of lactation and highlight the importance of investigating the microbiome at different stages of lactation. The large majority of species significantly associated with later lactation, such as *Sphingomonas yanoikuyae*, *Pseudomonas putida*, *Stenotrophomonas maltophilia*, *Cloacibacterium normanense*, *Comamonas testosteroni*, *Ottowia beijingensis*, and *Flavobacterium cucumis* are intriguing in having the common functional trait of aromatic hydrocarbon degradation. Whilst the contribution of specific bacterial species to infant metabolism and immunity is largely opaque, these distinct changes suggest active on-going remodeling of the milk microbiome throughout lactation that could contribute favorably to infant health. Moreover, these insights illustrate the need to study under-represented human communities in breast milk research given the complexity of cross-talk between the mother-infant dyad during lactation.

DATA AVAILABILITY STATEMENT

All data are made available within the manuscript or **Supplementary Data**. Raw sequence data has been deposited at the European Genome-Phenome Archive (EGAD00001004160) and are available upon request to KK, kristine.koski@mcgill.ca.

ETHICS STATEMENT

The studies involving human participants were reviewed and approved by McGill Institutional Review Board and CeSSIAM

Human Subjects Committee. All participating mothers provided written informed consent for participation.

AUTHOR CONTRIBUTIONS

EG and NB analyzed microbiome data, created figures, and drafted the manuscript. CL drafted the manuscript, prepared samples for the 16S rRNA sequencing and LL prepared data files of maternal characteristics. NS supervised milk sample collection. KK, CL, LA, and MS conceptualized the study design and edited the final manuscript. NS, LA, and KK provided the financial support. All authors contributed to the article and approved the submitted version.

FUNDING

This study was supported by the Natural Sciences and Engineering Research Council of Canada (NSERC): NSERC RGPIN-2015-04390 and NSERC RGPIN-2016-04961.

ACKNOWLEDGMENTS

Special thanks to McGill University and Genome Quebec Innovation Centre for technical assistance with 16S rRNA sequencing. We thank H. Wren, AM Chomat, and CeSSIAM field team for sample collection and the participating mothers for providing valuable milk samples.

SUPPLEMENTARY MATERIAL

The Supplementary Material for this article can be found online at: https://www.frontiersin.org/articles/10.3389/fmicb.2021.557180/full#supplementary-material

Supplementary File 1 | Total amplified community flower diagram illustrating raw count distribution across all OTUs.

– Count correlation of 200 OTUs including all mothers.

– *Streptococcus mitis* strain genome clustering. *Streptococcus mitis* DA is strain cluster. Strain level research has been conducted (Jensen et al., 2016) but this tree is based on all the up-to-date genomes submitted to NCBI.

Supplementary File 2 | OTU table and lactation DA table.

REFERENCES

Al-Mailem, D., Kansour, M., and Radwan, S. (2014). Bioremediation of hydrocarbons contaminating sewage effluent using man-made biofilms: effects of some variables. *Appl. Biochem. Biotechnol.* 174, 1736–1751. doi: 10.1007/s12010-014-1067-z

Anders, S., McCarthy, D. J., Chen, Y., Okoniewski, M., Smyth, G. K., Huber, W., et al. (2013). Count-based differential expression analysis of RNA sequencing data using R and Bioconductor. *Nat. Protoc.* 8:1765. doi: 10.1038/nprot.2013.099

Andreas, N. J., Kampmann, B., and Le-Doare, K. M. (2015). Human breast milk: A review on its composition and bioactivity. *Early Hum. Dev.* 91, 629–635. doi: 10.1016/j.earlhumdev.2015.08.013

Arulazhagan, P., Al-Shekri, K., Huda, Q., Godon, J.-J., Basahi, J. M., and Jeyakumar, D. (2017). Biodegradation of polycyclic aromatic hydrocarbons by an acidophilic *Stenotrophomonas* maltophilia strain AJH1 isolated from a mineral mining site in Saudi Arabia. *Extremophiles* 21, 163–174. doi: 10.1007/s00792-016-0892-0

Biagi, E., Quercia, S., Aceti, A., Beghetti, I., Rampelli, S., Turroni, S., et al. (2017). The bacterial ecosystem of mother's milk and infant's mouth and gut. *Front. Microbiol.* 8:1214. doi: 10.3389/fmicb.2017.01214

Bing, A., Loh, S., Morris, T., Hughes, H., Dixon, J., and Helgason, K. (2015). Actinomyces species isolated from breast infections. *J. Clin. Microbiol.* 53, 3247–3255. doi: 10.1128/jcm.01030-15

Bolyen, E., Rideout, J. R., Dillon, M. R., Bokulich, N. A., Abnet, C. C., Al-Ghalith, G. A., et al. (2019). Reproducible, interactive, scalable and extensible microbiome data science using QIIME 2. *Nat. Biotechnol.* 37, 852–857.

Bouvet, P. J., and Grimont, P. A. (1986). Taxonomy of the genus Acinetobacter with the recognition of *Acinetobacter baumannii* sp. nov., Acinetobacter haemolyticus sp. nov., Acinetobacter johnsonii sp. nov., and Acinetobacter junii sp. nov. and emended descriptions of Acinetobacter calcoaceticus and Acinetobacter lwoffii. *Int. J. Syst. Evol. Microbiol.* 36, 228–240. doi: 10.1099/00207713-36-2-228

Brereton, N., Gonzalez, E., Desjardins, D., Labrecque, M., and Pitre, F. (2019). Co-cropping with three phytoremediation crops influences rhizosphere microbiome community in contaminated soil. *Sci. Total Environ.* 711:135067. doi: 10.1016/j.scitotenv.2019.135067

Cabrera-Rubio, R., Collado, M. C., Laitinen, K., Salminen, S., Isolauri, E., and Mira, A. (2012). The human milk microbiome changes over lactation and is shaped by maternal weight and mode of delivery. *Am. J. Clin. Nutr.* 96, 544–551. doi: 10.3945/ajcn.112.037382

Cao, J., Lai, Q., Liu, Y., Li, G., and Shao, Z. (2014). Ottowia beijingensis sp. nov., isolated from coking wastewater activated sludge, and emended description of the genus Ottowia. *Int. J. Syst. Evol. Microbiol.* 64, 963–967. doi: 10.1099/ijs.0.054015-0

Cerqueira, V. S., Hollenbach, E. B., Maboni, F., Camargo, F. A., Maria, do Carmo, R. P., et al. (2012). Bioprospection and selection of bacteria isolated from environments contaminated with petrochemical residues for application in bioremediation. *World J. Microbiol. Biotechnol.* 28, 1203–1222. doi: 10.1007/s11274-011-0923-z

Chan, A. A., Bashir, M., Rivas, M. N., Duvall, K., Sieling, P. A., Pieber, T. R., et al. (2016). Characterization of the microbiome of nipple aspirate fluid of breast cancer survivors. *Sci. Rep.* 6:28061.

Chomat, A. M., Solomons, N. W., Koski, K. G., Wren, H. M., Vossenaar, M., and Scott, M. E. (2015). Quantitative methodologies reveal a diversity of nutrition, infection/illness, and psychosocial stressors during pregnancy and lactation in rural Mam-Mayan mother–infant dyads from the Western Highlands of Guatemala. *Food Nutr. Bull.* 36, 415–440. doi: 10.1177/0379572115610944

Coates, R., Moran, J., and Horsburgh, M. J. (2014). Staphylococci: colonizers and pathogens of human skin. *Fut. Microbiol.* 9, 75–91. doi: 10.2217/fmb.13.145

Cunliffe, M., and Kertesz, M. A. (2006). Effect of Sphingobium yanoikuyae B1 inoculation on bacterial community dynamics and polycyclic aromatic hydrocarbon degradation in aged and freshly PAH-contaminated soils. *Environ. Poll.* 144, 228–237. doi: 10.1016/j.envpol.2005.12.026

Cunningham, A. S., Jelliffe, D. B., and Jelliffe, E. P. (1991). Breast-feeding and health in the 1980s: a global epidemiologic review. *J. pediatr.* 118, 659–666. doi: 10.1016/s0022-3476(05)80023-x

Damaceno, Q. S., Souza, J. P., Nicoli, J. R., Paula, R. L., Assis, G. B., Figueiredo, H. C., et al. (2017). Evaluation of potential probiotics isolated from human milk and colostrum. *Probiot. Antimicrob. Prot.* 9, 371–379. doi: 10.1007/s12602-017-9270-1

Davé, V., Street, K., Francis, S., Bradman, A., Riley, L., Eskenazi, B., et al. (2016). Bacterial microbiome of breast milk and child saliva from low-income Mexican-American women and children. *Pediatr. Res.* 79:846. doi: 10.1038/pr.2016.9

Dekoning, E. P., and Karmaus, W. (2000). PCB exposure in utero and via breast milk. A review. *J. Expos. Sci. Environ. Epidemiol.* 10:285. doi: 10.1038/sj.jea.7500090

Delgado, S., Arroyo, R., Martín, R., and Rodríguez, J. M. (2008). PCR-DGGE assessment of the bacterial diversity of breast milk in women with lactational infectious mastitis. *BMC Infect. Dis.* 8:51. doi: 10.1186/1471-2334-8-51

Delorme, C., Abraham, A.-L., Renault, P., and Guédon, E. (2015). Genomics of Streptococcus salivarius, a major human commensal. *Infect. Genet. Evol.* 33, 381–392. doi: 10.1016/j.meegid.2014.10.001

Dewhirst, F. E., Chen, T., Izard, J., Paster, B. J., Tanner, A. C., Yu, W.-H., et al. (2010). The human oral microbiome. *J. Bacteriol.* 192, 5002–5017.

Douglas, C. A., Ivey, K. L., Papanicolas, L. E., Best, K. P., Muhlhausler, B. S., and Rogers, G. B. (2020). DnA extraction approaches substantially influence the assessment of the human breast milk microbiome. *Sci. Rep.* 10, 1–10.

Dunn, N., and Gunsalus, I. (1973). Transmissible plasmid coding early enzymes of naphthalene oxidation in *Pseudomonas* putida. *J. Bacteriol.* 114, 974–979. doi: 10.1128/jb.114.3.974-979.1973

Esposito, A., Pompilio, A., Bettua, C., Crocetta, V., Giacobazzi, E., Fiscarelli, E., et al. (2017). Evolution of *Stenotrophomonas* maltophilia in cystic fibrosis lung over chronic infection: a genomic and phenotypic population study. *Front. Microbiol.* 8:1590. doi: 10.3389/fmicb.2017.01590

Feist, C. F., and Hegeman, G. (1969). Phenol and benzoate metabolism by *Pseudomonas* putida: regulation of tangential pathways. *J. Bacteriol.* 100, 869–877. doi: 10.1128/jb.100.2.869-877.1969

Fernández, L., Langa, S., Martín, V., Maldonado, A., Jiménez, E., Martín, R., et al. (2013). The human milk microbiota: origin and potential roles in health and disease. *Pharmacol. Res.* 69, 1–10. doi: 10.1016/j.phrs.2012.09.001

Fernandez-Gonzalez, N., Sierra-Alvarez, R., Field, J. A., Amils, R., and Sanz, J. L. (2018). Adaptation of granular sludge microbial communities to nitrate, sulfide, and/or p-cresol removal. *Int. Microbiol.* 22, 305–316. doi: 10.1007/s10123-018-00050-4

Fischer, D., Gessner, G., Fill, T. P., Barnett, R., Tron, K., Dornblut, K., et al. (2019). Disruption of membrane integrity by the bacterium-derived antifungal jagaricin. *Antimicrob. Agents Chemother.* 63, 00707–00719e.

Fitzstevens, J. L., Smith, K. C., Hagadorn, J. I., Caimano, M. J., Matson, A. P., and Brownell, E. A. (2017). Systematic Review of the Human Milk Microbiota. *Nutr. Clin. Pract.* 32, 354–364. doi: 10.1177/0884533616670150

Gomez, A., and Nelson, K. E. (2017). The oral microbiome of children: development, disease, and implications beyond oral health. *Microbial. Ecol.* 73, 492–503. doi: 10.1007/s00248-016-0854-1

Gonzalez, E., Pitre, F., and Brereton, N. (2019). ANCHOR: A 16S rRNA gene amplicon pipeline for microbial analysis of multiple environmental samples. *Environ. Microbiol.* 21, 2440–2468. doi: 10.1111/1462-2920.14632

Graupner, K., Lackner, G., and Hertweck, C. (2015). Genome sequence of mushroom soft-rot pathogen Janthinobacterium agaricidamnosum. *Genome Announc.* 3, 277–215e.

Graupner, K., Scherlach, K., Bretschneider, T., Lackner, G., Roth, M., Gross, H., et al. (2012). Imaging mass spectrometry and genome mining reveal highly antifungal virulence factor of mushroom soft rot pathogen. *Angewandte Chem. Int. Edition* 51, 13173–13177. doi: 10.1002/anie.201206658

Gusberti, F., Mombelli, A., Lang, N., and Minder, C. E. (1990). Changes in subgingival microbiota during puberty: A 4—year longitudinal study. *J. Clin. Periodontol.* 17, 685–692. doi: 10.1111/j.1600-051x.1990.tb01054.x

Heikkilä, M., and Saris, P. (2003). Inhibition of Staphylococcus aureus by the commensal bacteria of human milk. *J. Appl. Microbiol.* 95, 471–478. doi: 10.1046/j.1365-2672.2003.02002.x

Hinić, V., Lang, C., Weisser, M., Straub, C., Frei, R., and Goldenberger, D. (2012). Corynebacterium tuberculostearicum: a potentially misidentified and multiresistant Corynebacterium species isolated from clinical specimens. *J. Clin. Microbiol.* 50, 2561–2567. doi: 10.1128/jcm.00386-12

Horinouchi, M., Koshino, H., Malon, M., Hirota, H., and Hayashi, T. (2018). Steroid degradation in Comamonas testosteroni TA441: identification of metabolites and the genes involved in the reactions necessary before D-ring cleavage. *Appl. Environ. Microbiol.* 84, 1324–1318e.

Hoyles, L., Falsen, E., Holmström, G., Persson, A., Sjödén, B., and Collins, M. D. (2001). Actinomyces suimastitidis sp. nov., isolated from pig mastitis. *Int. J. Syst. Evolut. Microbiol.* 51, 1323–1326. doi: 10.1099/00207713-51-4-1323

Hunt, K. M., Foster, J. A., Forney, L. J., Schütte, U. M. E., Beck, D. L., Abdo, Z., et al. (2011). Characterization of the Diversity and Temporal Stability of Bacterial Communities in Human Milk. *PLoS One* 6:e21313. doi: 10.1371/journal.pone.0021313

Hunt, K., Preuss, J., Nissan, C., Davlin, C., Williams, J., Shafii, B., et al. (2012). Human milk oligosaccharides promote the growth of staphylococci. *Appl. Environ. Microbiol.* 78, 4763–4770. doi: 10.1128/aem.00477-12

Jensen, A., Scholz, C. F., and Kilian, M. (2016). Re-evaluation of the taxonomy of the Mitis group of the genus Streptococcus based on whole genome phylogenetic analyses, and proposed reclassification of Streptococcus dentisani as Streptococcus oralis subsp. dentisani comb. nov., Streptococcus tigurinus as Streptococcus oralis subsp. tigurinus comb. nov., and Streptococcus oligofermentans as a later synonym of Streptococcus cristatus. *Int. J. Syst. Evolut. Microbiol.* 66, 4803–4820. doi: 10.1099/ijsem.0.001433

Jeurink, P., Van Bergenhenegouwen, J., Jiménez, E., Knippels, L., Fernández, L., Garssen, J., et al. (2012). Human milk: a source of more life than we imagine. *Benefic. Microbes* 4, 17–30. doi: 10.3920/bm2012.0040

Jiménez, E., de Andrés, J., Manrique, M., Pareja-Tobes, P., Tobes, R., Martínez-Blanch, J. F., et al. (2015). Metagenomic analysis of milk of healthy and mastitis-suffering women. *J. Hum. Lact.* 31, 406–415. doi: 10.1177/0890334415585078

Jonsson, V., Österlund, T., Nerman, O., and Kristiansson, E. (2016). Statistical evaluation of methods for identification of differentially abundant genes in comparative metagenomics. *BMC Genomics* 17:78. doi: 10.1186/s12864-016-2386-y

Jost, T., Lacroix, C., Braegger, C. P., Rochat, F., and Chassard, C. (2014). Vertical mother-neonate transfer of maternal gut bacteria via breastfeeding. *Environ. Microbiol.* 16, 2891–2904. doi: 10.1111/1462-2920.12238

Jost, T., Lacroix, C., Braegger, C., and Chassard, C. (2013). Assessment of bacterial diversity in breast milk using culture-dependent and culture-independent approaches. *Br. J. Nutrit.* 110, 1253–1262. doi: 10.1017/s0007114513000597

Kamimura, N., Aoyama, T., Yoshida, R., Takahashi, K., Kasai, D., Abe, T., et al. (2010). Characterization of the protocatechuate 4, 5-cleavage pathway operon in Comamonas sp. strain E6 and discovery of a novel pathway gene. *Appl. Environ. Microbiol.* 76, 8093–8101. doi: 10.1128/aem.01863-10

Kawai, Y., Kemperman, R., Kok, J., and Saito, T. (2004). The circular bacteriocins gassericin A and circularin A. *Curr. Prot. Peptide Sci.* 5, 393–398. doi: 10.2174/1389203043379549

Kilian, M., Riley, D. R., Jensen, A., Brüggemann, H., and Tettelin, H. (2014). Parallel evolution of Streptococcus pneumoniae and Streptococcus mitis to pathogenic and mutualistic lifestyles. *MBio* 5, 1490–1414e.

Klindworth, A., Pruesse, E., Schweer, T., Peplies, J., Quast, C., Horn, M., et al. (2013). Evaluation of general 16S ribosomal RNA gene PCR primers for classical and next-generation sequencing-based diversity studies. *Nucleic Acids Res.* 41:e1. doi: 10.1093/nar/gks808

Knight, R., Vrbanac, A., Taylor, B. C., Aksenov, A., Callewaert, C., Debelius, J., et al. (2018). Best practices for analysing microbiomes. *Nat. Rev. Microbiol.* 16, 410–422.

Könönen, E., Saarela, M., Karjalainen, J., Jousimies−Somer, H., Alaluusua, S., and Asikainen, S. (1994). Transmission of oral Prevotella melaninogenica between a mother and her young child. *Oral Microbiol. Immunol.* 9, 310–314. doi: 10.1111/j.1399-302x.1994.tb00077.x

Kou, S., Vincent, G., Gonzalez, E., Pitre, F. E., Labrecque, M., and Brereton, N. J. (2018). The Response of a 16S Ribosomal RNA Gene Fragment Amplified Community to Lead, Zinc, and Copper Pollution in a Shanghai Field Trial. *Front. Microbiol.* 9:366. doi: 10.3389/fmicb.2018.00366

Kovács, G., Burghardt, J., Pradella, S., Schumann, P., Stackebrandt, E., and Màrialigeti, K. (1999). Kocuria palustris sp. nov. and Kocuria rhizophila sp. nov., isolated from the rhizoplane of the narrow-leaved cattail (Typha angustifolia). *Int. J. Syst. Evol. Microbiol.* 49, 167–173. doi: 10.1099/00207713-49-1-167

Kumar, R., Verma, H., Haider, S., Bajaj, A., Sood, U., Ponnusamy, K., et al. (2017). Comparative genomic analysis reveals habitat-specific genes and regulatory hubs within the genus Novosphingobium. *MSystems* 2, 20–17e.

Lackey, K. A., Williams, J. E., Meehan, C. L., Zachek, J. A., Benda, E. D., Price, W. J., et al. (2019). What's Normal? Microbiomes In Human Milk And Infant Feces Are Related To Each Other But Vary Geographically: The INSPIRE Study. *Front. Nutrit.* 6:45. doi: 10.3389/fnut.2019.00045

LaTuga, M. S., Stuebe, A., and Seed, P. C. (2014). A review of the source and function of microbiota in breast milk. *Semin. Reprod. Med.* 2, 68–73.

Li, C., Solomons, N. W., Scott, M. E., and Koski, K. G. (2016). Minerals and trace elements in human breast milk are associated with Guatemalan infant

anthropometric outcomes within the first 6 months. *J. Nutrit.* 146, 2067–2074. doi: 10.3945/jn.116.232223

Li, Z., Wright, A.-D. G., Yang, Y., Si, H., and Li, G. (2017). Unique bacteria community composition and co-occurrence in the milk of different ruminants. *Sci. Rep.* 7:40950.

Lincoln, S. P., Fermor, T. R., and Tindall, B. (1999). Janthinobacterium agaricidamnosum sp. nov., a soft rot pathogen of Agaricus bisporus. *Int. J. Syst. Evol. Microbiol.* 49, 1577–1589. doi: 10.1099/00207713-49-4-1577

Love, M. I., Anders, S., Kim, V., and Huber, W. (2015). RNA-Seq workflow: gene-level exploratory analysis and differential expression. *F1000Research* 4:1070. doi: 10.12688/f1000research.7035.2

Love, M. I., Huber, W., and Anders, S. (2014a). Moderated estimation of fold change and dispersion for RNA-seq data with DESeq2. *Genome Biol.* 15:550.

Love, M., Anders, S., and Huber, W. (2014b). Differential analysis of count data–the DESeq2 package. *Genome Biol.* 15:550.

Marqués, S., and Ramos, J. L. (1993). Transcriptional control of the *Pseudomonas* putida TOL plasmid catabolic pathways. *Mol. Microbiol.* 9, 923–929. doi: 10.1111/j.1365-2958.1993.tb01222.x

Martín, R. O., Langa, S., Reviriego, C., Jiménez, E., Marín, M. A. L., Olivares, M., et al. (2004). The commensal microflora of human milk: new perspectives for food bacteriotherapy and probiotics. *Trends Food Sci. Technol.* 15, 121–127. doi: 10.1016/j.tifs.2003.09.010

Martín, R., Heilig, H. G., Zoetendal, E. G., Jiménez, E., Fernández, L., Smidt, H., et al. (2007). Cultivation-independent assessment of the bacterial diversity of breast milk among healthy women. *Res. Microbiol.* 158, 31–37. doi: 10.1016/j.resmic.2006.11.004

McGuire, M. K., and McGuire, M. A. (2017). Got bacteria? The astounding, yet not-so-surprising, microbiome of human milk. *Curr. Opin. Biotechnol.* 44, 63–68. doi: 10.1016/j.copbio.2016.11.013

McMurdie, P. J., and Holmes, S. (2013). phyloseq: an R package for reproducible interactive analysis and graphics of microbiome census data. *PLoS One* 8:e61217. doi: 10.1371/journal.pone.0061217

Mediano, P., Fernández, L., Jiménez, E., Arroyo, R., Espinosa-Martos, I., Rodríguez, J. M., et al. (2017). Microbial diversity in milk of women with mastitis: potential role of coagulase-negative staphylococci, viridans group streptococci, and corynebacteria. *J. Hum. Lactat.* 33, 309–318. doi: 10.1177/0890334417692968

Minerbi, A., Gonzalez, E., Brereton, N. J., Anjarkouchian, A., Dewar, K., Fitzcharles, M.-A., et al. (2019). Altered microbiome composition in individuals with fibromyalgia. *Pain* 160, 2589–2602. doi: 10.1097/j.pain.0000000000001640

Moossavi, S., Sepehri, S., Robertson, B., Bode, L., Goruk, S., Field, C. J., et al. (2019). Composition and variation of the human milk microbiota are influenced by maternal and early-life factors. *Cell Host Microbe* 25, 324–335 doi: 10.1016/j.chom.2019.01.011

Mousa, W. K., Athar, B., Merwin, N. J., and Magarvey, N. A. (2017). Antibiotics and specialized metabolites from the human microbiota. *Nat. Prod. Rep.* 34, 1302–1331. doi: 10.1039/c7np00021a

Oksanen, J., Blanchet, F. G., Kindt, R., Legendre, P., Minchin, P. R., O'hara, R., et al. (2017). *Package 'vegan' in Community ecology package, version*. Vienna: R Core Team.

Pandey, N., Malik, R., Kaushik, J., and Singroha, G. (2013). Gassericin A: a circular bacteriocin produced by lactic acid bacteria Lactobacillus gasseri. *World J. Microbiol. Biotechnol.* 29, 1977–1987. doi: 10.1007/s11274-013-1368-3

Parida, S., and Sharma, D. (2019). The power of small changes: comprehensive analyses of microbial dysbiosis in breast cancer. *Biochim. Biophys. Acta Rev. Cancer* 1871, 392–405. doi: 10.1016/j.bbcan.2019.04.001

Patel, S. H., Vaidya, Y. H., Patel, R. J., Pandit, R. J., Joshi, C. G., and Kunjadiya, A. P. (2017). Culture independent assessment of human milk microbial community in lactational mastitis. *Sci. Rep.* 7:7804.

Paviour, S., Musaad, S., Roberts, S., Taylor, G., Taylor, S., Shore, K., et al. (2002). Corynebacterium species isolated from patients with mastitis. *Clin. Infect. Dis.* 35, 1434–1440.

Pearce, C., Bowden, G., Evans, M., Fitzsimmons, S., Johnson, J., Sheridan, M., et al. (1995). Identification of pioneer viridans streptococci in the oral cavity of human neonates. *J. Med. Microbiol.* 42, 67–72. doi: 10.1099/00222615-42-1-67

Quigley, L., O'sullivan, O., Stanton, C., Beresford, T. P., Ross, R. P., Fitzgerald, G. F., et al. (2013). The complex microbiota of raw milk. *FEMS Microbiol. Rev.* 37, 664–698. doi: 10.1111/1574-6976.12030

Ramani, S., Stewart, C. J., Laucirica, D. R., Ajami, N. J., Robertson, B., Autran, C. A., et al. (2018). Human milk oligosaccharides, milk microbiome and infant gut microbiome modulate neonatal rotavirus infection. *Nat. Commun.* 9:5010.

Ramsay, D. T., Kent, J. C., Owens, R. A., and Hartmann, P. E. (2004). Ultrasound imaging of milk ejection in the breast of lactating women. *Pediatrics* 113, 361–367. doi: 10.1542/peds.113.2.361

Rasmussen, L., Dargis, R., Højholt, K., Christensen, J., Skovgaard, O., Justesen, U., et al. (2016). Whole genome sequencing as a tool for phylogenetic analysis of clinical strains of Mitis group streptococci. *Eur. J. Clin. Microbiol. Infect. Dis.* 35, 1615–1625. doi: 10.1007/s10096-016-2700-2

Riegel, P., De Briel, D., Prévost, G., Jehl, F., and Monteil, H. (1994). Genomic diversity among Corynebacterium jeikeium strains and comparison with biochemical characteristics and antimicrobial susceptibilities. *J. Clin. Microbiol.* 32, 1860–1865. doi: 10.1128/jcm.32.8.1860-1865.1994

Rodríguez, J. M. (2014). The origin of human milk bacteria: is there a bacterial entero-mammary pathway during late pregnancy and lactation? *Adv. Nutr.* 5, 779–784. doi: 10.3945/an.114.007229

Ruiz, L., García-Carral, C., and Rodriguez, J. M. (2019). Unfolding the human milk microbiome landscape in the omics era. *Front. Microbiol.* 10:1378. doi: 10.3389/fmicb.2019.01378

Sakwinska, O., and Bosco, N. (2019). Host microbe interactions in the lactating mammary gland. *Front. Microbiol.* 10:1863. doi: 10.3389/fmicb.2019.01863

Schloss, P. D., Westcott, S. L., Ryabin, T., Hall, J. R., Hartmann, M., Hollister, E. B., et al. (2009). Introducing mothur: open-source, platform-independent, community-supported software for describing and comparing microbial communities. *Appl. Environ. Microbiol.* 75, 7537–7541. doi: 10.1128/aem.01541-09

Selle, K., and Klaenhammer, T. R. (2013). Genomic and phenotypic evidence for probiotic influences of Lactobacillus gasseri on human health. *FEMS Microbiol. Rev.* 37, 915–935. doi: 10.1111/1574-6976.12021

Simpson, M. R., Avershina, E., Storrø, O., Johnsen, R., Rudi, K., and Øien, T. (2018). Breastfeeding-associated microbiota in human milk following supplementation with Lactobacillus rhamnosus GG, Lactobacillus acidophilus La-5, and Bifidobacterium animalis ssp. lactis Bb-12. *J. Dairy Sci.* 101, 889–899. doi: 10.3168/jds.2017-13411

Singh, D., and Fulekar, M. H. (2010). Biodegradation of petroleum hydrocarbons by *Pseudomonas* putida strain MHF 7109. *Clean Soil Air Water* 38, 781–786. doi: 10.1002/clen.200900239

Soeorg, H., Metsvaht, T., Eelmäe, I., Merila, M., Treumuth, S., Huik, K., et al. (2017). The role of breast milk in the colonization of neonatal gut and skin with coagulase-negative staphylococci. *Pediatr. Res.* 82, 759–767. doi: 10.1038/pr.2017.150

Sørensen, U. B. S., Yao, K., Yang, Y., Tettelin, H., and Kilian, M. (2016). Capsular polysaccharide expression in commensal Streptococcus species: genetic and antigenic similarities to Streptococcus pneumoniae. *MBio* 7, 1844–1816e.

Summers, R. M., Mohanty, S. K., Gopishetty, S., and Subramanian, M. (2015). Genetic characterization of caffeine degradation by bacteria and its potential applications. *Microbial Biotechnol.* 8, 369–378. doi: 10.1111/1751-7915.12262

Treven, P., Mahnič, A., Rupnik, M., Golob, M., Pirš, T., Matijašić, B. B., et al. (2019). Evaluation of Human Milk Microbiota by 16S rRNA Gene Next-Generation Sequencing (NGS) and Cultivation/MALDI-TOF Mass Spectrometry Identification. *Front. Microbiol.* 10:2612. doi: 10.3389/fmicb.2019.02612

Tuominen, H., Rautava, S., Collado, M. C., Syrjänen, S., and Rautava, J. (2018). HPV infection and bacterial microbiota in breast milk and infant oral mucosa. *PLoS One* 13:e0207016. doi: 10.1371/journal.pone.0207016

UNICEF (2018). *"Infant and young child feeding"*. New York, NY: UNICEF.

Urbaniak, C., Angelini, M., Gloor, G. B., and Reid, G. (2016). Human milk microbiota profiles in relation to birthing method, gestation and infant gender. *Microbiome* 4:1.

Walker, A. (2010). Breast milk as the gold standard for protective nutrients. *J. Pediatr.* 156, S3–S7.

Wang, J., Wang, C., Li, J., Bai, P., Li, Q., Yuan, S. M., et al. (2018). Comparative genomics of degradative Novosphingobium strains with special reference to the

microcystin-degrading Novosphingobium sp. THN1. *Front. Microbiol.* 9:2238. doi: 10.3389/fmicb.2018.02238

Ward, T. L., Hosid, S., Ioshikhes, I., and Altosaar, I. (2013). Human milk metagenome: a functional capacity analysis. *BMC Microbiol.* 13:116. doi: 10.1186/1471-2180-13-116

Wei, T., and Simko, V. (2017). *corrplot: Visualization of a Correlation Matrix*. Vienna: R Core Team.

Weiss, S., Xu, Z. Z., Peddada, S., Amir, A., Bittinger, K., Gonzalez, A., et al. (2017). Normalization and microbial differential abundance strategies depend upon data characteristics. *Microbiome* 5:27.

Williams, J. E., Carrothers, J. M., Lackey, K. A., Beatty, N. F., Brooker, S. L., Peterson, H. K., et al. (2019). Strong Multivariate Relations Exist Among Milk, Oral, and Fecal Microbiomes in Mother-Infant Dyads During the First Six Months Postpartum. *J. Nutrit.* 149, 902–914. doi: 10.1093/jn/nxy299

Williams, J. E., Carrothers, J. M., Lackey, K. A., Beatty, N. F., York, M. A., Brooker, S. L., et al. (2017). Human milk microbial community structure is relatively stable and related to variations in macronutrient and micronutrient intakes in healthy lactating women. *J. Nutr.* 147, 1739–1748.

World Health Organization (2014). *Global nutrition targets 2025: Breastfeeding Policy Brief*. Geneva: WHO.

Wren, H. M., Solomons, N. W., Chomat, A. M., Scott, M. E., and Koski, K. G. (2015). Cultural determinants of optimal breastfeeding practices among indigenous Mam-Mayan women in the Western Highlands of Guatemala. *J. Hum. Lact.* 31, 172–184. doi: 10.1177/0890334414560194

Yabuuchi, E., Yano, I., Oyaizu, H., Hashimoto, Y., Ezaki, T., and Yamamoto, H. (1990). Proposals of Sphingomonas paucimobilis gen. nov. and comb. nov., Sphingomonas parapaucimobilis sp. nov., Sphingomonas yanoikuyae sp. nov., Sphingomonas adhaesiva sp. nov., Sphingomonas capsulata comb, nov., and Two Genospecies of the Genus Sphingomonas. *Microbiol. Immunol.* 34, 99–119. doi: 10.1111/j.1348-0421.1990.tb00996.x

Zhang, X., Liu, Y., Lin, Y., Wang, L., Yao, S., Cao, Y., et al. (2017). Novosphingobium clariflavum sp. nov., isolated from a household product plant. *Int. J. Syst. Evol. Microbiol.* 67, 3150–3155. doi: 10.1099/ijsem.0.001803

Conflict of Interest: The authors declare that the research was conducted in the absence of any commercial or financial relationships that could be construed as a potential conflict of interest.

Copyright © 2021 Gonzalez, Brereton, Li, Lopez Leyva, Solomons, Agellon, Scott and Koski. This is an open-access article distributed under the terms of the Creative Commons Attribution License (CC BY). The use, distribution or reproduction in other forums is permitted, provided the original author(s) and the copyright owner(s) are credited and that the original publication in this journal is cited, in accordance with accepted academic practice. No use, distribution or reproduction is permitted which does not comply with these terms.

Advantages of publishing in Frontiers

OPEN ACCESS
Articles are free to read for greatest visibility and readership

FAST PUBLICATION
Around 90 days from submission to decision

HIGH QUALITY PEER-REVIEW
Rigorous, collaborative, and constructive peer-review

TRANSPARENT PEER-REVIEW
Editors and reviewers acknowledged by name on published articles

Frontiers
Avenue du Tribunal-Fédéral 34
1005 Lausanne | Switzerland

Visit us: www.frontiersin.org
Contact us: frontiersin.org/about/contact

REPRODUCIBILITY OF RESEARCH
Support open data and methods to enhance research reproducibility

DIGITAL PUBLISHING
Articles designed for optimal readership across devices

FOLLOW US
@frontiersin

IMPACT METRICS
Advanced article metrics track visibility across digital media

EXTENSIVE PROMOTION
Marketing and promotion of impactful research

LOOP RESEARCH NETWORK
Our network increases your article's readership